

University of Southampton Research Repository
ePrints Soton

Copyright © and Moral Rights for this thesis are retained by the author and/or other copyright owners. A copy can be downloaded for personal non-commercial research or study, without prior permission or charge. This thesis cannot be reproduced or quoted extensively from without first obtaining permission in writing from the copyright holder/s. The content must not be changed in any way or sold commercially in any format or medium without the formal permission of the copyright holders.

When referring to this work, full bibliographic details including the author, title, awarding institution and date of the thesis must be given e.g.

AUTHOR (year of submission) "Full thesis title", University of Southampton, name of the University School or Department, PhD Thesis, pagination

UNIVERSITY OF SOUTHAMPTON

**THE BIOGEOCHEMISTRY OF SOME TRACE METALS
IN SOME EUTROPHIC AREAS: THE ADRIATIC SEA
AND THE NORTH-WESTERN BLACK SEA**

by S.P.C. Tankéré

Department of Oceanography

June 1998

UNIVERSITY OF SOUTHAMPTON

ABSTRACT

FACULTY OF SCIENCE

OCEANOGRAPHY

Doctor of Philosophy

THE BIOGEOCHEMISTRY OF SOME TRACE METALS IN SOME EUTROPHIC

AREAS: THE ADRIATIC SEA AND THE NORTH-WESTERN BLACK SEA

by Sophie Pierrette Christine Tankéré

Measurements of dissolved trace metals (Mn, Fe, Co, Pb, Cd, Zn, Cu, Ni), total particulate trace metals (Mn, Fe, Pb, Zn, Cu, Ni), dissolved nutrients, oxygen, chl.*a* have been made in the Adriatic Sea. Measurements of dissolved trace metals (Mn, Fe, Co, Pb, Cd, Zn, Cu, Ni) were made in the Strait of Otranto. Measurements of dissolved trace metals (Mn, Fe, Co, Pb, Cd, Zn, Cu, Ni), acetic acid leachable particulate trace metals (Mn, Fe, Co, Pb, Cd, Zn, Cu, Ni), total particulate Mn and Fe, dissolved nutrients, oxygen, Chl.*a* have been made in the north western Black Sea.

In the northern Adriatic and north western Black Sea, relatively high concentrations of nutrients, inducing eutrophication, have been observed. The biodegradation of organic matter, which occurred below the thermocline or at the sediment-water interface, influence the reduction-oxidation potential in the water column. Fluctuation of the reduction-oxidation potential in the water column influences the distribution of redox sensitive metals (Mn, Fe and Co). Dissolved Mn and Fe concentrations were high in some cases mainly due to the reduction of Mn- and Fe- oxides which occurred in microenvironments in the dominantly oxic medium at the thermocline or in low O₂ zones near the bottom. The distributions were also influenced by riverine inputs. Dissolved Mn, Fe and Co concentrations were generally higher in the north-western Black Sea than in the Adriatic Sea suggesting that diagenetic reactions involving the destruction of organic carbon are more intense in the north-western Black Sea than in the Adriatic Sea. Total particulate concentrations of Mn and Fe were high, due to reprecipitation of Mn²⁺ and Fe²⁺ in presence of oxygen, riverine inputs and advective transport. Trace metal distributions (Co, Pb, Cd, Zn, Cu, Ni) were influenced by the Mn and Fe cycling and by riverine inputs. Relatively high dissolved and leachable or total particulate concentrations were generally found in surface waters at stations directly influenced by the River Po and the River Danube. High dissolved metal concentrations were found at the thermocline or near the sediment-water interface where dissolution of Mn- and Fe- oxides, on which metals were adsorbed, occurs under suboxic or anoxic conditions. Dissolved concentrations of Pb, Cd, Cu, Ni and Zn are generally similar in the northern Adriatic Sea and in the north-western Black Sea. Particulate Fe, Pb, Cu, Ni, Cd and Zn concentrations were higher in the northern Adriatic Sea than in the north-western Black Sea reflecting the strong influence of riverine inputs on the shallow northern part of the Adriatic where the depth hardly ever exceeds 40 m. In the north-western Black Sea, the Iron Gate dams significantly reduce the particulate metal loads.

A first order mass balance of 6 different trace metals (Mn, Fe, Pb, Zn, Cu and Ni) is presented for a one year period for the Adriatic Sea. The Adriatic Sea appears to be a source of dissolved Cu, Mn, Co, Cd and Fe for the Mediterranean Sea whereas for dissolved Zn and Pb the Adriatic Sea appears to be a net sink. Calculations of turnover time of metals with respect to different processes in the different parts of the Adriatic Sea show that in the northern and central Adriatic Sea, sedimentation is the main process which affect the metal distributions whereas in the southern Adriatic Sea the water flux exchanges with the Strait of Otranto play an important role for Zn, Cu and Ni.

ACKNOWLEDGEMENTS

I would like to thank my supervisor Dr Peter Statham for giving me the opportunity to carry on some work in the Adriatic Sea as part of the EUROMARGE-AS Project and for giving me the opportunity to do this Ph. D. Thesis. I would like to thank Prof. Dennis Burton for introducing me to the “Trace metal World”, for giving me the opportunity to carry on some work in the Western Mediterranean Sea and Black Sea as part of the EROS 2000 Project, and for encouraging me. I would also like to thank them both for discussing the writing of this thesis.

I would like to thank Dr Adrian Mc Donald, for helping me during the sampling trips in the Adriatic Sea, and Christophe Lerebourg for his technical assistance during analyses of particulate trace metals.

I would like to thank Dr Nick Morley and Paul Goody who have been there when help was needed.

I would like to thank all my friends particularly Dr Christine Gommenginger, Dr Susan Shimwell, Val Byfield, Dr Raoul Aguirre and Daniel Balestero for encouraging me and helping me.

Finally I would like to thank Anna who took care of Lawrence when I was busy writing this thesis, Hélène, Geneviève and Jack who helped the family in different ways over the last years and François for taking care of the house when I was busy and for his valued discussions during the writing of this thesis.

THE BIOGEOCHEMISTRY OF SOME TRACE METALS IN SOME EUTROPHIC AREAS: THE ADRIATIC SEA AND THE NORTH-WESTERN BLACK SEA

LIST OF CONTENTS

ABSTRACT

ACKNOWLEDGEMENTS

CHAPTER 1: Introduction.....	1
1.1 Trace metals in rivers and marine environments and major processes at work.....	1
1.1.1 Trace metals in rivers.....	1
1.1.2 Trace metals in estuaries.....	3
1.1.3 Trace metals in coastal waters.....	5
1.1.4 Trace metals in open ocean.....	5
a) Conservative-type vertical trace metal profiles (Rb, Cs).....	5
b) Nutrient-type vertical trace metal profiles (Cd, Zn, Cu, Ni).....	6
c) Surface enrichment and depth depletion type of vertical trace metal profiles (Pb, Mn, Co, Fe).....	7
1.1.5 Trace metals in anoxic environments.....	8
1.1.6 Importance of advective transport processes.....	10
1.1.7 Importance of boundary exchanges processes.....	11
1.1.7.1 Atmosphere.....	11
1.1.7.2 Sediment.....	11
1.2 The aims of this work.....	12
CHAPTER 2: Eutrophication.....	13
2.1 Manifestation of the problem in two semi-enclosed marginal seas: consequences for benthic-pelagic coupling.....	13
2.2 Consequences of eutrophication on trace metal behaviour.....	17
2.2.1 Cycling of iron and manganese.....	17
2.2.2 The role of phytoplankton in the uptake of trace metals.....	20
CHAPTER 3: Sampling and analytical procedures.....	23
3.1 Procedures used to minimise contamination for trace metal analyses.....	23
3.2 Dissolved trace metals (Cd, Co, Cu, Fe, Mn, Ni, Pb and Zn) in seawater and river water.....	24
3.2.1 Sampling.....	24
3.2.2 Analytical procedure for total dissolved trace metals.....	24
3.2.2.1 Generation of reagents and necessary apparatus.....	24
a) Apparatus.....	25
b) Reagents.....	25
c) Reagent preparation.....	26
3.2.2.2 Procedure.....	27

3.2.2.3 Measurement by atomic absorption spectrometry.....	27
3.2.2.4 Calculation of sample concentration, and method performance....	29
3.3 Particulate trace metals (Cd, Co, Cu, Fe, Mn, Ni, Pb and Zn) in seawater and river water.....	30
3.3.1 Samples in the Adriatic Sea.....	30
3.3.2 Samples in the Black Sea.....	30
3.3.2.1 Sample collection.....	30
3.3.2.2 Determination of leachable and total trace metals in suspended particulate material (SPM).....	31
A. The choice of analytical method for the determination of particulate trace metals.....	32
B. Analytical procedure for the determination of leachable trace metals... a) Apparatus.....	33
b) Reagents.....	33
c) Reagents preparation.....	34
d) Procedures.....	34
e) Analysis by atomic absorption spectrophotometry.....	34
C. Analytical procedures for the determination of total metal content of SPM.....	36
a) Apparatus and reagents.....	36
b) Digestion procedure.....	37
c) Assessment of the analytical quality of the total particulate trace metal measurement.....	37
3.4 Manganese and iron in pore water samples.....	38
3.4.1 Sampling.....	38
3.4.2 Analytical procedures for pore waters.....	38
3.4.2.1 Apparatus and reagents.....	39
a) Apparatus	39
b) Reagents.....	39
c) Reagent preparation.....	39
3.4.2.2 Procedures.....	39
3.4.2.3 Measurement by atomic absorption spectrometry.....	40
3.5 Auxiliary data.....	40
3.5.1 Salinity.....	40
3.5.2 Nutrients.....	40
CHAPTER 4: Trace metals in the Adriatic Sea.....	41
4.1 The study area.....	41
4.1.1 Geomorpholgy of the Adriatic Sea.....	41
4.1.2 Hydrography.....	41
4.1.3 River inputs to the Adriatic Sea.....	44
4.2 The database for the study.....	45
4.3 Hydrographic and chemical setting.....	45
4.3.1 Temperature, salinity and density.....	48
4.3.1.1 The Northern Adriatic Sea.....	48
4.3.1.2 The Central Adriatic Sea.....	48
4.3.1.3 The Strait of Otranto.....	51

4.3.2 Oxygen and Chl <i>a</i> in the Northern Adriatic Sea.....	54
4.3.3 Nitrogen and phosphorus in the Northern Adriatic Sea.....	56
4.4 Trace metals in the Po River.....	60
4.5 Trace metal distribution in the Northern Adriatic Sea.....	64
4.5.1 Manganese.....	64
4.5.2 Iron.....	69
4.5.3 Cobalt.....	73
4.5.4 Lead.....	73
4.5.5 Cadmium.....	76
4.5.6 Zinc.....	79
4.5.7 Copper.....	81
4.5.8 Nickel.....	85
4.6 Trace metal distribution in the central Adriatic Sea.....	89
4.6.1 Manganese and iron.....	89
4.6.2 Cobalt.....	94
4.6.3 Lead.....	96
4.6.4 Zinc and cadmium.....	98
4.6.5 Copper and nickel.....	100
4.7 Trace metal distributions in the Strait of Otranto.....	102
4.7.1 Manganese.....	103
4.7.2 Iron.....	106
4.7.3 Cobalt.....	106
4.7.4 Lead.....	106
4.7.5 Cadmium.....	108
4.7.6 Zinc.....	108
4.7.7 Copper and nickel.....	110
CHAPTER 5: Mass Balance of trace metals in the Adriatic Sea.....	112
5.1 Introduction.....	112
5.2 A simple box model for the Adriatic Sea.....	114
5.2.1 Description.....	114
5.2.2 Equations.....	116
5.3 Estimation of annual fluxes.....	118
5.3.1 Rivers inputs.....	118
5.3.1.1 The River Po.....	118
5.3.1.2 Total riverine inputs for the Adriatic	118
5.3.2 Atmospheric inputs.....	119
5.3.3 Internal cycling.....	123
5.3.3.1 Water Fluxes: Upwelling, downwelling, exchanges between compartments 1 and 2 and exchanges between the Adriatic and Ionian Sea.....	123
5.3.3.2 Trace metal fluxes between compartments 1 and 2.....	127
5.3.3.3 Trace metals fluxes through the Strait of Otranto.....	128
5.3.3.4 Trace metals fluxes associated with upwelling and downwelling within the Adriatic Sea.....	130
5.3.3.5 Down column fluxes of particles.....	131
5.3.4 Sedimentation.....	132

5.3.5 Advectional transport of sediments from the shelf.....	134
5.4 Results of the mass balance.....	134
5.4.1 Mass balance in compartment 1.....	135
5.4.2 Mass balance in compartment 2.....	136
5.4.3 Mass balance in compartment 3.....	137
5.5 Time scales.....	138
5.5.1 Turnover time.....	138
5.5.2 Residence time.....	139
5.6 Uncertainties.....	140
CHAPTER 6: Trace metals in the north-western Black Sea.....	141
6.1 The study area.....	141
6.1.1 Geomorphology of the Black Sea.....	141
6.1.2 Anoxia in the Black Sea.....	144
6.1.3 Hydrography.....	146
6.1.4 River inputs to the Black Sea.....	147
6.2 Database for the study.....	149
6.3 Hydrographic and chemical setting.....	151
6.3.1 Temperature, salinity, density and fluorescence.....	151
6.3.2 Dissolved oxygen and chl <i>a</i>	159
6.3.3 Nitrogen, ammonia, phosphorus and silicate.....	162
6.3.4 DOC and POC.....	167
6.4 Trace metals in the Danube River.....	171
6.5 Trace metals in the north western Black Sea shelf.....	172
6.5.1 Manganese.....	172
6.5.2 Iron.....	178
6.5.3 Cobalt.....	182
6.5.4 Lead.....	186
6.5.5 Copper.....	189
6.5.6 Nickel.....	196
6.5.7 Cadmium.....	200
6.5.8 Zinc.....	203
6.6 Trace metals in the slope region of the north western Black Sea.....	205
6.6.1 Manganese.....	205
6.6.2 Iron.....	211
6.6.3 Trace elements: Co, Pb, Cu, Ni, Cd and Zn.....	213
CHAPTER 7: Summary and conclusions.....	219
7.1 Introduction.....	219
7.2 The Adriatic Sea.....	219
7.3 The Black Sea.....	222
7.4 Comparison between the Adriatic Sea and the Black Sea.....	223
7.5 Recommandations for further work.....	228
REFERENCES.....	230
APPENDIX I: EUROMARGE-AS DATA BASE.....	255

LIST OF TABLES

Table 1.1: Concentrations of dissolved and particulate trace metals in some European rivers.....	2
Table 2.1: Equilibrium constants for redox processes in aquatic conditions at 25 °C.....	19
Table 3.1: Standard conditions for GFAAS.....	28
Table 3.2: Typical blank, detection limits and recovery data for Mn, Fe, Co, Pb, Cd, Cu, Ni and Zn.....	29
Table 3.3: Analyses of reference seawater samples (NASS4 and CASS2).....	29
Table 3.4: GFAAS conditions for analyses of AcOH leachate and total digestion trace metals.....	35
Table 3.5: The determination of total trace metals in reference estuarine sediment material (BCSS-1).....	38
Table 4.1: Data collection details.....	45
Table 4.2: Characteristic temperatures and salinities of the different water masses in the Strait of Otranto.....	51
Table 4.3: Average trace metal concentrations in the Po River. Comparison with the averages for the Rhone and Ebro rivers and for “global river” concentrations.....	60
Table 4.4: Correlation coefficients (r^2) between particulate trace metals and particulate Al, Fe, Mn and organic carbon in the River Po.....	64
Table 4.5: Trace metal concentrations of the different water masses in the Strait of Otranto.....	103
Table 5.1: Dissolved and particulate trace metal concentrations in the river Po and estimations of total riverine fluxes for compartments 1 and 2 for the entire Adriatic Sea	120
Table 5.2: Total atmospheric trace metal inputs for the Western Mediterranean Sea (Guieu <i>et al.</i> , 1996).....	121
Table 5.3: Atmospheric inputs for the Adriatic Sea.....	123
Table 5.4: Water fluxes for winter and summer periods (Fluxes are in km^3/y).....	125

Table 5.5: Fluxes of dissolved and particulate trace metals in and out of compartment 1...	128
Table 5.6a: Fluxes of dissolved trace metals entering the Adriatic Sea through the Strait of Otranto.....	129
Table 5.6b: Fluxes of dissolved trace metals leaving the Adriatic Sea through the Strait of Otranto.....	130
Table 5.6c: Trace metal mass balance for the Adriatic across the Strait of Otranto (t/y)....	130
Table 5.7: Vertical exchanges of dissolved trace metals.....	131
Table 5.8: Estimation of particulate trace metal fluxes from compartment 2 to compartment 3 in the southern Adriatic Sea (Flux of particles is $0.012 \text{ g cm}^{-2} \text{ y}^{-1}$, Heussner <i>et al.</i> (1995)).....	132
Table 5.9: Sedimentation rates in different parts of the Adriatic Sea	132
Table 5.10: Trace metal composition of cores (total values for the first cm) in different parts of the Adriatic Sea.....	133
Table 5.11: Fluxes of trace metals into sediments in the Adriatic Sea.....	134
Table 5.12: Mass balance for the Adriatic Sea.....	135
Table 5.13: Turnover time of metals with respect to different processes.....	139
Table 5.14: Residence time (R.T.) of water and metals in the Adriatic Sea.....	140
Table 6.1: Major river inputs to the Black Sea.....	149
Table 6.2: Trace metals concentrations in the Danube river. Comparison with mean values for the Rhône and Ebro rivers and with the world rivers average.....	172
Table 6.3: Concentrations (nM) of dissolved Co, Pb, Cu, Ni, Cd and Zn in Black Sea surface waters (Station 3) and comparison with Mediterranean surface waters and northwestern Black Sea.....	214
Table 6.4: Concentrations ($\mu\text{g/g}$) of leachable particulate Co, Ni, Cu, Zn, Cd and Pb in Black Sea surface waters (Station 3) and comparison with the Mediterranean surface waters and the northwestern Black Sea.....	216
Table 7.1: Comparison of metal loadings in the rivers Po and Danube, in the Adriatic Sea and in the Black Sea	226
Table 7.2: Dissolved and total particulate metal concentrations in the northern Black Sea and the northern Adriatic Sea.....	227

Table AI1a: General sample parameters (Cruise May 1994).....	258
Table AI1b: Dissolved trace metals and other parameters (Cruise May 1994).....	259
Table AI2a: General sample parameters (Cruise June 1994).....	260
Table AI2b: Dissolved trace metals and other parameters (Cruise June 1994).....	262
Table AI3a: General sample parameters (Cruise July 1994).....	264
Table AI3b: Dissolved trace metals and other parameters (Cruise July 1994).....	265
Table AI4a: General sample parameters (Cruise September 1994).....	266
Table AI4b: Dissolved trace metals and other parameters (Cruise September 1994).....	267
Table AI5a: General sample parameters (Cruise November 1994).....	268
Table AI5b: Dissolved trace metals and other parameters (Cruise November 1994).....	271
Table AI6a: General sample parameters (Cruise February 1995).....	274
Table AI6b: Dissolved trace metals and other parameters (Cruise February 1995).....	275
Table AI7a: Sampling parameters and dissolved trace metals (River Po).....	276
Table AI7b: Particulate trace metals and organic carbon (River Po, from Mowbray <i>et al.</i> , 1995).....	277
Table AI8: Mn and Fe in pore waters (Cruise February 1994).....	278
Table AI9: Mn and Fe in pore waters (Cruise June 1994).....	279
Table AI10: Mn and Fe in pore waters (Cruise September 1994).....	280
Table AI11: Mn and Fe in pore waters (Cruise February 1995).....	281
Table AII1: General sample parameters.....	283
Table AII2: Dissolved trace metals and other parameters.....	287
Table AII3: General sampling parameters and particulate Mn and Fe (L=leachable fraction; R=residual fraction).....	291
Table AII4: Leachable particulate trace metals.....	294

LIST OF FIGURES

Figure 4.1: Topography of the Adriatic Sea.....	42
Figure 4.2: Sampling locations in the Adriatic Sea.....	46
Figure 4.3: Sampling locations in the Strait of Otranto.....	47
Figure 4.4: Temperature and salinity distributions in the Northern Adriatic Sea.....	49
Figure 4.5: Sigma theta distribution in the Northern Adriatic Sea.....	50
Figure 4.6: Temperature-Salinity diagrams for Stations 4 and 10.....	52
Figure 4.7: Temperature-Salinity diagrams for stations in the Strait of Otranto; numbers refer to station positions in the Strait of Otranto.....	53
Figure 4.8: Oxygen saturation and Chl. α distributions in the Northern Adriatic Sea.....	55
Figure 4.9: Phosphate and nitrate + nitrite distributions in the Northern Adriatic Sea.....	58
Figure 4.10: Phosphate and nitrate + nitrite plotted against salinity (Northern Adriatic Sea).....	59
Figure 4.11: Dissolved and particulate Mn and Fe in the river Po (at Pontelagoscuro) plotted against sampling dates simultaneously with the flow rate of the Po (day 0 = 1/1/1994)...	62
Figure 4.12: Total particulate Mn and Fe versus particulate Al.....	63
Figure 4.13: Dissolved and particulate Mn in the Northern Adriatic Sea.....	66
Figure 4.14: Mn in pore waters in the Northern Adriatic Sea.....	67
Figure 4.15: Dissolved and particulate Fe in the Northern Adriatic Sea, () indicates suspect data (see text).....	70
Figure 4.16: Fe in pore waters in the Northern Adriatic Sea.....	71
Figure 4.17: Dissolved Co versus salinity in the Northern Adriatic Sea.....	74
Figure 4.18: Dissolved and particulate Pb in the Northern Adriatic Sea, () indicates suspect data.....	75
Figure 4.19: Dissolved Cd in the Northern Adriatic Sea.....	77

Figure 4.20: Dissolved Cd versus salinity in the Northern Adriatic Sea in May 1994, June 1994, September 1994 and February 1995.....	78
Figure 4.21: Dissolved and particulate Zn in the Northern Adriatic Sea.....	80
Figure 4.22: Dissolved and particulate Cu in the Northern Adriatic Sea.....	82
Figure 4.23: Dissolved Cu versus salinity in the Northern Adriatic Sea.....	83
Figure 4.24: Dissolved Cu versus DOC in the Northern Adriatic Sea.....	84
Figure 4.25: Dissolved and particulate Ni in the Northern Adriatic Sea.....	86
Figure 4.26: Dissolved Ni versus salinity in the Northern Adriatic Sea.....	87
Figure 4.27: Dissolved Ni versus DOC in the Northern Adriatic Sea.....	88
Figure 4.28: Manganese in the central Adriatic Sea.....	90
Figure 4.29: Dissolved Mn plotted versus salinity in the central Adriatic Sea.....	90
Figure 4.30: Iron in the central Adriatic Sea.....	92
Figure 4.31: Dissolved Co in the central Adriatic Sea.....	95
Figure 4.32: Dissolved Co-Salinity plot.....	95
Figure 4.33: Lead in the central Adriatic Sea.....	97
Figure 4.34: Zinc in the central Adriatic Sea.....	97
Figure 4.35: Dissolved Cd in the central Adriatic Sea.....	99
Figure 4.36: Copper in the central Adriatic Sea.....	101
Figure 4.37: Dissolved Cu and Ni versus salinity in the central Adriatic Sea.....	101
Figure 4.38: Nickel in the central Adriatic Sea.....	101
Figure 4.39: Dissolved Mn in the Strait of Otranto (stations are arranged in order, from West to East across the Strait.....	104
Figure 4.40: Dissolved metals versus salinity in the Strait of Otranto: a) Mn, b) Fe, c) Co, d) Pb, e) Cd, f) Zn, g) Ni, h) Cu.....	105
Figure 4.41: Dissolved Fe in the Strait of Otranto, () indicates suspect data (see text).....	104
Figure 4.42: Dissolved Co in the Strait of Otranto.....	107

Figure 4.43: Dissolved Pb in the Strait of Otranto.....	107
Figure 4.44: Dissolved Cd in the Strait of Otranto, () indicates suspect data.....	109
Figure 4.45: Dissolved Zn in the Strait of Otranto, () indicates suspect data.....	109
Figure 4.46: Dissolved Cu in the Strait of Otranto.....	111
Figure 4.47: Dissolved Ni in the Strait of Otranto, () indicates suspect data.....	111
Figure 5.1: Processes involved in the biogeochemical cycle of trace metals in the Adriatic Sea. Arrows represents fluxes of metals.....	113
Figure 5.2: Three- compartment box model of the Adriatic Sea.....	116
Figure 5.3: Horizontal and vertical fluxes, salinities and densities in compartments 1, 2 and 3.....	124
Figure 6.1a: Topography of the Black Sea.....	142
Figure 6.1b: Physiographic provinces of the Black Sea.....	143
Figure 6.2: Depths for the 23 μM sulfide isopleth in the Black Sea.....	145
Figure 6.3: General circulation in the surface layer of the Black Sea.....	148
Figure 6.4: Sampling locations in the north western Black Sea.....	150
Figure 6.5: Hydrographic data for Stations 0, 1 and 3.....	152
Figure 6.6: Hydrographic data for Stations 4, 5 and 6.....	153
Figure 6.7: Hydrographic data for Stations 7, 8, 9 and 10.....	155
Figure 6.8: Temperature-salinity plots for Stations 7, 8, 9 and 10.....	156
Figure 6.9: Hydrographic data for Stations 20, 21, 22, 23, 25 and 24.....	157
Figure 6.10: Temperature-salinity plots for Stations 20, 21, 22, 23, 24 and 25.....	158
Figure 6.11a: Distributions of dissolved O_2 and Chlorophyll α at Stations 6, 5, 4, 9, 10, 8, 7, 11, 17.....	160
Figure 6.11b: Distributions of dissolved O_2 and Chlorophyll α at Stations 20, 21, 22, 23, 24, 0, 1 and 3.....	161
Figure 6.12a: Distributions of nutrients at stations influenced by the Danube river.....	163

Figure 6.12b: Distributions of nutrients at stations on the shelf and on the slope.....	164
Figure 6.13: NH_4^+ (a), $\text{NO}_3^- + \text{NO}_2^-$ (b), $\text{Si}(\text{OH})_4$ and PO_4^{3-} (d) plotted versus salinity.....	168
Figure 6.14a: Distributions of DOC and POC at Stations 6, 5, 4, 9, 11, 17, 18 and 19.....	169
Figure 6.14b: Distributions of DOC and POC at Stations 20, 21, 22, 23, 25, 24, 0, 1 and 3	170
Figure 6.15a: Distributions of dissolved Mn (Mn_d), leachable particulate Mn (Mn_{lp}) and total particulate Mn (Mn_p) at Stations 6, 5, 4, 9, 10, 7, 11, 17 and 18.....	173
Figure 6.15b: Distributions of dissolved Mn (Mn_d), leachable particulate Mn (Mn_{lp}) and total particulate Mn (Mn_p) at Stations 19, 20, 21, 22, 23, 25, 0 and 1.....	174
Figure 6.16a: Distributions of dissolved Fe (Fe_d), leachable particulate Fe (Fe_{lp}) and total particulate Fe (Fe_p) at Stations 6, 5, 4, 9, 10, 7, 11, 17 and 18.....	179
Figure 6.16b: Distributions of dissolved Fe (Fe_d), leachable particulate Fe (Fe_{lp}) and total particulate Fe (Fe_p) at Stations 19, 20, 21, 22, 23, 25, 0 and 1	180
Figure 6.17a: Distributions of dissolved Co (Co_d) and leachable particulate Co (Co_{lp}) at Stations 6, 5, 4, 9, 10, 7, 11, 17 and 18.....	183
Figure 6.17b: Distributions of dissolved Co (Co_d) and leachable particulate Co (Co_{lp}) at Stations 19, 20, 21, 22, 23, 25, 0 and 1	184
Figure 6.18: Dissolved Co plotted versus dissolved Fe (a) and dissolved Mn (b).....	185
Figure 6.19a: Distributions of dissolved Pb (Pb_d) and leachable particulate Pb (Pb_{lp}) at Stations 6, 5, 4, 9, 10, 7, 11, 17 and 18.....	187
Figure 6.19b: Distributions of dissolved Pb (Pb_d) and leachable particulate Pb (Pb_{lp}) at Stations 19, 20, 21, 22, 23, 25, 0 and 1	188
Figure 6.20a: Distributions of dissolved Cu (Cu_d) and leachable particulate Cu (Cu_{lp}) at Stations 6, 5, 4, 9, 10, 7, 11, 17 and 18.....	190
Figure 6.20b: Distributions of dissolved Cu (Cu_d) and leachable particulate Cu (Cu_{lp}) at Stations 19, 20, 21, 22, 23, 25, 0 and 1	191
Figure 6.21: Dissolved Cu plotted versus salinity.....	193
Figure 6.22: Dissolved Cu plotted versus DOC.....	195
Figure 6.23a: Distributions of dissolved Ni (Ni_d) and leachable particulate Ni (Ni_{lp}) at Stations 6, 5, 4, 9, 10, 7, 11, 17 and 18.....	197

Figure 6.23b: Distributions of dissolved Ni (Ni_d) and leachable particulate Ni (Ni_{lp}) at Stations 19, 20, 21, 22, 23, 25, 0 and 1.....	198
Figure 6.24: Dissolved Ni plotted versus salinity.....	199
Figure 6.25a: Distributions of dissolved Cd (Cd_d) and leachable particulate Cd (Cd_{lp}) at Stations 6, 5, 4, 9, 10, 7, 11, 17 and 18.....	201
Figure 6.25b: Distributions of dissolved Cd (Cd_d) and leachable particulate Cd (Cd_{lp}) at Stations 19, 20, 21, 22, 23, 25, 0 and 1.....	202
Figure 6.26: Dissolved Cd plotted versus salinity.....	204
Figure 6.27a: Distributions of dissolved Zn (Zn_d) and leachable particulate Zn (Zn_{lp}) at Stations 6, 5, 4, 9, 10, 7, 11, 17 and 18.....	206
Figure 6.27b: Distributions of dissolved Zn (Zn_d) and leachable particulate Zn (Zn_{lp}) at Stations 19, 20, 21, 22, 23, 25, 0 and 1.....	207
Figure 6.28: Dissolved Zn plotted versus silicate.....	208
Figure 6.29: Distributions of dissolved Mn (Mn_d), leachable particulate Mn (Mn_{lp}) and total particulate Mn (Mn_p) at Stations 3 and 24.....	210
Figure 6.30: Distributions of dissolved Fe (Fe_d), leachable particulate Fe (Fe_{lp}) and total particulate Fe (Fe_p) at Stations 3 and 24.....	212
Figure 6.31: Distributions of dissolved and leachable particulate Co, Pb, Cu, Ni, Cd and Zn at Station 3.....	215
Figure 6.32: Distributions of dissolved and leachable particulate Co, Pb, Cu, Ni, Cd and Zn at Station 24.....	218

CHAPTER 1

INTRODUCTION

1.1 Trace metals in rivers and marine environments and major processes at work

One of the major challenges for marine chemistry is to determine the concentrations and distributions of trace metals (including Mn, Fe, Pb, Cd, Cu, Ni, Zn and Co) in waters ranging from rivers to estuaries, through ocean margins, to the open oceanic deep basins, and to understand the biogeochemical cycling processes influencing these elements. Most trace metals (e.g. Pb, Cd, Cu, Ni, Zn) are potentially toxic to marine organisms at high concentrations, but are present in coastal seas at levels only slightly above those found in the open ocean. There remains concern however, over areas very close to discharges contaminated with these metals, where concentrations may be very much higher than in the wider coastal environment.

This chapter reviews aspects of trace metal chemistry in rivers, estuaries, coastal waters, open ocean and anoxic environment. Attention will be paid to interactions between dissolved and particulate trace metals as these can play a major role in the cycling and fate of trace metals in the shelf environment (Sposito, 1985; Balls, 1989; Honeyman and Santschi, 1989; Turner *et al.*, 1992; Sung, 1995). The ocean margin is important in trapping continental particles and reducing their transport to deep waters (Meade, 1992). Recent studies suggest that less than 25-30% of the suspended sediment delivered by rivers escapes the continental shelf and, as a consequence, 75-95% of the trace metals fluxes associated with riverine transport are removed and deposited on the continental shelf (Milliman and Syvitski, 1992). Each of the major stages in the continuum between rivers and open ocean will be considered in turn.

1.1.1 Trace metals in rivers

Rivers drain the continents. They are carriers of water, salts, organic matter and mineral particles from land to sea. Continents influence the flow and composition of river waters in a number of ways:

Table 1.1: Concentrations of dissolved and particulate trace metals in some European rivers

River	Phase	Fe (nM)	Mn (nM)	Co (nM)	Pb (nM)	Cd (nM)	Cu (nM)	Ni (nM)	Zn (nM)	References	Flow (km ³ /y)	Catchment area (10 ³ km ²)	Loading (10 ⁶ t/y)
Rhine	Dissolved	55	330	3.5	1.1	0.63	36	57	170	(1)	69.4	224.4	0.72
	Particulate	2671	269	0.87	2.5	0.30	6.6	1.5	79				
Rhône	Dissolved	200	65	1.1	0.4	0.25	35	65	20	(2)	59.9	99	4.6
	Particulate	50714	1410	21.2	17.3	0.82	59	71	255				
Po	Dissolved	35			1.2	0.71	33	35	70	(3)	46.0	75	13
	Particulate	34988	1329		34.7	1.87	79	307	336	(4)			
Ebro	Dissolved	40	25		0.15	0.4	30	24	6	(2)	18.9	86	0.01
	Particulate	6715	546	2.04	3.26	0.80	14	7.7	40				
Clyde	Dissolved	3700	3180	4.3	5.5	0.81	34	48	190	(5)	1.4	1.9	0.11
	Particulate	7200	330	4.4	25	0.07	17	10	140				
Beaulieu	Dissolved	2235	1495	12.8	0.26	0.16	7	46.9	71.7	(6)	0.023		0.0002
	Particulate	24342	176	4.2	2.9	0.11	2.3	4.8	52				

(1) Althaus; (2) Guieu *et al.* (1997); (3) Pettine (1991); (4) Mowbray *et al.* (1995); (5) Muller *et al.* (1994); (6) Fang (1995)

- the height, shape and direction of mountain ranges in relation to the weather system determine the size and water drainage potential of a catchment area;
- rock type, climate and vegetation give characteristic imprints on the chemistry of the dissolved and particulate load of a river system;
- the impact of humans on the quality and distribution of water is felt in an ever increasing manner.

A compilation of recent data for trace metal concentrations in some European rivers, demonstrating a range of characteristics, is presented in Table 1.1.

Trace metal content in suspended matter differs widely because of changes in rock composition and in catchment morphology of rivers. Higher particulate trace metal concentrations are found in the Rhône and the Po rivers compared to the other rivers presented in Table 1.1. Although catchment areas and water flows are similar in magnitude for these rivers (see Table 1.1), particulate discharges of the Po river are twice those of the Rhône; the particulate loadings for these rivers are also higher than in the other rivers presented in Table 1.1. This may be due to the morphology and the composition of their catchment areas as erosion is more important in the Rhône and the Po than in the other rivers. We may consider that the Po and the Rhône are mildly polluted rivers since concentrations of anthropogenic metals such as Cd, Pb, Cu and Zn are higher than in other rivers presented in Table 1.1. Indeed the Rhône and Po rivers are surrounded by highly industrialised regions. With regard to particulate trace metals no definite relationships with the river discharges were established owing to the limited data set presented in Table 1.1.

For the dissolved discharges the situation is different, as the most particle reactive elements (Fe, Mn and Co) tend to have higher dissolved metal concentrations in small rivers like the Beaulieu (Fang, 1995) and the Clyde (Muller, 1994) than in larger rivers. For these metals, the dissolved concentrations decrease with increasing river discharge. For Cu and Ni which are less particle reactive, dissolved fractions exhibit a certain degree of uniformity and are not significantly related to long-term average water discharge. In the Po, Rhine and Clyde rivers dissolved Cd, Pb and Zn occur at levels exceeding some reported toxicity thresholds (Brand *et al.*, 1983; Bryan, 1984; Brand *et al.*, 1986). Consequently the Po, Rhine and Clyde may be considered as polluted rivers.

1.1.2 Trace metals in estuaries

Estuaries, which are located at the land/sea margin, are regions of rapid change, where river water of low ionic strength mixes with seawater (Cameron and Pritchard, 1963). When river water mixes with seawater various physicochemical processes may occur which can modify particulate and dissolved chemical fluxes to the continental shelf (Morel *et al.*, 1991). Estuaries can be regarded as filters of river-transported chemical signals (Garrels and Mackenzie, 1971; Turekian, 1977; Bewers and Yeats, 1989). This filter acts mainly via dissolved-particulate reactivity. Changes in environmental parameters such as: pH, alkalinity, chlorinity, organic complexing agents, all affect adsorption/desorption processes. The estuarine filter is selective in the manner in which it acts on individual elements. Some dissolved elements are simply diluted upon mixing of river and sea water (conservative behaviour), whereas others undergo dissolved-particulate reactions, which lead to their addition to, or removal from, the dissolved phase (non-conservative behaviour). Both conservative and non-conservative behaviour patterns have been reported for individual dissolved trace metals in different estuarine systems and these patterns are highly dependent on local conditions (Liss, 1976; Duinker and Nolting, 1977, 1978; Moore *et al.*, 1979; Boyle *et al.*, 1982; Danielsson *et al.*, 1983). In particular, complex estuaries with multiple sources of trace metals may produce apparently non-conservative behaviour. Although trace metals exhibit contrasting behaviour in different categories of estuaries, it has been shown that Cu, Ni, and Zn behave conservatively in most major world estuaries so that the net input of these trace metals to the shelf is not significantly different from their dissolved river input (Boyle *et al.*, 1982; Edmond *et al.*, 1985; Shiller and Boyle, 1985; Shiller and Boyle, 1991). The behaviour of Cd is different since it is partly mobilised from river suspended matter owing to the formation of soluble chloro-complexes in the mixing zone (Elbaz-Poulichet, 1987; Klinkhammer and Bender, 1981). Mn, Fe, Co and Pb generally show a non-conservative mixing behaviour in estuaries. These elements have a high affinity for particles and are often removed under estuarine conditions by coprecipitation with humic acids and iron hydroxides. Estuarine input and/or removal of Mn is a widely reported feature of many estuaries (Duinker *et al.*, 1979; Morris *et al.*, 1982; Sunda and Huntsman, 1994) and is probably the result of sediment-water exchanges. Seasonal variations for Mn and Fe have been observed in the Clyde estuary with Mn and Fe tending to show higher concentrations in the summer (Muller *et al.*, 1994).

1.1.3 Trace metals in coastal waters

The surface water concentrations of many trace elements are higher in coastal and shelf waters than they are in surface open-ocean waters (Burton and Statham, 1990; Davies, 1993; Laslett, 1995). This shows that trace metal sources are greater in nearshore receiving areas.

Nevertheless, a number of processes act to trap trace elements in the coastal zone (Burton *et al*, 1993). Chester (1990) gives an excellent summary of the driving forces affecting the distribution and behaviour of trace elements: adsorption/desorption at the suspended particle surfaces, precipitation/dissolution, flocculation/aggregation and destabilisation of colloids, uptake/release via organisms and benthic inputs. The processes that trap dissolved trace elements in the coastal zone include removal from solution to particulate phases (scavenging) followed by deposition of the particles to the sediment, and scavenging by biota. The elements that have been incorporated into reducing shelf sediments can be released by diagenetic processes and so escape into the overlying waters to be available for lateral transport. Martin and Thomas (1994) carried out a mass-balance of some dissolved trace metals (Cd, Cu, Ni and Zn) across the global ocean margin. They calculated that marine inputs exceed land-derived inputs by a factor of 2-3.5 for Cu, 2-7 for Zn, and of about 10 for Cd and Ni. They showed that the contribution of telluric sources (riverine and atmospheric) is small compared to the fluxes across the marine boundary. Nevertheless, trace metals from the coastal zone can be transported to the open ocean across the ocean margin zone. The nature of these transfer processes are currently poorly known or quantified.

1.1.4 Trace metals in open ocean

In open-ocean waters, dissolved trace metal concentrations are very low (down to nM and even lower). Such small concentrations lead to analytical problems which have been solved only in the last 20 years (Boyle *et al*, 1977; Danielsson *et al*, 1978). Bruland (1983) classifies trace metals into three groups:

- (a) Conservative-type vertical trace metal profiles (Rb, Cs)

Elements with conservative profiles have a constant concentration relative to salinity, which results from their generally low reactivity in seawater. Rb and Cs are examples of this group (Chester, 1990).

(b) Nutrient-type vertical trace metal profiles (Cd, Zn, Cu, Ni)

The characteristic features of the vertical concentration profiles of trace metals with nutrient-type profiles are a depletion in surface waters and an enrichment at some depth within the water column. These features arise from the involvement of the elements in the oceanic biogeochemical cycles. Phytoplankton utilise nutrients (phosphate, nitrate, silicate) in the euphotic zone and as they grow they extract trace elements from the water, thus leading to their depletion in these surface waters. As the organisms die and sink down the water column they undergo oxidative decay during which there is a regeneration of the nutrients, and the associated trace elements, back into solution. Cd is a labile nutrient-type element as it is associated with the soft tissue phases of organisms and undergo rapid regeneration in the upper water column. Some Cd values have been reported by Morley *et al.* (1993) for the Indian Ocean in the surface layer from 0.010 to 0.101 nM and in deeper water from 0.510 to 0.670 nM. Some values have also been reported for the North Atlantic Ocean by Saager (1994): 0.100-0.125 nM for the surface layer and 0.200-0.350 nM for the deep water. Zn is considered as a refractory nutrient-type element as it is associated more with hard skeletal parts of organisms and has a deeper water regeneration than N+P, which is similar to that of Si. Zn concentrations have been reported for the Indian and North Pacific Oceans to be respectively 0.8 nM and 0.08-1.89 nM for the upper water column and 2.7-7.3 nM and 4.97-9.07 nM for the deep water (Morley *et al.*, 1993; Bruland, 1980). Cu and Ni are combined labile-refractory type elements as they have both a shallow water and a deep water regeneration cycle. Morley *et al.* (1993) reported some data for the Indian Ocean which present maxima for Cu and Ni in the intermediate layer (210-1500 m) respectively 2.8 nM and 7.2 nM, the surface layer concentrations being respectively 0.8 nM and 2.6 nM and the deep water concentrations being respectively 1.3 nM and 5.6 nM. The Mediterranean Sea represents a special case which is relevant to the Adriatic Sea. The trace metal distribution and content of oceanic waters where the metal has a long oceanic residence time (typically $> 10^3$ years (Martin and Whitfield, 1983)) is largely controlled by processes which operate over long time scales. In the Mediterranean Sea where the water residence time is of the order of 100

years, there is insufficient time for very significant vertical or horizontal concentration patterns to develop. Thus although the same processes operate in the Mediterranean Sea as in the open ocean, it is largely the composition of incoming surface Atlantic Water (depleted in nutrient and therefore in Cd, Zn, Cu and Ni (Copin-Montegut *et al.* (1986))), that provides the background metal signature of Mediterranean waters. In the western Mediterranean Sea Cd levels are 0.040 nM in surface water (0-100 m), 0.090 nM in intermediate water (100-300 m) and 0.060 nM in deep water (300-2600 m); Zn is reported to have 1.5 nM in surface water and 5-6 nM in deep water column; Cu and Ni concentrations are respectively 1.4 and 2 nM in surface water, 1.7 and 4 nM at 100m, 1.5 and 4 in deeper water column with a slight increase near the bottom (Tankéré *et al.*, 1995).

(c) Surface enrichment and depth depletion type of vertical trace metal profiles (Pb, Mn, Co, Fe)

For elements which are more reactive and have a much shorter oceanic residence time (Mn, Fe, Co, and Pb) then boundary inputs and scavenging can have a more significant impact on their concentrations and distributions. This group of metals are introduced into surface waters mainly by atmospheric inputs and horizontal surface water transport following delivery from rivers or release from shelf sediments. They are removed rapidly from solution by particles. In the central part of the Western Mediterranean Sea, concentrations of Mn and Pb in surface water are reported to be 4 nM and 0.100 nM respectively. In deeper water column concentrations decrease down to 0.2 nM for Mn and 0.040 nM for Pb (Tankéré *et al.*, 1995). In the Gulf of Lion surface concentrations of Mn and Pb are higher. They have been reported to be 10 nM and 0.3 nM respectively by Morley *et al.* (1990). This may be due to the influence of the Rhone river. These elements have short residence times compared to the mixing time of the ocean (Brewer, 1975). This results from the combination of 2 factors: these elements are transported to the oceans mainly in particulate material and they undergo generally rapid hydrolysis in solution, which leads to their uptake by particle scavenging. Deep water maxima may be observed for Mn and Fe. Those maxima may result from in situ redox processes which convert the insoluble, oxidised forms of Mn and Fe into relatively soluble reduced species. Klinkhammer and Bender (1980) and Murray *et al* (1983) have reported sub-oxic Mn concentration maxima associated with an oxygen minimum zone in the Pacific Ocean. Major perturbations to the typical down-column Mn profile can also be found in the regions of

hydrothermal activity in the Atlantic and the Pacific Oceans (Edmond *et al.*, 1982; Klinkhammer *et al.*, 1986). The high Mn concentrations depend on the dispersal of the anoxic hydrothermal plume (Edmond *et al.*, 1982).

1.1.5 Trace metals in anoxic environments

In oxygenated ocean, molecular oxygen is recharged much faster than it is consumed by the oxidation of organic matter in deep water, whereas upon stratification of the water, O₂ is not transported below the interface and anoxic conditions develop. These two contrasting environments differ not only in oxygen and hydrogen sulphide content, but in a number of chemical such as mineral nutrients (nitrate, phosphate, ammonia and silica), trace metals and dissolved gases.

Anoxic waters will be formed in basins where the input of organic matter is high compared to the oxygen input. This will occur, for example, in landlocked bays, gulfs, fjords and basins like the Baltic Sea (Dyrssen and Kremling, 1990), the Black Sea (Deuser, 1974), Framvaren fjord (Jacobs *et al.*, 1985; Haraldsson and Westerlund, 1988). Intermittently anoxic conditions have also been described in different areas: the Northern Adriatic Sea (Justic, 1991), the Gulf of Elefsis (Scoullos, 1983) and the Northern Western Black Sea. These anoxia are characterised by an average annual increase in the O₂ content in the surface layers with a dramatic decrease at the bottom, the hypoxia becoming a recurrent phenomenon during summer months.

Trace metal distributions in permanent anoxic environment has some particularities. In the oxic layer of the Black Sea, the concentrations of Zn, Cd and Pb show features characteristic generally of open sea profiles elsewhere but the increases in concentration of Zn and Cd with depths are sharply reversed around the top of the redoxcline through the existence of the sink in the anoxic layers. Concentrations for Zn, Cd and Pb vary respectively between 1.5 and 10 nM, 0.010 and 0.130 nM, 0.010 and 0.600 nM (Lewis and Landing, 1992). In the oxic layer of the Framvaren Fjord, concentrations of Zn, Cd and Pb are higher in the surface layer and decrease with depth with the apparition of the sulphides. Concentrations of Zn, Cd and Pb vary respectively between 10 and 1 nM, 100 and 10 pM, 100 and 25 pM (Haraldsson and Westerlund, 1988). For Cu, the upper water column distribution appears to be affected by

scavenging processes. Concentrations decrease from 6 to 0.5 nM in the Baltic Sea (Dyrssen and Kremling, 1990), from 7 to 0.5 nM in the Black Sea (Lewis and Landing, 1992), and from 5 to 0.5 nM in the Framvaren Fjord (Haraldsson and Westerlund, 1988). For Cu, Cd, Pb and Zn, dissolved concentrations are very low in the anoxic layers. Those metals have strong sulphide complexes and consequently the transport of particulate matter through the water column is the controlling process below the transition zone for these elements (Dyrssen, 1985). In Framvaren fjord, the Black Sea and the Baltic Sea, average Ni concentrations are respectively 5.2-7.5 nM, 9-10 nM and 10-15 nM. In all cases Ni appears to be unaffected by the effects of sulphidic waters and no seasonal variation has been observed for this element. It is possible that nickel forms some inert unknown chelate or macrocyclic complexes that react slowly against scavenging in both oxic and anoxic seawaters (Dyrssen and Kremling, 1990). The metals that are capable of changing redox state (Mn, Fe, Co) show profiles with marked maxima in the redoxcline. For Mn, concentrations are low in the upper water column oxic waters and increase markedly to a maximum in the redoxcline. The Mn maxima are respectively 8 μ M, 15 μ M and 12 μ M for the Black Sea, Framvaren fjord and the Baltic Sea (Haraldsson and Westerlund, 1988; Dyrssen and Kremling, 1990). The pattern of subsequent decrease with depth in the anoxic waters indicates a sink due to solid phase formation or scavenging. The shape of the Mn maximum is controlled by diffusion and oxidation of Mn(II) and sinking and dissolution of solid phase MnO_x . The controls on the concentration of Fe are qualitatively similar and result in a similar distribution but with a deeper maximum for dissolved Fe, related to more rapid oxidation in the redoxcline, and a more marked decrease in deep water concentration reflecting the insolubility of Fe(II)S. The Fe maxima are respectively 0.3 μ M, 0.4 μ M and 2.0 μ M for the Black Sea, Framvaren fjord and the Baltic Sea (Haraldsson and Westerlund, 1988; Dyrssen and Kremling, 1990). The distribution of Co closely resembles that of Mn in the upper water column and redoxcline probably reflecting coupling through scavenging although an independent redox behaviour of Co is also possible; the marked decrease in concentration in the anoxic layer reflects efficient removal by scavenging or insoluble sulphide formation. The Co maxima are respectively 4.5 μ M, 1.8 μ M and 2.0 μ M for the Black Sea, Framvaren fjord and the Baltic Sea (Haraldsson and Westerlund, 1988; Dyrssen and Kremling, 1990).

Scoullos (1983) described several particular trace metal features in the Gulf of Elefsis which is an intermittently anoxic basin during the summer because of the strong stratification of the water column:

- a decrease of the concentration of the soluble species of certain trace metals (Cu, Zn, Pb and Cd) in favour of their particulate forms. These metals may be controlled by various reactions with particulate and dissolved organic matter.
- dissolution and reprecipitation of Fe and Mn either in the anoxic zone or at the oxic-anoxic interface due to redox processes. Fe although tends to react with particles.

Trace metal concentrations in this area were found to be several times higher than in the Aegean Sea and similar to those found in known polluted regions elsewhere like the North Sea.

1.1.6 Importance of advective transport processes

The processes that control the motions of the water in the ocean system are complex. In the oceans, water undergoes both horizontal and vertical movements. The principal forces driving these movements are wind and gravity and the resultant circulation patterns are modified by the effects of factors such as the rotation of the earth, the topography of the sea bed and the positions of the land masses that form the ocean boundaries (Knauss, 1978). In the surface ocean the currents are wind-driven and move in mainly horizontal flows at relatively high velocities. In the deep ocean circulation is largely driven by gravity and thermohaline velocity currents; these can have a vertical component (downwelling and upwelling) as well as a horizontal component (Bolin *et al.*, 1983).

Trace element distributions in seawater are controlled by a complex interaction between sources, removal and water circulation patterns. Dissolved trace elements are mainly transported with water mass movements. For example, Martin and Knauer (1985) and Martin *et al.* (1986) show the importance of lateral transport of Mn in the north-east Pacific Gyre oxygen minimum. Dissolved trace elements can also be removed from the water column by particles, via scavenging-type or biological active uptake-type mechanisms. These particles are transported by water mass movements or settle down to the sediment.

1.1.7 Importance of boundary exchange processes

1.1.7.1 Atmosphere

The atmosphere is an important route by which trace metals are transported to marine waters. The particles carried in the marine atmosphere have a different history from those transported to the oceans via the river runoff (Guieu *et al.*, 1997). One of the most important differences is that they do not undergo trapping or modification in the estuarine filter at the land/sea margins. Potentially, therefore, the atmosphere is the most important pathway for the long-range transport of particulate material to remote open-ocean areas from continents (Martin *et al.*, 1989). For the Western Mediterranean Sea the main air flows are as follows: 38 % of the air masses come in from the western sector, which includes the North Atlantic Ocean and the Iberian Peninsula; 28 % are from the North and cross the European land mass; 13 % are from the south and carry Saharan aerosols (Chester *et al.*, 1993b). The metals in aerosols can reach the sea surface following different pathways (Chester *et al.*, 1993a): (1) by the dry deposition mode in which aerosols reach the sea surface directly and where they can dissolve to varying extents depending on the element and the aerosol source; (2) by wet deposition mode in which aerosols (rainwater) contain trace metals in solubilized form or in non-solubilized particulate fraction.

1.1.7.2 Sediment

Trace metals from both natural and anthropogenic sources are transported from land by rivers and the atmosphere and finally buried in the sediment. While sediments provide the ultimate sink, they can also act as an intermediate source for metals as a result of biogeochemical processes.

Of the organic carbon produced in the surface waters of the ocean only a small fraction reaches the sediment surface, but because of rapid vertical transport a close coupling exists between the organic carbon arriving at the seabed and surface water productivity (Deuser and Ross, 1980). The organic carbon rain to the sediment surface is the driving force for a characteristic sequence of diagenetic reactions, in which organic carbon is oxidised first by molecular oxygen and then successively by NO_3^- and MnO_2 , Fe_2O_3 and SO_4^{2-} , deeper in the

sediment (Froelich *et al.*, 1979; Bender and Heggie, 1984). As those reactions proceed, concentrations of Mn²⁺ and Fe²⁺ and other trace metals associated with MnO₂ and Fe₂O₃ increase in pore waters. These dissolved metals migrate towards the surface of the sediment-water interface and may be a source of metals for the water column (see Chapter 4).

1.2 The aims of this work

This work on the sources, sinks and cycling of trace metals in the Adriatic Sea and the Black Sea was carried out within the framework of EU funded projects: the EUROMARGE AS Project, a component of the Mediterranean Targeted Project, and the pilot phase of EROS 21. The Adriatic Sea and the Black Sea are of particular biogeochemical interest because of concerns over inputs of potentially toxic trace metals into the Northern Adriatic Sea from the Po river and into the north-western Black Sea from the Danube river. Moreover, strong periodic eutrophic conditions characterise these regions and the effects of the associated biological processes on the cycling and fate of introduced trace metals are a major concern. The main objectives of this thesis are:

- (1) to investigate the distributions and concentrations of some trace metals representing a range of geochemical behaviour (Mn, Fe, Co, Pb, Cd, Zn, Ni and Cu) in the Adriatic Sea and the Black Sea.
- (2) to evaluate the factors and biogeochemical processes influencing the distribution of these trace metals under eutrophic and non-eutrophic conditions.

This thesis is organised into 7 Chapters and 2 Appendices. The first appendix contains the EUROMARGE AS data base and the second contains the EROS 2000 data base. Chapter 2 discusses the problem of eutrophication with the environmental consequences of this phenomenon. Chapter 3 gives details on the sampling and analytical procedures used to measure dissolved trace metals, particulate trace metals, salinity and nutrients in the water column, and Mn and Fe in pore water samples. The results obtained for the Adriatic Sea and the Black Sea are reported and discussed in Chapters 4 and 6 respectively. In Chapter 5, a mass balance for trace metals is presented for the Adriatic Sea. This mass balance enables the evaluation of the relative importance of the processes involving trace metals occurring in the water column. A summary and conclusions are presented in Chapter 7.

CHAPTER 2

EUTROPHICATION

2.1 Manifestation of the problem in two semi-enclosed marginal seas: consequences for benthic–pelagic coupling

The term “marine eutrophication” refers to a variety of complex and interconnected processes resulting from the over-fertilization of coastal surface waters. In both the northern Adriatic and the northwestern Black Sea, the eutrophication phenomenon has important consequences for several trace metals due to the redox changes associated with the decomposition of the large quantities of algal biomass produced as a result of increased nutrient inputs. This chapter considers the phenomenon of eutrophication, and then considers its impact on trace metals in marine systems.

Over the last 20 years, the urban and industrial development of the Po and Danube catchment areas—together with the attendant intensification of agriculture—has raised the level of inorganic nutrient inputs to the adjoining coastal areas so much as to upset the previous dynamics of nutrient, oxygen, pH and organic carbon regulation in these waters. Increasing loads of dissolved and particulate organic contaminants have also contributed to the problem. However, the main cause of eutrophication is undoubtedly linked to the development of intensive agriculture and its contribution to the increased nutrient inputs from decomposing livestock wastes, fertilizer applications and fertilizer factories. In the last two decades N and P inputs to the northwestern Black Sea increased respectively by a factor of 3 and 10, reaching 3.4×10^5 and 6.0×10^4 t/y for N and P respectively (Sur *et al.*, 1996; Cociasu *et al.*, 1996). In the northern Adriatic Sea the load of phosphorus increased from 2×10^3 t/y in the years 1968–1970 to 5×10^3 t/y in 1980 and the load of nitrogen increased from 5×10^4 t/y to 10^5 t/y in the same period (Marchetti *et al.*, 1989; Justic *et al.*, 1993; Degobbis and Gilmartin, 1990). Long-term nutrient records that are available for some rivers indicate that major changes in riverine dissolved nitrogen and

phosphorus coincided with the increased use of synthetic fertilizers and detergents that occurred after World War II.

While nutrient inputs have increased, nutrient ratios have also changed substantially, although the exact values differ in the Adriatic and in the Black Sea. However, the trends in changes of nutrient input ratios are similar in both systems, namely a recent decrease in silicon relative to nitrogen and phosphorus. Justic *et al.* (1994) noted this trend in the nutrient loads to the northern Adriatic Sea but concluded that silicon limitation to phytoplankton growth was unlikely on account of the abundance of this element in seawater. A similar scenario has been taking place in the northwestern Black Sea from the 1970s onwards. It was explained by Cociasu *et al.* (1996) who noted that the sharp, two-fold decrease in silicon concentrations measured at the mouth of the Danube around 1974 coincided with the construction of dams along the Danube and its tributaries. Intense algal blooms in the reservoir lakes have had the effect of stripping Si, N and P from the water. While the removal of N and P is more than compensated by the multitude of sources throughout the drainage basin, there is no such downstream sources for Si which thus remained relatively impoverished. A slower—but still downward—trend in Si inputs from the Danube has been recorded by Cociasu *et al.* (1996) to the present day. As noted for the Adriatic, this is not likely to limit plankton production in any way. Neither have N or P ever been observed to fall to growth-limiting levels in the inshore waters of the northwestern Black Sea (Gomoiu, 1985).

The increase in nutrient levels causes many other chemical and ecological changes which could collectively be labeled as ‘eutrophication’. Because of the peculiarities of each marine system, however, it is not possible to define a single quantitative measure of eutrophication which could be used to compare the ‘degree of eutrophication’ of different systems. Parameters which are commonly measured in the context of eutrophication include: T, S, pH, dissolved O₂, dissolved and particulate organic carbon, Si, N, P, SPM, water transparency, abundance (diversity, biomass) of microorganisms, zooplankton, benthos, etc. When used collectively, these parameters can be interpreted in terms of a limited number of processes, all of which have been observed to varying degrees in the

Adriatic and the Black Sea over the last 30 years. Their relation to the overall picture of eutrophication can be described as follows:

In a first step, large increases in the discharges of N and P from rivers and coastal run-off cause excessive growth of phytoplankton, which decreases the depth to which light can penetrate. Red and brown algae give way to opportunistic green algae with short biological cycles (Vasiliu, 1980). Such large quantities of phytoplankton also exude considerable amounts of dissolved organic compounds, among which carbohydrates account for a large fraction (Moller-Jensen, 1983; Myklestad *et al.*, 1989). The amount and molecular weight of these polymers is higher under conditions of unfavourable nutrient ratios (Lancelot, 1984). In the stratified, low fluid shear conditions of the summer months polymeric exudates and dead phytoplankton cells aggregate into either loose masses of mucus (mucilage) or large flakes (marine snow). These are rapidly colonized by bacteria and, over time, scavenge large quantities of small organisms as well as inorganic and organic debris. However, common plankton grazers are unable to utilize the organic carbon locked up in these large flocs and are thereby denied access to 25–60% of the total primary production (Ott and Herndl, 1995), perhaps up to 80% in the northern Adriatic Sea under conditions (e.g. N:P ratio ≈ 70) leading to stress responses by phytoplankton (Kaltenböck and Herndl, 1996). Marine eutrophication thus manifests itself in an increase in the global quantities of phytoplankton, changes in the trophic structure such as reflected in the chronic appearance of red tides more intense every year (Gomoiu, 1985; Jenkinson, 1989), and a reduction in the number of zooplankton species in parallel with an increase in the biomass of the dominant forms (Gomoiu, 1985; Bochdansky and Herndl, 1996). For example, the diatoms:dinoflagellates ratio in several areas of the northwestern Black Sea has changed dramatically over the last three decades. Diatom cell densities decreased from 92.3% of the total in 1960–1970 to 62.2% in 1983–1988 in the inshore waters of Romania, while the proportion of dinoflagellates increased from 7.6% to 30.9% in the same period (Bodeanu, 1989). As the aggregates accumulate at or around the pycnocline, bacteria feeding on it gradually use up oxygen in the water. This explains why O_2 supersaturation of up to 200% prevails at the surface due to primary production (Justic *et al.*, 1987; Stoyanov, 1991; Cociasu *et al.*, 1996) whereas suboxic conditions brought about by metabolic processes are found below the pycnocline (Zaitsev, 1979; Cociasu *et al.*, 1996). With the breakdown of water column stability occurring in the autumn, the organic-rich

aggregates sink down the water column, carrying with them high concentrations of microorganisms embedded in their anoxic matrix. This leads to a further rapid drop in the O_2 concentrations of the bottom waters, and on to anoxia. After prolonged anoxic conditions, nearly all the bottom-dwelling macrofauna dies (Stachowitsch, 1984). The benthos is all the more sensitive to these external perturbations as the organic aggregates generally also cause physical damage by clogging feeding structures or by smothering. Mass mortality of clams and mud-dwelling mussels on the Romanian shelf has been occurring every year since 1972 (Gomoiu, 1985; Gomoiu and Tiganus, 1990), thus severely reducing the filtration capacity of the ecosystem, encouraging the persistence of anoxia and the replacement of complex macrofauna communities by an increasingly active microbial community.

It is clear that some very tight biogeochemical interdependencies exist between all of the processes discussed in the above paragraph. Demonstration of some possible linkages between them have been proposed by different authors. Justic *et al.* (1993) demonstrated that the main factor determining hypoxia in surface water and anoxia in the bottom water in the Northern Adriatic Sea is the riverine influence (nutrient loads combined with flowrate). Justic *et al.* (1993) carried out a cross correlation analysis (CCA) to determine time-lags between river flow data and surface and bottom oxygen anomaly data. CCA shows that correlation between the Po river flow and the surface O_2 surplus in the northern Adriatic Sea is the highest for time-lag 0 month. In contrast, CCA indicates a time-lag of 4 months between the maximum in Po river flow and the maximum in bottom O_2 deficit. This suggests that O_2 surplus in the surface layer is associated with the increasing primary productivity due to the river inputs of nutrient. The O_2 surplus indicates net primary productivity and consequently the presence of excess of organic matter derived from primary production, which may be redistributed within the system and eventually reach the sediments. It appears therefore, that periods of high river flow are major events leading to the development of phytoplankton blooms and subsequent oxidation of this pelagic production by the benthic community. This supports the hypothesis that the development of summertime suboxic conditions is associated with the decay of organic matter accumulated during the spring months in the form of phytoplankton blooms. Other workers have sought to link the extent of O_2 depletion below the pycnocline to the earlier production of organic carbon in the surface layer. In the Northern Adriatic Sea, for example, the annual rates of primary production range from 55 g C m^{-2} in the eastern region to

about 120 g C m⁻² in the region adjacent to the Po delta (Kevder *et al.*, 1971; Gilmartin and Revelante, 1983; Revelante and Gilmartin, 1991). The average sedimentation rate, as measured in the middle of the Adriatic Sea at a depth of 50 m, accounted for 28% of the primary production (Staresinic *et al.*, 1983). Assuming that the sediment coefficient is 0.3 and the respiration coefficient is 1, Justic *et al.* (1993) calculated an oxygen consumption rate of 64 g O₂ m⁻² yr⁻¹ (corresponding to 24 g C m⁻² yr⁻¹) for benthic and epibenthic respiration of the sedimented organic matter, which then induces an oxygen depletion rate of 0.50 ml O₂ l⁻¹ month⁻¹. This value supports his conclusion that the vertical flux of organic matter is sufficient to induce suboxia in the bottom layer of a highly stratified water column.

Behind the multiple symptoms of eutrophication lies one fundamental concept: the benthic–pelagic coupling in a shallow and stratified marine environment. Most benthic species in the Adriatic and the Black Sea are somewhat resilient to external perturbations provided these occur at long intervals. However—in the Black Sea in particular—the recent dramatic changes in the whole ecosystem (Kideys, 1994) suggest that the resilience of the benthos has been overstretched to the point where it can no longer exert a regulating influence on water column particulate production through suspension feeding (Ott and Herndl, 1995). The former seasonal cycle of organic matter production and decomposition has thus been replaced, at best by a one-way forcing of the benthos by escalating pelagic processes (algal blooms), at worst by a positive feedback loop leading to more frequent blooms fueled in part by the release of P when Fe-rich carrier particles dissolve under reducing conditions. This in turn leads to further organic floc production—hindering zooplankton in their regulatory role—and to more persistent bottom anoxia from one year to the next. Under these conditions, there is every justification for considering (see below) that the dominant processes influencing trace metal behaviour are associated to plankton growth and decay in the surface layer (biological factors) and to the redox cycling of Fe and Mn (chemical factors) near the sediment/water interface.

2.2 Consequences of eutrophication on trace metal behaviour

2.2.1 Cycling of iron and manganese

Iron and manganese are redox sensitive elements and consequently their speciation is determined by the pE of the environment (Stumm and Morgan, 1996). Fluctuations of the reduction-oxidation potential in the water column are related to the biodegradation of the organic matter produced during bloom periods. The degradation of organic matter is mainly used as a source of energy for bacteria which successively select the most efficient oxidant available as a terminal electron acceptor during the oxidation of organic matter. Oxygen is used up first, followed by the reduction of nitrate to nitrogen, the reduction of particulate manganese and iron species, of sulphate and finally of carbon dioxide (Wollast, 1981). Table 2.1 presents the equations for the different reactions associated with their redox potential. Myers and Nealson (1988a and b) managed to identify a bacterium which couples its growth to the reduction of manganese. The characteristics of this reduction are consistent with biological, and not an indirect chemical, reduction of manganese. This bacterium could also utilise a number of other compounds as terminal electron-acceptors; this versatility could provide a distinct advantage in environments where electron-acceptor concentrations may vary.

Scoullos (1983) detected dissolved manganese and iron maxima in the Gulf of Elefsis (Greece) when NH_3 was more than $10 \mu\text{M}$. This was possibly due to dissolution of Mn and Fe oxides from the bottom deposits. This hypothesis was strongly supported by the vertical distribution of Fe in the sediment cores which had distinctly lower iron concentrations on the surface than at 20 cm deep. The reduction of MnO_2 and FeO_3 in the sediment may result in a flux of dissolved Mn and Fe to seawater that is mixed and advected horizontally and vertically.

Table 2.1: Equilibrium constants for redox processes in aquatic conditions at 25 °C

Half reactions	Eh° (volts)
$\frac{1}{4}O_2 + H^+ + e^- \rightarrow \frac{1}{2}H_2O$	+0.811
$\frac{1}{5}NO_3^- + \frac{6}{5}H^+ + e^- \rightarrow \frac{1}{10}N_2 + \frac{3}{5}H_2O$	+0.746
$\frac{1}{2}MnO_2(s) + \frac{1}{2}HCO_3^- + \frac{3}{2}H^+ + e^- \rightarrow \frac{1}{2}MnCO_3 + \frac{3}{8}H_2O$	+0.502
$\frac{1}{8}NO_3^- + \frac{5}{4}H^+ + e^- \rightarrow \frac{1}{8}NH_4^+ + \frac{3}{8}H_2O$	+0.384
$FeOOH(s) + HCO_3^- + 2H^+ + e^- \rightarrow FeCO_3(s) + 2H_2O$	-0.099
$\frac{1}{8}SO_4^{2-} + \frac{5}{4}H^+ + e^- \rightarrow \frac{1}{8}H_2S + \frac{1}{2}H_2O$	-0.207
$\frac{1}{8}CO_2 + H^+ + e^- \rightarrow \frac{1}{8}CH_4 + \frac{1}{4}H_2O$	-0.244

Scoullos (1983) gave also an example in which the particulate forms of Mn and Fe occur at higher concentrations in deeper water, and their dissolved forms either do not vary with depth or are present at slightly lower concentrations. This example is typical of an area which has an anoxic layer only at the very bottom of the water column and/or in the sediment-water interface. In this case MnO_2 and FeO_3 in the sediment are reduced to Mn(II) and Fe(II) which diffuse from the sediment and mixes vertically. However because of the presence of oxygen, the dissolved Mn and Fe originating from the sediment quickly re-oxydise and precipitate at the interface of the oxic and anoxic layers which is very close to the bottom. The chemical oxidation of Mn(II) in seawater should be a slow process due to unfavorable oxidation kinetics at pH 8. For example, based on the kinetics of manganese oxidation by molecular oxygen, Morgan (1967) calculated a half-life for Mn(II) in seawater of 500 years. By contrast in oxygenated seawater above an anoxic basin, Emerson *et al.* (1982) found reaction times for Mn oxidation of only a few days. They demonstrated that the formation of particulate Mn was inhibited by biological poisons, suggesting that the enhanced particulate formation rates were biologically mediated presumably by bacteria.

This idea has been developed by several authors: Tebo and Emerson (1986) and Sunda and Huntsman (1987).

2.2.2 The role of phytoplankton in the uptake of trace metals

In eutrophic areas, fluorescence is generally higher than in other surrounding areas, indicating that organic particles and phytoplankton are at greater concentrations (Coble *et al.*, 1990; Coble *et al.*, 1991). A study of colloid composition by Sigleo *et al.* (1982) demonstrated that plankton can be a major source for colloidal material. Isotopic measurements (Sigleo, 1985) further indicated that colloids from surface waters were of planktonic origin whereas those in deeper waters corresponded to the less labile components of the organic matter. Organic matter (both dissolved and colloidal fractions) appears to originate from *in situ* biological activity produced either by the decay of dead organisms or by excretion from plankton. As mentioned by Søndergaard and Jensen (1986), dissolved organic matter (DOM) in the colloidal range can contribute about a quarter of the DOC excreted by phytoplankton. Colloidal material can play an important role in the removal of dissolved trace metals from the marine environment (Honeyman and Santschi, 1989; Stumm, 1993). Colloids in the submicron range are of particular interest because they may sorb significant quantities of contaminants due to their large specific area. The transfer of truly dissolved metal species to larger, filterable particles through a colloidal intermediate has been described by Honeyman and Santschi (1989) with the Brownian-pumping model. In this model, the transfer consists of two rate steps: (1) rapid formation of metal/colloid surface site complexes; (2) slow coagulation of colloids into filterable particles. Martin *et al.* (1995) show evidence in a highly productive coastal environment (the Venice Lagoon, Italy) that biologically produced colloids ultimately control the total dissolved metal concentrations: Fe and Mn were preferentially tied to macroparticulate organic matter, whereas Cu and Cd were preferentially tied to colloidal organic matter in seawater. Ultrafiltrated organic carbon appeared to be important for Ni. Lead was mainly associated with macroparticulate organic matter except in highly productive regions where Pb tends to be associated with colloidal organic carbon. However Martin *et al.* (1995) did not find evidence for any significant flocculation of colloids on the time scale of estuarine mixing, suggesting high stability of colloidal material in the study.

area. They concluded that such stability may come because of organic matter being produced *in situ*. This phenomenon has also been observed by Filella and Buffle (1993). Filella and Buffle (1993) show the existence of 3 well-defined size ranges for particules in aquatic systems with residence times ranging from hours to days: (1) the range 1-100 nm where fast coagulation forms aggregates of 100-700 nm almost immediately, (2) the range 100-700 nm where both coagulation and sedimentation are slow and (3) the range larger than 700 nm where particles are quickly eliminated by sedimentation. They also demonstrated in laboratory that the degree of colloidal destabilisation increases as the ionic strength and the charge of the counter-ions increase but at the same time organic matter adsorption on the surface enhances colloid stability either by steric stabilisation (Tipping and Higgins, 1982) or via electrostatic effects (Tipping and Ohnstad, 1984). Association between small colloids and organic material, which subsequently stabilize in solution the small colloids that otherwise will coagulate very fast, has been modelled by Tiller and O'Melia (1993). Studies of colloidal stability in lakes of differing solution composition have also shown that variations in the stability coefficient can be correlated with dissolved organic carbon (Ali *et al.*, 1985; Weilenmann *et al.*, 1984).

Most dissolved trace elements are ultimately removed from seawater to marine sediments primarily by adsorption onto sinking particles ("scavenging") or by incorporation into biological phases via active uptake by phytoplankton followed by sinking of biological detritus. Some diatom species aggregates to form rapidly sinking flocs (Passow, 1991). Given that newly formed aggregates have sinking rates of approximately 100 m day^{-1} (Alldredge and Gotschalk, 1989), sinking phytodetritus is probably an effective vector for particle reactive metals out of surface water. Marine microorganisms have also transport systems capable of accumulating essential trace metals present at low oceanic concentrations —1 pM to 1 nM. In marine phytoplankton, Fe, Mn, Zn and Ni transport has been shown to involve complexation by membrane carriers (Hudson and Morel, 1993). However, prior to their ultimate removal trace elements may undergo various degrees of recycling which can involve chemical desorption reactions or biodegradation of biogenic material. For example Cu, Zn, Cd, Fe are often depleted in surface waters in areas of high productivity due to uptake by phytoplankton and regenerated at depth (Bruland, 1983; Martin and Gordon, 1988; Fisher and Wente, 1993; Tankéré and Statham, 1996). Fe may

be the most important of all the trace elements essential to phytoplankton and evidence exists that Fe may limit primary production in nutrient-rich oligotrophic open ocean regimes having low atmospheric Fe inputs (Martin and Fitzwater, 1988).

CHAPTER 3

SAMPLING AND ANALYTICAL PROCEDURES

3.1 Procedures used to minimise contamination for trace metal analyses

In this section, procedures used to minimise contamination at all stages of the work are described.

Plastics made of either low density linear polyethylene (LDPE) or polytetrafluoroethylene (PTFE) or perfluoralkoxyl (PFA) were used at all stages of the trace metal analyses (Howard and Statham, 1993). Every piece of equipment was washed before use with detergent (2 % (v/v) Micro), HCl and/or HNO₃ acids (Howard and Statham, 1993). For example, the sampling (LDPE) bottles and/or (LDPE) bottles used for storage of seawater were cleaned prior to use by soaking for 1 week in detergent, 1 week in 8 M HCl and then 1 week in 8 M HNO₃. Between each step bottles were rinsed with Milli-Q water. The bottles were then dried in a class 100 laminar flow bench. Each bottle was retained in a resealable plastic bag after drying. The PTFE filter holders for the filtration of trace metal sample were cleaned by soaking for 4 or 5 day in detergent (2 % (v/v) Micro) for the first time use and then 1 week in 8 M HCl and 1 week in 8 M HNO₃ for subsequent time use. The filter holders were rinsed with Milli-Q water before use. The Nuclepore membrane filters used here were cleaned by soaking for 1 week in 10 % SBD (Sub-Boiling Distilled) HCl and then 1 week in 10 % SBD HNO₃. The filters were rinsed with Milli-Q water and then placed in a class 100 laminar flow bench located in the clean laboratory for three days to dry. Filters were weighed using a Sartorius electronic pan balance (five figures). The membranes were stored in plastic Petri dishes until use.

All reagents used for the analyses were purified prior to use. Sub-boiling distillation is employed to provide high quality water, nitric and hydrochloric acids. Extraction of dissolved trace metals and digestion of particulate material were carried out in the clean laboratory. Non-particle generating clothing were worn at all time by the operator (Howard and Statham, 1993). All manipulations were carried out in Class-100 laminar flow hoods.

3.2 Dissolved trace metals (Cd, Co, Cu, Fe, Mn, Ni, Pb and Zn) in seawater and river water

3.2.1 Sampling

Seawater samples were collected using 10 l Teflon-lined Go-Flo bottles, fitted with Teflon taps and deployed on a rosette or on 6 mm Kevlar line. Additional surface sampling was carried out by hand (see below). Samples from Go-Flo bottles were filtered immediately after collection using nitrogen pressure, directly through cleaned Nuclepore filters (0.4 µm pore diameter) mounted in Teflon filter holders (Morley *et al.*, 1988). River samples and surface seawater samples were collected by hand using 5 l polyethylene bottles attached on a Kevlar line with a 5 kg plastic coated weight. These samples were filtered through Nuclepore filters in a Teflon filter holder, directly into a storage bottle in a chamber which was evacuated by a vacuum pump. Both filtration systems enabled collection of the filtrates into 1 l acid cleaned polyethylene storage bottles. Aliquots of the filtrates were acidified with sub-boiling distilled nitric acid to a pH of about 2 (1 ml of acid per litre of sample).

3.2.2 Analytical procedure for total dissolved trace metals

A chelation-solvent extraction procedure was used to concentrate trace metals and to remove salt matrix interference during determination by Graphite Furnace Atomic Absorption Spectrophotometry (GFAAS). The method is based on Danielsson *et al.* (1978), and modified by Statham (1985). Metal-carbamate complexes formed with two reagents, ammonium pyrrolidine dithiocarbamate (APDC) and diethylammonium diethyldithiocarbamate (DDDC), are extracted into Freon TF, and subsequently back extracted into nitric acid for determination of Mn, Fe, Co, Pb, Cu, Cd, Zn and Ni by GFAAS. These dithiocarbamates derivatives were used, because of their non-selective complexing properties over a relatively broad pH range. Freon TF was chosen as the organic solvent because of its low toxicity and low solubility in water, and in addition it is easy to purify and thus to obtain low metal blanks.

3.2.2.1 Generation of reagents and necessary apparatus

The apparatus and reagents in the procedure described below are sufficient for the extraction of 12 blanks, 50 samples and 2 spiked samples.

a) Apparatus

- 500 ml FEP separatory funnels (3)
- 125 ml FEP separatory funnels (2)
- 125 ml FEP screw capped bottle (4)
- 1000 ml FEP screw capped bottle (1)
- 2000 ml FEP screw capped bottle (1)
- 500 ml polyethylene bottle (1)
- 25 ml polyethylene measuring cylinder (1)
- 250 ml polyethylene measuring cylinder (1)
- 500 ml polyethylene measuring cylinder (1)
- 8 ml screw-capped polyethylene vials (1 per sample)
- perpex holder for 8 ml vials
- Gilson variable volume micropipettes, 10-100 µl (2), 100-1000 µl (2), 500-5000 µl (1)
- polyethylene tips for micropipettes
- polypropylene stand to hold a 500 ml FEP separatory funnel
- polypropylene stand to hold two 125 ml FEP separatory funnel
- polypropylene rotating table for extraction

b) Reagents

- NaCl, analytical grade
- APDC (Ammonium pyrrolidine dithiocarbamate), analytical grade
- DDDC (Diethylammonium diethyldithiocarbamate), analytical grade
- Sub-boiling distilled (SBD) concentrated nitric acid
- SBD water
- SBD nitric acid, 4% (v/v) in SBD water

- Isothermally distilled ammonia solution
- Acid-washed Freon (TF)
- 0.1 mg/l mixed metal standards for Mn, Fe, Co, Pb, Cu, Cd, Zn and Ni in 4% (v/v) nitric acid, made up from 1000 ppm standards for atomic spectrometry

c) Reagent preparation

- Complexant

A mass of 9.14 g of NaCl is dissolved in 250 ml of SBD water in a 1000 ml beaker. The two complexing agents (10 g of each) are added. After dissolution the complexant is filtered through a Whatman n°1 filter to remove particles. The complexant solution is made up with sodium chloride to avoid any coagulation upon mixing with seawater samples. Aliquots (125 ml) of mixed complexant solution are stripped of trace metals by sequential extractions. Each aliquot is washed with 30 ml of acid stripped freon during a 5 minute extraction on a rotating table. The Freon is drawn off and collected for recycling. This cleaning step is repeated 3 times. When the complexant is not used immediately, it is stored refrigerated in a bagged 1000 ml FEP bottle. The life time of the complexant in solution is about 3 days.

- Freon TF

The Freon is distilled from a glass still outside the clean room. After the pre-cleaning distillation, Freon is acid washed in the clean room. A volume of 300 ml of distilled freon and 1 ml of SBD HNO₃ are added in a 500 ml FEP separatory funnel and rotated for 5 minutes. Then 120 ml of SBD H₂O are added and rotated for 5 minutes. The aqueous phase is discarded. The acid-washing is repeated 3 times. At the end of the operation, an additional 120 ml of SBD H₂O are added and rotated for 5 minutes and the aqueous phase is discarded. The wash with water is to ensure that there is no trace of acid left with the Freon. The operation is repeated once. Acid-washed freon is stored in a 2000 ml FEP bottle.

- SBD water

Highest purity water is prepared from Milli-Q water using a sub-boiling still.

- SBD concentrated nitric acid is generated by sub-boiling distillation of 16N AR nitric acid.
- SBD nitric acid (4% v/v) is prepared with sub-boiling concentrated nitric acid and sub-boiling distilled water.

3.2.2.2 Procedure

To a 500 ml FEP separatory on a balance, approximately 250 ml of seawater sample are added and accurately weighed. A predetermined volume of isothermally distilled ammonia solution is added to the sample with a 1000 μ l pipette to adjust the pH to between 7 and 9. Then 4 ml of complexant (using a 5 ml autopipette) and 25 ml of Freon taken into a 25 ml polyethylene measuring cylinder (from a 500 ml FEP separatory funnel on a stand used to store clean Freon) are added. For the blank, only 100 ml of SBD water, 250 μ l of SBD nitric acid, the predetermined volume of isothermally distilled ammonia solution, complexant and Freon are added together in the 500 ml funnel. In order to calibrate the method, standard additions are made to some samples. Two calibrations are made by adding 42 μ l of 0.1 mg/l mixed metal standard to 250 ml of sample.

Then the separatory funnel is rotated for 5 minutes. The Freon is drawn off into a 125 ml separatory funnel, taking care not to transfer any of the aqueous phase. 20 ml of Freon is then added to the 500 ml funnel. The separatory funnel is rotated for 5 minutes, then the second aliquot is drawn off and combined with the first.

For the back extraction, 50 μ l of sub-boiling distilled concentrated nitric acid (using a 100 μ l autopipette) are added to the organic phase. The 125 ml separatory funnel is shaken for 30 seconds by hand. 1000 μ l of SBD water are added (using the 1000 μ l pipette) and the funnel is shaken for 30 seconds again. The aqueous phase is drawn off into the 8 ml vial with the 1000 μ l pipette. The acid back extraction is repeated and the second aliquot is combined with the first one. The overall concentration factor is 119 times that in the original seawater.

3.2.2.3 Measurement by atomic absorption spectrometry

A Perkin-Elmer 1100B Atomic Absorption Spectrometer fitted with a HGA-700 graphite furnace and a AS-70 autosampler is used. The extracts are analysed for Mn, Fe, Co, Pb, Cu, Cd, Zn and Ni. The instrument runs with deuterium background correction and two replicate measurements of the absorption peak area are made for each sample. Other conditions and parameters for the setting up of the instrument are taken from manufacturers recommendations. Table 3.1 shows the AAS parameters. These parameters are stored in the memory of the instrument and recalled during setting up.

Table 3.1: Standard conditions for GFAAS

Element	Mn	Fe	Co	Pb	Cu	Ni	Cd	Zn
Wavelength (nm)	279.5	248.5	241.2	216.9	324.7	232.0	229.0	213.8
Slit (nm)	0.2	0.2	0.7	0.7	0.7	0.7	0.7	0.7
Lamp current (mA)	7	12	8	7	5	10	5	5
Injection temperature (T °C)	100	60	100	80	100	80	100	100
Injection vol. (µl)	10	10	30	20	10	10	10	10
Dry 1 (T °C)	150	150	180	150	150	130	150	120
Ramp (s)	5	5	10	12	5	5	5	5
Hold (s)	10	10	25	20	10	1	10	10
Dry 2 (T °C)	250	250	300		250	600		
Ramp (s)	5	5	15		5	15		
Hold (s)	10	10	20		10	5		
Dry 3 (T °C)			400					
Ramp (s)			15					
Hold (s)			5					
Ash (T °C)	1100	1500	1200	800	1250	1000	600	700
Ramp (s)	5	5	5	15	5	10	10	10
Hold (s)	10	10	10	10	10	10	10	10
Atomisation (T °C)	2200	2500	2550	1800	2300	2300	1600	1800
Ramp (s)	0	0	0	0	0	0	0	03
Hold (s)	3	3	5	2	5	3	4	3
Burn (T °C)	2800	2800	2800	2400	2800	2550	2300	2000
Ramp (s)	1	1	1	1	1	1	1	3
Hold (s)	3	5	4	3	3	3	2	3
Standard 1	20	20	2	2	20	20	2	20
Standard 2	40	40	4	5	40	40	4	40
Standard 3	60	60	6	10	60	60	6	60
Standard 4 (µg/l)	80	80			100	100		80

3.2.2.4 Calculation of sample concentration, and method performance

The final results in nM for the samples are obtained by subtracting the average analytical blank from the sample concentration ($\mu\text{g/l}$) and then dividing by the concentration factor (250/2.1).

$$\text{Metal concentration in sample (nM)} = \frac{\text{reading} - \text{blank}}{F} \times \frac{1000}{M}$$

F: concentration factor

M: atomic weight of the measured element

The limit of detection (Table 3.2) is calculated as three times the standard deviation of the blank given in nM. Corrections for the extraction efficiency have not been done as recoveries were within 15 % of being quantitative (except for Pb, see below).

Table 3.2: Typical blank, detection limits and recovery data for Mn, Fe, Co, Pb, Cd, Cu, Ni and Zn.

Element	Mn	Fe	Co	Pb	Cu	Ni	Cd	Zn
Blank (nM)	0.267	0.180	0.008	0.005	0.155	0.026	0.006	0.030
Detection limit (nM)	0.119	0.181	0.009	0.003	0.052	0.071	0.001	0.135
Recovery (%)	92	115	109	76	100	115	95.2	112

Nearshore (CASS2) and open ocean (NASS4) certified seawater reference material have been analysed regularly. For those samples, 95 % of samples from any bottle would be expected to have concentrations within the specified range 95 % of the time. Table 3.3 compares the certified values for CASS2 and NASS4 with the results of the analyses.

Table 3.3: Analyses of reference seawater samples (NASS4 and CASS2)

Element	Mn	Fe	Co	Pb	Cu	Ni	Cd	Zn
CASS2 certified value	36.22 ± 2.70	21.49 ± 2.15	0.424 ± 0.100	0.092 ± 0.029	10.62 ± 0.61	5.08 ± 0.61	0.169 ± 0.035	30.13 ± 1.83
CASS2 analyses n=8	35.41 ± 3.14	21.70 ± 2.87	0.379 ± 0.053	0.046 ± 0.005	10.33 ± 0.92	5.48 ± 0.66	0.154 ± 0.020	30.74 ± 2.34
NASS4 certified value	6.92 ± 0.42	1.88 ± 0.29	0.153 ± 0.017	0.063 ± 0.024	3.58 ± 0.17	3.88 ± 0.15	0.142 ± 0.027	1.76 ± 0.28
NASS4 analyses n=5	6.25 ± 0.19	1.88 ± 0.31	0.123 ± 0.020	0.026 ± 0.004	3.38 ± 0.22	3.38 ± 0.63	0.106 ± 0.008	1.57 ± 0.20

For Mn, Fe, Co, Cu, Ni, Cd and Zn results are within 10% of the certified values, which is satisfactory. For Pb, results were systematically lower than the reference materials which is consistent with the low recovery found during analyses. As the error is constant, the lead values have been corrected. For each sample, the lead results have been multiplied by 100 and divided by the recovery (%).

3.3 Particulate trace metals (Cd, Co, Cu, Fe, Mn, Ni, Pb and Zn) in seawater and river samples

3.3.1 Samples in the Adriatic Sea

For the study in the Adriatic Sea, samples were collected and analysed by the University of Edinburgh as the work was done in collaboration (EUROMARGE-AS project).

In the river Po and on the shelf, water samples were mainly collected using a pump attached to an oscillatory winch that could be raised and lowered in the water column. In the basins and on the shelf during the June 1994 cruise, samples were collected using 10 l Niskin and Go-Flo bottles at different depths.

Various known aliquots of water (0.1 to 7 l) were filtered through preweighed, 37 mm (0.4 µm pore diameter) polycarbonate Nuclepore membranes, washed with distilled water to remove sea salts in the case of seawater samples, and dried before analysis. Membranes were weighed to measure suspended particulate material (SPM).

Metals (Fe, Mn, Zn, Pb, Cu, Cd and Ni) in the SPM were determined by digestion using ultrapure acids (HF/HNO₃). According to Loring and Rantala (1990), this type of digestion is total.

3.3.2 Samples in the Black Sea

3.3.2.1 Sample collection

Water samples were collected and filtered as described for the dissolved phase. Samples were filtered under nitrogen pressure directly from the bottle to avoid any contamination

with oxygen, through Nuclepore filters (0.4 µm pore diameter) using an in-line Teflon filtration unit. Filters were rinsed with Milli-Q water and stored in acid cleaned containers at about -20°C. The work was undertaken with stringent precautions to avoid contamination.

The gravimetric determination of suspended particulate matter was by reweighing preweighed filters using a Sartorius electronic pan balance (five figures) following drying for 48 hours in a class 100 laminar flow bench in the clean laboratory.

3.3.2.2 Determination of leachable and total trace metals in suspended particulate material (SPM)

Trace metals arrive in the oceanic environment in dissolved or particulate phases. They are transported into the sediment via the suspended particulate material to be “permanently” buried or to be remobilized into the oceanic environment by resuspension or changes in environmental conditions. Therefore, measurement of trace metals in suspended particulate material is an important component in the study of natural geochemical processes.

Only part of the metals associated with SPM may take part in short-term geochemical processes and/or are bioavailable. The mobilisation of trace metals occurs from the non-residual fractions which however will behave according to environmental conditions and to their stabilities. For the differentiation of the relative bonding strength of metals in different phases, sequential extraction procedures have been developed (Tessier *et al.*, 1979; Förstner *et al.*, 1981; Loring and Rantala, 1990):

Step 1: Exchangeable cations [1 M ammonium acetate, solid/solution ratio 1:20, 2 hours shaking time];

Step 2: Carbonate fraction [1 M sodium acetate buffer, pH 5, 1:20, 5 hours shaking at 20 °C]

Step 3: Easily reducible phases (Mn oxide, partly amorphous Fe-oxyhydrates) [0.1 M NH₂OH·HCl + 0.01 M HNO₃, pH 2, dilution 1:100, 12 hours shaking]

Step 4: Moderately reducible phases (e.g., amorphous and poorly crystallized Fe oxyhydroxides) [0.2 M ammonium oxalate + 0.2 M oxalic acid, pH 3, dilution 1:100, 24 hours shaking]

Step 5: Organic fraction, including sulphides [30% H_2O_2 + HNO_3 , pH 2, 85 °C, extracted with 1 M ammonium acetate, dilution 1:100, 24 hours shaking]

Step 6: Residual fraction (e.g. detrital silicates, crystalline Fe-oxides)
[concentrated HNO_3 , 120°C, dilution 1:100]

However, there is no general agreement in the literature on the solutions preferred for the various SPM and sediment components to be extracted, due mostly to the practical impossibility of choosing reagents, which will act selectively to give complete dissolution of particular components in complex mixtures of sedimentary phases, which are often intermixed as with coatings of hydrous oxides on other minerals (Martin *et al.*, 1987)

A. The choice of analytical method for the determination of particulate trace metals

The analytical method adopted in the present work to release trace metals in association with suspended particulate matter (SPM) involves a two step extraction, the first removing the more geochemically available fraction. The filter membranes were first leached using acetic acid (25% v/v) then the residue was digested with concentrated nitric acid using microwave heating.

According to Loring *et al.* (1983), a 25% (v/v) AcOH leach is the weakest chemical treatment that can be effectively used to remove metals held in ion-exchange positions, easily soluble amorphous compounds of iron and manganese, and carbonates, and metals weakly bound to organic matter. The metals in those phases are considered more readily available for mobilization and to living organisms when physical-chemical conditions vary (Malo, 1977). Rantala and Loring (1985) found that the percentage of the total metal content released during a 24 hours leach in 25% (v/v) AcOH for Cd, Cu, Pb and Zn was 88-89%, 79-88%, 64-87% and 90-97% respectively.

The use of microwave energy associated with closed vessels offer several advantages (Neas and Collins, 1988):

- (1) higher pressures and temperatures can be achieved and therefore the digestion time is significantly reduced;

- (2) airborne contamination is eliminated;
- (3) the possibility of losing volatile elements is effectively eliminated;
- (4) no acid is lost during the digestion, allowing a reduction in the amount of acid used and thus reducing the blank;
- (5) potentially hazardous fumes generated during the digestion are contained within the closed vessel.

The use of microwave digestion in closed vessels has been used successfully in this laboratory for the total digestion of SPM by Hall (1993) and Fang (1995).

B. Analytical procedure for the determination of leachable trace metals.

a) Apparatus

- Plastic tweezers (3)
- 1000 ml FEP bottle for reagent storage (2)
- 125 ml FEP bottle for reagent storage (1)
- 15 ml HDPE centrifuge tubes for leaching procedures
- 8 ml HDPE tubes for leachate storage
- Polystyrene Petri dishes
- 5000 μ l micropipette and tips
- centrifuge

b) Reagents

- AnalaR concentrated acetic acid
- SBD water
- Palladium powder, 99.999% (Aldrich)
- Hydroxylammonium chloride, AnalaR
- 0.1 mg/l mixed metal standards for Mn, Fe, Co, Pb, Cu, Cd, Zn and Ni in 25% (v/v) acetic acid

c) Reagents preparation

- AnalaR concentrated acetic acid (AcOH) was sub-boiled in a clean wet bench in the clean laboratory. This distilled acid was stored in a double bagged 1000 ml FEP bottle.
- Distilled concentrated AcOH was diluted with sub-boiled Milli-Q water to 25% (v/v) and stored in a double bagged FEP bottle. The 25% (v/v) AcOH was dispensed from the 125 ml FEP working bottle.

- Matrix modifier:

For the stock solution, 55.1 mg of palladium was dissolved with 1ml of concentrated SBD hydrochloric acid and 1ml of concentrated SBD nitric acid in a 100 ml volumetric flask. The solution was diluted with 50 ml of SBD water and 1g of hydroxylammonium chloride was added and dissolved. Then the volume was brought up to 100 ml with SBD water. This solution was stored in a 125 ml FEP bottle. For the analysis, the matrix modifier was used diluted 10 times with SBD water.

d) Procedures

The 47 mm membranes were folded with the tweezers in half three times in succession, with the SPM held on the inner surface. The folded membranes are then transferred to centrifuge tubes and positioned so that the apex of the membrane is securely held within the bottom of the centrifuge tube. A volume of 5ml of SBD 25% (v/v) AcOH is added to the centrifuge tubes with a 5000 µl micropipette. The filters are leached for 24 hours. The tubes are centrifuged to 3000 rpm for 30 minutes to ensure complete mixing of the leachate and to avoid any carry-over of SPM when the leachate is poured into the storage tube.

e) Analysis by atomic absorption spectrophotometry

Analysis of the leachate for eight elements (Mn, Fe, Co, Pb, Cd, Zn, Cu, Ni) was performed using the Perkin-Elmer 1100B GFAAS. Because of high concentrations of Mn and Fe in the leachate, dilution was required for these elements prior to determination.

Table 3.4: GFAAS conditions for analyses of AcOH leachate and total digestion trace metals

Element	Mn	Fe	Co	Pb	Cu	Ni	Cd	Zn
Wavelength (nm)	279.5	248.5	241.2	216.9	324.7	232.0	229.0	213.8
Slit (nm)	0.2	0.2	0.7	0.7	0.7	0.7	0.7	0.7
Lamp current (mA)	7	12	8	7	5	10	5	5
Injection temperature (T °C)	100	60	100	80	100	80	100	100
Injection vol. (µl)	10	10	30	20	10	20	10	10
Dry 1 (T °C)	150	150	180	150	150	130	150	120
Ramp (s)	5	5	10	12	5	5	5	5
Hold (s)	10	10	25	20	10	15	10	10
Dry 2 (T °C)	250	250	300		250	600		
Ramp (s)	5	5	5		5	15		
Hold (s)	10	10	20		10	5		
Dry 3 (T °C)			400					
Ramp (s)			5					
Hold (s)			5					
Ash (T °C)	1200	1500	1200	700	1250	1250	500	700
Ramp (s)	5	5	5	15	5	10	10	5
Hold (s)	20	20	20	30	20	20	20	30
Atomisation (T °C)	2200	2500	2550	1800	2300	2300	1600	1800
Ramp (s)	0	0	0	0	0	0	0	03
Hold (s)	3	3	5	2	5	4	4	3
Burn (T °C)	2800	2800	2800	2400	2800	2550	2300	2000
Ramp (s)	1	1	1	1	1	1	1	3
Hold (s)	3	5	4	3	3	3	2	3
Standard 1	20	20	2	2	20	20	2	20
Standard 2	40	40	4	4	40	40	4	40
Standard 3	60	60	6	6	60	60	6	60
Standard 4 (µg/l)		80		8				

Samples were co-injected with palladium as modifier and hydroxylammonium chloride as a reductant in the GFAAS. The reductant ensures that the palladium is reduced to the metal in the early stages of the temperature program. The use of palladium solution as a modifier appears to stabilise the analyte (Schlemmer and Welz, 1986). The aim of matrix modification is to permit

high enough pyrolysis temperatures to remove the bulk of concomitants during thermal pre-treatment of the sample without losing any analyte element prior to the atomisation stage. Effective matrix modification greatly reduces a number of spectral interferences due to absorption of source radiation by overlapping molecular or atomic lines of concomitants and scattering of source radiation by non-volatilized particles formed by the concomitants. It also reduces volatilisation and vapour-phase interferences. By using a matrix modifier, no matrix effect (noisy signal and background) was observed for Mn, Fe, Co, Pb, Cd, Cu and Ni. Consequently, measurements were made with standard calibration curves. The metal standards used were made up in the same final matrix as the leachate. A matrix effect was observed for Zn and consequently measurements were made by standard additions. The instrument settings are listed in Table 3.4.

C. Analytical procedures for the determination of total metal content of SPM

a) Apparatus and reagents

- MDS-81D microwave oven, CEM
- Teflon PFA digestion vessels (6), Savilex Inc.#568
- 1000 ml Teflon PFA overflow reservoir, Savilex Inc.#1008
- polyethylene carousel
- Digestion vessel torque wrench
- Electronic pan balance
- tweezers
- 1000 ml FEP bottle for storage of reagent
- 125 ml FEP bottle for storage of reagent
- 60 ml LDPE wide mouth bottles for digest storage
- polyethylene gloves
- Ice bath
- 5000 μ l micropipette and tips
- Concentrated SBD-HNO₃
- Milli-Q water

b) Digestion procedure

Filters, which have gone through the acetic acid leach procedure, are placed on the base of the digestion vessel, and 2000 µl of SBD-HNO₃ are added to each reaction vessel. The acid should cover the filter. The caps to each vessel are secured with the torque wrench and the pressure relief valves adjusted to maximum pressure resistance. The digestion vessels are placed onto the carousel and attached to the central reservoir containing 50 ml of SBD-H₂O. The carousel is placed on the rotating table and the samples heated for 9 minutes with the microwave set at 90% of full power. After heating the carousel is transferred to an ice bath and cooled for 30 minutes. After digestion, the filters are completely dissolved. The contents of each vessel are poured into preweighed LDPE bottles. Each vessel is rinsed 3 times with Milli-Q water and the washings collected into each sample storage bottle. The volume of each digested solution is made up to 20 ml gravimetrically using an electronic pan balance.

In a typical analysis one reagent blank is run with each batch of five samples. The blank digestion vessel is rotated so that each vessel has a reagent blank every six cycles. Standard sediment (BCSS-1) was run to check the recovery of the method. For that, standard sediment was accurately weighed out (~ 5 mg) and transferred to a digestion vessel. Digestion vessels are cleaned between each batch of samples by running a complete set of blanks.

Analysis of the solution from the total decomposition was performed on a Perkin-Elmer 1100B (GFAAS) for eight elements (Mn, Fe, Co, Pb, Cd, Zn, Cu and Ni). The instrument setting conditions are the same as those describe in Table 3.4. Standards were made up in 10% (v/v) HNO₃.

c) Assessment of the analytical quality of the total particulate trace metal measurement

In order to examine the accuracy and precision of the total digestion analytical procedure employed in this study, a certified reference estuarine sediment (BCSS-1, National Research

Council Canada) has been analysed. A comparison of the obtained values and the certified ones is presented in Table 3.5. The measured values were in satisfactory agreement with the certified value. Concentrations for Fe, Mn, Co, Pb, Cd, Zn, Cu were within the range of the certified value. For Ni, measured values were lower than the certified value.

Table 3.5: The determination of total trace metals in reference estuarine sediment material (BCSS-1)

Element	BCSS-1 material Certified concentration ($\mu\text{g/g}$)	Analysis 1	Analysis 2	Analysis 3
Fe	3.05 ± 0.17 (%)	3.36	3.37	3.23
Mn	229 ± 15	188	196	197
Co	11.4 ± 2.1	10.1	9.77	9.25
Pb	22.7 ± 3.4	21.2	20.5	17.5
Cd	0.25 ± 0.4	0.397	0.327	0.237
Zn	119 ± 12	120	115	136
Cu	18.5 ± 2.7	17.4	16.5	18.7
Ni	55.3 ± 3.6	48.0	48.1	40.8

3.4 Manganese and iron in pore water samples

3.4.1 Sampling

Cores (50 cm long) were collected using a gravity water-sediment corer (Giordani *et al.*, 1994). Core extrusion and pore water extraction were performed in inert atmosphere (nitrogen gas). Cores were sectioned into 0.5 to 2 cm slices with higher resolution near the water-sediment interface. Each slice was placed in a tube and centrifuged at 5000 rpm for 10-15 minutes at the in-situ temperature of collection. The supernatant was then filtered through 0.40 μm Nuclepore filters and acidified with hydrochloric acid for trace metals measurements.

3.4.2 Analytical procedures for pore waters

Samples were diluted and co-injected with palladium as modifier and hydroxylammonium chloride as a reductant in the GFAAS (See Table 3.4).

3.4.2.1 Apparatus and reagents

a) Apparatus

- 1000 ml FEP bottle (1)
- 125 ml FEP bottle (3)
- 100 ml polyethylene volumetric flask (1).
- 100 ml polyethylene bottles (5)
- Gilson variable volume micropipettes, 10-100 μ l (1), 100-1000 μ l (1)
- polyethylene tips for micropipettes

b) Reagents

- SBD water
- manganese and iron standards (1000 ppm) spectrosol, BDH.
- SBD concentrated nitric acid.
- SBD concentrated hydrochloric acid
- Palladium powder 99.999 % (Aldrich)
- Hydroxylammonium chloride, AnalR, BDH

c) Reagent preparation

- Matrix modifier (see section, 3.2.2.2.B.c)
- Standards

Standards were made for Mn and Fe in 1% HNO_3 (v/v) at the following concentrations: 10 $\mu\text{g/l}$, 40 $\mu\text{g/l}$, 60 $\mu\text{g/l}$ and 100 $\mu\text{g/l}$. The blank is made of 1% HNO_3 (v/v). Standards were stored in 100 ml polyethylene bottles.

- 1 per thousand (v/v) HNO_3 solution was prepared with SBD concentrated nitric acid and SBD water and stored in a 1000 ml FEP bottles.

3.4.2.2 Procedures

Samples were diluted with 1 per thousand HNO₃ (v/v) 10, 20, 40 or 100 times depending of the sample concentration to diminish the salt effect during the measurement with the GFAAS.

3.4.2.3 Measurement by atomic absorption spectrometry

Sample concentrations were measured by graphite furnace atomic absorption spectrometry (Perkin Elmer 1100B) using the standard addition method. Three standard additions were made for each samples (20 µg/l, 40 µg/l and 100 µg/l). The instrument setting conditions are the same as those described in Table 3.4.

3.5 Auxiliary data.

3.5.1 Salinity

Samples for salinity measurement were collected in glass bottles. Salinity was determined by measuring the conductivity with a Guildline Autosal salinometer which had been calibrated with IAPSO standard seawater (P series), and the salinity calculated using the programme “octable”.

3.5.2 Nutrients

Samples for phosphate and nitrate + nitrite were also collected in the Adriatic Sea. These were filtered through GF/F filters, poisoned with mercury chloride (300 µl of a 3.5 % (w/v) solution per 100 ml of sample) to prevent changes in concentration, and stored in a refrigerator in brown glass bottles. Dissolved inorganic phosphate was analysed using the method of Murphy and Riley (1962) as modified by Strickland and Parsons (1977). The absorbance of the samples was measured using an Hitachi U2000 spectrophotometer and a 40 mm flow cell. A technique of flow injection analysis was used for the determination of nitrate plus nitrite (Anderson, 1979). With this method the nitrate is reduced to nitrite during passage through a copper-cadmium alloy column. Subsequently the reagents are added to the sample and the absorbance of the resulting pink complex measured.

CHAPTER 4

TRACE METALS IN THE ADRIATIC SEA

4.1 The study area

4.1.1 Geomorphology of the Adriatic Sea

The Adriatic Sea is a rectangular basin oriented in a NW-SE direction with a length of about 800 km and a width of about 200 km situated between Italy, the old Yugoslavia, and Albania (Fig. 4.1). It is connected to the Ionian Sea through the Strait of Otranto and consequently there are important water exchanges between the Adriatic Sea and the eastern Mediterranean Sea. The Adriatic has a volume of 36,000 km³ and its surface area is about 160,000 km². The Adriatic Sea can be divided into 3 sub-basins:

- the first part in the North is dominated by the continental shelf with very shallow depths with the bottom sloping gently southwards and reaching at most 90 m;
- the second part is situated between three pits located along a line perpendicular to the coast at Pescara, and by the Palagruza sill which is 170 m deep;
- the third part consists of the South Adriatic pit. The topography is characterised by isobaths of approximately circular shape. The maximum depth is about 1,200 m at the centre of the basin. The bottom rises towards the Strait of Otranto, which has a maximum sill depth of 780 m and a width of about 75 km.

4.1.2 Hydrography

The hydrographic properties of the Adriatic Sea result from its geographical location and morphology, climatic conditions of the area, fresh water inflow from rivers and water exchange with the Ionian Sea. Each of these factors act separately, but they also interact with each other in various combinations, thus determining the circulation pattern of the basin as well as its seasonal variability (Artegiani *et al.*, 1993). The surface circulation consists of a large-scale cyclonic meander with several smaller cells embedded in it (Barale *et al.*, 1984).

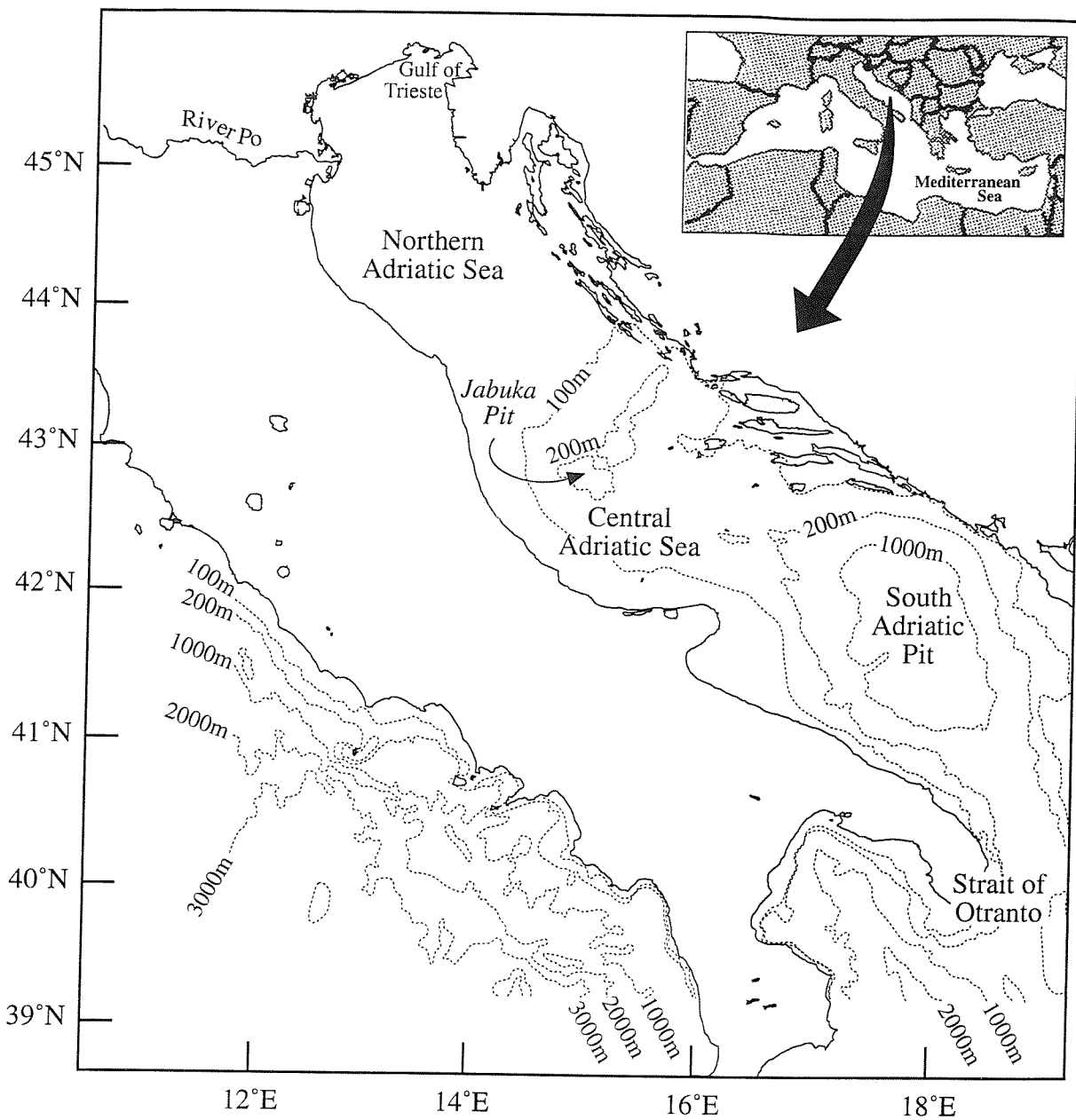


Fig. 4.1: Topography of the Adriatic Sea

Water mass analyses and direct current measurements indicate that the cyclonic meander also occurs in the intermediate layer, dominated by a current that inflows along the eastern coast. In the bottom layer, an outflowing current pressed against the western coast dominates (Orlic *et al.*, 1992). The Adriatic Sea is the main source of Eastern Mediterranean Deep Water (EMDW) which is formed in the southern Adriatic and the northern Ionian Sea near the Strait of Otranto (Artegiani and Salusti, 1987; Artegiani *et al.*, 1989; Bignami *et al.*, 1991; Zoccolotti and Salusti, 1987). Lascoros (1993) estimated the quantitative upper bounds of water type production inside the Mediterranean Sea. He found a 0.34 Sv figure for the formation of the EMDW in the Adriatic which is very similar to the 0.29 Sv figure suggested by Roether and Schlitzer (1991). During the winter, the Adriatic Sea is subject to meteorological perturbations: the Bora (a dry and cold wind blowing from the east coast) and the Scirocco (blowing from the south-east bringing rather humid and warm air into the Adriatic region). The Bora produces buoyancy fluxes through evaporative and heat loss, and consequently induces both wind driven and thermohaline circulation and is responsible for deep water formation (Orlic *et al.*, 1994). In the Adriatic Sea, three types of dense water are generated: the North Adriatic Water (NAW) with a temperature, salinity and sigma theta of 11°C, 38.5, 29.52 respectively; the Middle Adriatic Water (MAW) characterised by 12°C, 38.2, 29.09 for temperature, salinity and sigma theta respectively; the South Adriatic Water (SAW) characterised by 13°C, 38.6, 29.20 for temperature, salinity and sigma theta respectively. Also the Mixed Levantine Intermediate Water (MLIW) enters the Adriatic Sea by the Strait of Otranto and mixes with the Adriatic Water to form a high salinity and high temperature water mass (Orlic *et al.*, 1992; Artegiani *et al.*, 1993).

The very dense NAW is formed during winter in the shallow northern Adriatic Sea. The influence of the fresh water inflow, mainly by the river Po, and the strong Bora events inducing high evaporation (15mm/day) are the main factors which contribute to the formation of the NAW characterised by low temperature and relatively low salinity. This water mass flows southward pressed against the slope of the western coastal shelf, forming a vein of water which flows along the isobaths. This vein of water splits in two branches, one descending into the Jabuka Pit and one pouring over the Palagruza sill. The water flow of the vein is highly variable depending on the meteorological conditions.

The MAW is not a distinct water mass. It is formed in the area of the Jabuka pit during winter periods when there is weak inflow of Levantine Intermediate Water through the Strait of

Otranto (Zore-Armanda, 1963). According to Artegiani *et al.*, (1993), the bottom layer of the Jabuka pit is filled with NAW which has been modified with the MLIW flowing along the eastern coast. The MAW is then a mixture which is somewhat warmer and saltier than the original water mass. Its oxygen content is low in summer showing the long residence time of the water mass in the Jabuka pit (Artegiani and Salusti, 1987).

The SAW originates from the South Adriatic Pit in the centre of the South Adriatic gyre during the winter period. It is mainly the air-sea heat exchanges which induce the dense water formation processes. The dissolved oxygen content is very high over the entire water column during winter, showing that the water is well ventilated. The other very important controlling mechanism is the Mediterranean inflow through the Strait of Otranto. Both mechanisms can be related to each other: intense deep water formation processes can result from the strong air-heat exchange and consequently a strong Adriatic water outflow which means a strong demand for the Mediterranean inflow (Ferentinos and Kastanos, 1988). There are controversial ideas concerning the relationship between the NAW and the SAW: Ovchinnikov *et al.*, (1985) found that SAW is overlaying NAW in the south Adriatic pit whereas Zore-Armanda (1963) and Zoccolotti and Salusti (1987) think there is mixing between the two water masses and then the SAW body is a result of this process. Despite this controversy, all the authors agree that the SAW outflows in the Strait of Otranto and becomes the bottom layer of the Eastern Mediterranean Deep Water. Hopkins (1978) showed that the SAW mixes with LIW to form the EMDW in the Ionian Sea.

4.1.3 River inputs to the Adriatic Sea

The major fresh water source is the Po river in the Northern Adriatic Sea. Between 1918 and 1981, the mean flow rate of the Po was $1,515 \text{ m}^3/\text{s}$. Over this period the maximum flowrates have tended to increase while the minimum flowrates have tended to decrease (Dal Cin, 1983). As part of the EUROMARGE MAST program, Mowbray *et al.*, (1995) sampled the river Po at Pontelagoscuro covering all the seasons between August 1993 and December 1994. The flow rate ranged from $540 \text{ m}^3/\text{s}$ to $8,630 \text{ m}^3/\text{s}$, the mean flow rate being $2,149 \text{ m}^3/\text{s}$. The maxima were much higher than the mean flow rate and were associated with snow melt in spring and strong precipitation in autumn. The annual mean runoff of rivers other than the Po in the Northern Adriatic Sea is about $1121 \text{ m}^3/\text{s}$ (Cavazzoni Galaverni, 1972); the rivers

inflowing along the eastern coast contribute about 1150 m³/s of the fresh water inputs (Orlic *et al.*, 1992). The Po river input represents 60% of the total river inputs and therefore will have a great influence on the water mass bodies present in the Northern Adriatic Sea.

4.2 The database for the study

The dissolved metal and supporting hydrographic data for the Adriatic Sea obtained in this study are tabulated in Appendix I. Samples have been collected in the Adriatic Sea on 7 occasions, as detailed in Table 4.1.

Table 4.1: Data collection details

Area	Dates	Sampling
Adriatic Sea	February 13/2/94-19/2/94	pore waters
Northern Adriatic Sea	May 11/5/94-16/5/94	dissolved and particulate trace metals, nutrients, DOC, fluorescence, salinity
Adriatic Sea	June 25/6/94-3/7/94	dissolved and particulate trace metals, salinity, pore waters
Northern Adriatic Sea	July 7/7/94-8/7/94	dissolved and particulate trace metals, salinity
Northern Adriatic sea	September 27/9/94-1/10/94	dissolved and particulate trace metals, nutrients, DOC, fluorescence, salinity, pore waters
Strait of Otranto	November 11/11/94-25/11/94	dissolved trace metals, salinity
Northern Adriatic Sea	February 15/2/95-17/2/95	dissolved and particulate trace metals, nutrients, DOC, fluorescence, salinity, pore waters

Sampling locations are shown on 2 maps (Fig. 4.2 and Fig. 4.3).

River Po samples were also collected at monthly intervals at Pontelagoscuro.

4.3 Hydrographic and chemical setting

In order to interpret and better understand the metal data, it is important to have a sound knowledge of the hydrodynamic and biogeochemical processes at work.

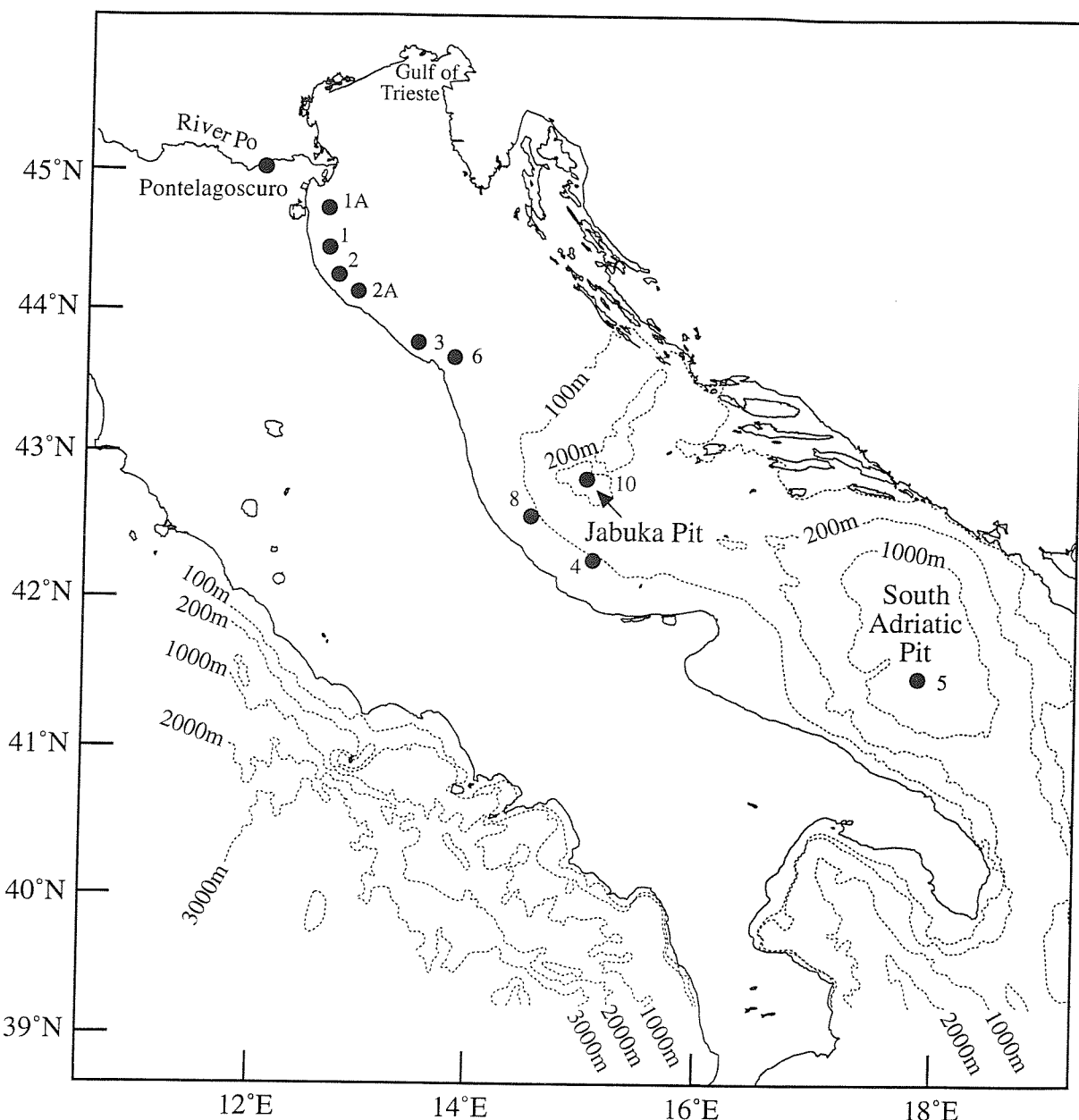


Fig. 4.2: Sampling locations in the Adriatic Sea

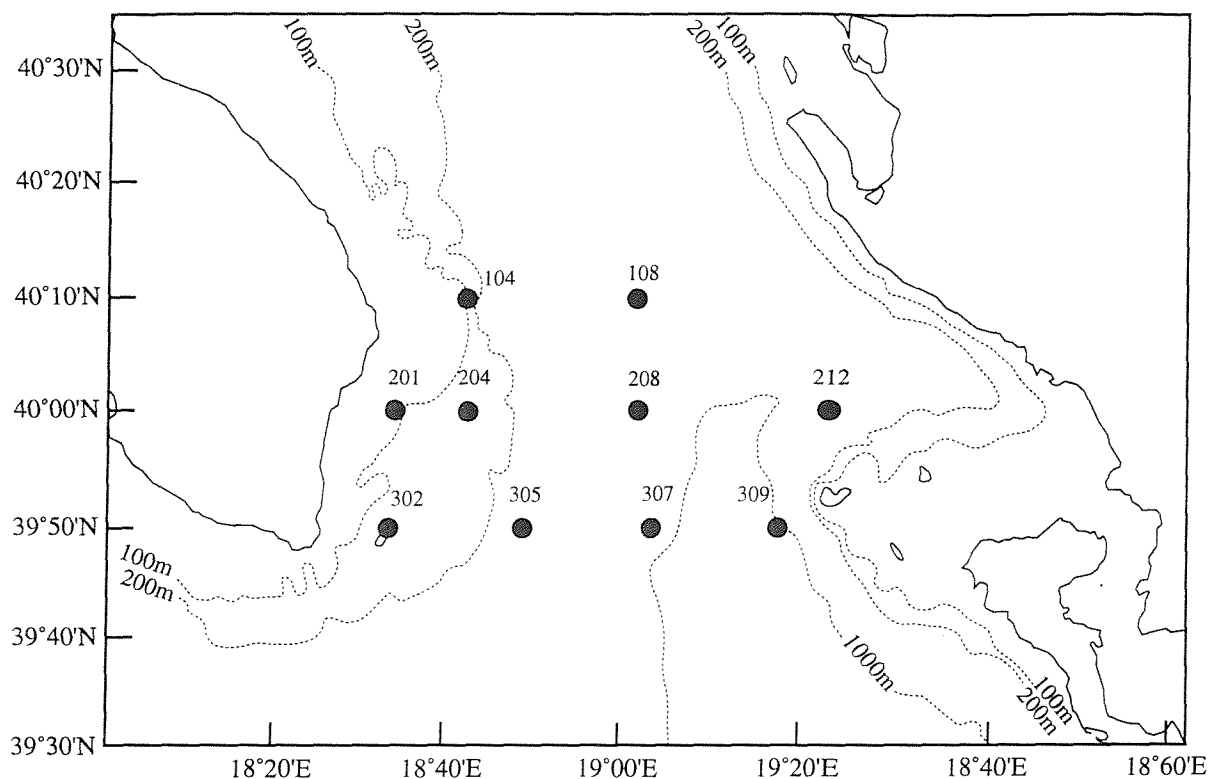


Fig. 4.3: Sampling locations in the Strait of Otranto

This section provides a description and interpretation of these background physical and chemical data which were obtained at the same time as the metal data.

4.3.1 Temperature, salinity and density

4.3.1.1 The Northern Adriatic Sea

Temperature and salinity data collected during the summers of 1911-1982 (Justic, 1991) show no significant trend of increase or decrease either near the surface or at the bottom. However, a decline in surface salinities on the western side of the Northern Adriatic Sea was identified from the 1975-1978 data suggesting more fresh water inputs recently.

Temperature and salinity distribution patterns below the Po river outflow are affected by the freshwater inputs to a decreasing extent southwards and vertically towards the bottom (Fig. 4.4 and Fig. 4.5). During the spring-summer period (May 1994 and September 1994) the water column is strongly stratified due to atmospheric heating: thermoclines and haloclines are well defined (4 m Station 1, 7 m Station 2 and 12 m Station 3). In September 1994 and February 1995 the thermoclines are not so apparent since the water column is well mixed. Temperatures are much lower during the winter (8 °C) than during the autumn (20 °C). The haloclines are still well defined for Stations 1 and 2 (4 m at Station 1 and 6 m at Station 2). At Station 3 salinity increases progressively from 35.86 to 36.78 from the surface to the bottom; there is a decrease in stratification in comparison to the other Stations. The Northern Adriatic basin shows typical shallow water mass characteristics which can be considered independent of the Middle and Southern basins as they are more affected by seasonal temperature and salinity variability.

4.2.1.2 The Central Adriatic Sea

Temperature - salinity diagrams have been plotted for Stations 4 and 10 (Fig. 4.6). On this diagram, mixing between 4 water masses can be identified: the Northern Adriatic Water (NAW), the mixed Levantine Intermediate Water (MLIW), the Mixed Adriatic Water (MAW) and surface water (SW). At Station 4 the low salinity in the surface layer shows the

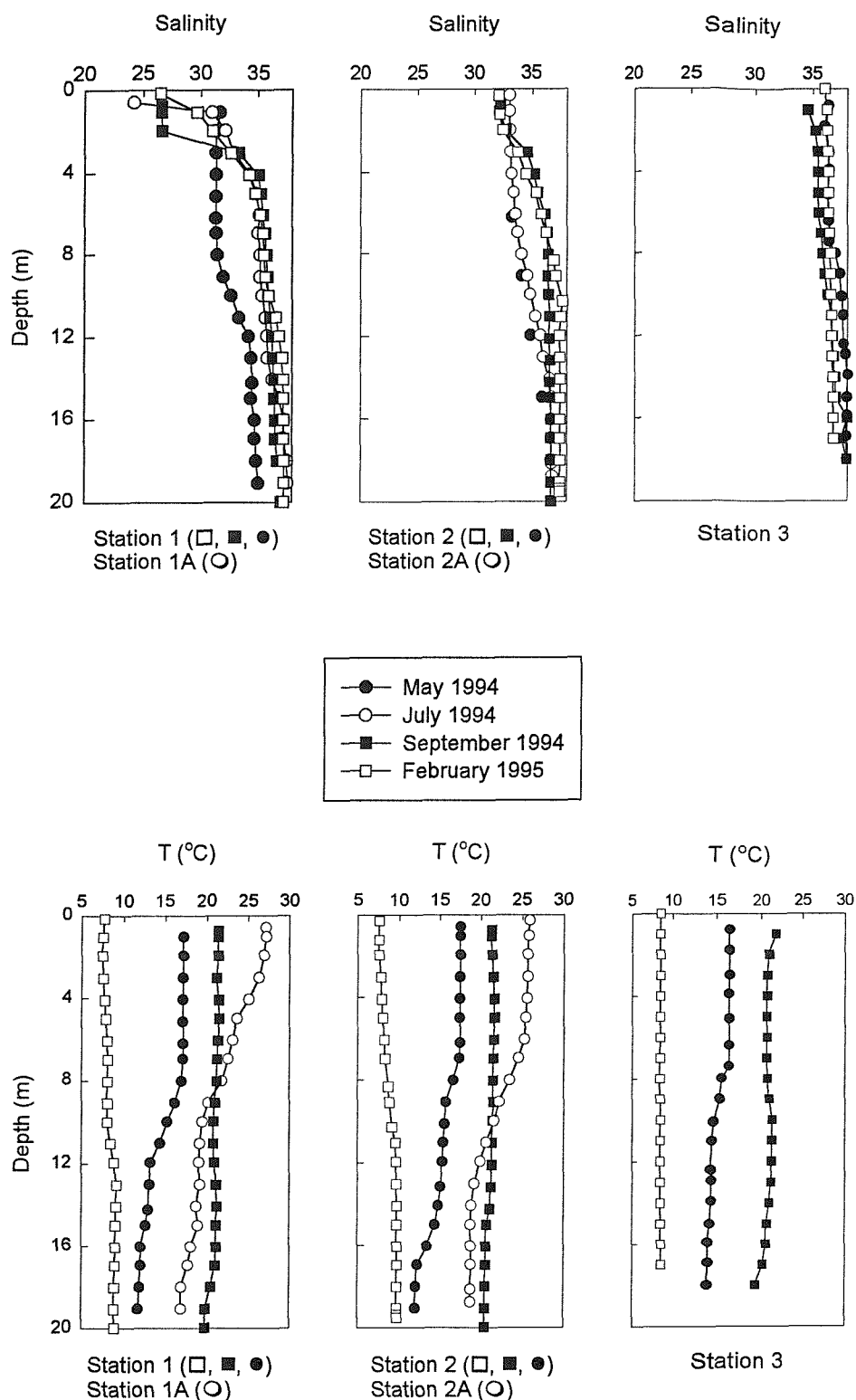


Fig. 4.4: Temperature and salinity distributions in the Northern Adriatic Sea

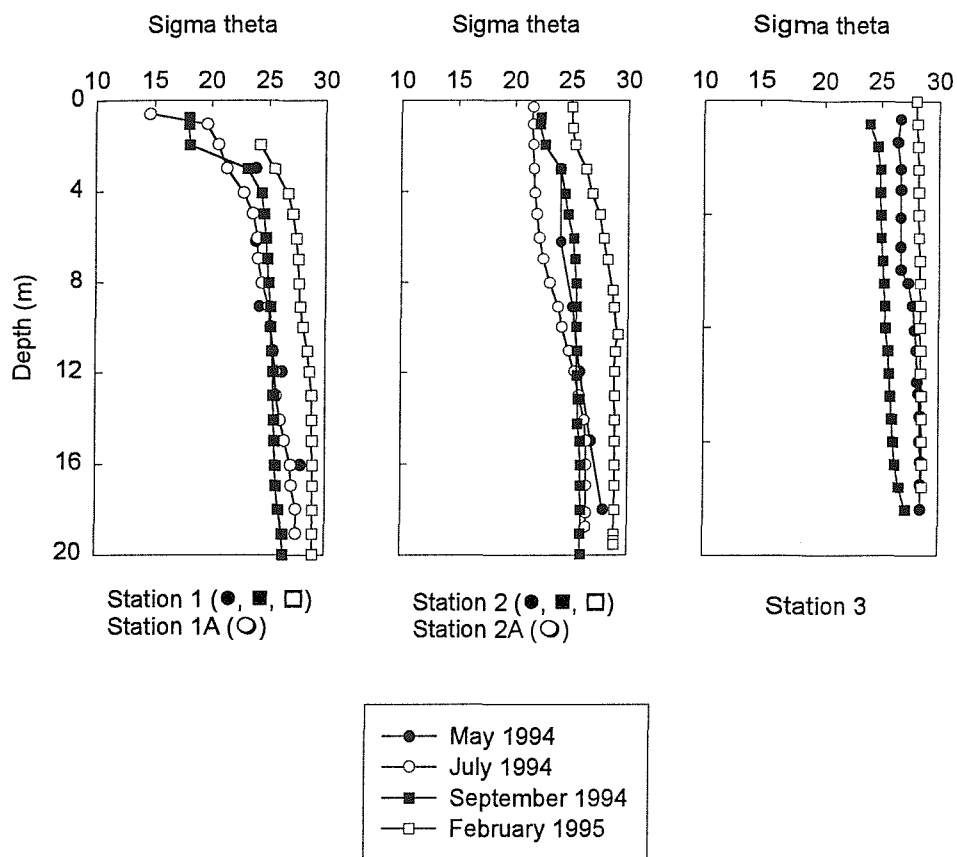


Fig. 4.5: Sigma theta distribution in the Northern Adriatic Sea

influence of fresh water coming mainly from the River Po along the Italian coast. At this time the water column is strongly stratified. Deeper in the water column there is mixing between surface water and MAW. At Station 10, the MAW mixes with the MLIW. In the central part of the Adriatic Sea the salinity of MLIW is lower than in the Southern Adriatic Sea suggesting some mixing with lower salinity water masses from Adriatic origin. The MLIW mixes with the NAW. According to Orlic *et al.*, (1992) the NAW is formed in the Northern Adriatic Sea during the winter period and is transported Southward along the Italian coast. With our limited data set, it is possible to determine its characteristics which are 38.45 for the salinity and 11 °C for the temperature.

4.3.1.3 The Strait of Otranto

Fig. 4.7 presents the temperature versus salinity plot for samples collected during the AEGAE0 cruise. It shows that five water masses, similar to those described by Orlic *et al.*, (1992), can be clearly identified (see Table 4.2): The West Surface Water (WSW) comes from the Ionian Sea and is characterised by a high salinity (38.4). The East Surface Water (ESW) comes from the Adriatic and is influenced by the Po river and has consequently a low salinity (37.7). These two water masses mix with the Mixed Adriatic Water (MAW) which has a low temperature (13.16) and a salinity about 38.3.

Table 4.2: Characteristic temperatures and salinities of the different water masses in the Strait of Otranto

	ESW	WSW	MAW	MLIW	SAW
Salinity	38.39	37.75	38.32	38.73	38.62
Temperature °C	19.04	18.80	13.16	13.59	13.11

On the T-S plot, it is possible to notice some lateral mixing between the different surface waters: surface water characteristics of Stations 208 and 108 fall exactly on the mixing line between WSW and ESW. Deeper in the water column, MAW mixes with the Mixed Levantine Intermediate Water (MLIW) which enters the Adriatic Sea through the Strait of Otranto. Then the MLIW mixes with South Adriatic Water (SAW).

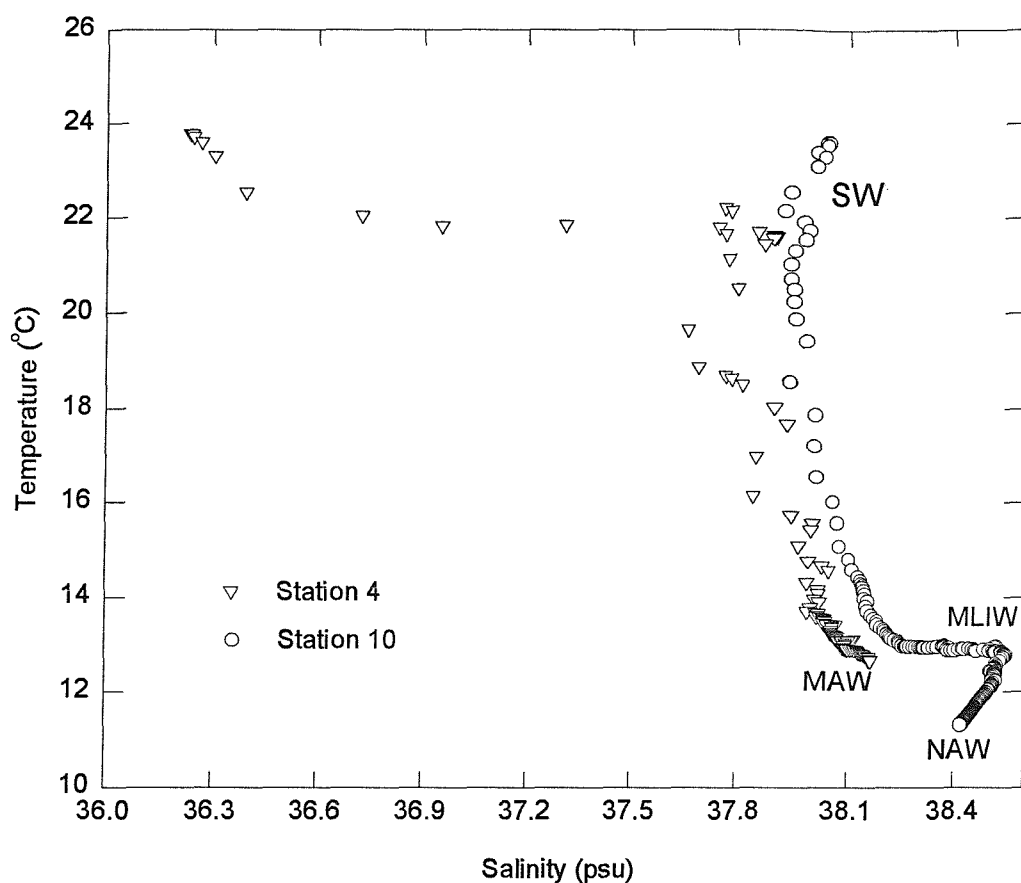


Fig. 4.6: Temperature-Salinity diagrams for Stations 4 and 10

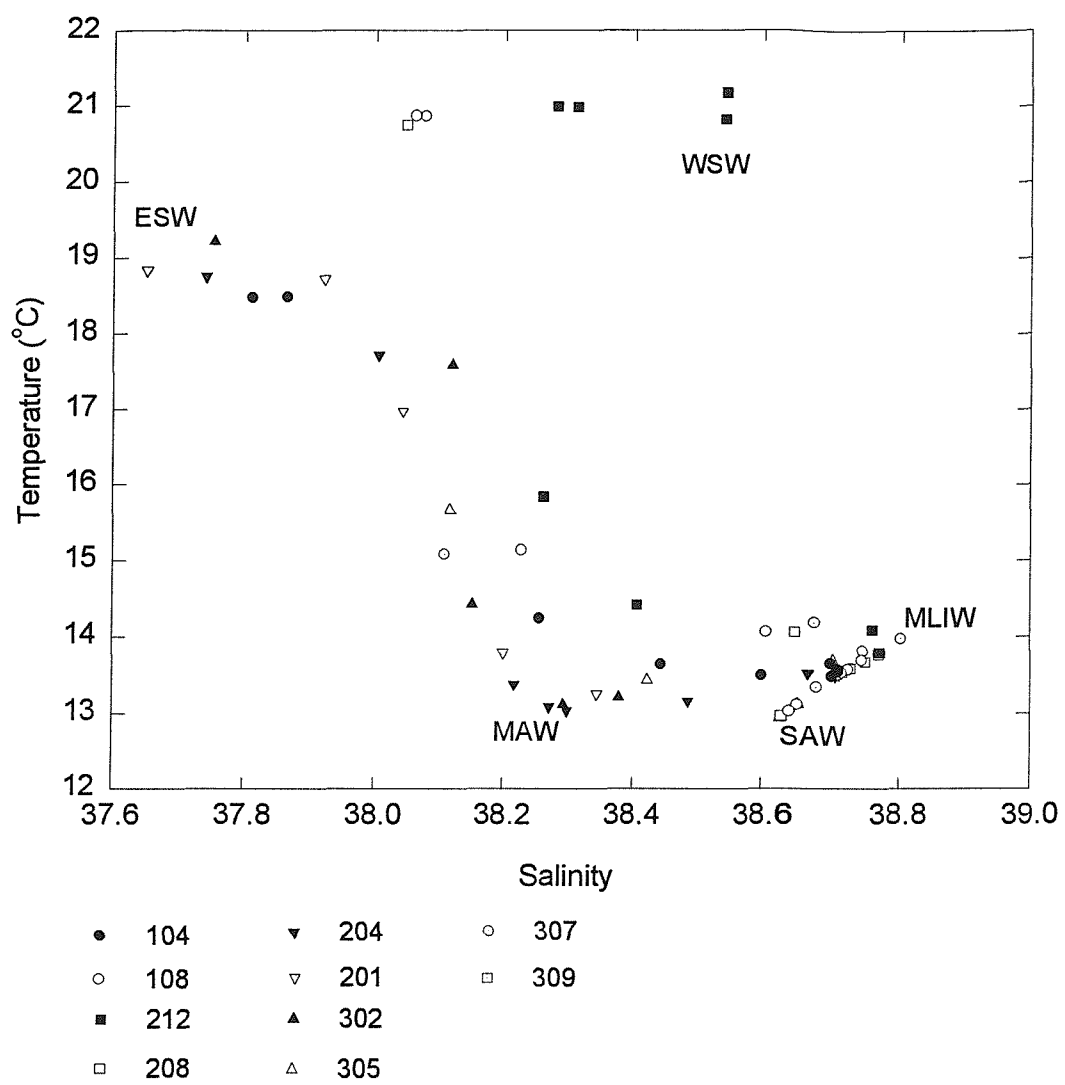


Fig. 4.7: Temperature-Salinity diagrams for stations in the Strait of Otranto; numbers refer to station positions in the Strait of Otranto

4.3.2 Oxygen and Chl α in the Northern Adriatic Sea

Justic (1991) used oxygen data collected during the period 1911-1984 in the Northern Adriatic Sea and demonstrated that there was a trend towards higher oxygen content in surface water and lower oxygen content deeper in the water column with a strong gradient near the bottom. The changes appear to be substantial: during the last 75 years, the oxygen concentration has increased by about 1.1 ml l^{-1} at the surface and decreased by about 2.2 ml l^{-1} at 2 m above the bottom (Justic, 1987; Justic *et al.*, 1987). The higher values in surface water may be due to the air-sea exchanges and to primary production (it is difficult to differentiate these inputs) whereas the bottom decrease may be due to oxidation of organic carbon (Justic, 1994). These trends are observed on our data set (Fig. 4.8), particularly for Stations 1 and 1A in July 1994, September 1994 and February 1995. For Station 2 and 2A higher oxygen saturation is observed in surface water in September 1994 and February 1995 whereas higher oxygen saturation is observed between 10 and 16 m in May 1994 and July 1994. According to Gilmartin and Revelante (1983) the seasonal cycle of primary production in the Northern Adriatic Sea is characterised by three periods of blooms: January-April, June-August and September-November. The spring and autumn primary productivity maxima tend to coincide with the maximum of Po River discharge whereas the winter maximum occurs during the period of winter overturn. Chlorophyll α is a good indicator of primary production. In our limited data set it is possible to observe 3 blooms during those periods in the years 1994 and 1995 at Station 1 and Station 1A, which is not very far from Station 1. In February 1995, maxima of Chl α and oxygen saturation are observed in surface waters suggesting a bloom in surface water then concentrations of Chl α and oxygen saturation decrease gradually with depth. In September a maximum of Chl α is observed at 3 m associated with a high oxygen saturation suggesting the occurrence of a bloom. Below 3 m concentrations decrease down to $2 \mu\text{g/l}$ suggesting sedimentation and decay of the chl α produced during a previous bloom since the oxygen saturation is decreasing. In July 1994 there are maxima of chl α and oxygen saturation in surface waters which suggest the appearance of a bloom. Between 10 m and 20 m there is a small maxima of Chl α ($10 \mu\text{g/l}$) and a strong decrease in oxygen saturation (32 % on the bottom) which suggest a sedimentation of chl α produced during previous blooms in surface water and a decay of organic matter. In May 1994 there is no apparent bloom in the

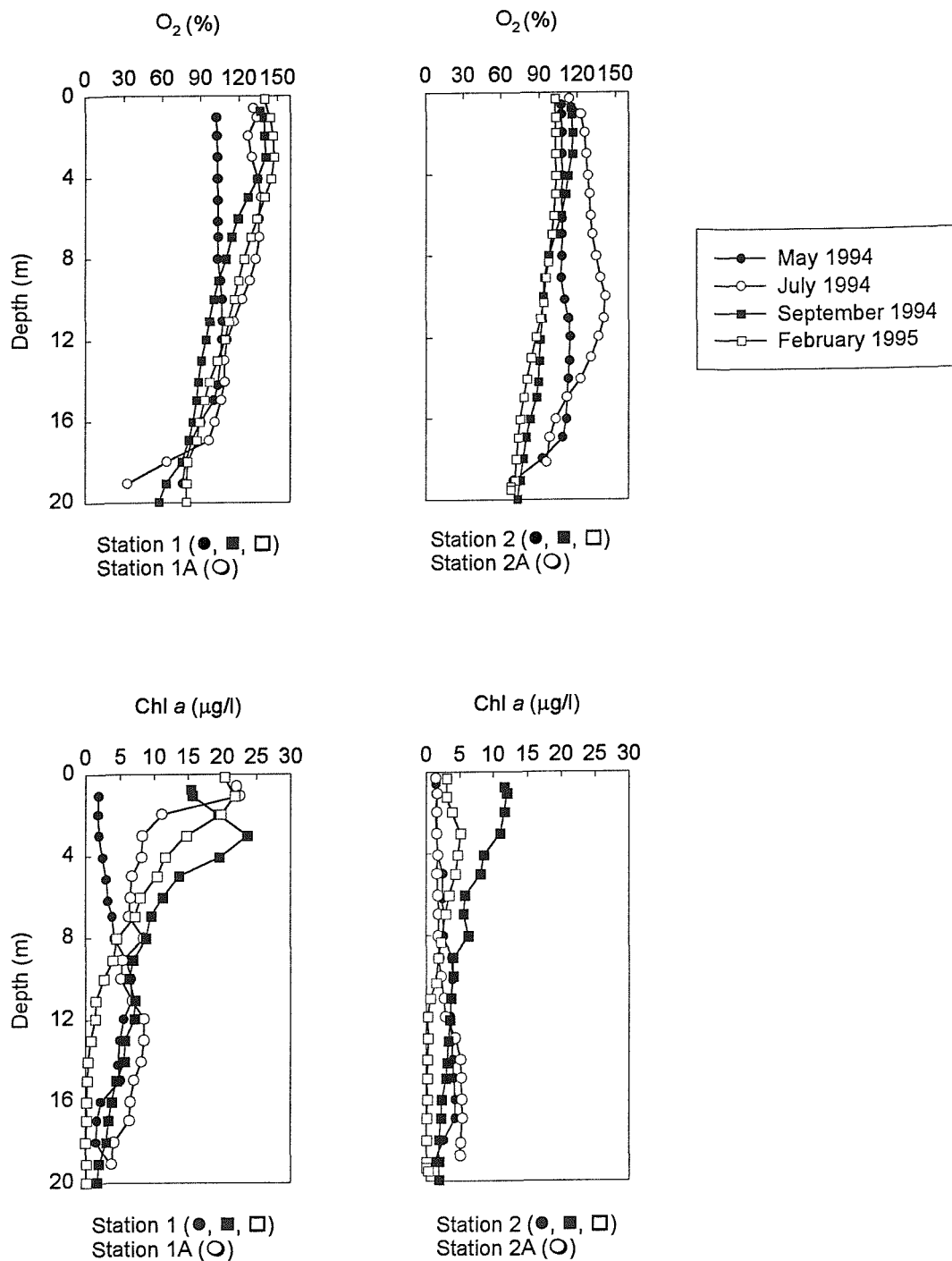


Fig. 4.8: Oxygen saturation and Chl *a* distributions in the Northern Adriatic Sea

surface water but an increase of Chl α and oxygen saturation between 8 and 18 m suggest an increase in primary production at greater depth. At Stations 2 and 2A blooms appear in the same periods but their amplitudes are less due to the lower influence of the river Po. The extremely low oxygen saturation (32 %) at the bottom during summer is due to the oxygen demand which increases with temperature and increasing flux of carbon to sediments (Justic, 1991). Moreover at that time of the year reoxygenation through the pycnocline decreases with the increasing stability of the water column. As a consequence, the oxygen concentration at the bottom decreases. The oxygen content of the bottom water also decreases, due to the fact that the pycnocline gradually progresses towards the deeper parts of the water column. During September, the pycnocline, which at this time is mostly at the thermocline, can be within 10 m above the bottom. On some occasion it may lie only a few meters above the bottom (Justic, 1991).

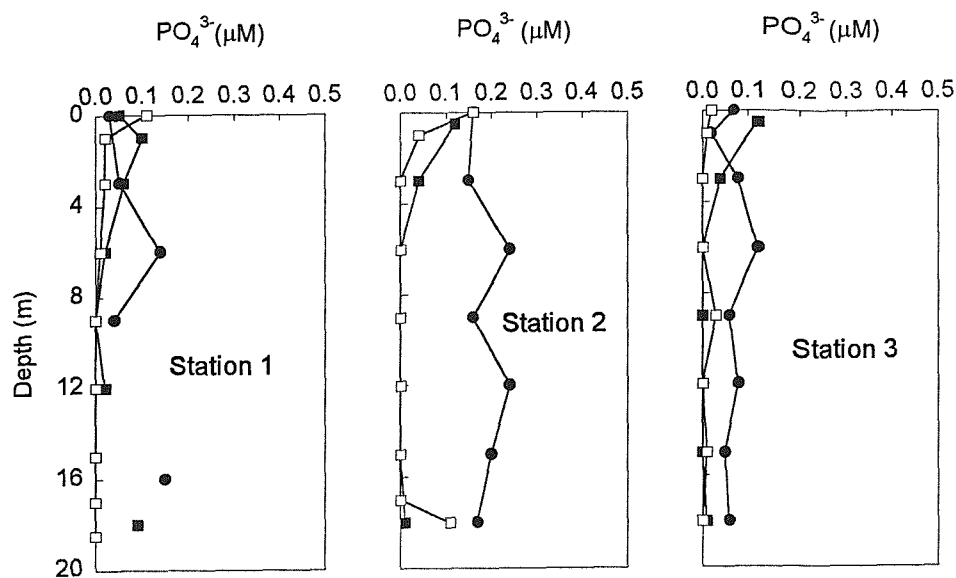
4.3.3 Nitrogen and phosphorus in the Northern Adriatic Sea

The trend of increase in oxygen concentration at the surface and a decrease near the bottom in recent decades may be explained by the fact that fertilisation practices changed and the use of detergents containing phosphorus started to increase rapidly 30 years ago (Justic, 1991). The consumption of phosphorus and nitrogen in the drainage areas of the Po River and other north Italian rivers, seems to have increased by at least a factor of five over the past forty years, thus increasing the influx of nutrients to the sea.

The concentrations of nutrients in the water column measured in this study confirm the trend recorded in previous investigations of the Adriatic Sea (Deggobis and Gilmartin, 1990) and of other areas in the Mediterranean Sea (Cruzado and Velasquez, 1989). Most of the dissolved reactive phosphorus concentrations are below the detection limit ($0.02\mu\text{M}$) except in May 1994 and September 1994 but even there, concentrations were very low (Fig. 4.9). In order to understand factors controlling biological productivity, both nutrient concentrations and their ratio have to be taken into account. Justic *et al.*, (1994) defined nutrient ratios for each element in limiting conditions: P is limiting if $\text{DIN}/\text{P} > 22$; N is limiting if $\text{DIN}/\text{P} < 10$ (DIN is dissolved inorganic nitrogen ($\text{NO}_2^- + \text{NO}_3^- + \text{NH}_4^+$) and P is dissolved reactive phosphorus). In this study, data for NH_4^+ were not available and consequently DIN is an underestimation of

the true DIN. However ammonia concentrations would not be significant since NH_4^+ is regenerated from the short-term recycling processes within the euphotic layer and is utilised by phytoplankton. At Station 1, nitrate concentrations are much higher in surface water in February 1995 than in May 1994 and September 1994. The high concentrations in February may be explained by the high River Po outflow that occurred at the same time. In May 1994, nitrate concentrations are relatively constant in the water column (10 μM) and decrease near the bottom (4.3 μM). In September 1994 and February 1995 there were maxima in surface waters which were respectively 16 μM and 75.3 μM ; concentrations decrease down to 1 μM and 6 μM respectively below 9 m. Phosphate concentrations are very low in all cases and consequently P could be a limiting factor at Station 1. At Station 2, nitrate concentrations are always higher in surface water and decrease deeper in the water column. Highest concentrations in surface waters are found in February 1995 (24 μM). Concentrations are in general higher in May 1994 than in September 1994. Phosphorus concentrations are always very low and P appears to be the limiting factor for primary production. At Station 3 reactive phosphorus concentrations are below 0.1 μM . Nitrate concentrations are in general lower than those in Stations 2 but the shape of the profiles is similar. In May 1994, P appears to be the limiting factor in surface water whereas N appears to be the limiting factor below 9 m. In September 1994 and February 1995, P appears to be a limiting factor.

In general nitrate concentrations are very high due the River Po influence. Surface concentrations decrease southward and downward towards the bottom. The nitrate-salinity diagram (Fig. 4.10) shows a conservative mixing line between 20 psu and 35 psu for the different seasons, the highest slope being for the winter situation. Between 35 and 37 psu there are changes of slopes due to the influence of additional processes, other than the simple mixing between the different water masses, on the concentrations such as the longer term effects of biological utilisation and recycling. Phosphorus concentrations are very low in the Northern Adriatic Sea and consequently P is generally the limiting factor, although inorganic phosphate is not the only form of phosphorus that can be used by organisms for their nutritional needs. Jackson and Williams (1985) have discussed the importance of dissolved organic phosphorus (DOP) in the nutrient economy of the ocean. The data provided by these authors showed that DOP concentrations increase as those of phosphate decrease, indicating a



● May 1994
 ■ September 1994
 □ February 1995

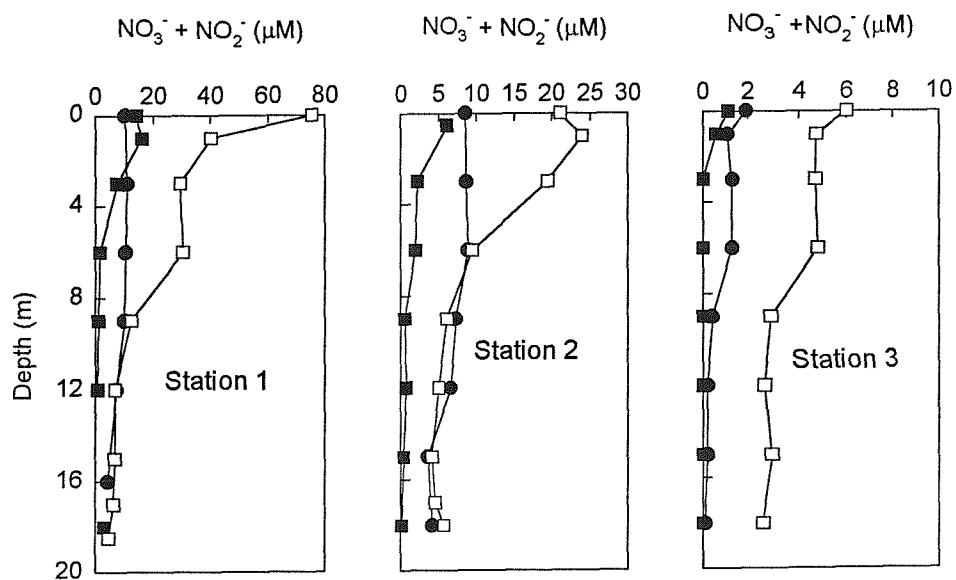


Fig. 4.9: Phosphate and nitrate + nitrite distributions in the Northern Adriatic Sea

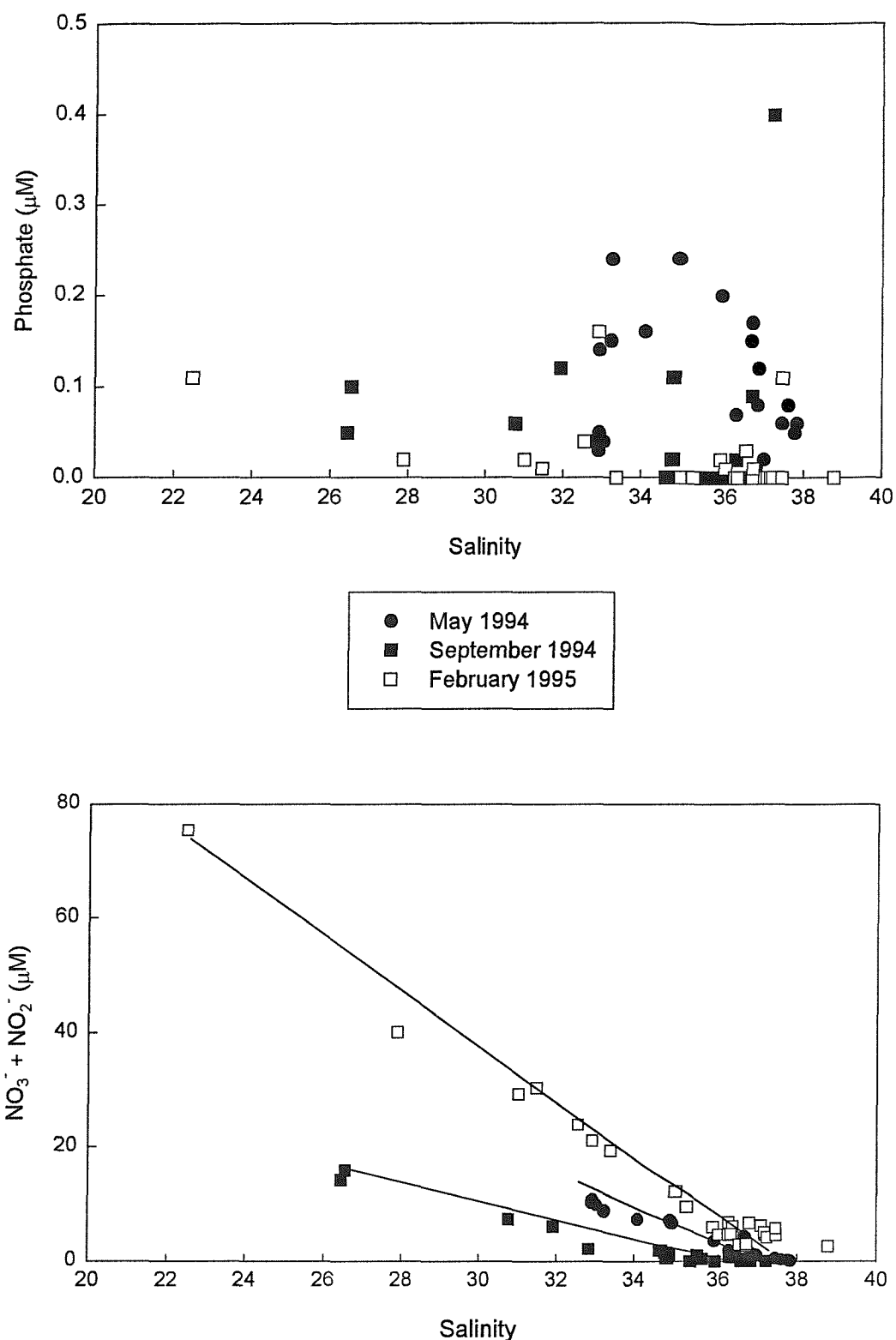


Fig. 4.10: Phosphate and nitrate+nitrite plotted against salinity (Northern Adriatic Sea)

change in the dominant chemical form of phosphorus from phosphate to DOP. The authors concluded that DOP constitute a significant fraction of the oceanic nutrient pool.

4.4 Trace metals in the Po river

Results for dissolved and particulate trace metals in the river Po are presented in Tables A7a and A7b of Appendix I. One noticeable feature is that samples provided by the Edinburgh group produced anomalously high values of dissolved Zn, Co, Pb and Cd compared with the set collected by Southampton. This casts suspicion on the reliability of the sampling and handling methods used by the Edinburgh group in the context of dissolved trace metal determinations.

Averaging values of dissolved and particulate metal concentrations allows an interesting comparison to be made with average trace metal concentrations previously reported in the Rhône and Ebro rivers, as well as those estimated for “average world rivers” (Table 4.3).

Table 4.3: Average trace metal concentrations in the Po river. Comparison with the averages for the Rhône and Ebro rivers and for “global river” concentrations.

		Mn	Fe	Co	Pb	Cd	Zn	Ni	Cu
Average Po river	Dissolved (nM)	39	69	1.1	0.610	0.146	42.3	45	27
	Particulate (µg/g) [3]	1137	29590	—	101	2.4	317	261	69
Average Rhône and Ebro [1]	Dissolved (nM)	61	184	10	0.375	0.265	18.6	25	34
	Particulate (µg/g)	1037	33100	—	43	1.6	200	48	47
Average world river [2]	Dissolved (nM)	150	720	1.7	0.150	0.090	9.0	8	23
	Particulate (µg/g)	1050	48000	—	35	1.2	250	90	100

[1] Guieu *et al.*, (1997)

[2] Martin and Windom (1991)

[3] Price *et al.*, (1996)

Dissolved Cu and Co do not show any significant differences with world river values whereas Cd, Pb, Zn and Ni show enrichment by factors of 1.6, 4, 4.7 and 5 respectively. These last three elements also show concentrations which are higher than in the rivers Rhône and Ebro by a factor of 2. One striking feature is that Fe concentrations are by far the lowest in the Po. Price *et al.*, (1996) showed that low dissolved Fe concentrations in the Po river are the result

of the alkaline character of the river ($\text{pH} \sim 8.0$), and probable precipitation of dissolved Fe within the feeding groundwaters. Manganese concentrations in the river Po are also lower than in either the average world river (by a factor of 4) or the Rhône and Ebro rivers (by a factor of 1.6). Particulate Mn, Fe, Zn and Cu concentrations in the Po river are similar to those in other rivers, whereas particulate Pb and Cd are higher by a factor of 2. Lead and cadmium are regarded as potentially presenting the greatest concern among toxic metals in terms of their land based inputs to coastal waters, and are accordingly classified as EU “Black List Substances”. Dissolved and particulate Cd and Pb concentrations are higher than the average world river values, and consequently the Po river may be considered as a mildly polluted river.

In Fig. 4.11 dissolved and total particulate Mn and Fe in the River Po together with the flow rate have been plotted against sampling dates. Dissolved Fe concentrations tend to vary seasonally with higher concentrations during the winter period. The low values in spring and summer periods may be attributable to biological uptake (Morel *et al.*, 1991). Particulate Fe and Mn correlate well with particulate Al (Fig. 4.12) suggesting that Mn- and Fe-oxyhydroxides mostly occur as coatings on alumino-silicate detritus. However for Mn, a few points lay above the regression line between particulate Mn and Al. These points correspond to a low flow regime associated with a period of high productivity. Under these circumstances, biological oxygen demand increases in the sediment-water interface inducing suboxic sediments. Then reduction of Mn oxides to Mn(II) occurs and Mn(II) diffuses from interstitial water into the overlying water. With the presence of O_2 , dissolved Mn precipitates into newly formed Mn-oxyhydroxides which increase the particulate Mn load. This is also consistent with higher dissolved Mn concentrations observed during the same period (Fig. 4.11). The particulate load depends very much on the dynamics of the flow regime (Price *et al.*, 1996) and since Fe-oxyhydroxides are mostly associated with alumino-silicate minerals, particulate Fe concentrations tend to have a positive and linear relationship with the flow rate whereas for particulate Mn concentrations there is no significant relationship.

Trace metals are scavenged from the water column by particles (Morel *et al.*, 1991; Santschi and Honeyman, 1991). Such scavenging processes may include: biological uptake, sorption (adsorption onto particle surface, absorption by particles and surface precipitation),

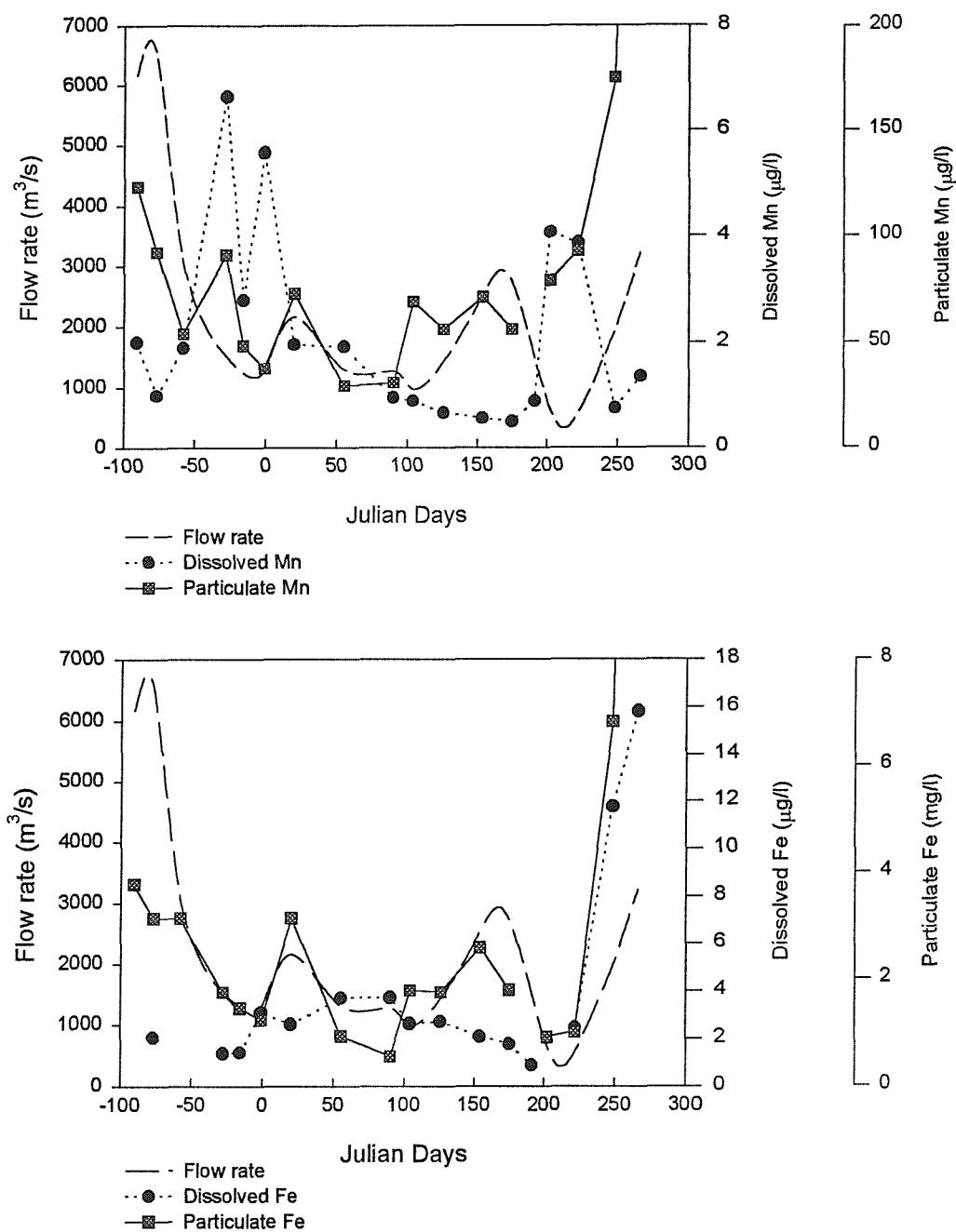


Fig. 4.11: Dissolved and particulate Mn and Fe in the river Po (at Pontelagoscuro) plotted against sampling dates simultaneously with the flow rate of the Po (day 0 = 1/1/1994).

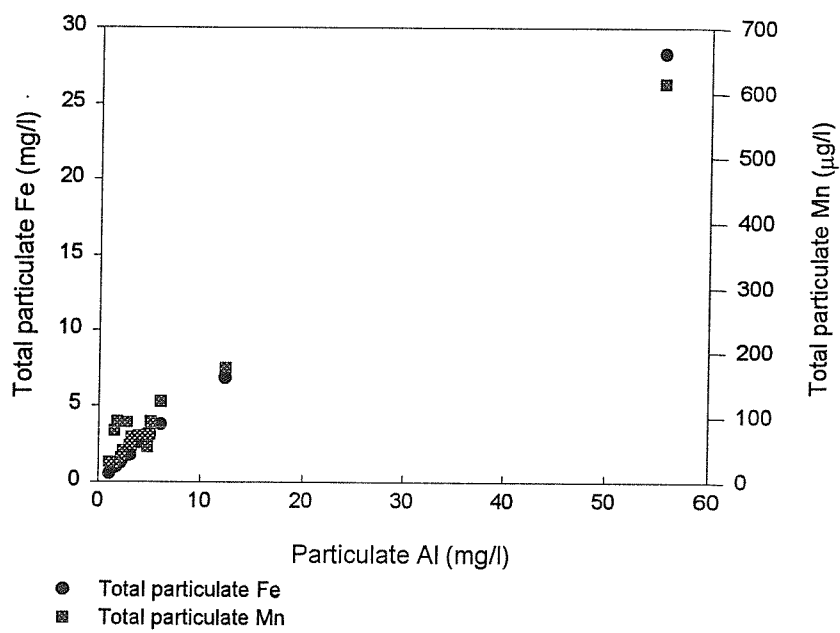


Fig. 4.12: Total particulate Mn and Fe versus particulate Al

coprecipitation by Fe- and Mn- oxides, and coagulation of colloids. Suspended particulate matter therefore largely influences the extent to which dissolved elements are transported out of the water column. Zinc, Cd, Ni, Cu and Pb can be adsorbed on surfaces of coated organics or metal oxyhydroxides or on surfaces of uncoated clays and oxides (Sung, 1995). Table 4.4 gives the correlation coefficient for total particulate trace metals (Pb, Cd, Zn, Ni, Cu) with total particulate Al, Fe, Mn and particulate organic carbon. Particulate trace metals (Pb, Cd, Zn, Ni, Cu) have high correlation coefficients with particulate Al, Fe and Mn, and low correlation coefficients with particulate organic carbon, suggesting that Pb, Cd, Zn, Ni, Cu are mainly associated with aluminosilicates and Fe- and Mn- oxyhydroxides.

Table 4.4: Correlation coefficients (r^2) between particulate trace metals and particulate Al, Fe, Mn and organic carbon in the River Po.

	Pb	Cd	Zn	Ni	Cu
Al	0.8348 n=22	0.9550 n=22	0.9069 n=22	0.9957 n=22	0.9561 n=22
Fe	0.8445 n=22	0.9553 n=22	0.9154 n=22	0.9951 n=22	0.9626 n=22
Mn	0.8619 n=22	0.9492 n=22	0.9187 n=22	0.9863 n=22	0.9528 n=22
Organic carbon	0.4459 n=18	0.0652 n=18	0.3793 n=18	0.3463 n=18	0.2285 n=18

For dissolved trace metals (Cu, Ni, Cd, Zn, Co, Pb), if samples which were collected in July 1994 and February 1995 are considered, concentrations are higher in winter than in Summer for Cu, Ni, Zn, Cd and Pb by respectively a factor of 1.5, 1.8, 1.5, 7.2 and 2.6. For Co, summer concentrations are similar to winter concentrations. There is no strong relationship between the flow rate and dissolved trace metal concentration in the River Po although we can say that concentrations tend to be higher during low flow regime of the River Po.

4.5 Trace metal distribution in the Northern Adriatic Sea

4.5.1 Manganese

Dissolved manganese concentrations are relatively high in this coastal environment, and concentrations vary from 10 nM to 200 nM with general increases towards the sediment

interface (Fig. 4.13). Manganese can have a large natural riverine source, but in this environment, there is no clear conservative mixing between Po and Northern Adriatic waters; and the metal-salinity diagram suggests significant sources of manganese from the shelf. The high concentrations seem attributable to mobilisation of dissolved manganese from particulate material either in suspension or in bottom sediments.

In May 1994, dissolved Mn concentrations vary between 10 and 60 nM. Dissolved Mn maxima are found around the pycnocline suggesting reduction of MnO_x is occurring. However O_2 concentrations are not particularly low, the oxygen saturation varying between 102 and 108 %, consequently it is not likely that bulk water conditions favour the release of Mn by dissolution of MnO_x phases. Some reduction may occur in microenvironments in the dominantly oxic medium. In the stratified water column of the spring and summer months, polymeric exudates and dead phytoplankton cells aggregate into either loose masses of mucus (mucilage) or large flakes (marine snow) around the pycnocline. These are rapidly colonized by bacteria and scavenge large quantities of inorganic and organic materials. As the aggregates accumulate around the pycnocline, bacteria feeding on it gradually use up the oxygen. This explains how suboxic conditions can be brought about by metabolic processes at the pycnocline and induce reduction of Mn(IV). Dissolved Mn concentrations also increase near the bottom suggesting benthic inputs. Particulate Mn concentrations vary between 5 and 100 nM with increases near the bottom which could be due to reprecipitation of Mn(II) in presence of oxygen and/or to resuspension.

In June 1994, dissolved Mn concentrations vary between 10 and 200 nM. At Station 1 there is a maximum in dissolved Mn at the pycnocline and at Stations 2 and 3 dissolved Mn concentrations increase below the pycnocline, suggesting the use of the MnO_x phase in the oxidation of organic matter within the “marine snow” since oxygen saturation varies between 120 and 130% around the pycnocline. Dissolved and particulate Mn concentrations also increase near the sediment-water interface at Stations 1, 2 and 3. This is associated with oxygen saturation of 30 % at Station 1 and 90 % at Station 2. In addition, the pore water profiles show increases of Mn^{2+} in the surface layer of the cores (Stations 1, 2, 3 respectively 63 μM , 52 μM , 141 μM) suggesting reduction of MnO_x to Mn(II) is occurring during remineralization of organic carbon. Dissolved manganese diffuses from the sediment into the

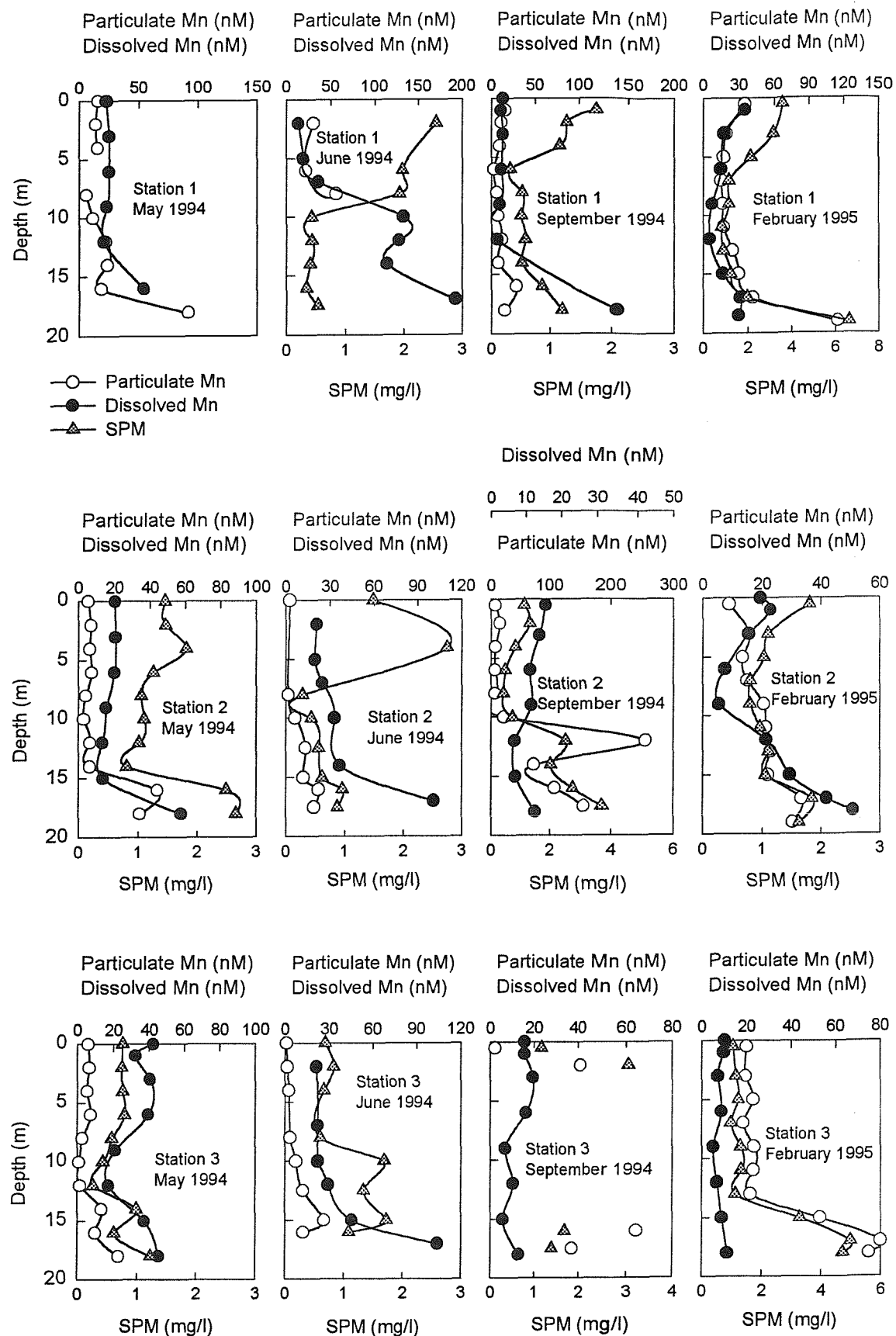


Fig. 4.13: Dissolved and Particulate Mn in the Northern Adriatic Sea

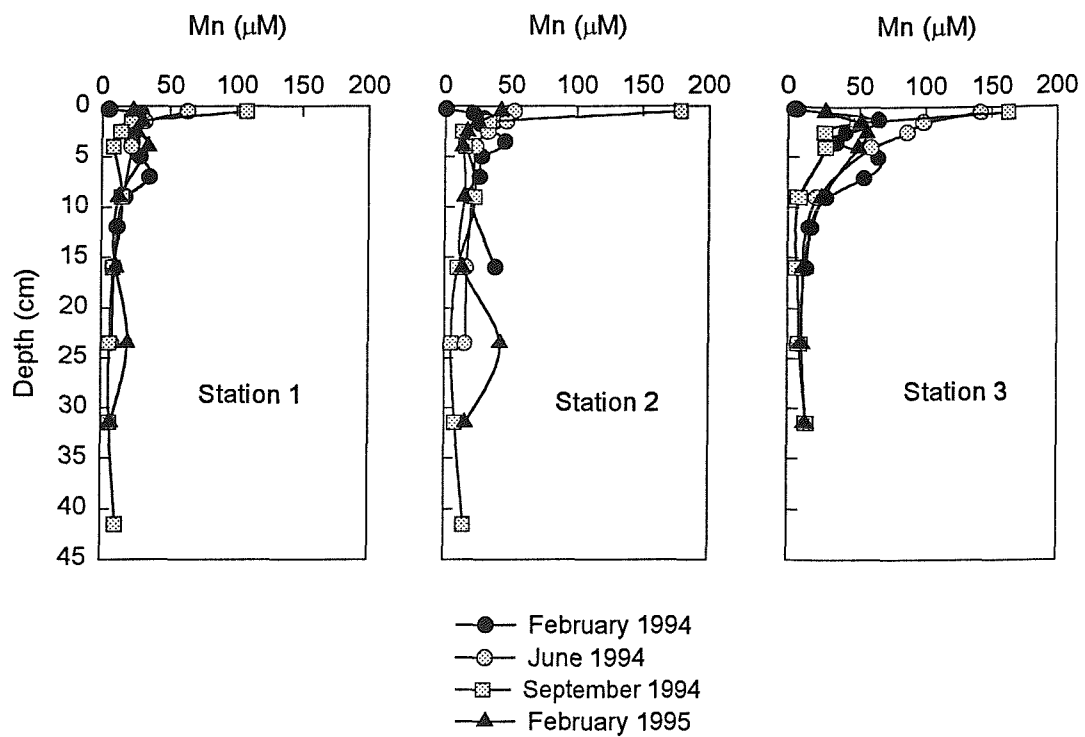


Fig. 4.14: Mn in pore waters in the Northern Adriatic Sea

water column and reprecipitates as MnO_2 due to the presence of oxygen inducing high concentrations in both dissolved and particulate Mn.

In September 1994, dissolved Mn concentrations tend to be lower than in June 1994 (10-150 nM), whereas particulate Mn concentrations tend to be higher (2-200 nM). Small maxima in dissolved Mn are found at the thermocline at Stations 2 and 3. These are also possibly due to reduction of MnO_x by bacteria within the mucilage or marine snow accumulated at the thermocline. However pore water profiles show increases of Mn^{2+} which are higher than in June 1994 at the surface of the core (Stations 1, 2 3 respectively 107 μM , 179 μM , 163 μM) suggesting that anoxic conditions in the sediment surface are more pronounced in September 1994 than in June 1994. With the breakdown of the water column stability occurring in the autumn, the organic-rich aggregates accumulated at the pycnocline, sink down the water column, carrying with them high concentrations of micro-organisms embedded in their anoxic matrix. This leads to a rapid drop in O_2 concentrations at the sediment-water interface. Justic *et al.* (1993) also found that minima of oxygen (saturation 20%) appeared in bottom waters of the Northern Adriatic Sea periodically in September. Particulate Mn concentrations are relatively high near the bottom which may in part be due to precipitation of Mn(II) in presence of oxygen outside the reducing organic rich micro-environments. The particulate Mn increase may also be enhanced by resuspension as suggested by the good correlation of SPM and particulate Mn at Stations 2 and 3.

In February 1995, dissolved Mn concentrations are relatively low and vary between 5 and 50 nM. The increases near the bottom are much less in amplitude than in summer or autumn, suggesting low benthic inputs. In February 1994 and 1995, Mn^{2+} pore water profiles show low concentrations in the surface layer of the cores (Stations 1, 2 and 3). This may be explained by the fact that the oxygen penetration depth in winter may be deeper than during the summer period in the surface of the core and consequently Mn^{2+} is oxidised. Giordani *et al* (1994) measured NH_4^+ in the pore waters of the same cores for February 1994 and June 1994 for Station 1, and found that NH_4^+ was more depleted in the surface of the core in February 1994 than June 1994. This data suggests reducing conditions in the surface of the cores are stronger in summer than in winter. The high concentrations of Mn^{2+} between 3 and 10 cm in February 1995 show that reducing conditions are still present at those depths during winter. Particulate

Mn concentrations are relatively high in February 1995 and increase near the bottom. The relatively high concentrations in the water column are possibly due to advective transport of particulate material which has been resuspended. Increases near the bottom are possibly due to resuspension of sediment material.

4.5.2 Iron

Samples for dissolved iron collected at Station 3 in February 1995 and at Station 1 in May 1994 may have been contaminated since dissolved Fe concentrations are not oceanographically consistent (Fig. 4.15). Surface samples are elevated and are away from the general trend in the absence of major changes (obvious sources) in the water mass structure.

Iron is also a redox sensitive element and consequently there are marked similarities in the distribution of Fe and Mn. Dissolved Fe concentrations are much lower than those of Mn and vary from 0.5 nM to 15 nM whereas particulate Fe concentrations are much higher than those of Mn, and vary between 50 nM and 4500 nM (Fig. 4.15). This is probably due to the quicker oxidation and precipitation of soluble iron species in the presence of oxygen relative to Mn (Stumm and Sulzberger, 1992). As for Mn, samples taken from bottom waters have higher dissolved Fe concentrations and suggest that there is an important release of dissolved Fe from the sediment-water interface which is possibly due to reduction of Fe-oxides by bacteria during mineralization of organic carbon (Lovley and Phillips, 1988; Nealon and Myers, 1990). The formation and precipitation of iron oxides also take place at the oxic-anoxic water interface giving rise to particulate Fe maxima above the bottom.

The distribution of Fe varies seasonally and depends on the oxygen distribution within the water column, cycling and benthic inputs. In spring the water column is well oxygenated. The deposition of the spring blooms, despite being the largest carbon input event of the year, does not cause anoxia. Very high particulate Fe concentrations were observed with relatively low dissolved Fe concentrations. During summer, the water column becomes stratified, inducing suboxic conditions within the marine snow and mucilage accumulated at the thermocline through microbial respiration, and lower oxygen concentrations, which reach the annual minimum in late summer, near the bottom. This led to increasing dissolved Fe concentrations

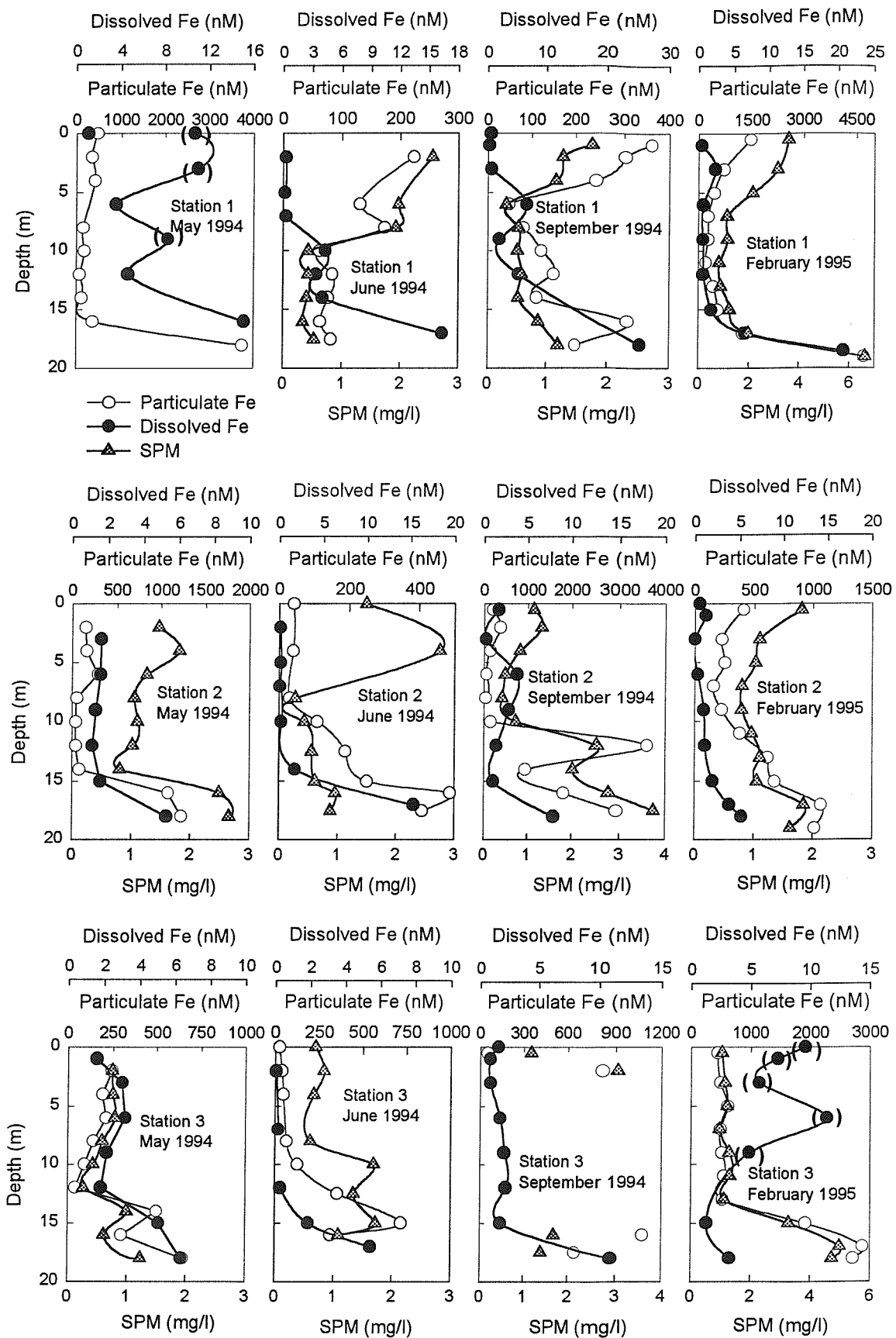


Fig. 4.15: Dissolved and particulate Fe in the Northern Adriatic Sea, () indicates suspect data (see text)

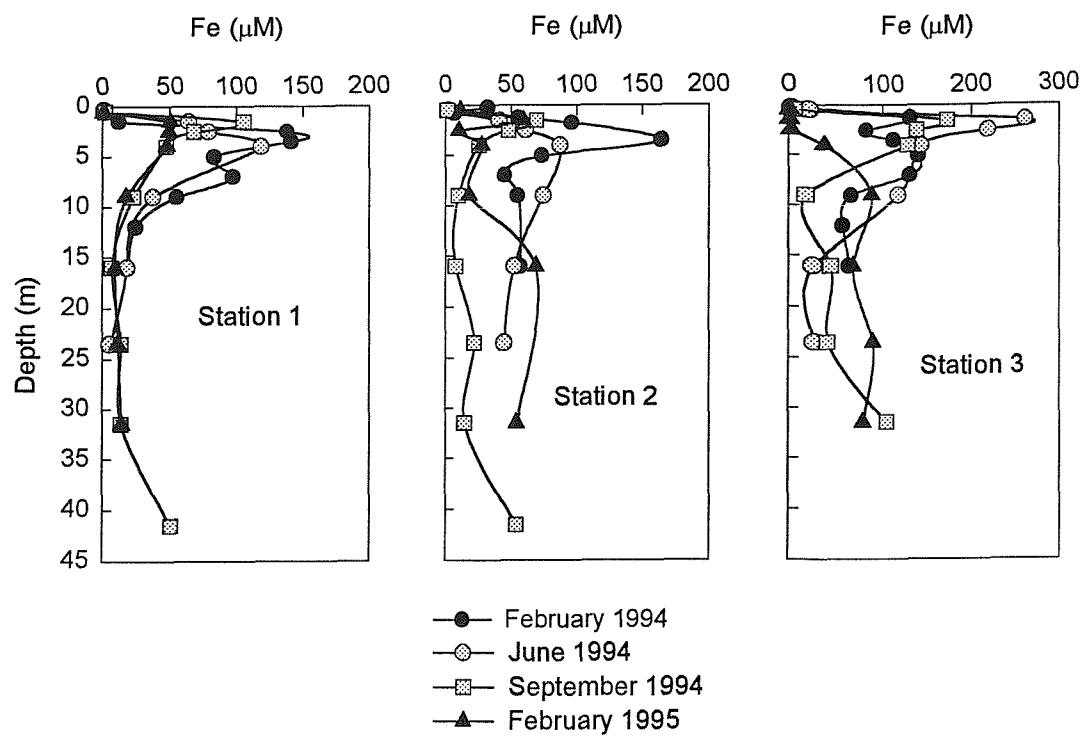


Fig. 4.16: Fe in pore waters in the Northern Adriatic Sea

in the lower part of the water column from May 1994 to September 1994. Small maxima in dissolved Fe were found at the thermocline (Station 3, May 1994; Station 1, June 1994; Stations 1, 2, 3, September 1994). These mid water column features are possibly due to reduction of Fe-oxides within the marine snow or mucilage. Nealson and Myers (1990) suggested that certain micro-organisms act as catalysts for the oxidation of organic matter coupled to the reduction of Fe(III) oxides. Higher dissolved Fe concentrations were also found near the bottom and are possibly due to benthic inputs. The relatively high Fe particulate concentrations near the bottom in September 1994 are possibly due to rapid oxidation of Fe(II) in presence of oxygen and to resuspension of iron enriched sediments. In winter, mixing of the water column with storms break down the stratification of the water column and aerates the water column and the sediments. Consequently dissolved Fe concentrations decrease rapidly and particulate Fe concentrations tend to increase.

Fig. 4.16 shows profiles of iron in pore waters collected in February 1994, June 1994, September 1994 and February 1995. At Station 1, Fe^{2+} profiles can be divided in 2 groups. In February 1994 and June 1994 profiles are very similar in shape: surface concentrations are low (0.8-1.0 μM) and there are maxima of 120-130 μM between 3 and 10 cm. In September 1994 and February 1995 profiles have similar shapes but the maxima appear at about 3 cm deep in the core and are much lower in concentration (50-100 μM). This suggests that there are changes in the redox conditions of the sediment between June 1994 and September 1994. Violent storms hit the north of Italy in August 1994 and the beginning of September 1994. These storms may have induced resuspension of sediments and modified their transport, and consequently may have changed the redox conditions in the surface of the core, the oxygen penetration having probably increased. At Stations 2 and 3 similar observations can be made, Fe^{2+} concentration maxima in February 1994, June 1994 and September 1994 tend to be higher than in February 1995 suggesting a shallower oxygen penetration depth before February 1995.

At Stations 1 and 2, higher particulate Fe concentrations are also found in surface waters. These are due to the River Po inputs. Iron as ferric hydroxide appears as the major carrier phase of particulate trace metals (Section 4.4) in the River Po.

4.5.3 Cobalt

Cobalt has only been measured in the dissolved phase. Dissolved Co concentrations vary from 0.3 to 1.1 nM. These concentrations are higher than those found in the Gulf of Lions by Morley *et al.* (1992) and suggest important benthic or riverine inputs. Dissolved Co concentrations are higher near the mouth of the River Po and decrease southwards, the influence of the Po being weaker (Fig. 4.17). On the metal-salinity diagram, the slope of the mixing line between the Po river water and the NAW appears to change at 35 psu and some data points lay above the general trend. This may be evidence for additional inputs. Benthic inputs do not appear as significant as for manganese and iron but may influence distribution as there is an increase in Co concentrations towards the bottom. Manganese cycling near the sediment-water interface may influence the cobalt distribution (Sundby *et al.*, 1986; Chiffolleau *et al.*, 1994). Cobalt can be adsorbed onto Mn-oxides and under low oxygen concentration may be released into the water column as manganese oxides are reduced to Mn(II). Since the distribution of Co is coupled with manganese cycling, a seasonal variation in the cobalt distribution is expected and the highest cobalt concentrations have been found in September 1994 when bottom waters are suboxic/anoxic (see section 4.3.2).

4.5.4 Lead

Lead is mainly associated with the particulate phase (Fig. 4.18). In the Northern Adriatic Sea, dissolved Pb concentrations vary from 0.04 nM to 0.75 nM whereas particulate Pb concentrations vary from 0.1 nM to 7.2 nM. These observations may be ascribed to efficient scavenging of lead from solution onto particles (Mart *et al.*, 1982; Balls, 1985, 1988). Pb concentrations in both dissolved and particulate phases are higher in February 1995 than in the other seasons. A similar seasonal pattern has been observed in the North Sea (Tappin *et al.*, 1995). In the coastal zones of the North Sea, the winter enrichment in particulate Pb was attributed to both estuarine inputs and resuspension of sediments enriched in Pb. In the Northern Adriatic Sea, dissolved Pb concentrations are rather uniform with depth except at Stations 1 and 2 in February 1995 where there is an increase near the bottom which is associated with an increase in particulate Pb concentrations. This may be due to benthic

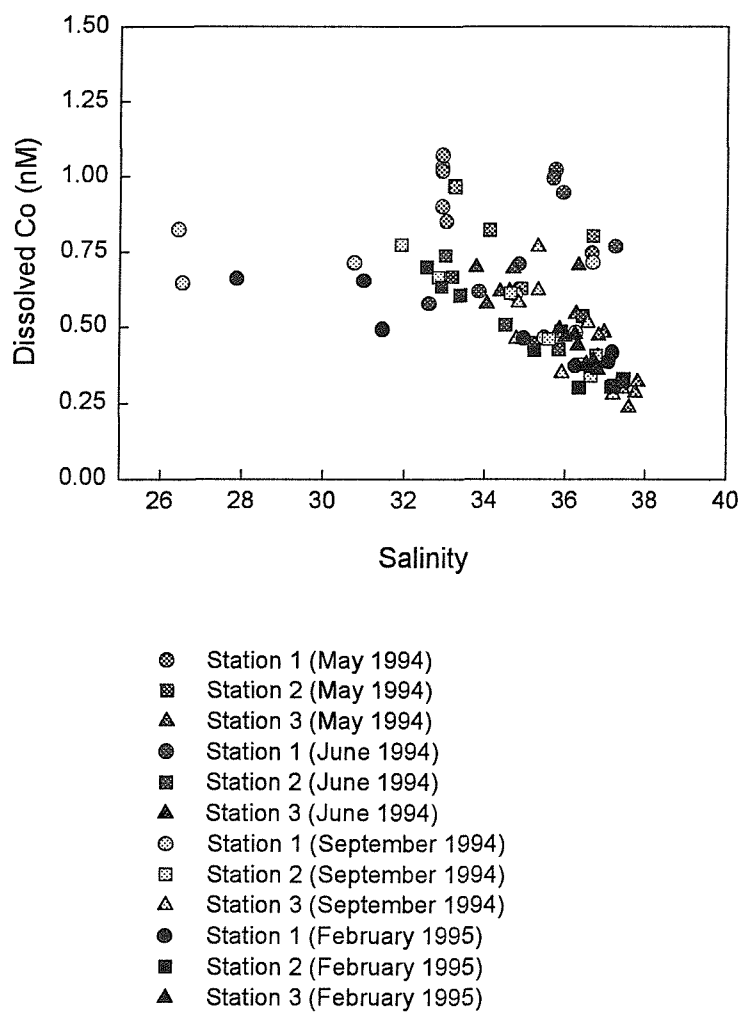


Fig. 4.17: Dissolved Co versus salinity in the Northern Adriatic Sea

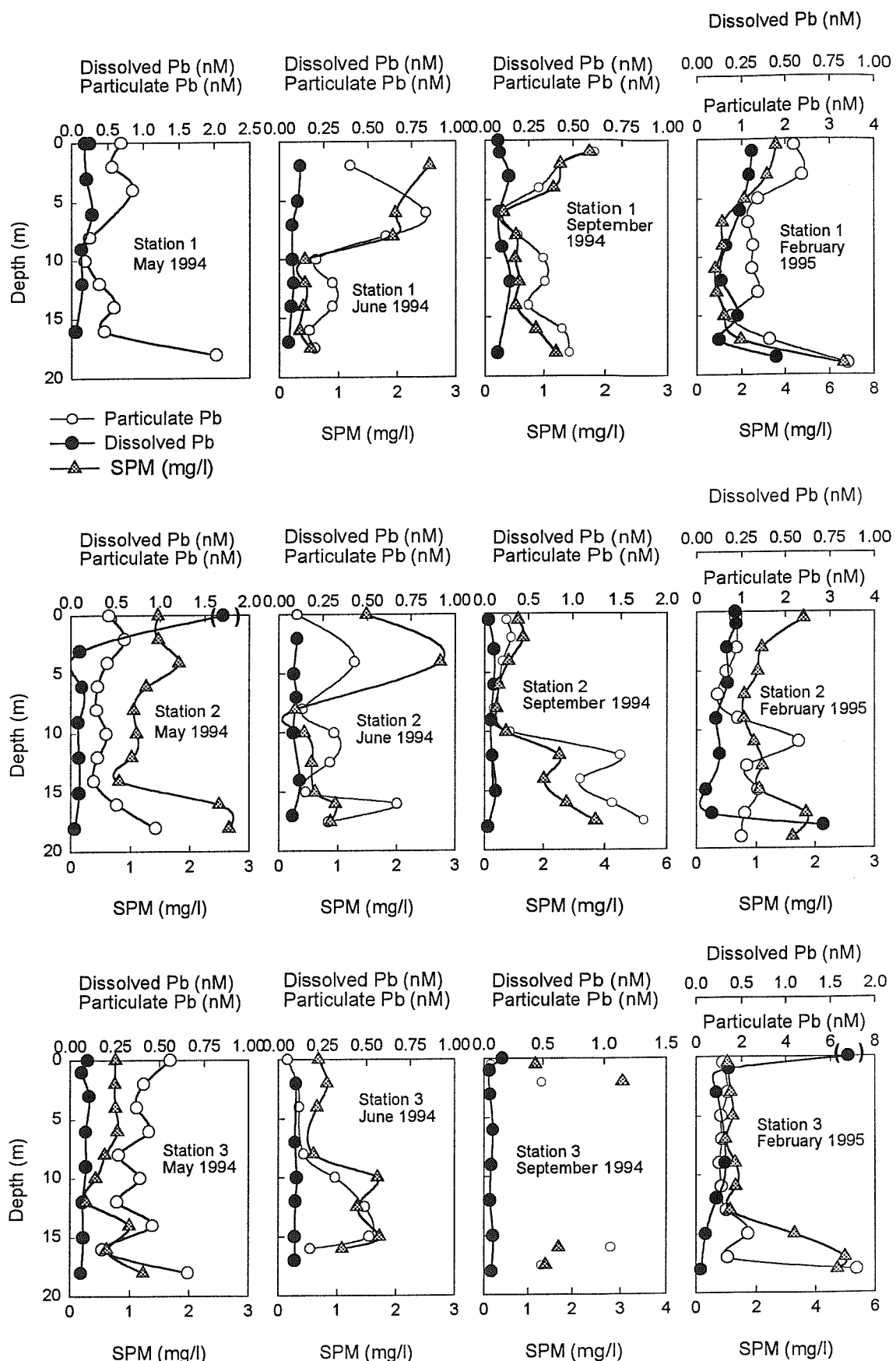


Fig. 4.18: Dissolved and particulate Pb in the Northern Adriatic Sea, () indicates suspect data

inputs linked to Mn and Fe cycling. Although the winter mixing aerates the water column and sediments, resuspension and redeposition of organic matter (winter inputs) may create suboxic episodes during the winter season. Lead which is adsorbed onto Mn- and Fe- oxides may be released from the sediment because of the reduction of the Mn- and Fe- oxide carrier phases. This dissolved Pb may be quickly re-adsorbed onto newly formed Fe- and Mn- oxides in the oxic-anoxic interface creating a maximum in particulate Pb concentrations. Particulate Pb distributions show maxima in surface waters and in bottom waters at all Stations. Maxima in surface waters are due to riverine inputs. In section 4.4, it was suggested that Pb is mainly associated with alumino-silicates and Fe- and Mn- oxyhydroxides in the suspended particulate material of the river Po which is transported southwards along the Italian coast. Particulate Pb maxima without maxima in the dissolved phase near the bottom may be explained by the resuspension phenomenon or/and Mn and Fe cycling. The low dissolved Pb concentrations may be due to rapid adsorption onto Mn- and Fe- oxides.

4.5.5 Cadmium

In the northern Adriatic Sea, Cd concentrations vary from 0.08 nM to 0.22 nM (Fig 4.19). These values are similar to the average value found in the North Western Mediterranean Sea (Morley *et al.*, 1990). Profiles of dissolved Cd (Fig. 4.19) show that dissolved Cd concentrations tend to be higher in surface water than in deep water. This is possibly due to strong riverine inputs from the River Po and/or atmospheric inputs. In May 1994 and February 1995, the Cd-salinity diagrams (Fig. 4.20) show conservative behaviour during mixing between the Po river water and the NAW. Nevertheless some other anthropogenic or natural inputs must be present as there are data points above the general trend in the metal-salinity diagrams. In May and February 1995, some of these points correspond to bottom water and may be due to release from resuspended sediments. Salomon (1978) has shown that in laboratory experiments, more than 50 % of Cd can be released from resuspended sediments. In May 1994 some elevated points correspond to surface water at Station 1 and reflect localised inputs other than riverine. In June 1994, dissolved Cd concentrations at Stations 2 and 3 are much lower than those at Station 1. This is possibly due to biological uptake or scavenging by Fe- and Mn- oxides which are present in relatively high concentrations at Stations 2 and 3 due to oxidation of Mn(II) diffused from the sediment- water interface.

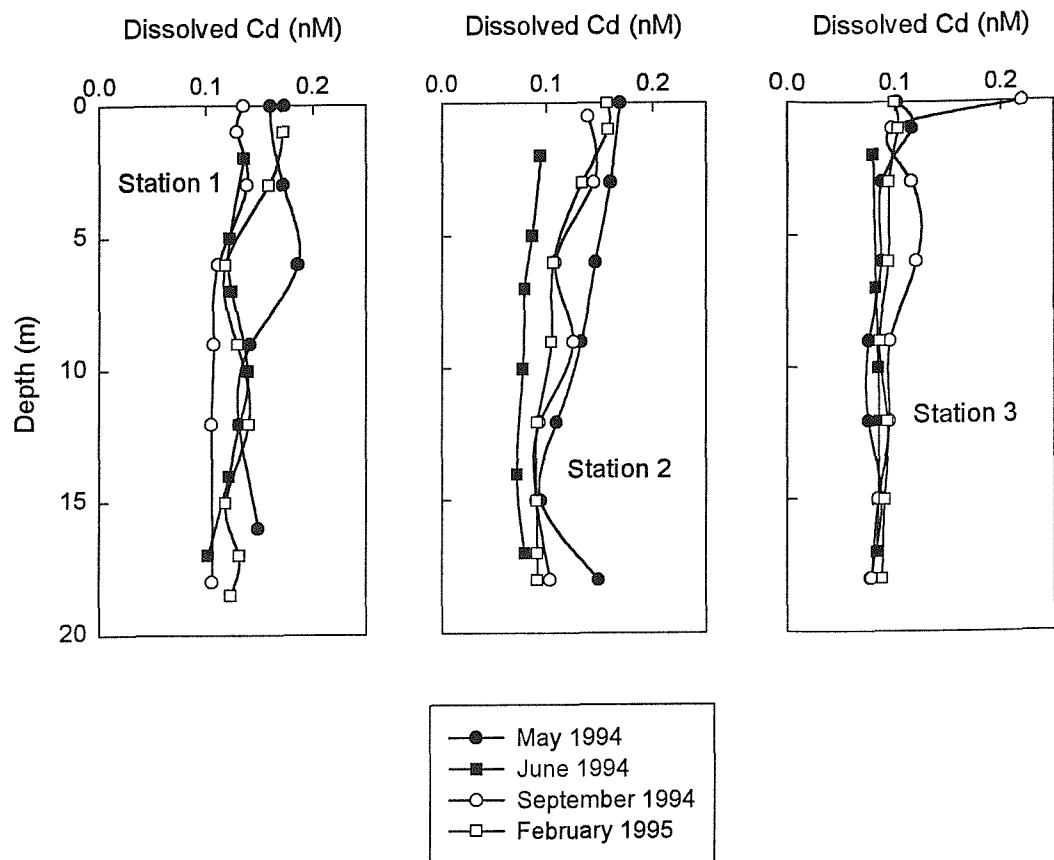


Fig. 4.19: Dissolved Cd in the Northern Adriatic Sea

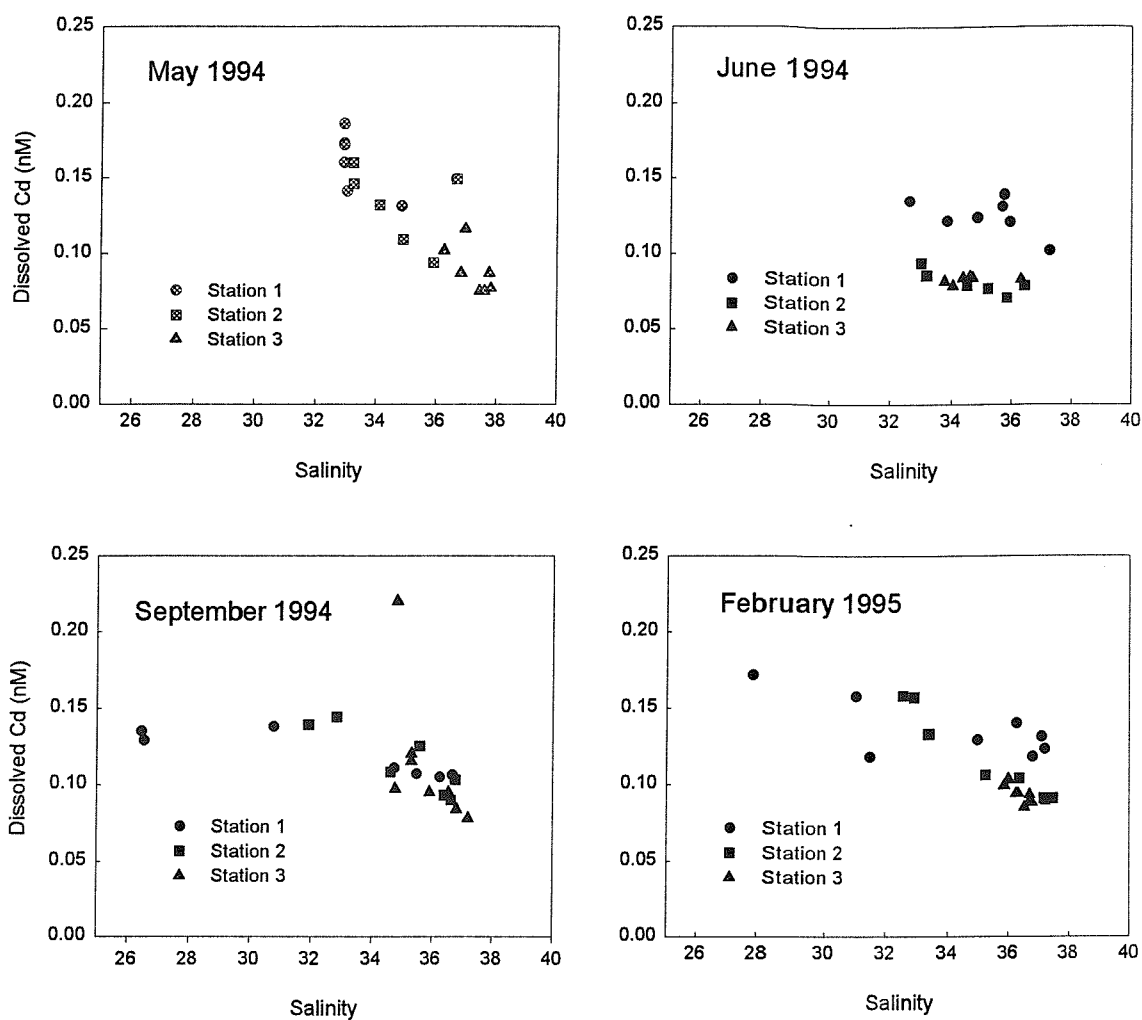


Fig. 4.20: Dissolved Cd versus salinity in the Northern Adriatic Sea in May 1994, June 1994, September 1994 and February 1995.

In September 1994, the Cd-salinity diagram exhibits a maximum in Cd concentration at a salinity of 33. The low Cd concentrations at salinity 26 are coincident with high concentrations of SPM and may be due to biological uptake or scavenging by other particles.

4.5.6 Zinc

Dissolved zinc concentrations varied from 2 nM to 10 nM in May 1994, June 1994 and September 1994 (Fig. 4.21). Martin *et al.*, (1994) found concentrations around 8.3 nM in the Venice Lagoon which are similar to that found in the River Po area. Higher concentrations are found in February 1995 and vary from 3 nM to 22 nM. Zn concentrations in the Northern Adriatic Sea are not significantly higher than in the western Mediterranean sea, where they are reported to be about 4-5 nM in the open-sea (Ruiz-Pino, 1991) and about 10 nM in the Gulf of Lions (Morley *et al.*, 1990). Dissolved Zn concentrations tend to be lower in surface waters during the spring-summer-autumn period when there is high productivity. This may be due to removal by biological activity. Hudson and Morel (1993) demonstrated that marine micro-organisms have systems capable of accumulating trace metals (Zn, Ni, Mn and Fe) present at low concentrations in the marine environment. This is consistent with higher particulate Zn concentrations in surface water. However, particulate concentrations at Stations 1 and 2 are higher than what is expected if the transfer from dissolved phase to particulate phase by biological activity is taken into account alone. The particulate Zn maxima in surface water may possibly be influenced by riverine or atmospheric inputs. As an example for calculations, Station 1 in February 1995 has been chosen. The dissolved and particulate Zn concentrations in the River Po are 70-86 nmol/l and 255 nmol/l respectively. The surface water salinity at Station 1 is 27.88 which corresponds to 26.6% of River Po water diluted with 73.3% of Adriatic Sea water. If the dilution process is taken into account alone, the surface concentrations at Station 1 would be 22 nM for the dissolved phase and 69 nM for the particulate phase. However 13.5 nM and 48 nM have been measured for dissolved phase and particulate phase respectively. The low dissolved Zn concentration could be due to transfer from the dissolved phase to the particulate phase and the low particulate Zn concentrations could be due to sedimentation. In the water column, Zn composition of particles vary between 256 and 981 µg/g. This large range reflects different particle origins.

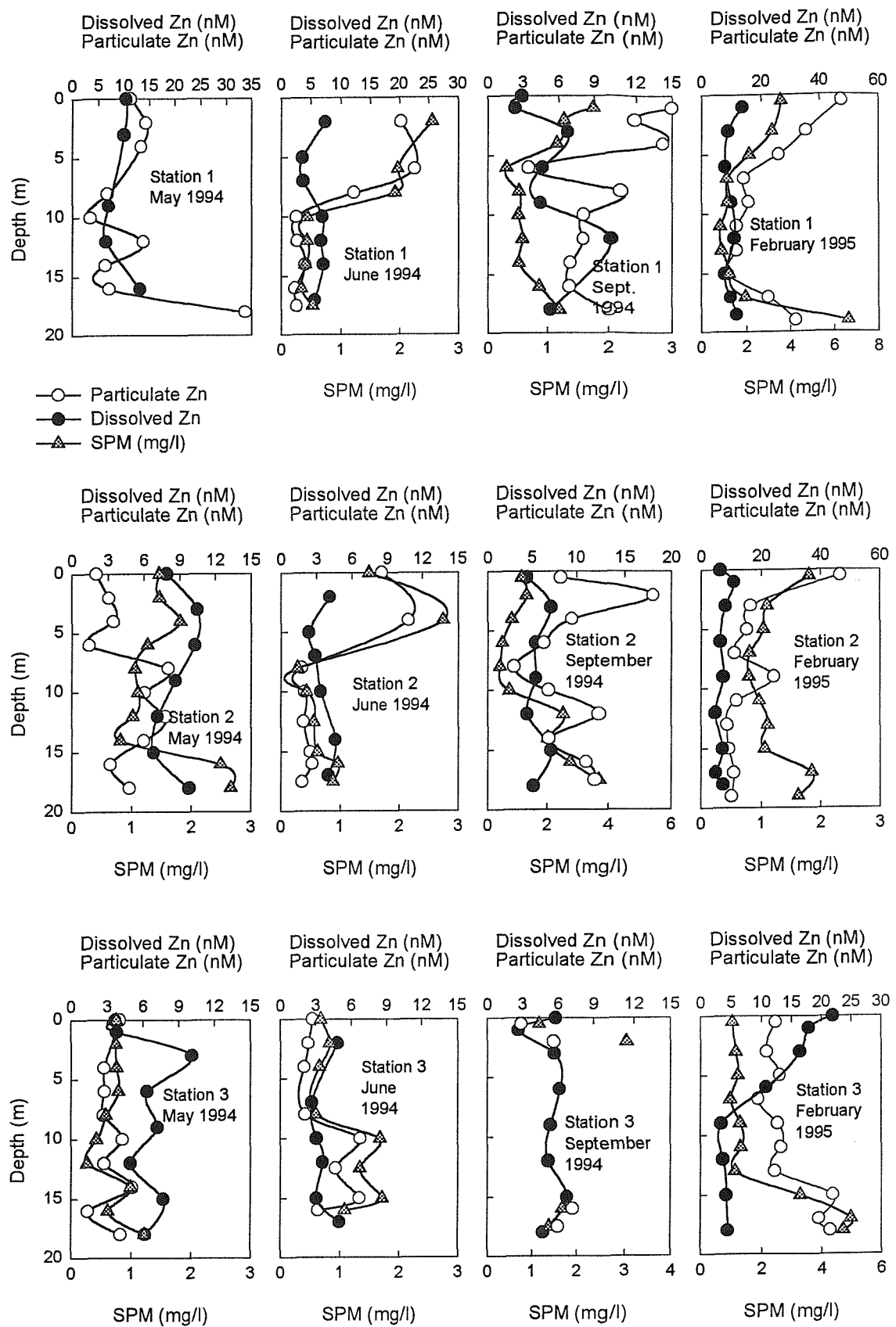


Fig. 4.21: Dissolved and particulate Zn in the Northern Adriatic Sea

Near the bottom, Zn composition of particles vary between 256 and 406 µg/g which is similar to the Zn composition of surface sediment (155-192 µg/g) in the Northern Adriatic Sea (Price *et al.*, 1993). This suggest that particulate Zn maxima near the bottom could be attributable to resuspension. Higher dissolved Zn concentrations have also been observed in bottom waters and may be due to benthic inputs (Westerlund *et al.*, 1986).

4.5.7 Copper

When approaching the river Po dissolved Cu concentrations in surface water increase and can reach 25 nM (Station 1, June 1994) suggesting strong riverine inputs (Fig. 4.22); below 3 m, dissolved Cu concentrations are essentially constant at circa 8 nM. The concentration decrease is essentially due to mixing with higher salinity water containing lower dissolved metal concentrations. On the metal-salinity diagrams (Fig 4.23), dissolved Cu shows generally conservative mixing between the two end members: river Po water and NAW. Several data points for dissolved Cu between salinities of 32 and 34 lie above the general trend of the metal-salinity diagram. These are surface samples and the elevated concentrations reflect higher Cu concentrations in river inputs associated with unusual high river flow when the water is highly stratified. In June and September 1994, dissolved Cu concentrations tend to vary between 8 and 9 nM and particulate Cu concentrations tend to vary between 0 and 3 nM whereas in May 1994 and February 1995 dissolved Cu concentrations are lower and vary between 5 and 6 nM with particulate Cu concentrations being higher varying between 1 and 12 nM. These observations suggest that scavenging of dissolved Cu by particles or the transfer of colloidal Cu into particulate phase by flocculation of colloids are more pronounced in May 1994 and February 1995 than in June and September 1994 when there is high productivity. Several authors found that Cu was preferentially tied to colloidal material (Donat *et al.*, 1994; Martin *et al.*, 1995). The stability of colloidal material in waters enriched in organic material (areas of intense productivity) may prevent the flocculation of colloids and consequently prevent the transfer of dissolved Cu to the particulate phase (Martin *et al.*, 1995). In Fig. 4.24, dissolved Cu concentrations have been plotted against dissolved organic carbon (DOC). Dissolved Cu correlates well with DOC at each season ($r^2 = 0.787$ for September 1994). Both elements are fairly conservative and have strong gradient in the mixing zone. The higher DOC concentrations in September reflects production of DOC from decomposing phytodetritus,

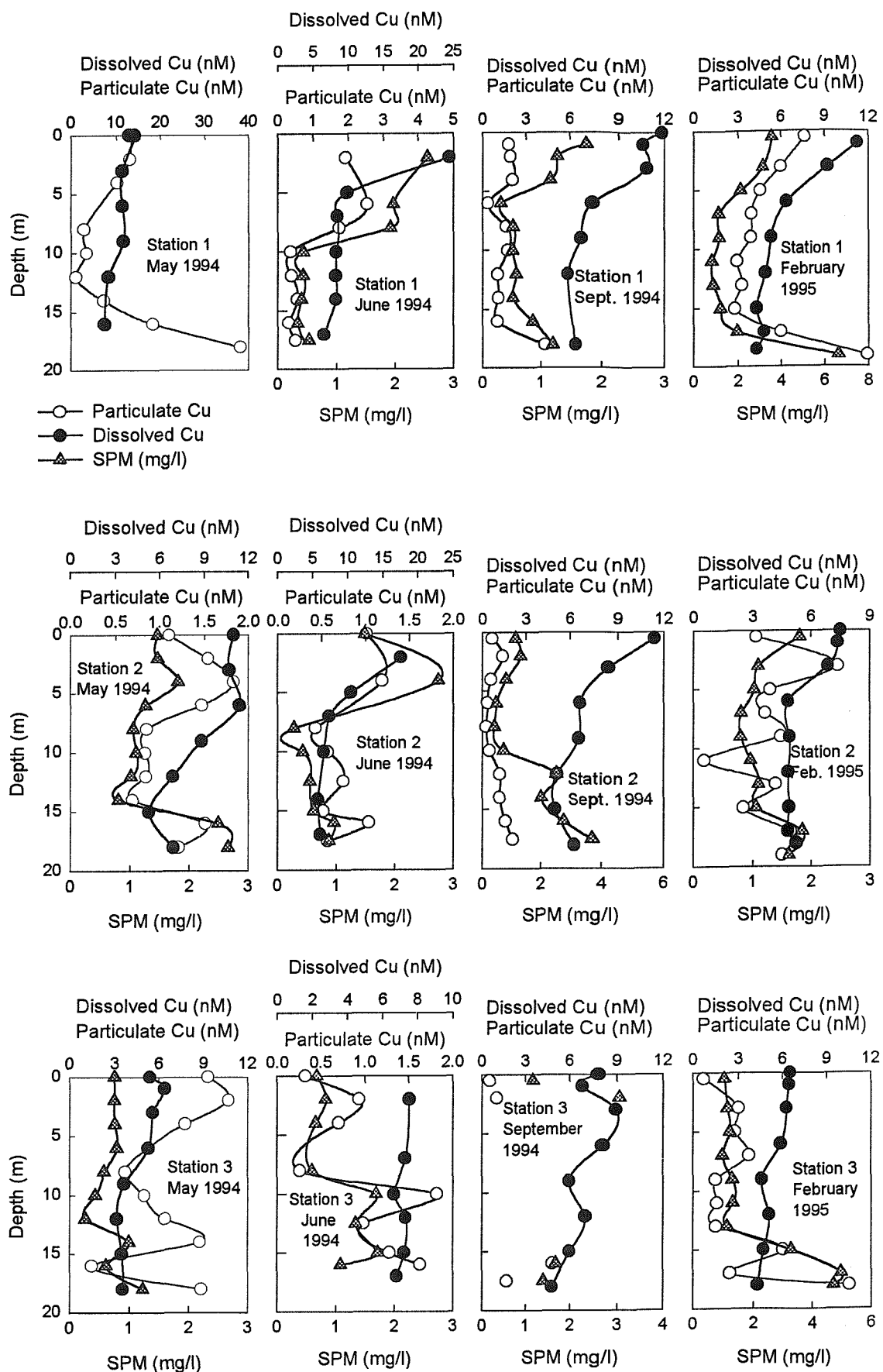


Fig. 4.22: Dissolved and particulate Cu in the Northern Adriatic Sea

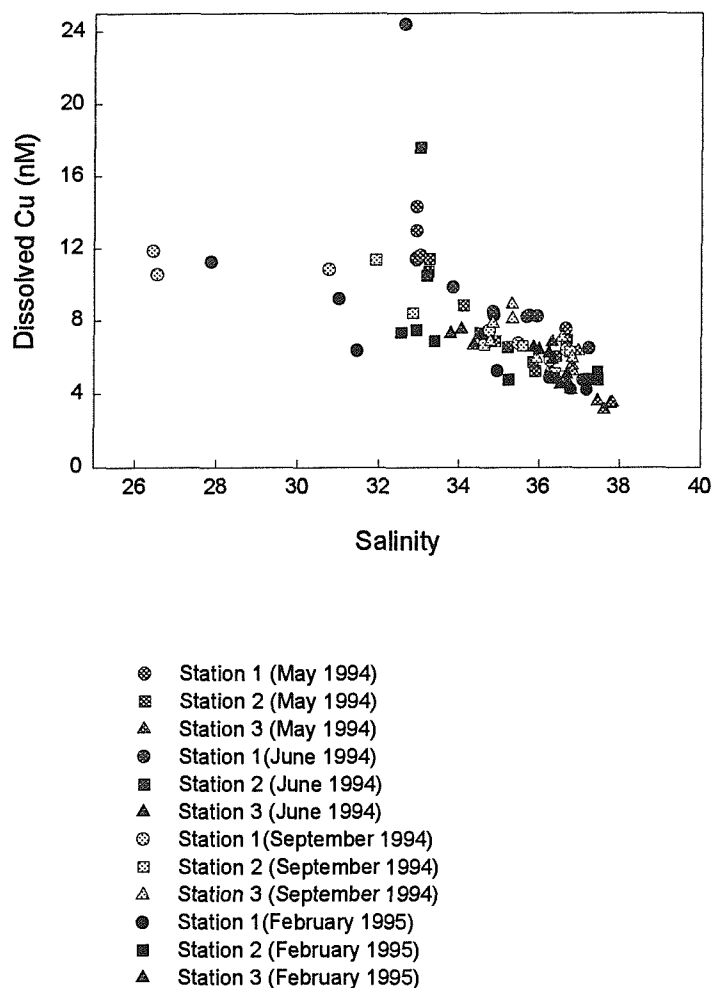


Fig. 4.23: Dissolved Cu versus salinity in the Northern Adriatic Sea

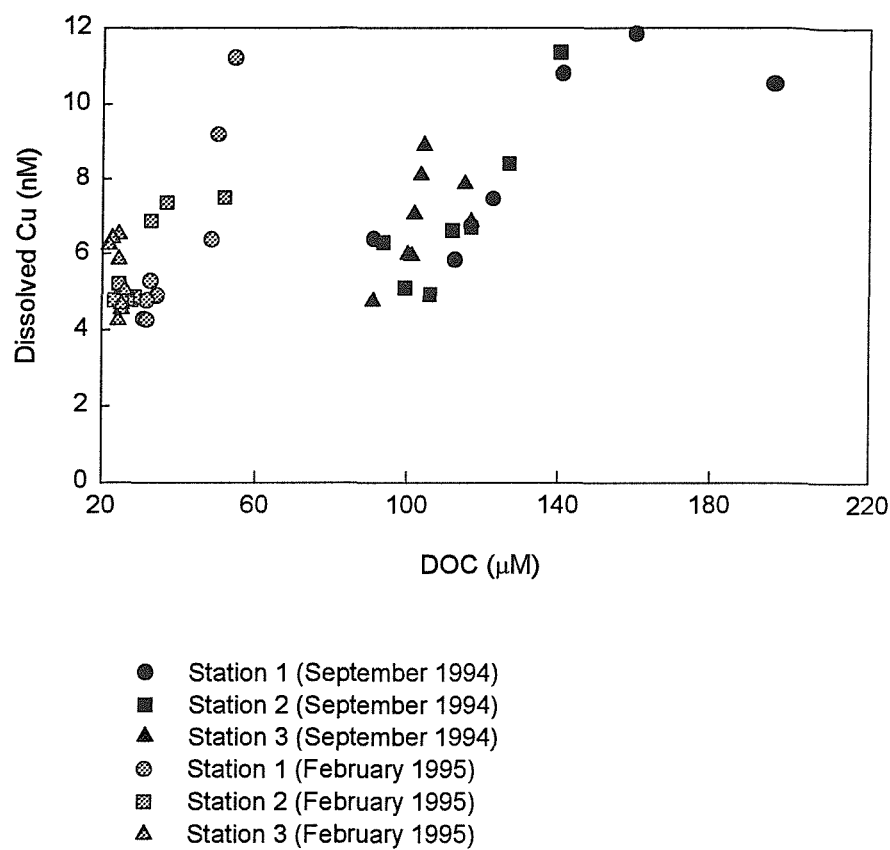


Fig. 4.24: Dissolved Cu versus DOC in the Northern Adriatic Sea

which are metabolised or diluted away by the following February. Particulate Cu profiles show maxima in surface water and near the bottom. Particulate Cu is delivered to the coastal zone by the Po and smaller rivers on the north-western Adriatic coast mainly associated with alumino-silicate and Mn- and Fe- oxyhydroxides (Table 4.3). These inputs cause maxima in surface waters which decrease in a southward direction. Maxima of particulate Cu near the bottom is attributable to resuspension. Maxima are highest in May 1994 and February 1995 when meteorological conditions are favourable to resuspension.

4.5.8 Nickel

Dissolved Ni concentrations vary between 6 nM and 22 nM (Fig. 4.25). Higher concentrations are found in surface water and appear to be due to riverine inputs. Dissolved Ni concentrations tend to be higher in May and June 1994. On the metal-salinity diagram Ni show conservative mixing between the two end members: the Po River and the NAW (Fig. 4.26). The different mixing lines show that there is seasonal variations of the two end-members. Conservative behaviour has also been reported by Windom *et al.*, (1991) for well mixed estuaries, by Shiller and Boyle (1991) for the Mississippi plume, and by Althaus (1992) for the Humber-Wash plume. This lack of particle-reactivity contrasts markedly with the recycled behaviour of the metal in oceanic environment (see Section 1.1.4) reflecting differences in the time-scale of processes and in concentrations. Particulate Ni concentrations vary between 0.5 nM and 10 nM and tend to be higher in February 1995 than in May, June and September 1994. Higher particulate concentrations are found in surface water and near the bottom. In surface water this may be due to riverine inputs (Po river and Northern Adriatic rivers) whereas near the bottom this may be due to resuspension. In Fig. 4.26, dissolved Ni concentrations have been plotted against DOC. As for Cu, there is a good correlation between dissolved Ni concentrations and DOC. This good correlation could be coincidental, reflecting that both elements have the same riverine source and behave conservatively in the mixing zone. However, Martin *et al.*, (1995) observed that Ni was mainly associated with ultrafiltrated organic carbon. Van den Berg and Nimmo (1987) and Nimmo *et al.*, (1989) found that 30 to 50% of dissolved Ni in the U.K. coastal waters was bound in extremely strong organic complexes. In waters rich in organic material, Ni may form some inert chelate

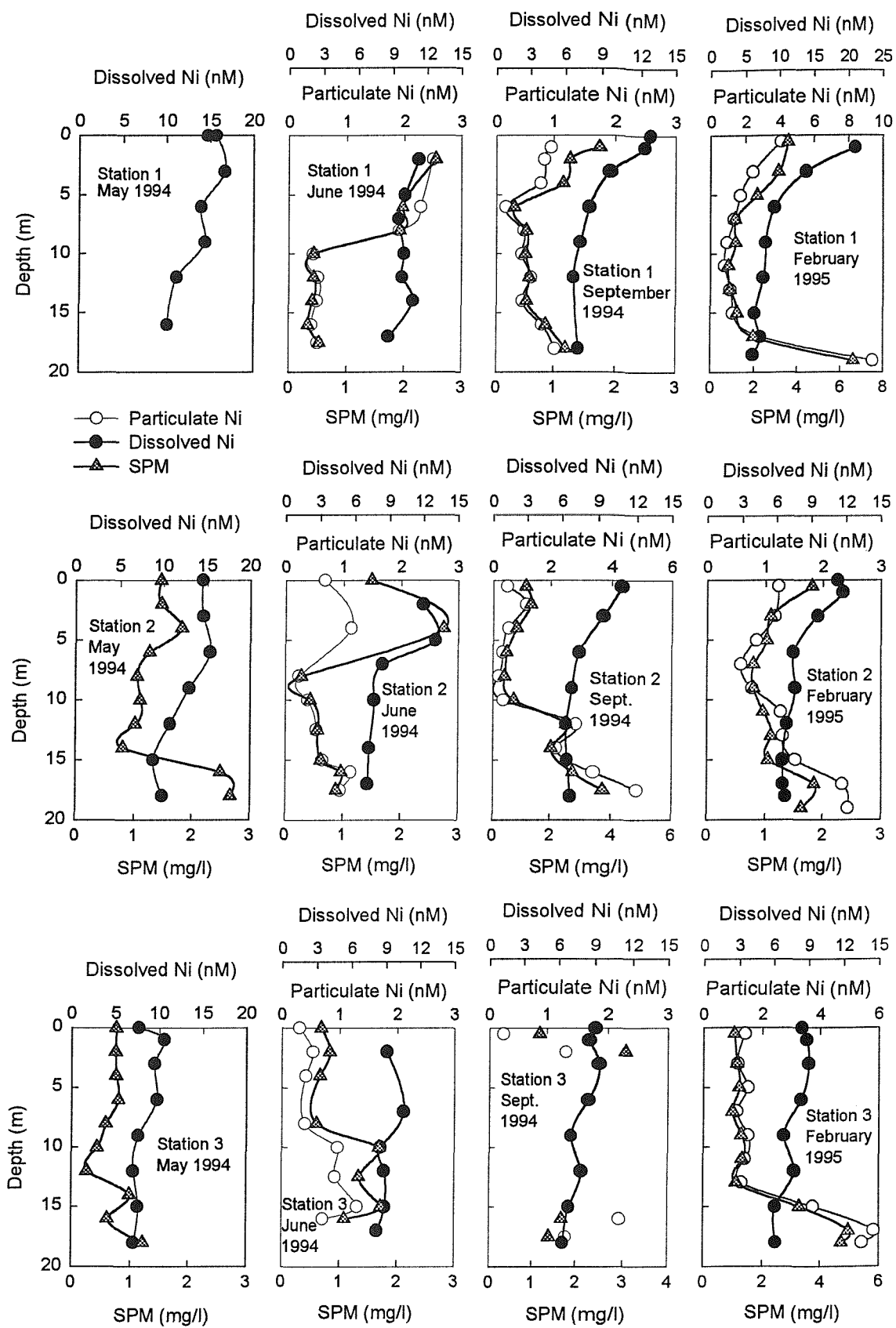


Fig. 4.25: Dissolved and particulate Ni in the Northern Adriatic Sea

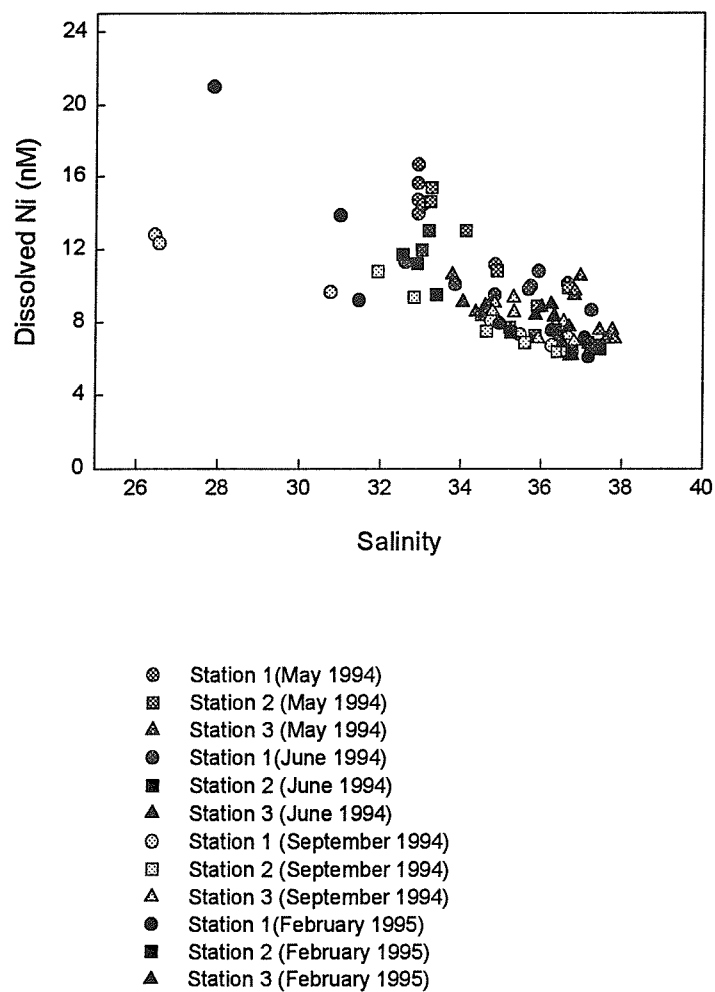


Fig. 4.26: Dissolved Ni versus salinity in the Northern Adriatic Sea

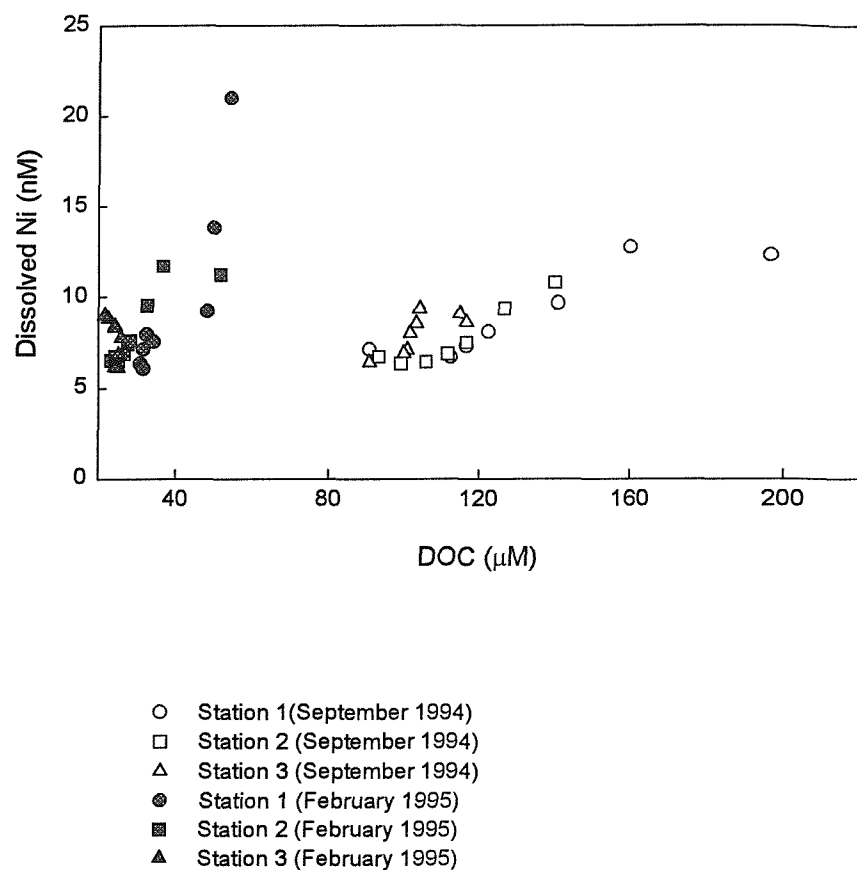


Fig. 4.27: Dissolved Ni versus DOC in the Northern Adriatic Sea

or macrocyclic complexes that react slowly against scavenging and consequently higher dissolved Ni concentrations can be observed simultaneously with lower particulate concentrations.

4.6 Trace metal distribution in the central Adriatic Sea

4.6.1 Manganese and iron

At Station 4, dissolved and particulate Mn have similar distributions (Fig. 4.28). High concentrations are found in surface water (32 nM for dissolved Mn and 22 nM for particulate Mn) then concentrations decrease rapidly down to 30 m to reach 10 nM for the dissolved phase and 1 nM for the particulate phase. The higher concentrations in surface water in both dissolved and particulate phases are most probably due to atmospheric and riverine inputs and to advective transport from the Northern Adriatic Sea. The Mn-salinity diagram (Fig. 4.29) shows the importance of inputs other than riverine since the mixing line between the River Po water and the Adriatic Sea water is well above the theoretical dilution line. The surface layer (first 30 m) originates from the North Adriatic Sea where eutrophication and resuspension phenomena induce high concentrations in Mn. This water mass flows southward pressed against the slope of the western coastal shelf forming a vein of water which flows along the isobaths. Below 30 m, the water mass has a different origin, salinity is higher and characteristic of the Mixed Adriatic Water. This water mass has lower dissolved and particulate Mn concentrations. Because of the strong summer stratification there is no mixing between the surface layer (NAW) and the deeper water mass (MAW). Near the bottom, dissolved and particulate Mn concentrations increase from 8 nM to circa 18 nM. The relatively high dissolved Mn concentrations observed near the bottom could be due to diffusive inputs from the sediment-water interface. The summer stratification may also cause an oxygen depletion which could lead to an increase in dissolved Mn inputs from the sediment. This has also been observed in the California margin by Johnson *et al.*, (1992). The particulate increase could be attributed to resuspension of sediment material and precipitation of Mn(II) in presence of oxygen.

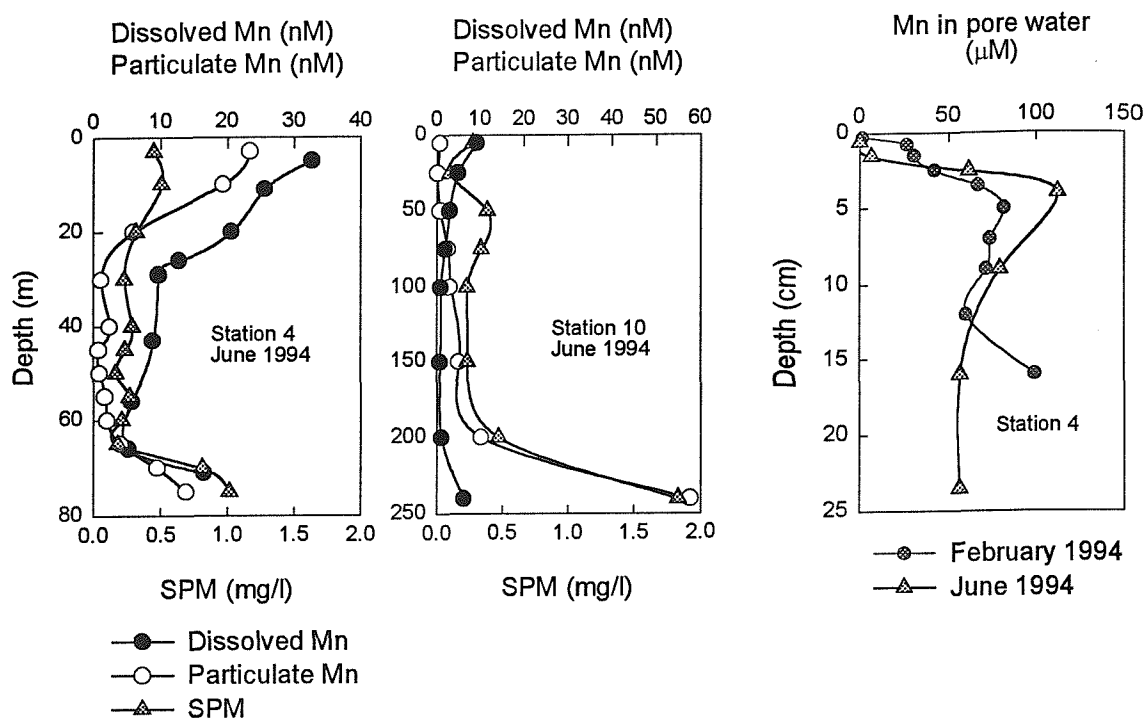


Fig. 4.28: Manganese in the central Adriatic Sea

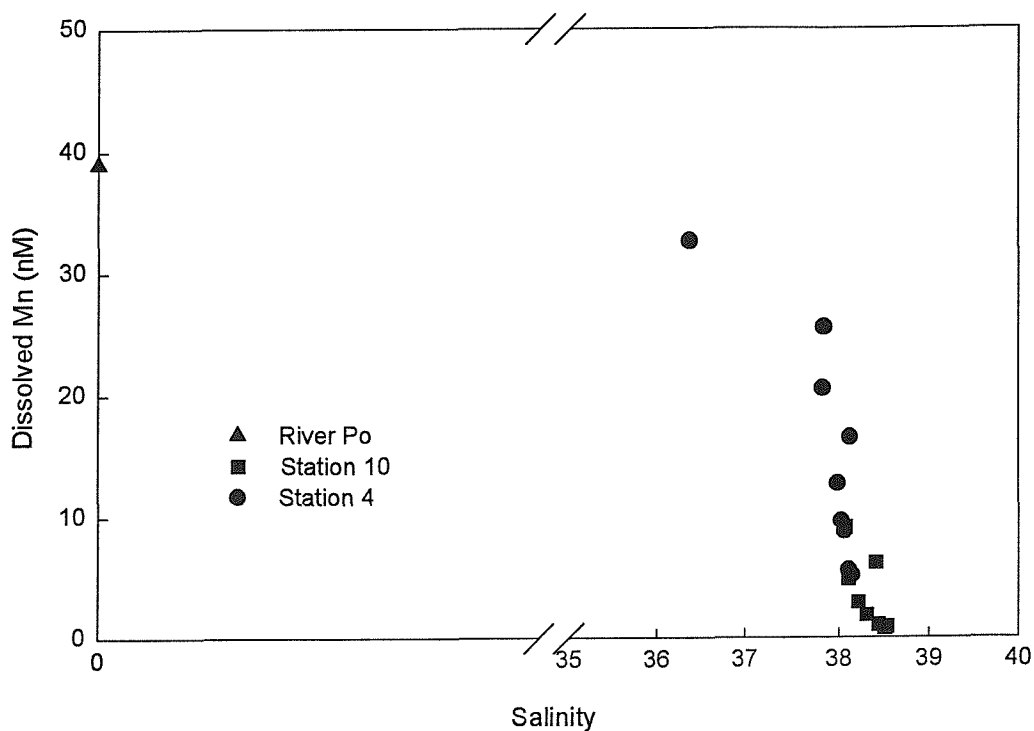


Fig. 4.29: Dissolved Mn plotted versus salinity in the central Adriatic Sea

At Station 10, the dissolved manganese profile shows a marked rapid decrease in concentration from 9 nM in the near surface water to 1 nM below 60 m. This rapid decrease shows the strongly scavenged behaviour of Mn. The small surface maximum may be due to atmospheric or riverine inputs. Particulate Mn concentrations are low in the surface layer. The formation of particulate Mn can be inhibited by sunlight. Sunda and Huntsman (1988) demonstrated that sunlight can cause photoinhibition of manganese oxidising micro-organisms. Sunda *et al.*, (1983) also reported experiments that demonstrate photoreduction of manganese oxides by dissolved organic substances. Such reactions appeared to be important in maintaining Mn in a dissolved reduced form in photic waters. Below 50 m, particulate Mn concentrations tend to increase slightly from 0.7 nM to 3 nM. This is consistent with the particle reactivity of Mn. Near the bottom, dissolved and particulate Mn concentrations increase respectively to 10 nM and 60 nM. According to Artegiani *et al.*, (1993) the bottom layer of the Jabuka Pit is filled with NAW which has been modified with MLIW flowing along the eastern coast. The high particulate Mn concentrations may be explained by resuspension and advective transport of resuspended material from the shelf. Because of the long residence time of the water mass in the Jabuka Pit, suspended material tend to accumulate inducing higher particulate Mn concentrations than at Station 4. The high dissolved Mn concentrations may possibly be due to diffusion from the sediment-water interface. This Mn(II) may also reprecipitate into Mn-oxides in the presence of oxygen.

The profiles of Fe at Stations 4 and 10 are generally similar to those of Mn (Fig. 4.30). At Station 4, particulate Fe concentrations are high in surface water and vary from 570 nM to 100 nM. Dissolved Fe concentrations vary between 1.5 nM and 6 nM with a maximum at 10 m. Fe is the most important of all the trace elements essential to phytoplankton (Martin and Gordon, 1988; Martin *et al.*, 1989) and the decrease in surface water may be due to biological uptake. If the biological uptake of metals is only by incorporation into phytoplankton, the biological flux of Fe could be estimated using the ratio Fe:C in phytoplankton and the primary production rate. The trace metal composition of phytoplankton is poorly characterised and the few studies which have examined it indicate a high degree of variability both between areas and species (Martin and Knauer, 1973; Collier and Edmond, 1983). Martin and Knauer (1973) analysed phytoplankton samples collected under bloom conditions in the Californian

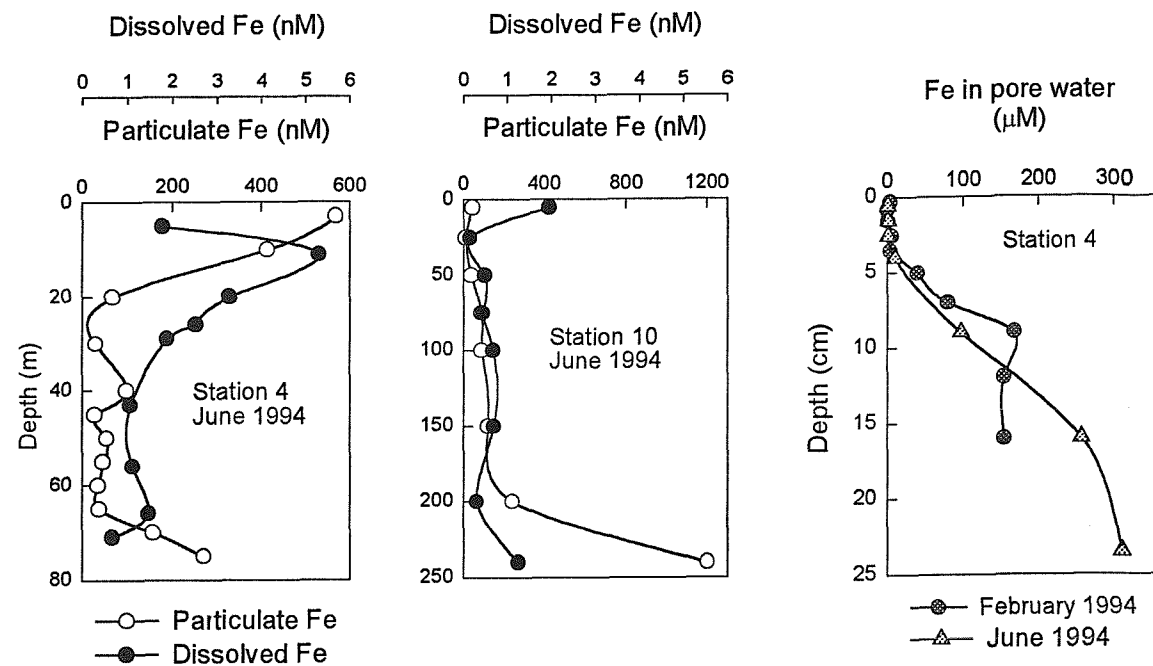


Fig. 4.30: Iron in the central Adriatic Sea

coastal waters (Monterey Bay) and reported a value of 660 mg/kg (dry weight) for Fe, giving a Fe:C ratio of $394 \cdot 10^{-6}$ (molar). Primary production has been measured monthly in the Northern Adriatic Sea (Poniz *et al.*, 1996). They reported a maximum value at 5 m depth in June 1994 (29.1 mgC/m³h). This bloom was due to the diatom *Pseudo-Nitzschia* representing about 90 % of the total phytoplankton cells. The biological uptake for Fe is then estimated to 0.955 nM/h. This value is large compared to the observed depletion in surface water (3.52 nM) suggesting that biological uptake of Fe is potentially an important process. The high concentrations between 0 and 40 m in both dissolved and particulate phases may be due to atmospheric and riverine inputs. Iron is mainly transported southward in the particulate phase in the water pressed against the slope of the western coastal shelf. Below 40 m concentrations are relatively low (around 40 nM for the particulate phase and 1 nM for the dissolved phase). This water mass has a different origin from the surface layer and is characterised by low Fe concentrations. Near the bottom, particulate Fe concentrations increase whereas dissolved Fe concentrations decrease. This may reflect resuspension and rapid scavenging of dissolved Fe onto particles.

Station 10 is away from the influence of the Po outflow and consequently particulate Fe concentrations are relatively low. They vary between 40 nM and 100 nM with an increase towards deeper water which is consistent with the particle reactivity of Fe. The profile of dissolved Fe shows a rather uniform distribution with depth with concentrations of 0.5 nM below 25 m. There is a maximum of 2 nM in surface water. This may be due to atmospheric inputs and to photoreductive dissolution of Fe(III)-oxides, Fe colloids and organically chelated Fe. Waite and Morel (1984) and Rich and Morel (1990) demonstrated the importance of photoreductive dissolution of particulate and colloidal Fe in seawater. Below 200 m, concentrations of dissolved and particulate Fe are high and reach respectively 1.25 nM and 1200 nM. As for Mn, the high particulate Fe concentrations are possibly due to resuspension and advective transport of resuspended material from the shelf. Because of the long residence time of water inside the Jabuka Pit, particulate material are not transported away and higher concentrations of particulate Fe than at Station 4 can be observed near the bottom. The high dissolved Fe concentrations near the bottom are possibly due to diffusive inputs from the sediment surface.

At Station 4, manganese (II) and iron (II) profiles in pore waters are clearly decoupled (Figs. 4.28 and 4.30). The manganese concentrations in the first centimetre of the core at Station 4 are low (between 0.09 and 1.46 μM) and increase up to 100 μM at 4-5cm deep in the core. There is no data available for the oxygen penetration depth but the manganese profile suggests an oxygen penetration of 1 or 2 cm only. At 2-3 cm the nitrates would be expected to be reduced. There is a decrease in manganese concentrations down to 60-70 μM between 5 and 10 cm, below which concentrations stay constant. Fe concentrations are very low in the surface layers of the core (between 0.5 and 4 μM) and down to 4 cm where organic carbon is oxidised by oxygen, nitrates and manganese oxides. Below 4 cm, the Fe^{2+} concentrations increase with depth to reach 150 μM between 8 and 16 cm in June 94 and 300 μM at 14 cm in February 95: at these depths oxidation of the organic carbon by bacteria using the iron oxides as electron acceptors is occurring. This is consistent with the relatively low concentrations in dissolved Mn and Fe in bottom waters and suggest there is less diffusion of Fe and Mn from the sediment-water interface here than in the Northern Adriatic Sea where there is a much greater supply of carbon to the sediments. No seasonal variations in the distribution of Fe^{2+} and Mn^{2+} in pore water has been observed at Stations 4. This is due to the low rate of sedimentation and associated carbon which allows relatively deep oxygen penetration into the sediment.

4.6.2 Cobalt

In the central Adriatic Sea, distribution of dissolved Co is similar to the distribution of Mn (Fig. 4.31). At Station 10, profiles of Co show higher concentrations in surface waters (0.3 nM) than deeper in the water column (0.05 nM). At Station 4, Co concentrations in surface water tend to be higher than at Station 10 (0.5 nM) suggesting stronger riverine or atmospheric inputs and/or advective transport of resuspended sediment from the shelf along the Italian coast. As for Mn, the Co-salinity diagram (Fig. 4.32) shows the importance of inputs other than riverine since the mixing line between the River Po water and the Adriatic Sea water is well above the theoretical dilution line. Near the bottom, Co concentrations increase slightly from 0.12 nM to 0.16 nM. This may be linked to the reduction of MnO_x which has been observed in this area (see section 4.6.1). Cobalt, which can be adsorbed onto

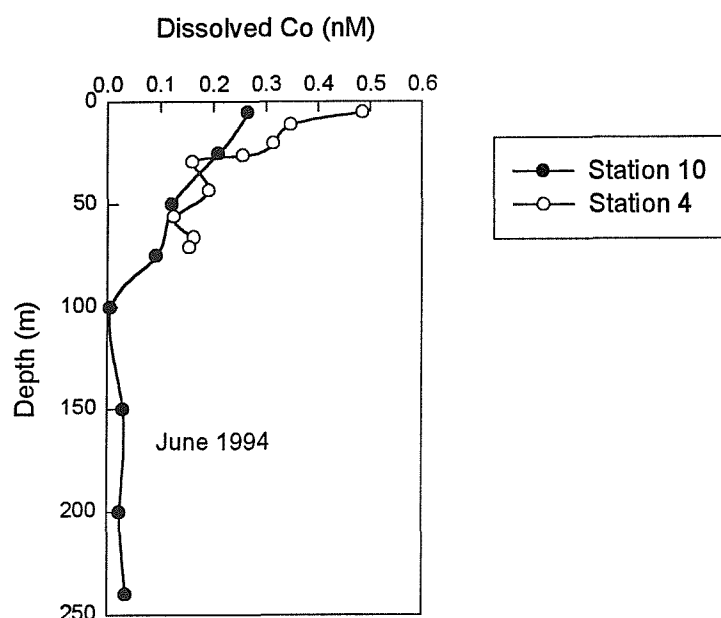


Fig. 4.31: Dissolved Co in the central Adriatic Sea

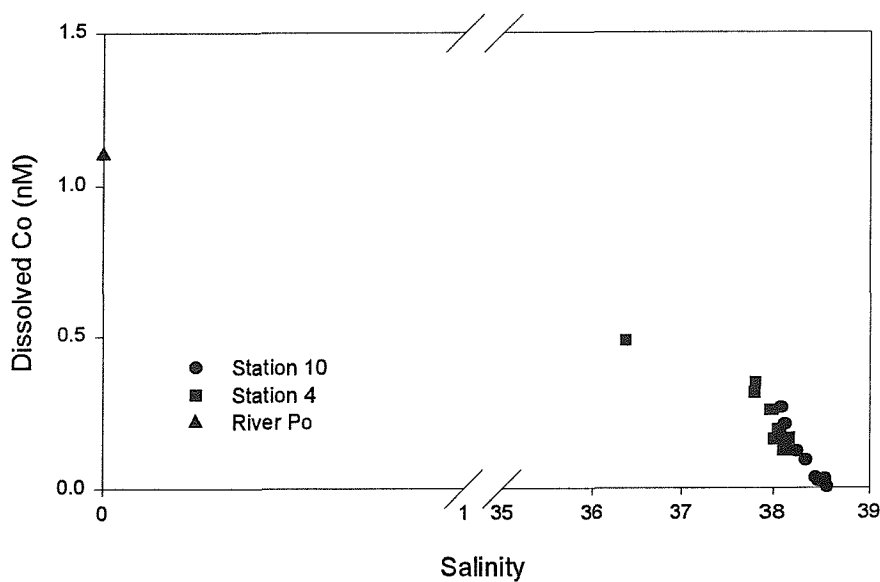


Fig. 4.32: Dissolved Co-Salinity plot

MnO_x , may be released into the water column as MnO_x are reduced to Mn(II) in the sediment-water interface. Concentrations of Co tend to be lower in the central Adriatic Sea than in the Northern Adriatic Sea. This also reflects the small influence of the NAW, which is enriched in metals, onto the central Adriatic Sea.

4.6.3 Lead

At Station 4, dissolved Pb concentrations are about 0.15 nM in surface water and 0.04 nM deeper in the water column (below 50 m). The higher concentrations in surface water may be due to atmospheric or river inputs (Fig. 4.33). For this metal, input through the atmosphere is an important pathway. The importance of this route, which may account for more than 90 % of the input to coastal Mediterranean waters, mainly reflects the use of petrol containing tetraethyl lead (IAEA, 1996; Guieu *et al.*, 1997). Morley *et al.* (1990) found a similar distribution in the Western Mediterranean Sea with an average dissolved Pb concentration of 130 ± 72 pM. At Station 4, particulate Pb concentrations vary between 0.3 and 0.4 nM in the surface layer (0-25 m), decrease to 0.1 nM at 30 m and increase in deeper water to reach 0.45 nM near the bottom. Lead has no known biological function, however its characteristics show a high particle affinity (Balls, 1989; Burton *et al.*, 1993). The surface maximum is mainly due to higher SPM concentrations which have a riverine origin. Particulate Pb concentrations in the river Po are high and vary between 9 and 147 nM. The river Po water which is enriched in particulate Pb mixes with the NAW in the surface and is transported southward along the Italian coast. The bottom maximum is attributed to resuspension.

Station 10 is less influenced by the river Po plume and particulate Pb concentrations are relatively low (0.1 nM) in surface water then increase below 50 m from 0.2 nM to 0.7 nM near the bottom. Particulate Pb concentrations in the central Adriatic Sea (50-220 $\mu\text{g/g}$) are higher than in the Western Mediterranean Sea (0.1-22 $\mu\text{g/g}$; Tankéré *et al.*, 1995) but are lower than in the North Sea (2-844 $\mu\text{g/g}$; Tappin *et al.*, 1995), suggesting that the Adriatic Sea is affected by anthropogenic inputs which originate from industrial areas around the coast line.

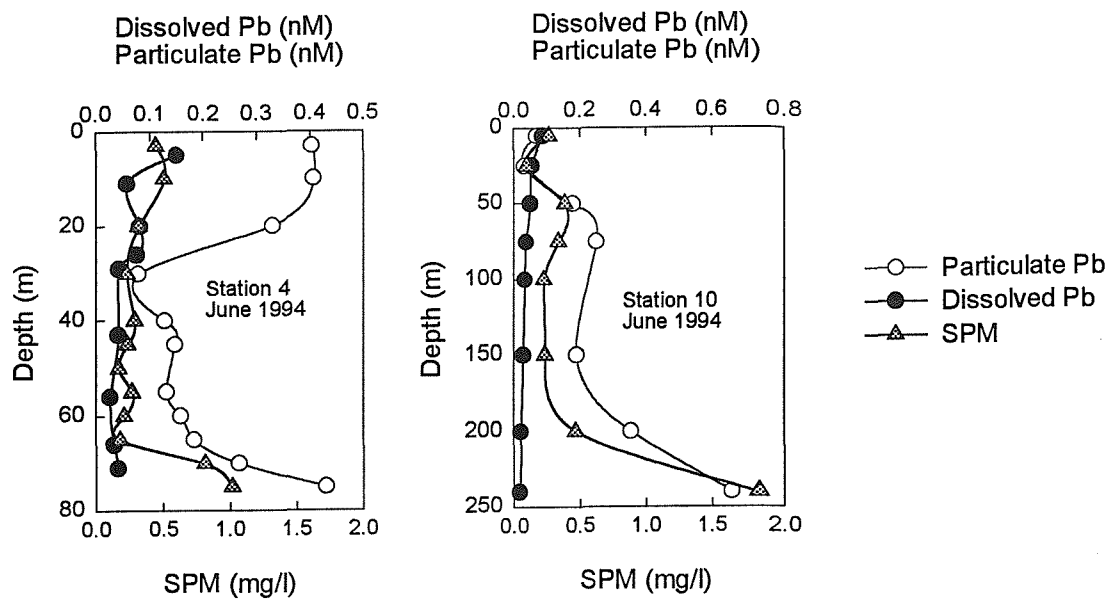


Fig. 4.33: Lead in the central Adriatic Sea

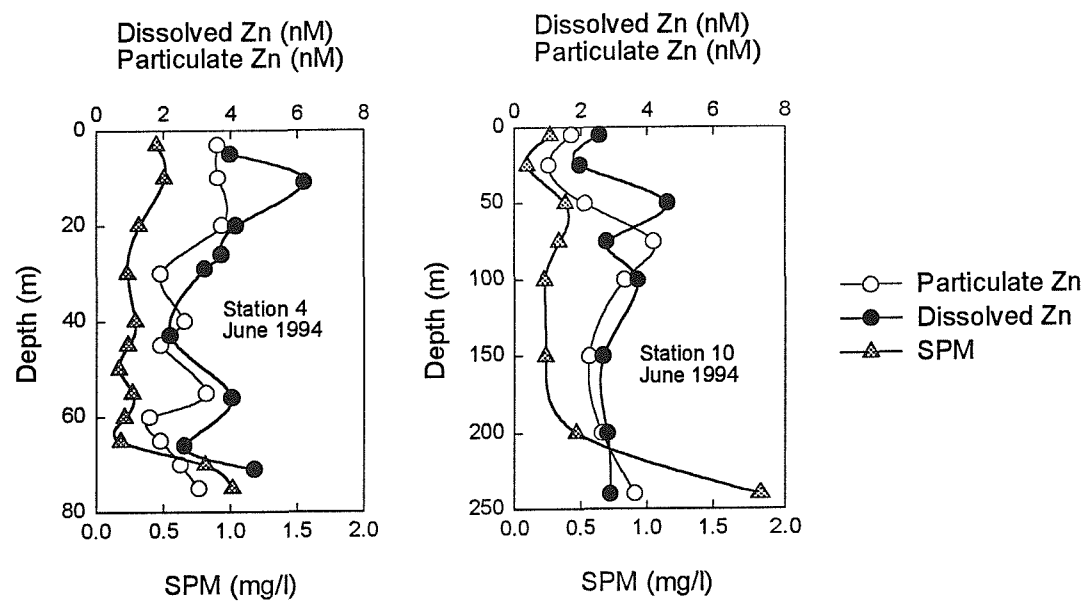


Fig. 4.34: Zinc in the central Adriatic Sea

The distribution of particulate Pb at both stations paralleled those of Fe and Mn suggesting an association with Mn- and/or Fe- rich solid phases. For Pb, transport in the suspended particulate phase is a dominant factor.

4.6.4 Zinc and cadmium

At Station 10, dissolved and particulate Zn distributions are similar. There is a low concentration in surface water (2 nM), concentrations increase to 4 nM below 50 m and decrease to 2.5 nM below 150 m (Fig. 4.34). The maximum in the dissolved phase may be due to mixing with MLIW which has a concentration of 6 nM when entering the Adriatic Sea through the Strait of Otranto. The minimum in surface water may be enhanced by biological uptake although there is no significant increase in particulate Zn concentrations. The higher dissolved Zn concentrations (6 nM) in surface water at Station 4 also suggest that the Zn distribution is not directly linked to the cycle of biological utilisation and regeneration of nutrients and its distribution is more influenced by boundary inputs. Zn is not a redox sensitive element although dissolved and particulate Zn distributions are similar to those of iron at Station 4 suggesting that particulate Zn may be associated with Fe-oxides. Similar observations have been made in the North Sea (Tappin *et al.*, 1995).

In the central Adriatic Sea, concentrations of dissolved Cd are lower in the top 100 m (60 pM) than in the deeper water column (91 pM), (Fig. 4.35). The lower values in surface water may be due to biological uptake. Martin and Knauer (1973) measured Cd in phytoplankton and reported a value of 2.3 mg/kg. The biological uptake of Cd by phytoplankton in surface water has been estimated using the same method as for Fe (section 4.61). A rate of incorporation of 1.65 pM/h has been calculated. This rate is in agreement with the observed depletion (29 pM) in surface water of the central Adriatic Sea in June 1994. The variation in dissolved Cd concentrations with depth could also reflect mixing of different water masses with different Cd content. The Jabuka pit is partly filled with NAW which has relatively high dissolved Cd concentrations (0.1 nM). Benthic inputs may also contribute to enhance Cd concentrations in bottom waters (Westerlund *et al.*, 1986).

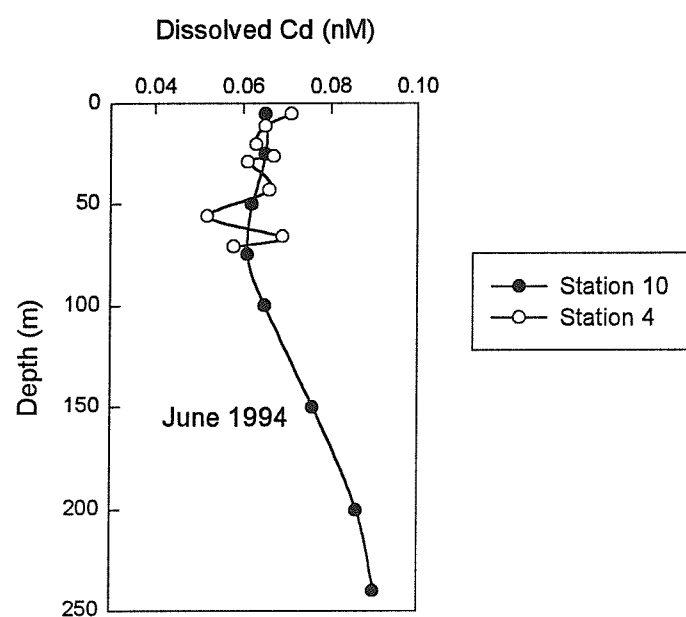


Fig. 4.35: Dissolved Cd in the central Adriatic Sea

4.6.5 Copper and nickel

At Station 10, surface concentrations of dissolved Cu are around 5 nM; there is a minimum of 2.5 nM between 20 and 100 m, then concentrations increase to reach 3-4 nM near the bottom (Fig. 4.36). The surface maximum may be due to eolian and/or remote riverine inputs. The minimum between 20 and 100 m may be due to mixing with MLIW. In the Strait of Otranto, the MLIW composition for Cu is 1.5 nM (Tankéré and Statham, 1996). On the metal-salinity diagram, Cu shows a fairly conservative mixing between the NAW and the MLIW (Fig. 4.37). Some data points lie above the mixing line, however, and are possibly due to eolian inputs in surface water and to benthic inputs near the sediment-water interface. In the intermediate layer, the MAW contains a higher percentage of MLIW than in deeper water and consequently the mixture of MLIW with NAW has a concentration of around 2.5 nM. The bottom of the Jabuka Pit is filled with dense NAW and consequently concentrations tend to be higher. This may also be enhanced by benthic inputs. When moving onto the shelf (Station 4), dissolved Cu concentrations show a similar distribution to Station 10. Slightly higher concentrations are observed near the bottom and may be due to benthic inputs. Recent studies on the distribution of dissolved Cu in marine sediments showed near-surface maxima of the element in pore waters from different kinds of sediments (Pedersen, 1985; and references cited therein). A similar conclusion is reached by Shaw *et al.*, (1990), who indicate that Cu released from sediments is not dependent on redox conditions but on sediment binding capacity. At both Stations (Stations 4 and 10), particulate Cu concentrations are relatively low compared to the Northern Adriatic Sea and are around 0.5 nM. Increases in particulate Cu concentrations are observed near the bottom and may be due to resuspension since SPM concentrations increase simultaneously.

There is little variation of dissolved Ni concentrations with depth in the central Adriatic Sea (Fig. 4.38). Concentrations vary between 5.4 and 6.5 nM with a minimum at 50 m (5.4 nM) which corresponds to the influence of mixing with MLIW. The MLIW enters the Adriatic Sea through the Strait of Otranto with a concentration for Ni of 4.9 nM. Mixing between NAW and MLIW is conservative for Ni (Tankéré and Statham, 1996). As for Cu, there is no depletion for Ni in surface waters which may be attributed to atmospheric and remote riverine inputs. At Station 4, particulate Ni concentrations are around 1 nM in surface water and near

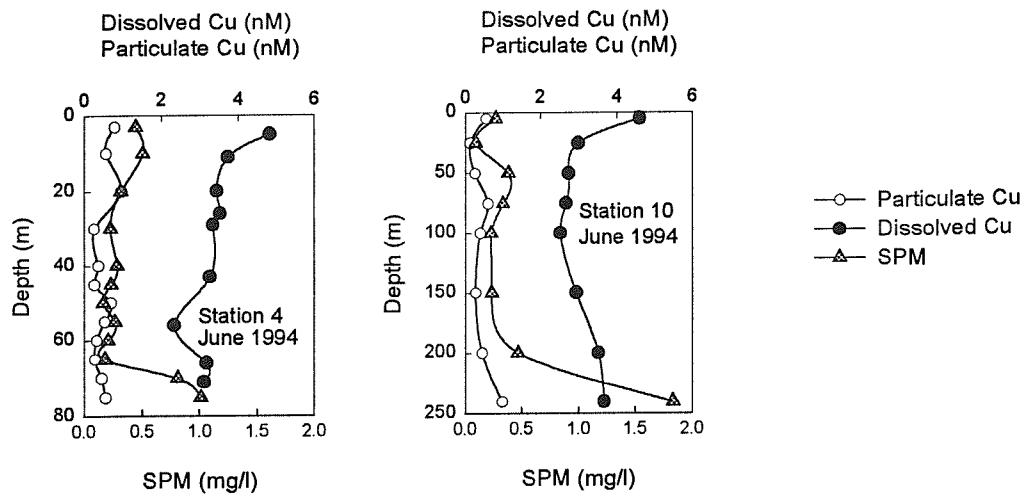


Fig. 4.36: Copper in the Central Adriatic Sea

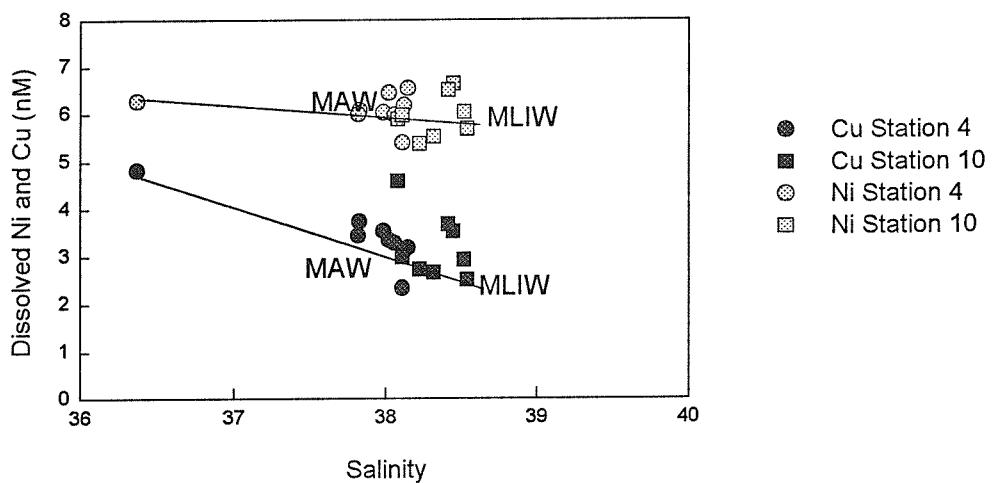


Fig. 4.37: Dissolved Cu and Ni versus salinity in the central Adriatic Sea

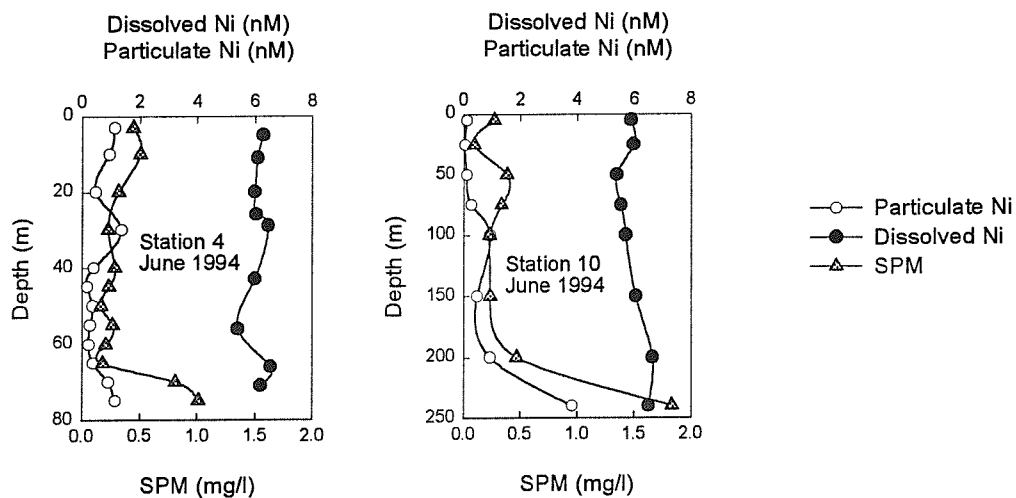


Fig. 4.38: Nickel in the central Adriatic Sea

the bottom with a minimum of 0.3 nM in mid-water column. The higher concentrations in surface water may be due to riverine inputs whereas near the bottom, they may be due to resuspension. Both maxima are associated with higher SPM concentrations. At Station 10, particulate Ni concentrations are low in surface water (0.2 nM), increase to 1 nM between 100 and 200 m and reach 3.8 nM near the bottom. The distribution of particulate Ni is similar to the distribution of particulate Mn. The highly absorptive properties of particulate and colloidal Mn-oxides may contribute significantly to the behaviour of Ni which may be scavenged by Mn-oxides (Morris and Bale, 1979).

4.7 Trace metal distributions in the Strait of Otranto

In the Strait of Otranto, dissolved trace metal data only are available. However suspended particulate matter has been studied in detail by Rabitti *et al.*, (1994) in the same area. They found a 3 layer structure which can be described by:

- (a) a surface layer rich in suspended matter, related to the biological production and the coastal dynamics, with W-E and N-S gradients depending on the seasonal conditions;
- (b) an intermediate layer (below 200m) with very low particle content and stable in time;
- (c) a bottom nepheloid layer, the extent of which varies in time and space in relation to the flow of dense bottom waters of Adriatic origin and with the supply of material from the coastal region along the shelf.

In surface waters on the western side of the strait, transmittance values were found to vary between 85.48 and 95.50 % whereas on the eastern side they were higher and were varying between 94.00 and 95.50 % (Rabitti *et al.*, 1994). These transmittance values suggest that particulate metal fluxes are relatively low in this area and could be neglected compared to dissolved metal fluxes. However a quantitative assessment needs to be done.

Concentrations of dissolved trace metals in the different water masses in the Strait of Otranto have been identified and are summarised in Table 4.5. Metal concentrations have been averaged for depth intervals which have ranges of salinity corresponding to the water masses identified above.

Table 4.5: Trace metal concentrations of the different water masses in the Strait of Otranto

Water mass	Mn (nM)	Fe (nM)	Co (nM)	Pb (nM)	Cd (nM)	Cu (nM)	Ni (nM)	Zn (nM)
ESW	4.45	1.59	0.12	0.17	0.05	2.52	5.08	4.15
WSW	6.14	2.12	0.22	0.13	0.07	3.97	5.07	3.77
MAW	1.31	0.74	0.04	0.10	0.06	2.66	4.21	4.71
MLIW	0.20	0.66	0.02	0.12	0.05	1.50	4.90	5.60
SAW	0.23	0.33	0.01	0.10	0.04	1.91	4.01	3.36

ESW: East Surface Water; **WSW:** West Surface Water; **MAW:** Mixed Adriatic Water
MLIW: Mixed Levantine Intermediate Water; **SAW:** South Adriatic Water

4.7.1 Manganese

Dissolved manganese profiles show higher concentrations in surface waters (0-100 m) than in deeper waters, suggesting some atmospheric and riverine inputs in surface waters (Fig 4.39). In surface waters concentrations are about 8 nM whereas in the deeper water column concentrations range from 0.2 to 3 nM. Manganese profiles show higher concentrations in the water column on the western side of the Strait of Otranto than on the eastern side suggesting that the MAW flowing along the Italian coast and through the Strait of Otranto is influenced by riverine inputs (mainly the Po river). On the western side of the strait, manganese benthic inputs seem also greater than on the eastern side. Manganese enrichment in bottom waters is found at Stations 201, 302 and 305 (Fig. 4.39) suggesting changes in the composition and chemical and physical characteristics of the sediments between the western side of the Strait of Otranto and the eastern side. These changes may possibly increase the diffusion of Mn from the sediment-water interface on the west side. When the metal-salinity diagram (Fig 4.40 a) is taken into account, manganese shows a quasi-conservative mixing behaviour between the different water masses. Conservative behaviour is favoured by the low particulate loading of the different water masses which induces less scavenging of dissolved manganese onto particles. Nevertheless some data points lay above the mixing lines: for Stations 201 and 302 those points correspond to the bottom water where there are benthic inputs; for Stations 108, 204 and 212 the points corresponds to surface waters suggesting some higher riverine or atmospheric inputs than the general background mean.

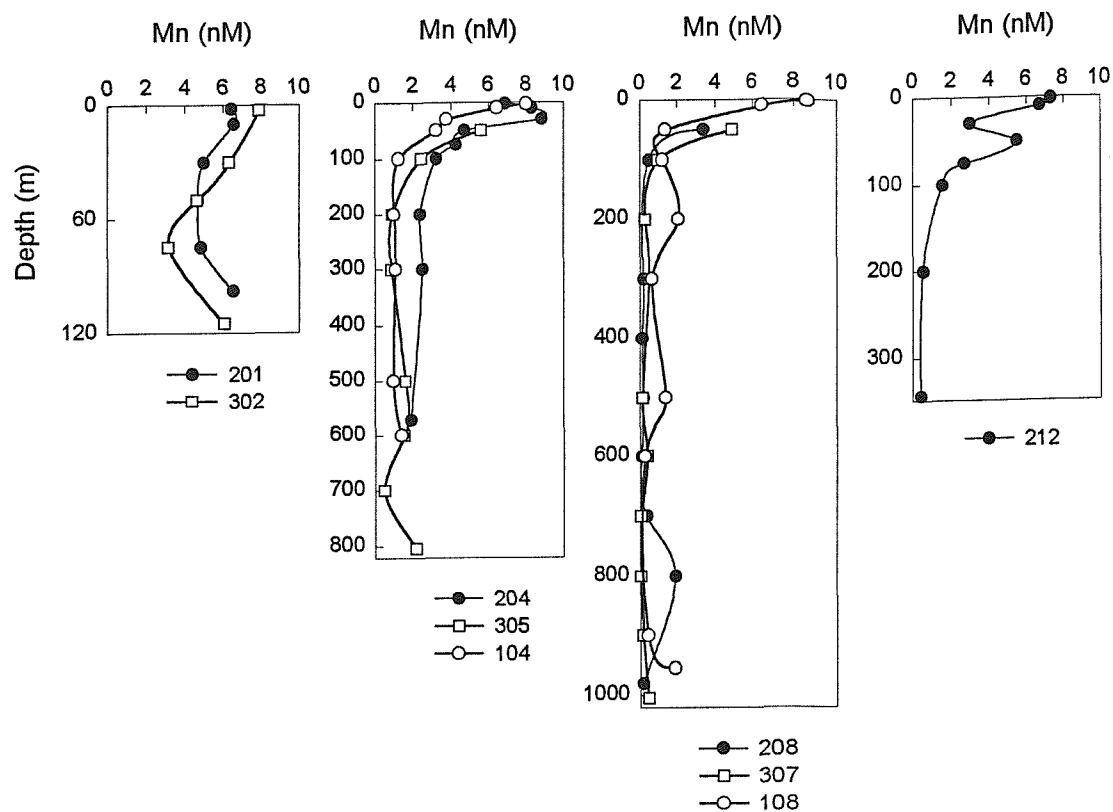


Fig. 4.39: Dissolved Mn in the Strait of Otranto (stations are arranged in order, from West to East across the Strait)

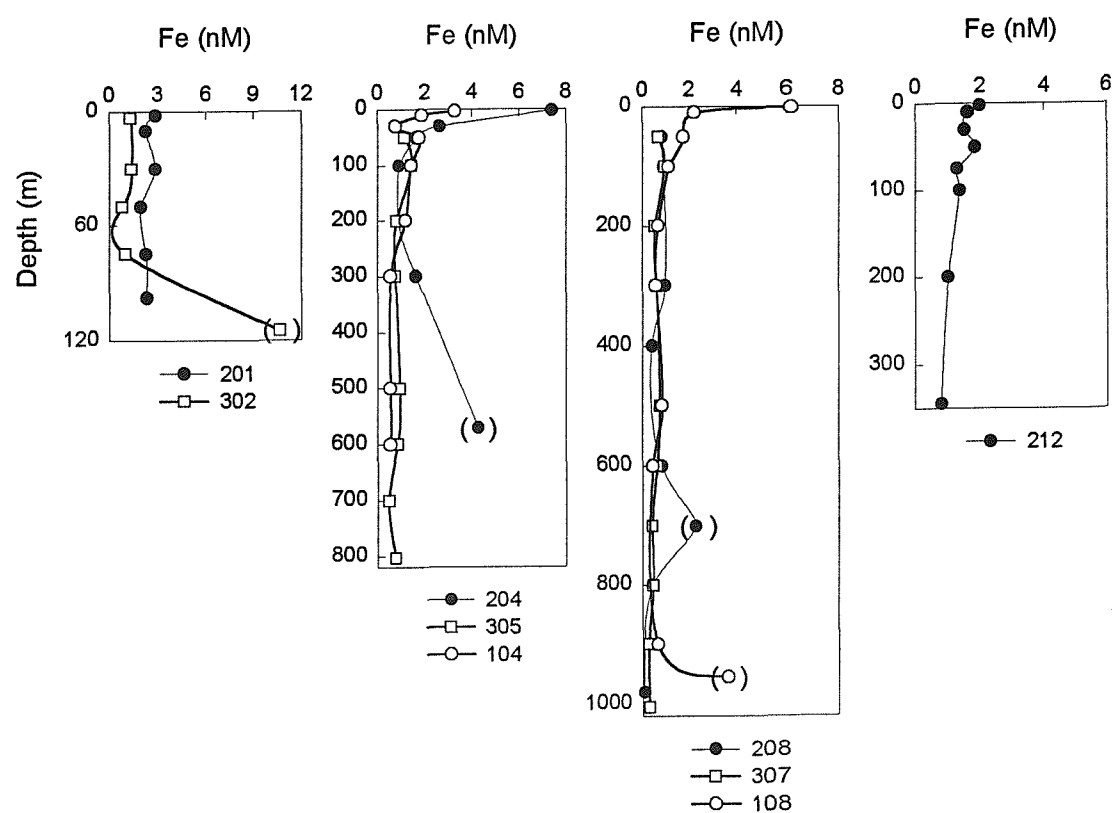


Fig. 4.41: Dissolved Fe in the Strait of Otranto, () indicates suspect data (see text).

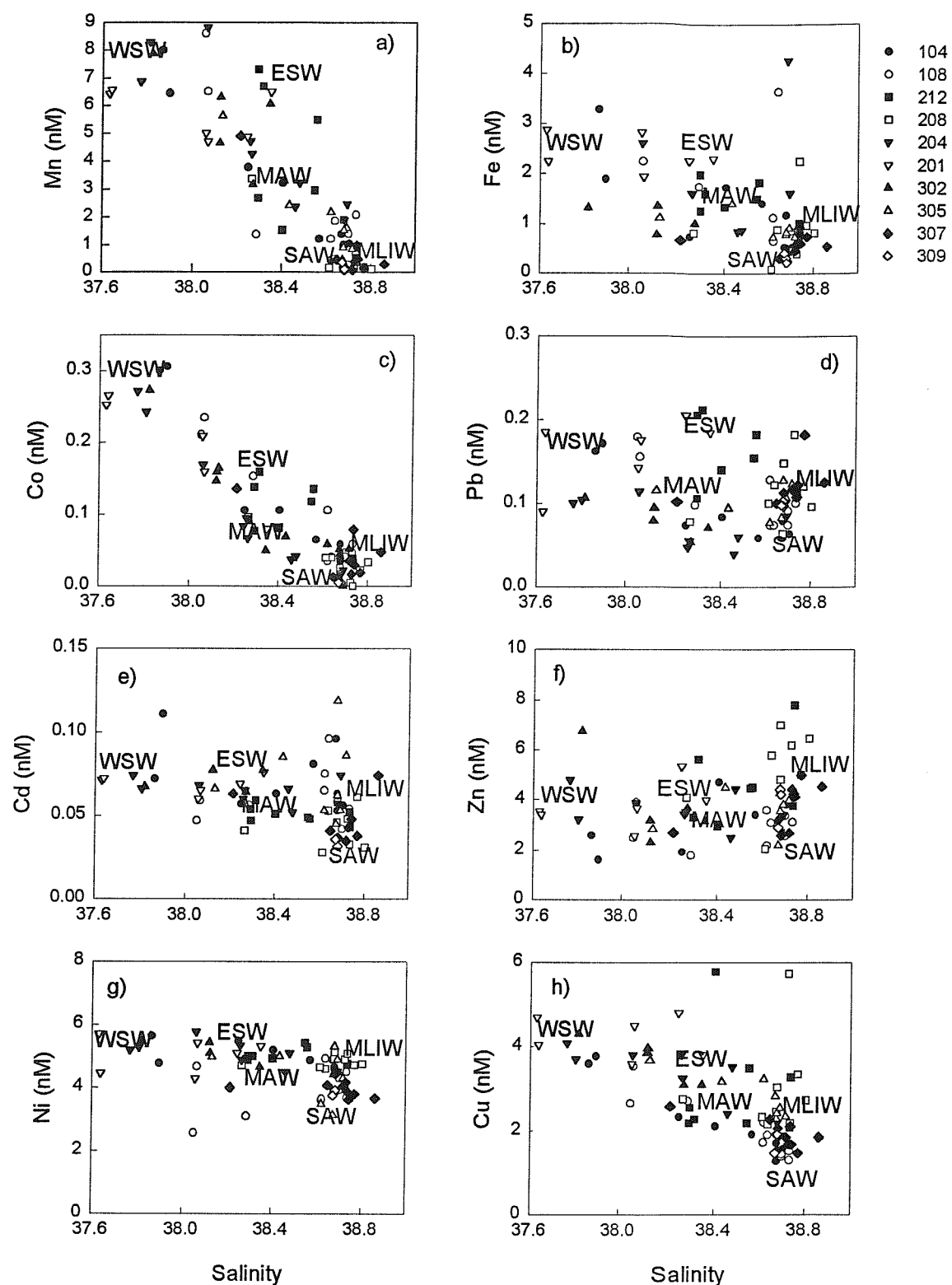


Fig. 4.40: Dissolved metals versus salinity in the Strait of Otranto: a) Mn, b) Fe, c) Co, d) Pb, e) Cd, f) Zn, g) Ni, h) Cu.

4.7.2 Iron

The high concentrations found in bottom waters at Stations 302, 204 and 108, and at about 700 m for Station 208 are not oceanographically consistent and samples may have been contaminated (Fig. 4.41). In general, higher concentrations are found in surface waters (2.5-4 nM) than in the deeper water column (about 1 nM) particularly in the central part of the Strait of Otranto where scavenging by particles in the euphotic zone is possibly less than in shelf waters. The difference in iron concentrations between the western side and the eastern side of the Strait is not as marked as with manganese. On the metal-salinity diagram (Fig. 4.40 b), Fe shows a conservative behaviour during mixing between SAW and MLIW and between MLIW and MAW whereas the behaviour is rather non-conservative for mixing between MAW and WSW or ESW reflecting atmospheric and riverine inputs in surface water and some removal occurring into the water column.

4.7.3 Cobalt

Cobalt reflects the characteristics of scavenged metals. There are relatively high concentrations in surface waters (0.15-0.3 nM) (Fig. 4.42). These concentrations decrease rapidly with depth to 0.015-0.030 nM at 200 m. Below this depth concentrations stay constant. There is a marked increase in surface concentrations from east to west, suggesting that riverine inputs of Co are greater on the western side than the eastern side of the Strait of Otranto. On the metal-salinity diagram (Fig. 4.40 c), Co behaviour is conservative during the mixing of the different water masses; this is favoured by the low particle loading of the different water masses. There is a good correlation between Co and Mn ($r^2 = 0.847$). This good relationship with Mn has also been observed in the western Mediterranean Sea (Morley *et al.*, 1997) and in the Strait of Dover (James *et al.*, 1993). Cycling of Co may be linked to cycling of Mn (Section 4.5.3).

4.7.4 Lead

Lead concentrations are typical for open Mediterranean waters and vary between 0.05 and 0.20 nM (Tankéré *et al.*, 1995; Yoon *et al.*, 1995). Higher Pb concentrations are found in

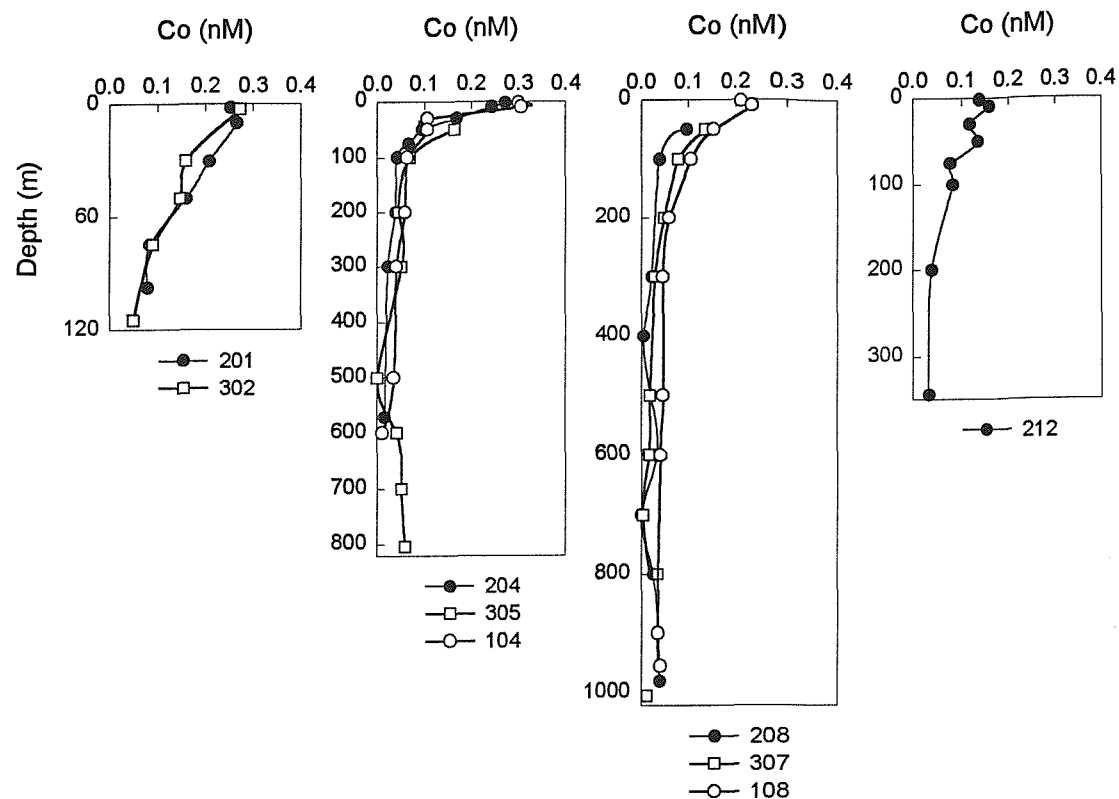


Fig. 4.42: Dissolved Co in the Strait of Otranto

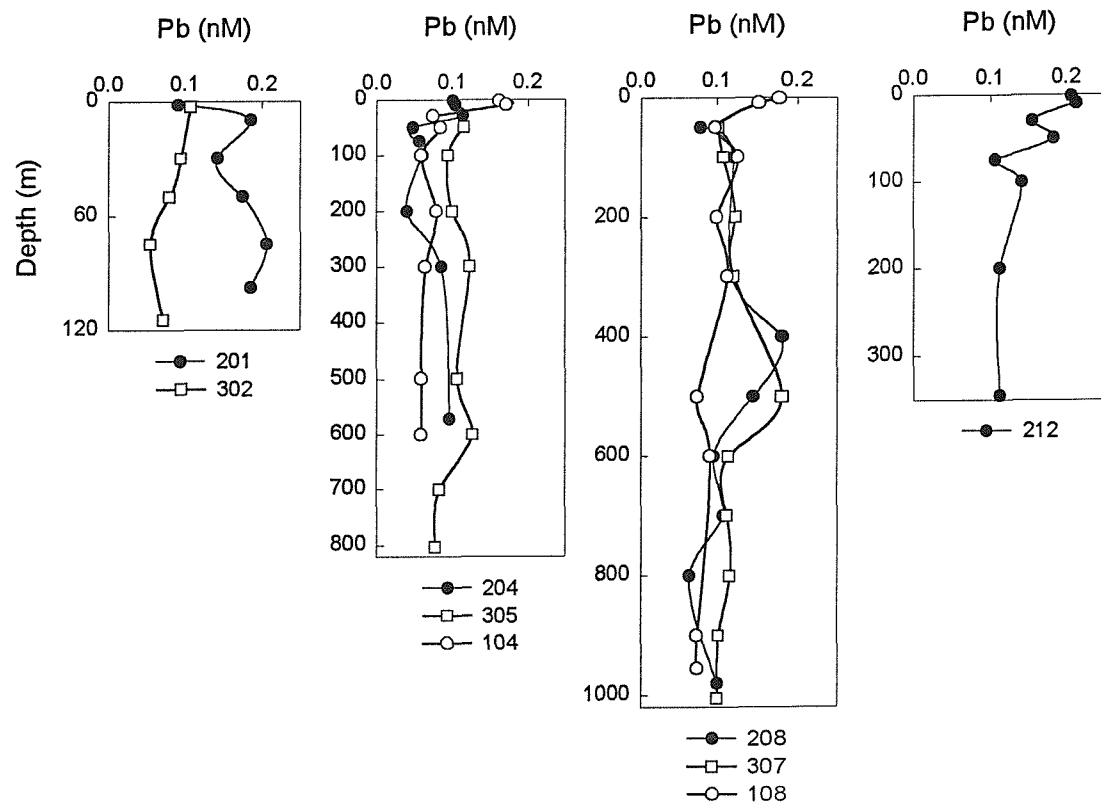


Fig. 4.43: Dissolved Pb in the Strait of Otranto

surface waters and may reflect anthropogenic inputs with an atmospheric origin (Guieu *et al.*, 1997), (Fig. 4.43). Higher concentrations are also found at Station 201 compared to Station 302 and may reflect local coastal inputs. From the metal-salinity diagram (Fig. 4.40 d), Pb shows a conservative behaviour during mixing between SAW and MLIW. For the mixing between the other water masses (MAW, ESW, WSW) Pb shows a non-conservative behaviour since the data points do not fall within boundaries delimited by the mixing lines between the contributing water masses. The metal-salinity diagram shows evidence for inputs to surface waters which have possibly riverine and/or atmospheric origins. Some removal is occurring in the water column since some data points fall below the mixing lines between the contributing water masses. Dissolved Pb may possibly be scavenged by suspended particulate material.

4.7.5 Cadmium

For deep stations in the Strait of Otranto (208, 307, 108), Cd profiles show a small minimum in surface waters (≈ 40 pM), then an increase in concentration between 200 and 300 m (Fig. 4.44). Below 300 m concentrations are homogenous with depth (≈ 60 pM). Increases near the bottom can be observed at Stations 108, 104, 305, 201 and 302. This may be due to benthic remobilization. Salomons (1978) has shown in laboratory experiments, that more than 50 % of Cd present in resuspended sediments can be released. At Station 212, concentrations are homogenous with depth (0.050 nM). At Stations 201 and 302, concentrations are slightly higher between 0.060 nM and 0.072 nM suggesting riverine and anthropogenic inputs coming from the northern Adriatic Sea. The NAW flows in a surface layer southward pressed against the slope of the western coastal shelf and leaves the Adriatic Sea on the western side of the Strait of Otranto. On the metal-salinity diagram (Fig. 4.40 e) Cd data points fall largely within boundaries delimited by the mixing lines between the main contributing water masses, except for samples near the bottom which reflect benthic inputs, suggesting a conservative behaviour for Cd during mixing between the different water masses.

4.7.6 Zinc

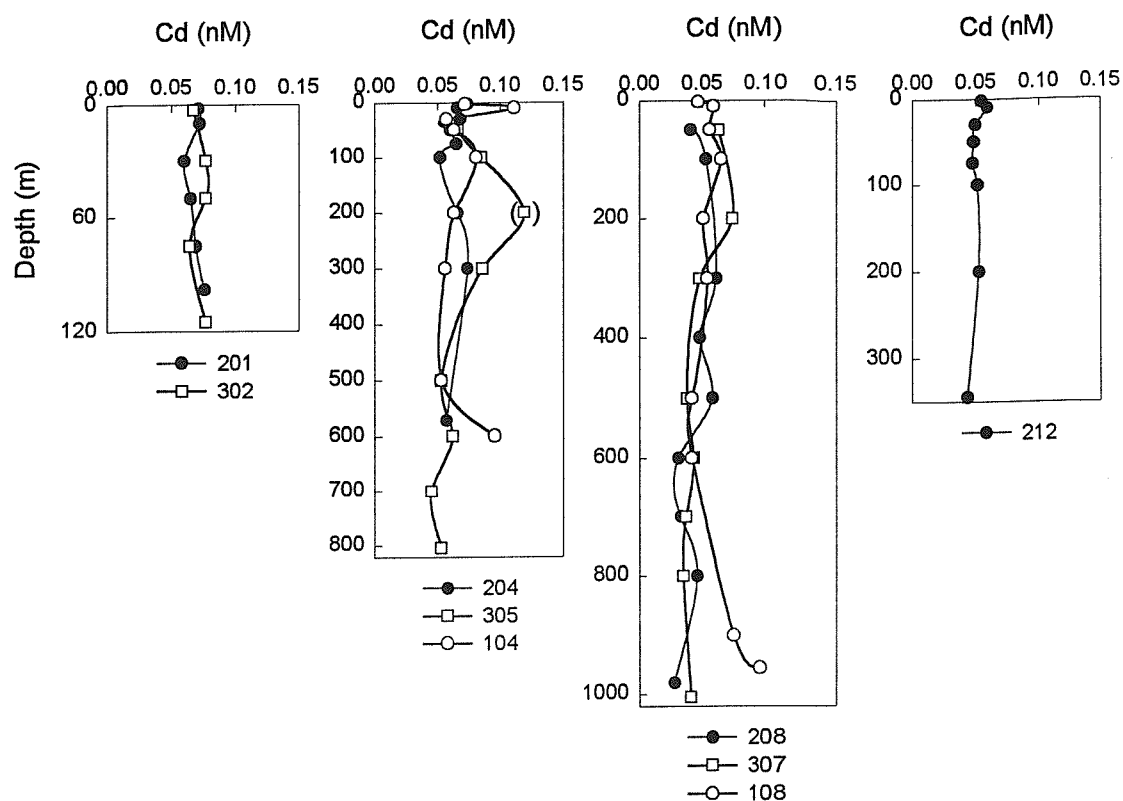


Fig. 4.44: Dissolved Cd in the Strait of Otranto, () indicates suspect data

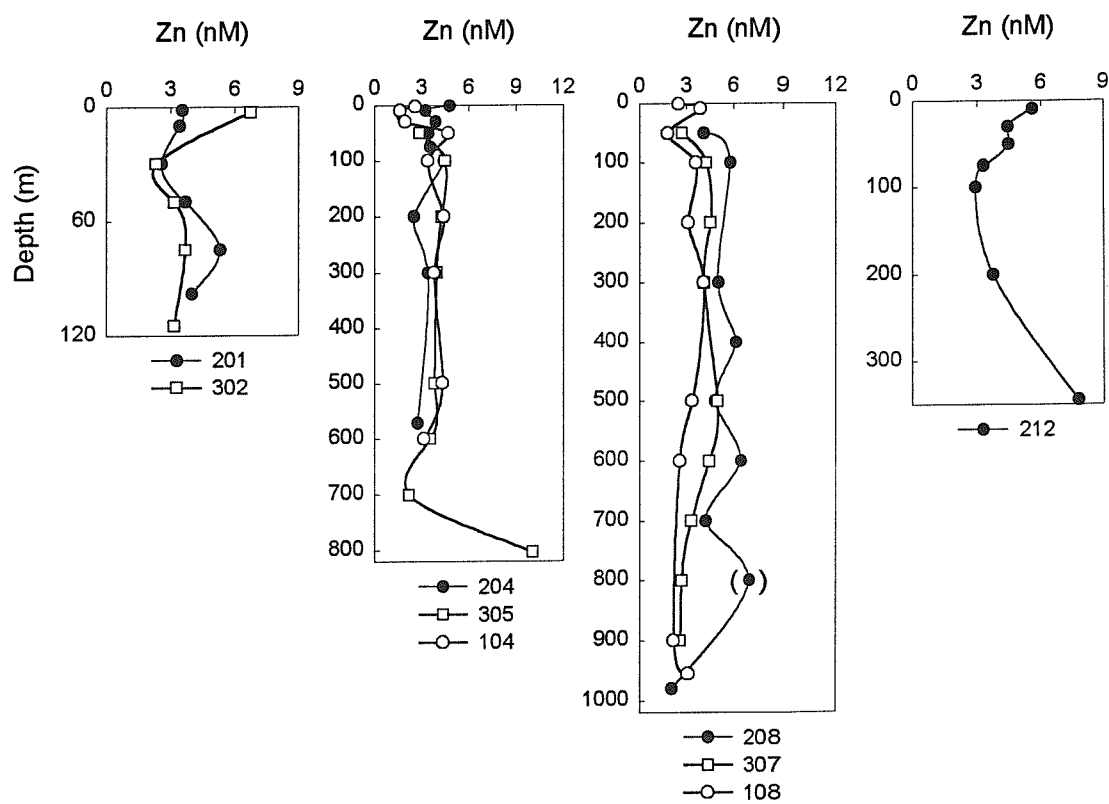


Fig. 4.45: Dissolved Zn in the Strait of Otranto, () indicates suspect data

Data on the zinc profiles are relatively scattered (Fig. 4.45). Zinc is one of the most difficult elements to sample and analyse accurately because of the potential for contamination.

Dissolved Zn concentrations vary between 2 and 10 nM. These values are in the same range as those in the Western Mediterranean Sea (1.5-7 nM; Tankéré *et al.*, 1995). The Otranto profiles away from shore show a minimum in surface water (2.5 nM) and an increase to about 100m (5-6 nM). Below 100 m concentrations tend to be homogenous with depth (4-5 nM). Shallow water profiles show maxima in the surface layer (6 nM) and near the bottom (8-9 nM), suggesting some atmospheric and riverine inputs in surface waters and benthic inputs in bottom waters. On the metal-salinity diagram (Fig. 4.40 f), Zn shows a conservative mixing between the different water masses although some points have elevated concentrations at salinity 38.7 and reflect benthic inputs.

4.7.7 Copper and nickel

Copper and nickel have similar profiles (Fig. 4.46 and Fig. 4.47). Some samples may have been contaminated for Cu at Stations 208 (400 m) and 212 (100 m) since the corresponding data points are not oceanographically consistent. Concentrations are homogeneous with depth ranging from 1.5 to 4 nM for Cu and from 4 to 6 nM for Ni. The highest concentrations are found in surface waters. The lack of surface depletion for Cu and Ni has also been observed in the western Mediterranean Sea (Morley *et al.*, 1997). It was then suggested that mixing processes predominate and that there is little influence of recycling on the composition of the upper and deeper water. Table 4.5 presents the concentrations for the different water masses. The average values for Cu and Ni in MLIW in the Strait of Otranto (respectively 1.50 nM and 4.90 nM) are similar to those given by Yoon *et al.*, (1995) in the western Mediterranean Sea. On the metal-salinity diagram (Fig. 4.40 g and h) Cu and Ni show essentially conservative.

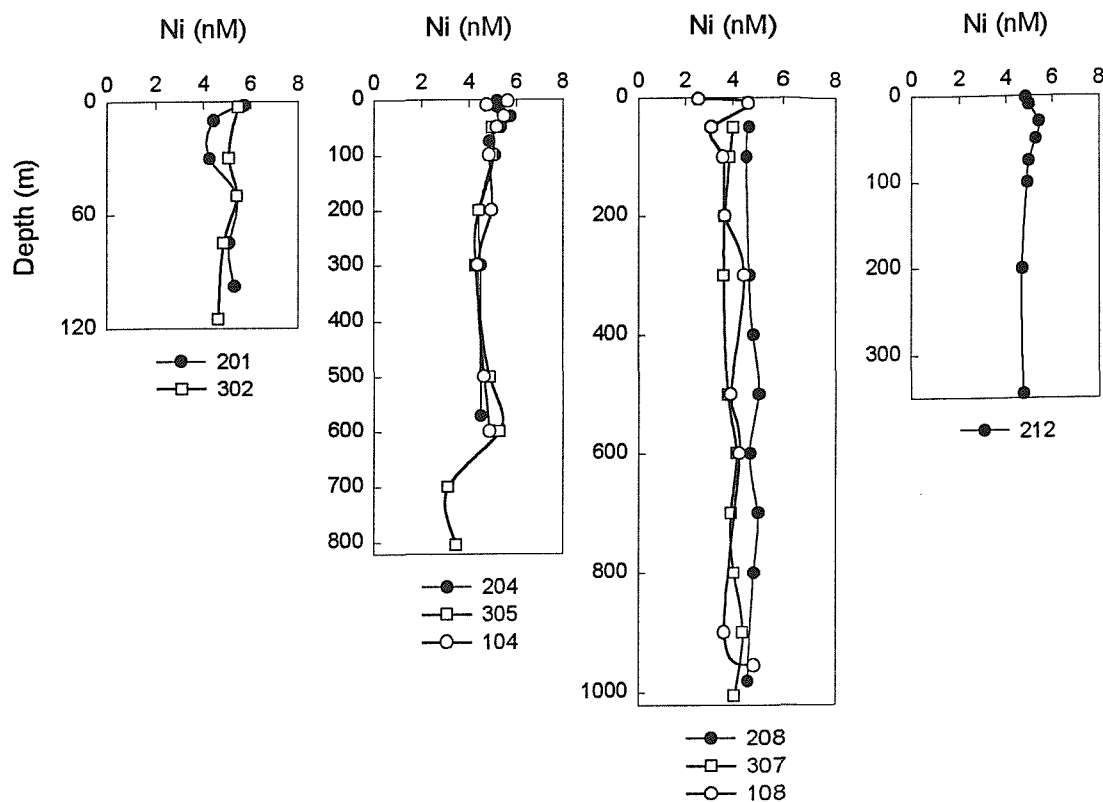


Fig. 4.46: Dissolved Cu in the Strait of Otranto

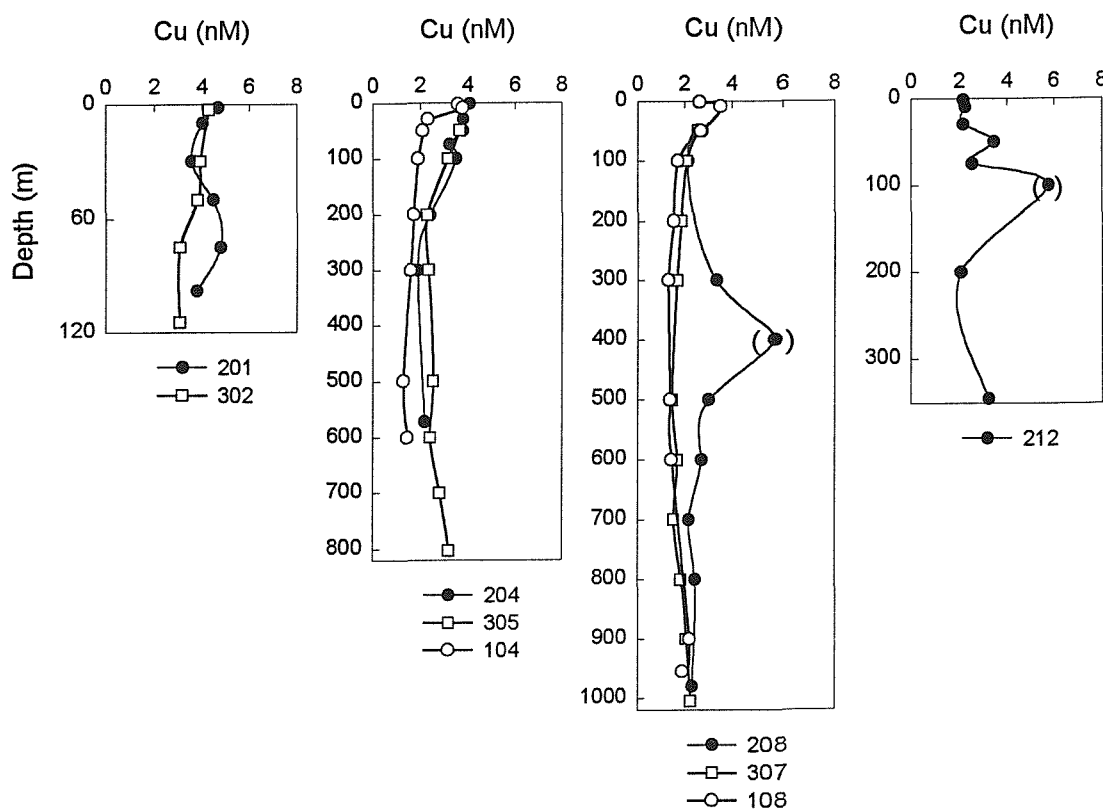


Fig. 4.47: Dissolved Ni in the Strait of Otranto, () indicates suspect data



CHAPTER 5

MASS BALANCE OF TRACE METALS IN THE ADRIATIC SEA

5.1 Introduction

In this chapter, cycling of trace metals and their mass balance in the Adriatic Sea will be considered. Fig. 5.1 shows the different cycling and transport processes which occur in the cycle of trace metals in the Adriatic Sea. The continental shelf and the margin represent ca. 70 % of the Adriatic surface sediments. These areas receive important amounts of material mainly supplied by rivers. During the period 1956-1973 the average total sediment transport of the Po averaged $13.7 \cdot 10^6$ t/y which includes a bedload transport of $1.8 \cdot 10^6$ t/y. The second most important discharge is from the Adige, with a loading of $886 \cdot 10^3$ t/y. Shelf waters also receive dissolved inputs from rivers, in which trace metal concentrations are generally higher than in coastal water. The impact on biota, as well as the actual flux to the open sea of these inputs, will be controlled by their fate during estuarine mixing. Other factors such as benthic remobilization and eolian inputs may also be important in determining the distribution of trace metals in shelf waters. To describe the distribution of trace metals in the Adriatic Sea, a two-box vertical model is used for the Southern Adriatic Sea and the central Adriatic Sea (one box representing the surface layer of the Southern Adriatic Sea and the central Adriatic Sea and the other one representing the deep water of the Southern Adriatic Sea) while the Northern Adriatic Sea continental shelf is represented by a single box. The three reservoirs are coupled. The parameters used to run the model are the dissolved and particulate concentrations of the elements, the fluxes of water between the reservoirs and the input and output fluxes of the elements at the boundaries. This type of model provides a steady-state description of fluxes, reservoir contents and turnover times. It gives a basis for quantitative modelling and it helps to estimate the relative magnitudes of fluxes.

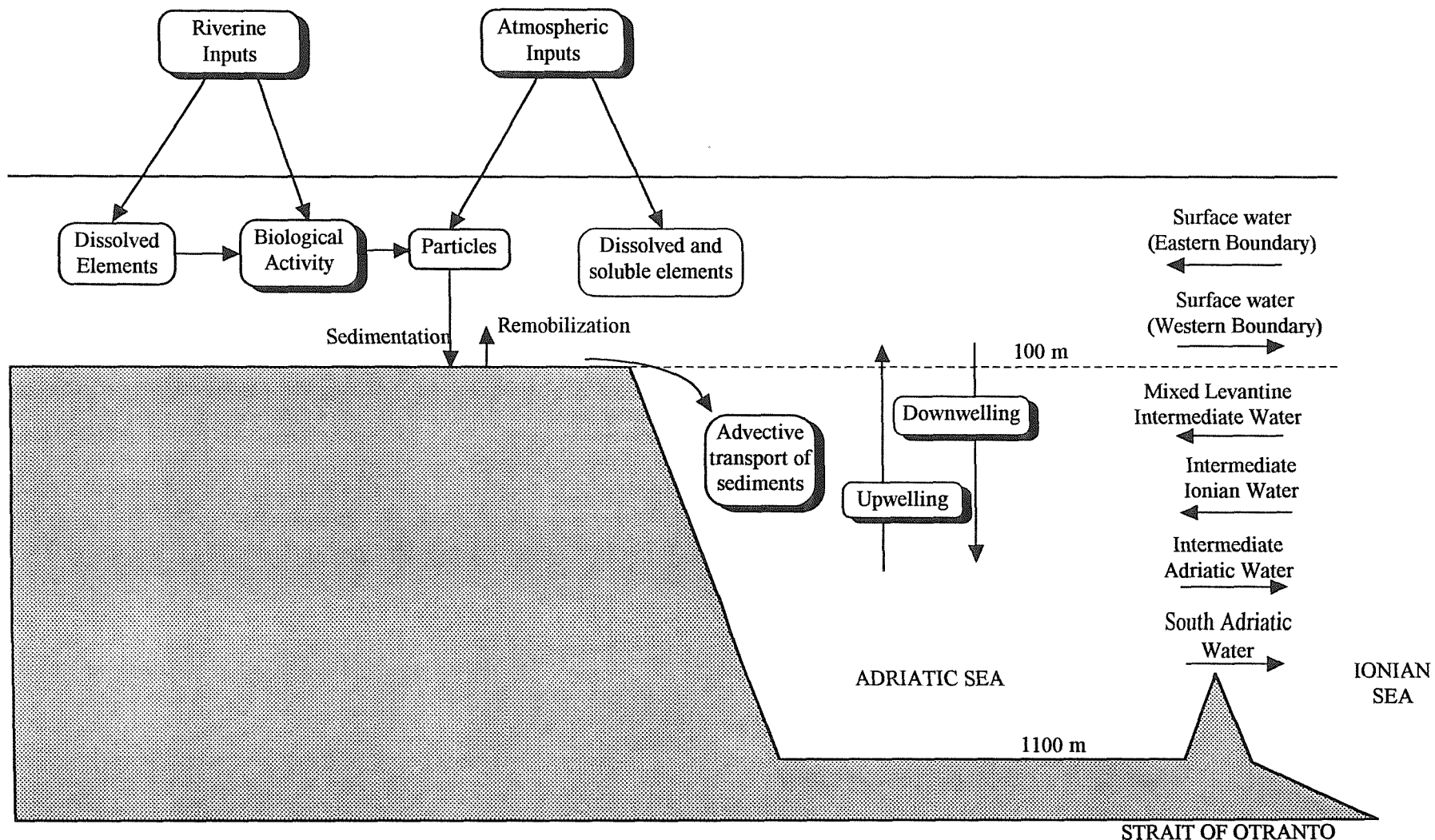


Fig. 5.1: Processes involved in the biogeochemical cycle of trace metals in the Adriatic Sea. Arrows represent fluxes of metals.

5.2 A simple box model for the Adriatic Sea

5.2.1 Description

A box model has to take into account all processes influencing the distribution of trace metals in the Adriatic. Compartments have to be defined by physical and hydrographic characteristics, so that each compartment can be considered as reasonably homogenous. Salinity and temperature profiles show 3 different patterns: the northern Adriatic contains a typical water mass independent from the central and southern Adriatic Sea. In the central Adriatic, T-S diagrams resemble the T-S sections for the surface layer in the southern Adriatic Sea. In the southern part, surface and deep water characteristics have to be considered separately. In order to consider the biochemical cycle of trace metals, a euphotic zone of 100 m has been chosen. Photosynthesis requires light in the wavelength range 370-720 nm, and even in clear tropical waters only 1 % of the visible light energy penetrates to a depth of 100 m. Photosynthesis is therefore generally restricted to the upper 100 m of the water column (Chester, 1990)

The Adriatic Sea may thus be represented by a 3-compartment box model (Fig. 5.2).

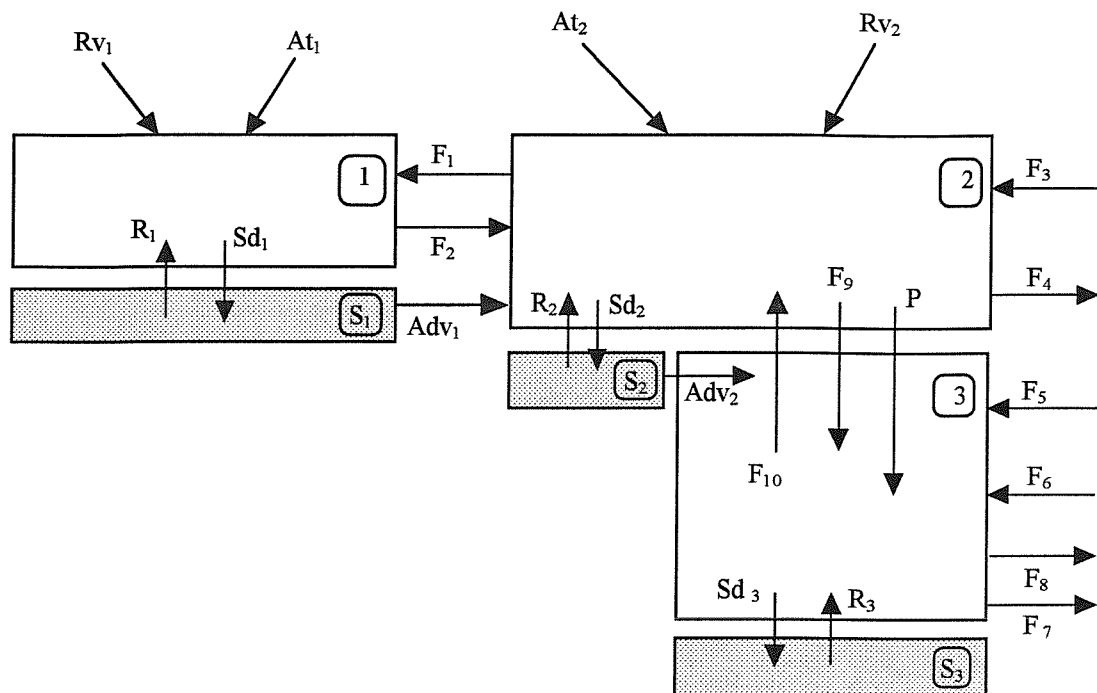
Compartment 1 represents the continental margin of the northern Adriatic Sea from the Gulf of Trieste to the Jabuka Pit. The southern Adriatic Sea is represented by 2 compartments: One for the surface layer (0-100 m) (compartment 2) and one for the deep water (100-1100 m) (compartment 3). The central Adriatic Sea is included in compartment 2 as the hydrographic properties are similar to the southern Adriatic surface water.

Compartments receive and lose trace metals in different ways (Fig. 5.2):

- Atmospheric inputs (At_1 and At_2): there is dry deposition (elements are associated to aerosols) and there is wet deposition (trace metals are in dissolved or particulate phases). In this study we differentiate total dissolved inputs (dissolved phase + particulate phase which is solubilised in contact with surface water) from the net particulate flux (insoluble fraction of the particulate phase).
- Riverine inputs (Rv_1 and Rv_2) are in dissolved and particulate phases.
- Dissolved and particulate trace metals are transported with water mass exchanges between the different compartments. Water mass exchanges take place between

compartment 1 and compartment 2 due to horizontal advection. There is a general clockwise circulation; along the east coast, the surface water from compartment 2 is entering compartment 1 (water flux V_1); along the west coast, the surface water from compartment 1, is entering compartment 2 (V_2). In the strait of Otranto, exchanges take place in the surface layer between the Ionian Sea and compartment 2. On the east side of the Strait, surface water from the Ionian Sea enters the Adriatic Sea (V_3); on the west side of the Strait, surface water hugging the Italian coast exits the Adriatic Sea (V_4). Deeper in the water column (compartment 3) there is exchange of water masses and associated trace metals with the Ionian Sea. An ingress of Mixed Levantine Intermediate Water (V_5) and Ionian Intermediate Water (V_6) into the Adriatic Sea is counterbalanced by an export of South Adriatic Water (V_7) leaving the Adriatic Sea along the bottom and an export of Intermediate Adriatic Water (V_8). There are also exchanges between the surface layer (compartment 2) and the deep layer (compartment 3); further, dynamic processes such as upwelling (V_{10}) and downwelling (V_9) also result in transport of trace metals between the 2 compartments. During the winter period, the formation of dense water along the west coast produces downwellings.

- There is a downward flux of particles between compartments 2 and 3 which result from sedimentation. These particles may be detrital or biogenic in origin. There are sedimentation fluxes in each compartment representing settling of particles on the bottom.
- In each compartment there is, additionally, a remobilization flux which is due to the diffusion of trace metals from the pore waters into the bottom layer.
- Advective transport of sediments (Adv_1 and Adv_2) can be a major source of metals for compartments 2 and 3 respectively.



At_i : Total atmospheric input for compartment i (dissolved and particulate phases)

Rv_i : Total riverine input for compartment i (dissolved and particulate phases)

P : Flux for particulate trace metals from compartment 2 to compartment 3.

Sd_i : Sedimentation flux for compartment i

R_i : Remobilization flux for compartment i

Adv_i : Advective transport of sediments from compartment i

S_i : Sediment box for compartment i

F_i : Total (dissolved + particulate) trace metals fluxes associated with water mass exchanges (V_i , $i = 1, 10$)

Fig. 5.2: Three-compartment box model of the Adriatic Sea

5.2.2 Equations

The equation describing the rate of change of mass within a reservoir can be written as:

$$\frac{dM}{dt} = Q - S$$

$\frac{dM}{dt}$ is the variation of mass of metal within of the reservoir

Q represents the sources (flux of metal into the reservoir)

S represents the sinks (flux of metal out of the reservoir).

The working assumption is that the 3 compartments are coupled and are in a steady-state,

that is to say: $\frac{dM}{dt} = 0$. Consequently sources (Q) and sinks (S) must balance in out each

compartment. Metal fluxes between compartments are proportional to chemical

concentrations in the compartment where they originate. The flux F_{ij} from reservoir i to reservoir j is given by:

$$F_{ij} = V_{ij} \cdot C_i$$

where V_{ij} represents the water flux from reservoir i to reservoir j and C_i represents the metal concentration in the reservoir i

The rate of change of the mass of metal (M_i) in the reservoir i is thus:

$$\frac{dM_i}{dt} = \sum_{j=1,n} V_{ij} C_{Mj} - C_{Mi} \cdot \sum_{j=1,n} V_{ij} \quad \text{for } i \neq j$$

where n is the total number of reservoirs in the system.

If we apply this concept to the Adriatic Sea model, the dynamic behaviour of the system is governed by the three differential equations:

$$\frac{dM_1}{dt} = -V_2 \cdot (C_1 + C_1') + V_1 \cdot (C_2 + C_2') + At_1 + Rv_1 + R_1 - Sd_1$$

$$\frac{dM_2}{dt} = V_2 \cdot (C_1 + C_1') - V_1 \cdot (C_2 + C_2') + V_{10} \cdot C_3 - V_9 \cdot C_2 - P \cdot C_2' + V_3 \cdot (C_{Is} + C_{Is}') - V_4 \cdot (C_2' + C_2) + At_2 + Rv_2 + Adv_1 + R_2 - Sd_2$$

$$\frac{dM_3}{dt} = V_9 \cdot C_2 + P \cdot C_2' - V_{10} \cdot C_3 + V_5 \cdot (C_{Lv} + C_{Lv}') + V_6 \cdot (C_{Id} + C_{Id}') - V_8 \cdot (C_3 + C_3') - V_7 \cdot (C_3 + C_3') + Adv_2 + R_3 - Sd_3$$

- $C_1, C_2, C_3, C_{Is}, C_{Lv}, C_{Id}$ are the dissolved trace metal concentrations for compartments 1, 2 and 3, for the Ionian Sea surface layer, the Levantine Intermediate water and for the Ionian Sea deep water.
- $C_1', C_2', C_3', C_{Is}', C_{Lv}', C_{Id}'$ are the particulate trace metal concentrations for compartments 1, 2 and 3, for the Ionian Sea surface layer, the Levantine Intermediate water and for the Ionian Sea deep water.
- V_i is a water flux ($i=1,10$), see section 6.2.1 for description
- P is the mass flux of particles between compartments 2 and 3
- At_1 and At_2 : atmospheric inputs in compartments 1 and 2
- Rv_1 and Rv_2 : riverine inputs in compartments 1 and 2
- R_1, R_2 and R_3 : remobilization in compartments 1, 2 and 3 respectively

- Sd_1 , Sd_2 and Sd_3 : sedimentation in compartments 1, 2 and 3 respectively
- Adv_1 and Adv_2 : advective transport of sediments from compartments 1 and 2 respectively

5.3 Estimation of annual fluxes

5.3.1 Rivers inputs

5.3.1.1 The River Po

The Po river accounts for 49 % of the total riverine inputs to the Adriatic Sea. Details about the flow rate variations are described in Chapter 2. The Po delta is a micro-tidal estuary which is stratified. Consequently there is a short residence time of the fresh water inputs in the mixing zone, the fresh water being rapidly transported southward.

Dissolved trace metals concentrations (Mn, Co, Fe, Cu, Ni, Zn, Cd, Pb) for the river Po have been reported in Chapter 4. On metal-salinity diagrams Cd, Cu, Ni and Pb show conservative mixing suggesting that only dilution influences the distribution of these trace metals in the mixing between the two end members. Other metals (Mn, Fe, Co and Zn) have been affected by removal processes. Dissolved riverine inputs have been calculated by multiplying concentrations in the upper reaches of the river (at Pontelagoscuro) by the river flow.

Particulate inputs are discussed in Chapter 4. Particulate concentrations are positively correlated with the river flow and consequently particulate fluxes are calculated by multiplying particulate trace metals concentrations by the river flow.

5.3.1.2 Total riverine inputs for the Adriatic

Such an estimation is difficult because of the large number of rivers with unknown inputs into the Adriatic Sea. The Po river represents 49 % of the total river inputs, with a runoff of $67.7 \text{ km}^3/\text{y}$. The other rivers in the Northern Adriatic Sea have an estimated runoff of $35.4 \text{ km}^3/\text{y}$. Consequently the total riverine input for compartment 1 is $103.1 \text{ km}^3/\text{y}$. The river inputs for compartment 2 have been estimated at $36.3 \text{ km}^3/\text{y}$.

Fluxes of trace metals for compartments 1 and 2 are reported in Table 5.1. To determine these fluxes several assumption have been made:

- 1) dissolved and particulate trace metal concentrations from the Po river have been extrapolated to the other rivers.
- 2) seasonal variations for river flow and trace metal concentrations have been observed. In the light of these observations, 2 periods have been differentiated: autumn-winter and spring-summer. Trace metal concentrations have been estimated for these 2 periods and are presented in Table 5.1 The river flow has been estimated as 60 % of the annual flow for the autumn-winter period and as 40 % for the spring-summer period.
- 3) the behaviour of dissolved trace elements in the mixing zone is taken as conservative. According to Table 5.1 most of the trace metals are associated with the suspended particulate material. The seasonal variation of trace metal concentrations is more pronounced for the dissolved phase than for the particulate phase. Riverine inputs are larger in compartment 1 than in compartment 2 by a factor of 2.8.

5.3.2 Atmospheric inputs

The estimation of trace metal atmospheric fluxes is difficult because of the variability of meteorological conditions. The Adriatic Sea is situated between the subtropical high-pressure zone and the mid-latitude or westerlies belt, in which atmospheric disturbances generally move from west to east. These zones shift throughout the year causing sharp seasonal differences. Through most of the year, the effects of the westerlies belt dominate the region, with frequent cyclones and anticyclones appearing in the lower troposphere. In winter, the dominant winds are the Bora (blowing from the Northeast) and the Sirocco (Southeast). In summer, Etesian winds (blowing from the Northwest) prevail, particularly in the southern Adriatic Sea where 53% of all winds come from this direction. Along the coast, land and sea breezes develop during the warmer part of the year. Relative humidity is at a minimum in summer, a maximum in autumn. However, more pronounced are its “synoptic” variations: a pulse of the Bora can lower humidity by 60-70%. Cloud amount depends on the passage of atmospheric disturbances, being greatest in late autumn and least in summer. As a consequence, maximum precipitation occurs in late autumn, with minimum precipitation characterising the summer period.

Table 5.1: Dissolved and particulate trace metal concentrations in the river Po and estimations of total riverine fluxes for compartments 1 and 2 and for the entire Adriatic Sea (AS).

	Dissolved trace metals					Particulate trace metals					the Total flux for AS
	conc. (nM) Summer	conc. (nM) Winter	flux (t/y) comp (1)	flux (t/y) comp (2)	flux (t/y) AS	conc. (µg/l) Summer	conc. (µg/l) Winter	flux (t/y) comp (1)	flux (t/y) comp (2)	flux (t/y) AS	
Mn	17.4	33.9	154.7	54.4	209	85.67	64.8	7543	2653	10196	10405
Fe	12.5	40.0	167.0	58.7	226	2390	2138	230865	81201	312066	312292
Co	0.483	0.424	2.7	1.0	3.7						4<
Pb	0.199	0.510	8.2	2.9	11.1	9.72	5.5	741	261	1002	1013
Cd	0.116	0.176	1.8	0.6	2.4	0.333	0.133	22	8	30	32
Zn	11.2	78.0	345.7	121.6	467	25.84	20.06	2307	811	3118	3586
Cu	28.2	43.6	245.3	86.3	332	5.19	4.72	506	178	684	1016
Ni	32.2	56.9	284.6	100.1	385	18.56	17.18	1829	643	2472	2856

Precipitation is greater at inland (about 1000 mm/year) than at coastal stations (approximately 400 mm/year).

The Adriatic Sea is surrounded by a number of contrasting aerosol source regions which supply trace metals to the atmosphere. There are anthropogenic inputs: the Adriatic is bordered by nations having a variety of economies, which range from industrial and semi-industrial to agricultural. There are natural inputs such as Saharan dusts: to the south-west it is bounded by the Western Mediterranean Sea and the Eastern Mediterranean Sea where there is the influence of the major desert belts of the African coast and the Middle East. In addition there is volcanic activity in the region (Etna) bringing volcanic dust into the system. Total atmospheric trace metal deposition was studied in the Western Mediterranean Sea by Guieu *et al.* (1991), Guerzoni *et al.* (1991), Nicolas *et al.* (1995) and Chester *et al.* (1993b), as part of the EROS 2000 European Union programme. To estimate atmospheric inputs of the Adriatic Sea, data from Guieu *et al.* (1997) have been used since these include information for all the trace metals studied in the Adriatic Sea (see Table 5.2).

Atmospheric inputs are similar for the 3 stations presented in Table 5.2 for Cd and Ni. For stations on the French coast (Tour du Valat and Cap Ferrat) deposition of Mn, Fe, Co, Cu and Pb tend to be higher than in Corsica (Ajaccio). This may be due to coastal inputs and anthropogenic inputs from industries and traffic.

Table 5.2: Total atmospheric trace metal inputs for the Western Mediterranean Sea (Guieu *et al.*, 1997)

	Tour du Valat kg/km ² /y	Cap Ferrat kg/km ² /y	Ajaccio kg/km ² /y
Mn	19	5.5	5.5
Fe	73	37	9
Co	0.04	0.02	0.011
Pb	4.0	6	2.5
Cd	0.2	0.36	0.25
Zn	1.8	1.8	2.2
Cu	2.0	0.65	0.6
Ni	0.4	0.3	0.5

Data from Ajaccio will be used to extrapolate the numbers to the southern Adriatic Sea because this station is remote from the coast and is less influenced by any anthropogenic inputs which could give an overestimate of atmospheric inputs for this area, whereas data from Tour du Valat will be used to extrapolate the numbers to the northern Adriatic Sea

which is more influenced by coastal and anthropogenic inputs than the southern part of the Adriatic Sea.

Atmospheric inputs occur by two mechanisms:

1) dry deposition

Aerosol fluxes are directly related to the wind systems. It is possible to characterise the aerosol by their chemical composition (Chester *et al.*, 1993b); winds from the north have high concentrations in anthropogenic elements (Cd, Zn, Pb), and winds from the south have high concentrations in terrigenous elements (Fe and Al).

2) wet deposition

In general Cd, Cu, Ni, Pb and Zn are primarily in the dissolved phase because of their higher solubility and of the natural acidity of the rain water. For Al and Fe, which are less soluble, the particulate phase is more important. According to Guieu (1991), there is a chemical signature for wet deposition; Saharan rain is characterised by high concentrations in Al and Fe; European rain is enriched in Cd, Pb and Zn which are anthropogenic metals; Co, Cu, Mn and Ni have mixed origins. Consequently it was suggested that trace metals could be used to indicate the origin of the different air masses.

The extent of dissolution of particulate trace metals after dry and during wet deposition depends on the characteristics of the particles. Once immersed in seawater, a fraction of particulate trace metals may be solubilised. The solubility coefficient depends on the nature of the element. According to Chester *et al.* (1993a) it is the chemical character of aerosols which constrains the fate of the metals in seawater; for example the dissolution of trace metals is considerably greater from anthropogenic than from crustal components.

Partitioning between the dissolved and the particulate fractions of trace metal depositions has been studied in detail by Guieu *et al.* (1997) but for the purpose of constructing the mass balance of the Adriatic Sea only total fluxes have been taken into account (Table 5.2). Total atmospheric inputs were partitioned in proportion to the relative surface areas of compartment 1 (45 % of the whole of the Adriatic) and compartment 2 (55 %). Results in t/y for the Adriatic atmospheric inputs are presented in Table 5.3. These estimates are based on data collected in the Northern Western Mediterranean Sea and on the hypothesis that fluxes are uniform throughout the entire Adriatic Sea. However Guerzoni *et al.* (1995) demonstrated that Saharan aerosol fluxes decrease exponentially with latitude.

Consequently, the estimated values may represent upper limits for trace metals with a Saharan origin.

Table 5.3: Atmospheric inputs for the Adriatic Sea

	Compartment 1 (t/y)	Compartment 2 (t/y)	Adriatic Sea (t/y)
Mn	1368	484	1852
Fe	5256	792	6048
Co	0.792	0.968	1.76
Pb	288	220	508
Cd	18	22	40
Zn	130	194	324
Cu	144	53	197
Ni	29	44	73

5.3.3 Internal cycling

5.3.3.1 Water Fluxes: Upwelling, downwelling, exchanges between compartments 1 and 2 and exchanges between the Adriatic and Ionian Sea.

In this chapter, a quantitative estimation of the mean water fluxes in the Adriatic Sea is proposed, on the basis of the water and salt budgets for each compartment (Bethoux, 1980).

On the basis of the water and salt mass balances, it is possible to write the following equations:

- water mass balance for compartment 1:

$$V_1 - V_2 - (E - P) = 0 \quad (1)$$

- salt mass balance for compartment 1:

$$\rho_2 S_2 V_2 = \rho_1 S_1 V_1 \quad (2)$$

- water mass balance for compartment 2:

$$V_2 - V_1 + V_3 - V_4 + V_{10} - V_9 - (E - P) = 0 \quad (3)$$

- salt mass balance for compartment 2:

$$\rho_3 S_3 V_3 - \rho_4 S_4 V_4 + \rho_{10} S_{10} V_{10} - \rho_9 S_9 V_9 + \rho_2 S_2 V_2 - \rho_1 S_1 V_1 = 0 \quad (4)$$

- water mass balance for compartment 3:

$$V_5 + V_6 - V_7 - V_8 + V_9 - V_{10} = 0 \quad (5)$$

- salt mass balance for compartment 3:

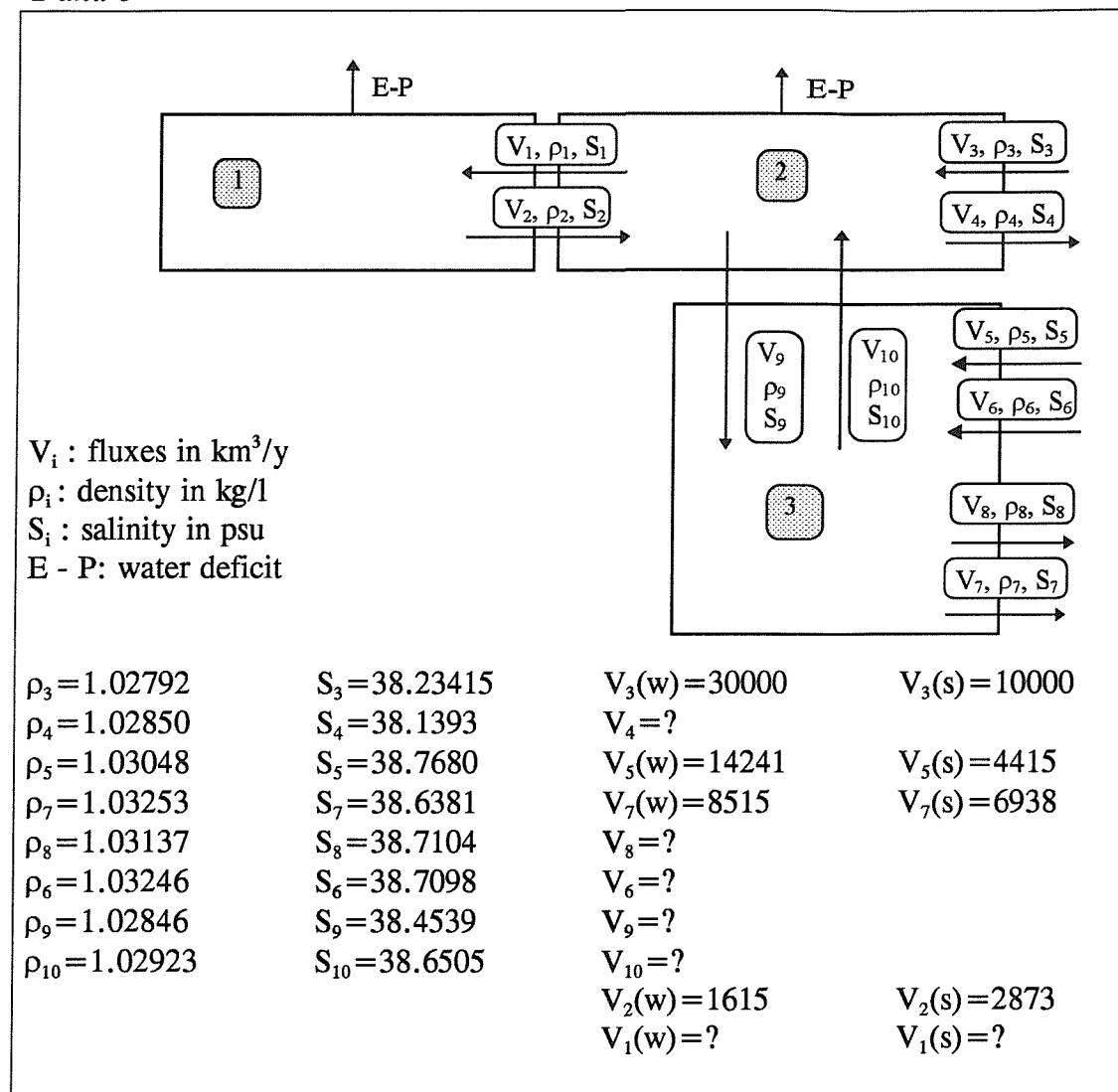
$$\rho_9 S_9 V_9 - \rho_{10} S_{10} V_{10} + \rho_5 S_5 V_5 + \rho_6 S_6 V_6 - \rho_7 S_7 V_7 - \rho_8 S_8 V_8 = 0 \quad (6)$$

- water mass balance for the entire Adriatic Sea:

$$V_4 + V_7 + V_8 = To \text{ (total outflow)} \quad (7)$$

$$V_3 + V_5 + V_6 = Ti \text{ (total inflow)} \quad (8)$$

Fig. 5.3: Horizontal and vertical fluxes, salinities and densities in compartments 1, 2 and 3



In order to determine the fluxes, observed salinity (S_i, i = 1,10) and density (ρ_i, i = 1,10) values have been introduced into the mass balance equations. Bethoux (1980) also estimated the water deficits (E-P) in the different surface compartments of the Adriatic Sea. The northern part of the Adriatic Sea has a positive water budget (E-P = -3 km³/y), loss by

evaporation (E) being slightly less than river influx and precipitation (P) whereas the southern part of the Adriatic has a negative budget (E-P = 21 km³/y).

V_3 , V_5 , V_7 , T_i and T_o have been measured by Poulain *et al.* (1996). V_2 has been determined by Mosetti *et al.* (1996). V_8 , V_4 , V_6 , V_{10} , V_9 , and V_1 have been calculated using equations (1), (2), (3), (4), (5), (6), (7) and (8).

$$V_8 = \frac{1}{\rho_4 \cdot S_4 - \rho_8 \cdot S_8} [-\rho_3 \cdot S_3 \cdot V_3 + \rho_4 \cdot S_4 \cdot (T_o - V_7) + \rho_7 \cdot S_7 \cdot V_7 - \rho_3 \cdot S_3 \cdot V_5 - \rho_6 \cdot S_6 \cdot (T_i - V_5 - V_3)]$$

$$V_4 = T_o - V_7 - V_8$$

$$V_6 = T_i - V_5 - V_3$$

$$V_{10} = \frac{1}{\rho_{10} \cdot S_{10} - \rho_9 \cdot S_9} [-\rho_3 \cdot S_3 \cdot V_3 + \rho_4 \cdot S_4 \cdot V_4 + \rho_9 \cdot S_9 \cdot (V_7 - V_5 + V_8 - V_6)]$$

$$V_9 = V_7 - V_5 + V_{10} + V_8 - V_6$$

$$V_1 = V_2 + (E - P)$$

Results are shown in Table 5.4.

**Table 5.4: Water fluxes for winter and summer periods
(Fluxes are in km³/y)**

	Winter/ Autumn	Summer/ Spring
Total Inflow	52665	31851
Total Outflow	52720	31851
V_3	30000	10000
V_4	28534	7430
V_5	14191	4415
V_6	8474	17436
V_7	8515	6938
V_8	15671	17483
V_9	3185	2888
V_{10}	1664	318
V_1	1618	2876
V_2	1615	2873

In Poulain *et al.* (1996) total outflow and total inflow are significantly different. This difference may be due to low spatial resolution of current meters and consequently some recirculation due to mesoscale eddies, occurring especially in the shear zone between inflow and out flow may have been lost. To satisfy the water budget the net water flux

through the Strait of Otranto has been taken as equal to zero using the highest values of total outflow and total inflow in the data given by Poulain *et al.* (1996).

The calculated results for water fluxes, require data from independent measurements, each of which is subject to a random uncertainty and each of which contribute to the net random error of the result. For the purpose of showing how such random uncertainties affect the outcome of the results, the independency of the fluxes, on which the calculated results depend, has to be assumed. This means that the calculated errors are overestimated since fluxes are linked with the water budget and salt budget equations. Nevertheless it gives an idea of the reliability of the calculated fluxes. Standard deviations of V_5 , V_7 and Total outflow are respectively 5046, 3154 and 8200 km³/y for the winter and autumn seasons (Poulain *et al.*, 1996). Standard deviations of V_8 , V_4 , V_6 , V_{10} and V_9 have been calculated according to the standard error propagation equations assuming the independency of the fluxes:

$$\sigma_{V_8}^2 = \frac{1}{(\rho_4 S_4 - \rho_8 S_8)^2} \cdot \left[(\rho_6 S_6 - \rho_3 S_3)^2 \cdot \sigma_{V_3}^2 + (\rho_6 S_6 - \rho_5 S_5)^2 \cdot \sigma_{V_5}^2 + (\rho_4 S_4 - \rho_6 S_6)^2 \cdot \sigma_{To}^2 \right. \\ \left. + (\rho_7 S_7 - \rho_4 S_4)^2 \cdot \sigma_{V_7}^2 \right]$$

$$\sigma_{V_4}^2 = \sigma_{To}^2 + \sigma_{V_7}^2 + \sigma_{V_8}^2$$

$$\sigma_{V_6}^2 = \sigma_{To}^2 + \sigma_{V_7}^2 + \sigma_{V_8}^2$$

$$\sigma_{V_{10}}^2 = \frac{1}{(\rho_{10} S_{10} - \rho_9 S_9)^2} \cdot \left[(\rho_3 S_3)^2 \cdot \sigma_{V_3}^2 + (\rho_4 S_4)^2 \cdot \sigma_{V_4}^2 + (\rho_9 S_9)^2 \cdot (\sigma_{V_7}^2 + \sigma_{V_5}^2 + \sigma_{V_8}^2 + \sigma_{V_6}^2) \right]$$

$$\sigma_{V_9}^2 = \sigma_{V_7}^2 + \sigma_{V_5}^2 + \sigma_{V_{10}}^2 + \sigma_{V_8}^2$$

After calculations, standard deviations of V_8 , V_4 , V_6 , V_{10} and V_9 are respectively:

$$\sigma_{V_8}^2 = 0.90 \cdot \sigma_{V_3}^2 + (9199)^2$$

$$\sigma_{V_4}^2 = (12720)^2 + 0.90 \cdot \sigma_{V_3}^2$$

$$\sigma_{V_6}^2 = (9628)^2 + \sigma_{V_3}^2$$

$$\sigma_{V_{10}}^2 = 83941 \cdot \sigma_{V_3}^2 + 5.82 \cdot 10^{11}$$

$$\sigma_{V_9}^2 = 83942 \cdot \sigma_{V_3}^2 + 5.82 \cdot 10^{11}$$

The standard deviation of V_3 (σ_{V_3}) is not known since V_3 has been fixed. The standard deviations of calculated fluxes depends on σ_{V_3} . σ_{V_3} can be considered as small since it has been chosen using current measurements data obtained by Poulain *et al.* (1996). In these

conditions, standard deviations σv_4 , σv_8 , σv_6 are relatively small compared to the calculated fluxes V_4 , V_8 and V_6 and consequently these fluxes can be considered as reliable. This is not the case for σv_{10} and σv_9 which exceed V_{10} and V_9 by several order of magnitude. This probably reflects the actual variability of V_{10} and V_9 . According to Lascoros (1993), the water mass formation which occurs in the Southern Adriatic Sea during the winter period is $10,722 \text{ km}^3/\text{y}$. This number is much higher than the value (V_9) calculated in Table 5.4. Poulain *et al.* (1996) found that the outflow of ADW in the deepest central portion of the strait and on the western continental margin is not continuous, and appears as a series of bursts of southward flows lasting for about a week. They found also that these bursts correspond to a bottom intensified pulsation of the entire water column. The value for water formation (V_9) represents a mean for 6 months and consequently is compatible with the value given by Lascoros (1993) which is representative of a short period of time.

5.3.3.2 Trace metal fluxes between compartments 1 and 2

Water fluxes between compartments 1 and 2 were combined with dissolved and particulate trace metal data. Stations 4 and 3 gave an estimate for trace metal concentrations in waters leaving compartment 1 on the west coast of the Adriatic Sea. The east side of the Adriatic Sea was not sampled, consequently trace metal concentrations in waters entering compartment 1 were estimated using data from the surface layer of Station 5. A seasonal variation has been taken into account for the calculation of fluxes out of compartment 1 since a high variability in trace metal concentrations has been observed in the North Adriatic Sea. Table 5.5 gives results for trace metal fluxes in and out of compartment 1. Particulate trace metals were not available for Co and Cd and consequently trace metal fluxes between compartments 1 and 2 were underestimated for those metals. Trace metals are exported from compartment 1 to compartment 2. Fe, Mn, Pb and Zn are mainly transported in the particulate phase whereas the other elements (Cu and Ni) are primarily transported in the dissolved phase.

Table 5.5: Fluxes of dissolved and particulate trace metals in and out of compartment 1

	Mn	Fe	Co	Pb	Cd	Zn	Ni	Cu
concentration D (S) (nM) OUT	16.5	2.42	0.27	0.067	0.064	3.94	6.04	3.5
concentration P (S) ($\mu\text{g/l}$) OUT	0.35	8.26		0.054		0.18	0.035	0.034
concentration D (W) (nM) OUT	8.45	1.73	0.42	0.207	0.093	6.45	7.68	5.45
concentration P (W) ($\mu\text{g/l}$) OUT	1.95	62		0.395		0.96	0.143	0.213
flux D OUT (t/y)	1677	272	43	55	19	711	873	599
flux P OUT (t/y)	2077	61930		397		1034	166	221
Total Flux OUT	3754	62203	43	451	19	1744	1039	820
concentration D (nM) IN	3.92	0.73	0.138	0.052	0.064	3.14	5.7	3.11
concentration P ($\mu\text{g/l}$) IN	0.046	1.61		0.024		0.155	0.008	0.021
flux D IN	484	92	18	24	16	461	752	444
flux P IN	103	3618		54		348	18	48
Total Flux IN	587	3709	18	78	16	810	770	492
IN-OUT	-3167	-58493	-25	-373	-3	-935	-269	-328

D: dissolved; P: particulate; S: summer; W: winter.

5.3.3.3 Trace metals fluxes through the Strait of Otranto

First estimates of dissolved metal fluxes were generated by multiplying the metal concentrations in Tables 5.6a and 5.6b by the appropriate water mass inflow and outflow data given in the same Tables for the Adriatic Sea in winter and summer.

Since particulate trace metal data were not available for the Strait of Otranto, particulate trace metals were not included in the budget for the Strait. However SPM was very low in this area consequently particulate trace metals could be taken as a negligible fraction of the total trace metals (Civitarese *et al.*, 1998).

Table 5.6a: Fluxes of dissolved trace metals entering the Adriatic Sea through the Strait of Otranto

	Flow km ³ /y	Mn	Fe	Co	Pb	Cd	Zn	Ni	Cu
surface layer									
metal concentrations (nM)		4.45	1.59	0.118	0.17	0.05	4.15	5.08	2.52
winter flux (t/y)	30000	7334	2664	209	1057	169	8140	8944	4804
summer flux (t/y)	10000	2445	888	70	352	56	2713	2981	1601
Mean Flux (t/y)	4889	1776	139	704	112	5427	5963	3203	
Levantine Intermediate Water									
metal concentration (nM)		0.317	0.637	0.032	0.086	0.053	4.53	3.68	1.66
winter flux (t/y)	14241	248	506	27	253	85	4224	3079	1502
summer flux (t/y)	4415	77	157	8	78	26	1310	954	466
Mean Flux (t/y)	162	332	18	166	56	2767	2016	984	
Ionian Intermediate Water									
metal concentration (nM)		0.190	0.507	0.019	0.069	0.038	3.47	4.04	1.68
winter flux (t/y)	8474	88	240	9	121	37	1921	2011	906
summer flux (t/y)	17435	182	493	20	249	75	3952	4137	1865
Mean Flux (t/y)	135	367	15	185	56	2936	3074	1386	

For dissolved Fe and Ni, inflows and outflows cancel out to within 10 % (Table 5.6c). For dissolved Mn, Co, Cd and Cu there is net export out of the Adriatic Sea. Rivers and benthic inputs are the main sources of dissolved Mn, Co, Cd and Cu to the Adriatic. For dissolved Zn and Pb the Adriatic Sea appears to be a net sink. This is particularly so for Zn where the concentrations are lower in the Adriatic Sea than in the Ionian Sea. Zn is probably imported into the system through the Strait of Otranto and is trapped in the sediment. Zn is a biological reactive element. It is taken up by phytoplankton during blooms and transported to the sediment when the phytoplankton die. The trapping efficiency of the Adriatic Sea towards Pb is comparable to that for Zn, though probably not for the same reasons: Pb has no known biological function but tends to adhere strongly to the surface of particles.

Table 5.6.b: Fluxes of dissolved trace metals leaving the Adriatic Sea through the Strait of Otranto

	Flow km ³ /y	Mn	Fe	Co	Pb	Cd	Zn	Ni	Cu
surface layer									
metal concentrations (nM)		5.65	1.89	0.16	0.13	0.07	3.77	5.07	3.65
winter flux (t/y)	28534								
summer flux (t/y)	7431	8857	3012	269	769	225	7033	8491	7198
Mean Flux (t/y)		2307	784	70	200	58	1832	2211	1875
		5582	1898	170	484	141	4432	5351	4169
Intermediate Adriatic Water									
metal concentrations (nM)		1.12	0.74	0.048	0.063	0.062	3.37	4.10	2.42
winter flux (t/y)	15671								
summer flux (t/y)	17481	964	648	45	205	108	3453	3771	2410
Mean Flux (t/y)		1076	722	50	228	121	3852	4206	2688
		1020	685	47	216	115	3652	3989	2549
Adriatic Deep Water									
metal concentrations (nM)		0.23	0.33	0.008	0.062	0.036	3.36	3.83	1.47
winter flux (t/y)	8515								
summer flux (t/y)	6938	108	157	4	109	34	1868	1914	795
Mean Flux (t/y)		88	128	3	89	28	1522	1560	648
		98	142	3	99	31	1695	1737	722

Table 5.6.c: Trace metal mass balance for the Adriatic Sea across the Strait of Otranto (t/y)

	Mn	Fe	Co	Pb	Cd	Zn	Ni	Cu
IN-OUT	-1512	-251	-49	256	-64	1350	-23	-1867
IN/OUT	0.77	0.91	0.78	1.32	0.78	1.14	1.00	0.75
% variation	23	9	22	-32	22	-14	0	25

5.3.3.4 Trace metal fluxes associated with upwelling and downwelling within the Adriatic Sea

Vertical water fluxes were estimated in 5.3.3.1. The winter fluxes take into account the water mass formation which occurs in the Southern Adriatic Pit. The amounts of dissolved trace metals transported by upwelling and downwelling, expressed as yearly fluxes, are reported in Table 5.7.

Table 5.7: Vertical exchanges of dissolved trace metals

	Mn	Fe	Pb	Co	Cu	Ni	Cd	Zn
concentrations (nM) compartment (2)	4.43	2.83	0.14	0.18	2.64	3.48	0.06	2.94
Downwelling (t/y)	739	480	88	32	509	620	20	584
concentrations (nM) compartment (3)	1.12	1.15	0.09	0.05	1.62	4.15	0.06	3.06
Upwelling (t/y)	61	64	3	18	7	198	102	241

5.3.3.5 Down column fluxes of particles

Trace metals are transferred from the dissolved phase to the particulate phase through adsorption or biological uptake depending on the type of element and particle. In Chapter 1, two major types of trace metals have been defined: the nutrient type (Ni, Cu, Zn and Cd) and the scavenged type (Pb, Mn, Co and Fe). The distribution of scavenged elements reflects boundary inputs and interactions with the particulate phase in suspension in the water column. In contrast, the nutrient-type distribution reflects the involvement of the trace metals in the major biological cycles which, in the open ocean, results in surface depletion and subsurface enrichment in their dissolved concentrations. Vertical trace metal distributions may be interpreted in terms of either a scavenging-type or a nutrient-type behaviour or by a combination of both, all of which involve the transfer of dissolved species onto particulate matter. The distinction between the scavenged-type and the nutrient-type behaviours not only draws attention to the central role played by particulate matter in the removal of trace metals from seawater, but also highlights the importance of the nature and reactivity of individual particles; thus internally-produced biotic particles (responsible for the nutrient-type behaviour) are involved in different trace metal cycles than are the externally-produced non-biotic particles (scavenged-type). The importance of particulate material in the removal of trace metals from seawater has been widely acknowledged for many years, to the extent that Turekian (1977) referred to the overall process as the “great particle conspiracy”. Particles from detritic or biogenic origin will sink in the water column, the sedimentation rate depending of the size and shape of the particles. Small particles have a low sedimentation rate and consequently do not sink rapidly; they can be degraded by bacterial activity and remineralized. Large particles or aggregates have sufficient mass to sink at an appreciable rate and thus reach the sediments.

Mass fluxes vary greatly between different marine environments: in shallow water sedimentation rates are greater than in deep water. The vertical transport is dominated by the global carbon flux and depends on the primary production.

Heussner *et al.* (1995) reported some data on downward fluxes of particles in the Southern part of the Adriatic (Station 5) obtained by a sediment trap technique. They reported a mass flux of $0.012 \text{ g cm}^{-2} \text{ y}^{-1}$. Particulate metal data for Mn, Fe, Cu and Ni were available for the Adriatic Sea (Price, pers. communication). For particulate Pb, Zn, Co and Cd data from the Western Mediterranean Sea (Tankéré *et al.*, 1995) were extrapolated to the Adriatic Sea. These data were combined with the particle flux data of Heussner *et al.* (1995) to give an estimate of particulate trace metal fluxes for the Southern Adriatic Sea, which represents 27.5 % of the total surface of the Adriatic (see Table: 5.8).

Table 5.8: Estimation of particulate trace metal fluxes from compartment 2 to compartment 3 in the southern Adriatic Sea (Flux of particles is $0.012 \text{ g cm}^{-2} \text{ y}^{-1}$, (Heussner *et al.* (1995)).

	Mn	Fe	Co	Pb	Cu	Ni	Cd	Zn
concentrations ($\mu\text{g/g}$)	180	6158	0.74	4.4	84	31	0.38	41
Flux (t/y)	950	32514	4	23	444	164	2	214

5.3.4 Sedimentation

The assessment of sediment accumulation rates is crucial to understand the role played by the sediments as marine sinks for components that have flowed through the seawater reservoirs. Frignani and Langone (1991) and Frignani *et al.* (1996) discussed apparent accumulation rates from a series of sediment cores collected in the Po delta, in the western side of the Adriatic continental shelf and in the Southern Adriatic Basin (Table 5.9).

Table 5.9: Sedimentation rates in different parts of the Adriatic Sea

Station	% of total surface area	sedimentation rate ($\text{g cm}^{-2} \text{ y}^{-1}$)
1A	10	0.77
2	10	0.3
3	25	0.13
4	27.5	0.26
5	27.5	0.06

The sediment accumulation rate studies were conducted using ^{210}Pb and ^{137}Cs measurements. Generally there was a good agreement between the accumulation rates derived by the different techniques.

The highest accumulation rates occur near the Po delta where the supply of sedimentary material from the land is greatest. There the accumulation rates lie in the range 1.80 ± 0.29 to $0.53 \pm 0.04 \text{ g cm}^{-2} \text{ y}^{-1}$. A mean value $0.77 \text{ g cm}^{-2} \text{ y}^{-1}$ for the Po delta area (10 % of the total surface area) has been calculated. Accumulation rates south of the delta are lower and fairly constant ($0.29 \text{ g cm}^{-2} \text{ y}^{-1}$). At Station 3, the ^{210}Pb and ^{137}Cs measurements give respectively mass accumulations of $0.12 \text{ g cm}^{-2} \text{ y}^{-1}$ and $0.14 \text{ g cm}^{-2} \text{ y}^{-1}$. In the central Adriatic Sea (Station 4), accumulation rates vary with time (Frignani *et al.*, 1996). The core collected at Station 4 showed a sediment accumulation rate of $0.31 \text{ g cm}^{-2} \text{ y}^{-1}$ until 1945; after this date and up to 1965, the accumulation rate reduces to $0.12 \text{ g cm}^{-2} \text{ y}^{-1}$ and since this date the accumulation rate appears to be around $0.26 \text{ g cm}^{-2} \text{ y}^{-1}$. In the Southern Adriatic Basin, a sediment accumulation rate of $0.06 \text{ g cm}^{-2} \text{ y}^{-1}$ has been measured using ^{210}Pb measurements.

During the EUROMARGE-AS project, a large number of cores were collected in the Adriatic Sea and were analysed for trace metals (Price *et al.*, 1995). These results are presented in Table 5.10.

Table 5.10: Trace metal composition of cores (total values for the first cm) in different parts of the Adriatic Sea.

Station	Mn (%)	Fe (%)	Cu ($\mu\text{g/g}$)	Ni ($\mu\text{g/g}$)	Pb ($\mu\text{g/g}$)	Zn ($\mu\text{g/g}$)
1A	0.080	3.54	42.8	84.9	42.7	152
2A	0.080	3.89	32.2	82.9	25.9	106
6	0.107	3.66	23.6	63.2	25.9	104
8	0.084	3.65	23.6	63.2	25.9	104
10	0.373	3.52	26.4	135	24.6	99
5	0.158	3.71	49.4	153	27.7	99

Trace metal sedimentation fluxes have been estimated in different parts of the Adriatic Sea and are presented in Table 5.11.

Table 5.11: Fluxes of trace metals into sediments

	Mn (t/y)	Fe (t/y)	Cu (t/y)	Ni (t/y)	Pb (t/y)	Zn (t/y)
compartment 1	192970	8140240	8047	17723	7855	29164
compartment 2	96096	4175600	2700	7230	2964	11897
compartment 3	41712	979440	1303	4039	731	2629
Adriatic Sea	330778	13295280	12050	28992	11550	43690

5.3.5 Advectional transport of sediments from the shelf

Advectional transport of sediments from compartment 1 to compartment 2 is evident from sedimentation rate measurements: sedimentation in compartment 2 ($0.26 \text{ g cm}^{-2} \text{ y}^{-1}$) is exceeding *in situ* production and sedimentation in compartment 1 ($0.12 \text{ g cm}^{-2} \text{ y}^{-1}$). The “Marine snow” produced in the Northern Adriatic waters is composed of aggregated biogenic and inorganic particles which flocculate and are easily resuspended when reaching the sediment floor (Stachowitzsch *et al.*, 1990). The transport of this material in deeper water is facilitated by resuspension and is topography driven: it is transported along the Italian coast in a southward direction. A first estimate of this transport shows that 54 % of the sediment in compartment 2 has possibly been advected from compartment 1. Advectional transport of sediment from the shelf could also be a major source of metals for compartment 3 since sedimentation rates obtained by ^{210}Pb and ^{137}Cs measurements in sediments are significantly higher than the sedimentation rate obtained by sediment trap technique. As much as 80% of the sediments in compartment 3 might have been advected from the shelf. However a more detailed study of the particle transfer from the Northern Adriatic Sea to the South Adriatic Pit needs to be done with sediment traps which would allow to identify and measure the influence of the general and local factors controlling the particle transfer.

5.4 Results of the mass balance

A first order mass balance of 6 different trace elements (Mn, Fe, Pb, Zn, Cu and Ni) in the Adriatic Sea is presented for a one year period for the different compartments (Table 5.12). Remobilization from sediments has been calculated by difference, when all other fluxes have been estimated. Remobilization fluxes are high in the Northern and Central Adriatic Sea. Although remobilization is not quantified directly, the results of the mass balance suggest that the process is potentially important and needs to be assessed.

5.4.1 Mass balance in compartment 1

In compartment 1, trace metal inputs are from rivers, the atmosphere and remobilization.

Riverine inputs tend to be higher than atmospheric inputs for all metals (Mn, Fe, Pb, Zn, Cu and Ni) and are mainly associated with particles.

Table 5.12: Mass balance for the Adriatic Sea

COMPARTMENT 1		Phase	Mn (t/y)	Fe (t/y)	Pb (t/y)	Zn (t/y)	Cu (t/y)	Ni (t/y)
Rivers	D	155	167	8	346	245	285	
	P	7543	230865	741	2307	506	1829	
Atmosphere	T	1368	5256	288	130	144	29	
Exchanges between compartments 1 and 2	D	-1193	-180	-31	-250	-155	-121	
	P	-1974	-58312	-343	-686	-173	-148	
Sedimentation	P	-192970	-8140240	-7855	-29164	-8047	-17723	
Remobilization	D	187071	7962444	7192	27317	7480	15849	
COMPARTMENT 2		Phase	Mn (t/y)	Fe (t/y)	Pb (t/y)	Zn (t/y)	Cu (t/y)	Ni (t/y)
Rivers	D	54	59	3	122	86	100	
	P	2653	81201	261	811	178	643	
Atmosphere	T	484	792	220	194	53	44	
Exchanges between compartments 1 and 2	D	1193	180	31	250	155	121	
	P	1974	58312	343	686	173	148	
Exchanges with the Strait of Otranto	D	-693	-122	220	995	-966	612	
Upwelling	D	61	64	18	198	102	241	
Downwelling	D	-739	-480	-88	-584	-509	-620	
Particle flux	P	-950	-32514	-23	-214	-444	-164	
Advectional transport of sediments	P	51700	2246473	1595	6401	1452	3890	
Sedimentation	P	-96096	-4175600	-2964	-11897	-2700	-7230	
Remobilization	D	40359	1821636	384	3039	2419	2215	
COMPARTMENT 3		Phase	Mn (t/y)	Fe (t/y)	Pb (t/y)	Zn (t/y)	Cu (t/y)	Ni (t/y)
Exchanges with the Strait of Otranto	D	-821	-128	36	356	-901	-636	
Upwelling	D	-61	-64	-18	-198	-102	-241	
Downwelling	D	739	480	88	584	509	620	
Particle flux	P	950	32514	23	214	444	164	
Advectional transport of sediments	P	33370	783552	585	2103	1042	3231	
Sedimentation	P	-41712	-979440	-731	-2629	-1303	-4039	
Remobilization	D	7535	163089	17	-430	311	901	

D: dissolved; P: particulate; T: total.

A fraction of these inputs is likely to be carried southward into compartment 2 via water fluxes. The contribution of the Northern Adriatic to the rest of the Adriatic Sea is relatively small because of the restricted water exchange and the losses due to burial in the sediment. Only 35% (Mn), 25% (Fe), 36% (Pb), 34% (Zn), 37% (Cu) and 13% (Ni) of total telluric inputs in compartment 1 may possibly be transported to the Central Adriatic Sea.

In the northern Adriatic Sea regeneration of Mn, Fe, Pb, Zn, Cu, Ni from deposited sediment represents most of the sedimentary flux. The remobilization and recycling of trace elements in the sediment–interstitial water–seawater complex is intimately related to the diagenetic environment under which the sediment is deposited. This suggest that diagenetic reactions occur in the sediment surface in the northern Adriatic Sea. The organic carbon that reaches the sea–floor is oxidised successively by O₂, nitrate, MnO₂ and Fe₂O₃ and remobilization of Mn and Fe occurs in the sediment (Sundby *et al.*, 1986). Metals like Pb, Zn, Cu, Ni which can be adsorbed onto Mn– and Fe– oxides, can simultaneously be released during dissolution of Mn and Fe solid phases (Sawlan and Murray, 1983). The recycled elements (Cu, Ni, Zn) may also be released during the decomposition of organic debris (Sawlan and Murray, 1983).

Westerlund *et al.* (1986) measured fluxes of trace metals (Cd, Cu, Ni, Zn and Pb) across the sediment–water interface *in situ* at 6 m depth in Gullmarsfjorden (Sweden), using diver-operated stirred benthic flux-chambers. The measured release rate with benthic chamber was high for Cd, Cu, Zn and Ni and was attributed to breakdown of labile organic matter during oxidation. Scavenging by particles, in particular by Fe and Mn oxide coatings was an important process in maintaining the low trace metal concentrations for Cu and Zn observed in pore waters in the surface of the core. Remobilization fluxes for trace elements, estimated with the mass balance, are consistent with the high concentrations of dissolved metals observed in bottom waters of the northern Adriatic Sea, particularly during the summer period (Chapter 4).

5.4.2 Mass balance in compartment 2

Though a lesser factor in the Southern Adriatic Sea than in the Northern part, riverine inputs still represent a major contribution to the mass balance of compartment 2 and most of the metals are associated with the particulate phase. Compartment 2 receives metals from

compartment 1 via water fluxes because of a net export of metals from the Northern Adriatic Sea to the Southern Adriatic Sea. In the Strait of Otranto Pb, Zn and Ni tend to be imported into compartment 2 from the Ionian Sea whereas Mn, Fe and Cu are exported towards the Ionian Sea. Upwelling and downwelling tend to mix the water column and, consequently, metals which have higher concentrations in the surface layer due to riverine and atmospheric inputs (Mn, Fe, Pb, Zn and Cu) are transported from the surface layer to the underlying layers. Downward fluxes of particles through the water column represents a major transport for Mn and Fe. In general, advective transport of sediments from the sediment floor in compartment 1 and sedimentation fluxes for the coastal zone exceed by several orders of magnitude, the other fluxes as do remobilization fluxes which are calculated by difference (Table 5.12). In the central Adriatic Sea, remobilization of Mn and Fe accounts for 42 and 44 % respectively of the deposited sediment which is less than in compartment 1 where 96.9 and 97.8 % have been found respectively, suggesting that diagenesis processes appear deeper in the sediment in the central Adriatic Sea. In the central Adriatic Sea, the dissolved Mn and Fe concentrations in the interstitial waters are low in the surface of the core and increase below 2 cm and 4 cm respectively (Chapter 4). This is characteristic of sub-oxic pore waters and results from the utilisation and solubilisation of Mn- and Fe- oxides in the diagenetic sequence. There is less remobilization of Pb in compartment 2 (13 % of deposited sediments). A similar observation has been made by Westerlund *et al.*, (1986) in Gullmarsfjorden (Sweden) and suggested that most Pb in these sediments was present in a non-mobile form. Remobilization of Zn, Cu and Ni accounts for 26, 90 and 31 % respectively of the deposited sediment. These metal releases are possibly due to oxidation of their organic carrier phases in the sediment column via secondary oxidants such as Mn oxides. As a result of this, the concentration gradients are greater here than higher up in the sediment column, and the concentration gradients set up lead to an upward migration via diffusion through the interstitial waters (Sawlan and Murray, 1983).

5.4.3 Mass balance in compartment 3

All metals but Pb and Zn are exported from the Adriatic to the Ionian Sea across the Strait of Otranto. Advective transport of sediments from compartment 2 constitute a major input of metals for compartment 3. Remobilization fluxes are significantly less in compartment 3 than

in compartments 2 and 1. This is consistent with the fact that the southern Adriatic sea floor is made of hemi-pelagic sediments where dissolved Mn concentrations in interstitial waters increase below 17 cm (Chapter 4). Remobilization fluxes for Mn, Fe, Cu and Ni account for 18 %, 17 %, 24 % and 22 % respectively of deposited sediments. Similar results have been found by Hartmann and Muller (1982) for Mn, Cu and Ni in oxic pelagic sediments from the central Pacific.

5.5 Time scales

5.5.1 Turnover time

By definition (Junge, 1974; Hamrud, 1983), the turnover time is the ratio between the contents (M) of a reservoir and the total flux out of it or into it (S):

$$\tau_0 = \frac{M}{S}$$

The turnover time may be thought of as the time it would take to empty the reservoir if the sink (S) remained constant while the sources were zero. A long turnover time is usually associated with a small variability in the total inventory (Junge, 1974; Hamrud, 1983). If material is removed from the reservoir by two or more separate processes, each with a flux S_i , where i is a particular process, then the turnover time with respect to each such process is

defined by:

$$\tau_{0i} = \frac{M}{S_i}$$

Table 5.13 presents turnover times of metals for the different processes involved in the removal. Turnover times of metals with respect to sedimentation are short for compartments 1 and 2 compared with other processes. In compartment 3, sedimentation is the main sink for Fe, Mn and Pb and consequently the turnover time for these metals with respect to sedimentation is short. For the other metals, the exchange with the Ionian Sea has a greater impact on the contents of the reservoir than upwelling or sedimentation and so the corresponding turnover times are relatively short.

Table 5.13: Turnover time of metals with respect to different processes

compartment 1	Mn	Fe	Pb	Zn	Cu	Ni
contents (t)	9695	4549	252	1761	1860	2060
exchange with 2 (y)	2.6	0.1	0.6	1.0	2.3	2.0
sedimentation (y)	0.050	0.001	0.032	0.060	0.231	0.116
Compartment 2	Mn	Fe	Pb	Zn	Cu	Ni
contents (t)	2450	21514	319	3215	1942	3055
exchange with 1 (y)	4.2	5.8	4.1	4.0	4.0	4.0
exchange with Ionian Sea (y)	0.44	11.3	0.66	0.73	0.43	0.57
downwelling (y)	3.3	44.8	3.6	5.5	3.8	4.9
particle flux (y)	2.6	0.7	13.9	15.0	4.4	18.6
sedimentation (y)	0.03	0.01	0.11	0.27	0.72	0.42
compartment 3	Mn	Fe	Pb	Zn	Cu	Ni
contents (t)	2149	62456	721	9837	3592	8000
exchange with Ionian Sea (y)	1.9	75.5	2.3	1.8	1.1	1.4
upwelling (y)	35	976	40	50	35	33
sedimentation (y)	0.05	0.06	0.99	3.7	2.8	2.0

5.5.2 Residence time

The residence time is the average time spent in a reservoir by an individual molecule. It is therefore the age of a molecule counted from its introduction into the reservoir when it leaves the reservoir. When the reservoir is in steady state ($\frac{dM}{dt} = 0$), sources (Q) and sinks (S) must balance and the residence time is equal to the turnover time. Table 5.14 presents the residence time of metals in the different compartments of the Adriatic.

The residence time of water in compartment 1 (Northern Adriatic Sea) is 2 years which is longer than in compartment 2 (less than 4 months) and compartment 3 (less than 1 year). Compartments 2 and 3 are subject to rapid exchanges and consequently the water is rapidly renewed. In compartment 1, the residence time of metals are significantly shorter than that for water, which suggest that metals are rapidly removed from the system. In compartment 2, the residence time for Zn, Cu and Ni are longer than for Mn, Fe and Pb and similar to that of water. Zn, Cu and Ni are mainly in the dissolved form, this may be due to low particle reactivity of those elements which therefore stay longer in the system. In compartment 3, residence time of metals (Zn, Cu, Ni and Pb) are generally longer than in compartment 2 and similar to the residence time of water. Mn and Fe exhibit short residence times indicating significant removal.

Table 5.14: residence time (R.T.) of water and metals in the Adriatic Sea

compartment 1	Mn	Fe	Pb	Zn	Cu	Ni	water
contents (t)	9695	4549	252	1761	1860	2060	3600.10⁹
annual inputs (t/y)	196724	8202441	8307	30910	8867	18762	1776.10 ⁹
R.T. (y)	0.049	0.001	0.030	0.057	0.210	0.110	2.03
compartment 2	Mn	Fe	Pb	Zn	Cu	Ni	water
contents (t)	2450	21514	319	3215	1942	3055	8800.10⁹
annual inputs (t/y)	103954	4214194	3636	17936	8318	14135	22769.10 ⁹
R.T. (y)	0.024	0.005	0.088	0.179	0.233	0.216	0.386
compartment 3	Mn	Fe	Pb	Zn	Cu	Ni	water
contents (t)	2149	62456	721	9837	3592	8000	23600.10⁹
annual inputs (t/y)	42891	980331	1064	8174	4676	10006	25319.10 ⁹
R.T. (y)	0.050	0.064	0.677	1.203	0.768	0.799	0.932

5.6 Uncertainties

Uncertainties in the estimates of fluxes of metals arise from the errors associated with estimated water fluxes and with suspended particulate fluxes, from the assumptions made in interpolation procedures, and from analytical errors. The analytical error can be considered small compared to the error associated with the estimated water fluxes since there was a good accuracy in the determination of metal concentrations. Evaluation of the errors on the estimates of metals fluxes is difficult because there are insufficient observations to test all the assumptions involved in the interpolation of data.

CHAPTER 6

TRACE METALS IN THE NORTHWESTERN BLACK SEA

6.1 The study area

6.1.1 Geomorphology of the Black Sea

The Black Sea is an elliptical basin with an area of 423,000 km² and a volume of 534,000 km³. It is located in an east-west intermontane depression between two Alpine fold belts. South of the Black Sea are the Pontic Mountains with a maximum elevation of 3,937 m, and east of it are the Caucasus Mountains with a maximum elevation of 4,040 m.

Echo-sounding data (Ross *et al.*, 1974) show that the Black Sea basin can be divided into 4 physiographic provinces (Fig. 6.1a and b): shelf (29.9 % area), basin slope (27.3 % area), basin apron (30.6 % area) and abyssal plain (12.2 % area) — the last three are crossed by the Danube fan, which is a relict sedimentary feature formed as the result of the high rate of sediment supply by rivers entering the northwestern part of the Black Sea (Danube, Dnestr, Bug and Dnepr rivers). Studies of Holocene sediments (Ross *et al.*, 1970) indicate that, at present, little fluvial sediment is being supplied to the fan; most of the particles are being trapped in the river estuaries — a phenomenon typical of many areas because of the rise in sea level 9,000 years ago. The maximum development of the shelf is west of the Crimean Peninsula where it is more than 190 km wide. Along the Turkish coast, eastern Russia, and south of the Crimea peninsula, the shelf exceeds 20 km in width in only a few places. The basin slopes are of 2 types: a steep, highly dissected slope where erosion was the dominant process in the recent past, and possibly the present, and a smooth slope where deposition has been predominant. The steep slope is present where the shelf is narrow and submarine canyons reach nearly to the present shore. The smooth slope occurs where the shelf is widest and where pelagic sedimentation is the dominant mode of sedimentation. Most basin aprons at the base of the slopes are continuous and are interrupted only locally

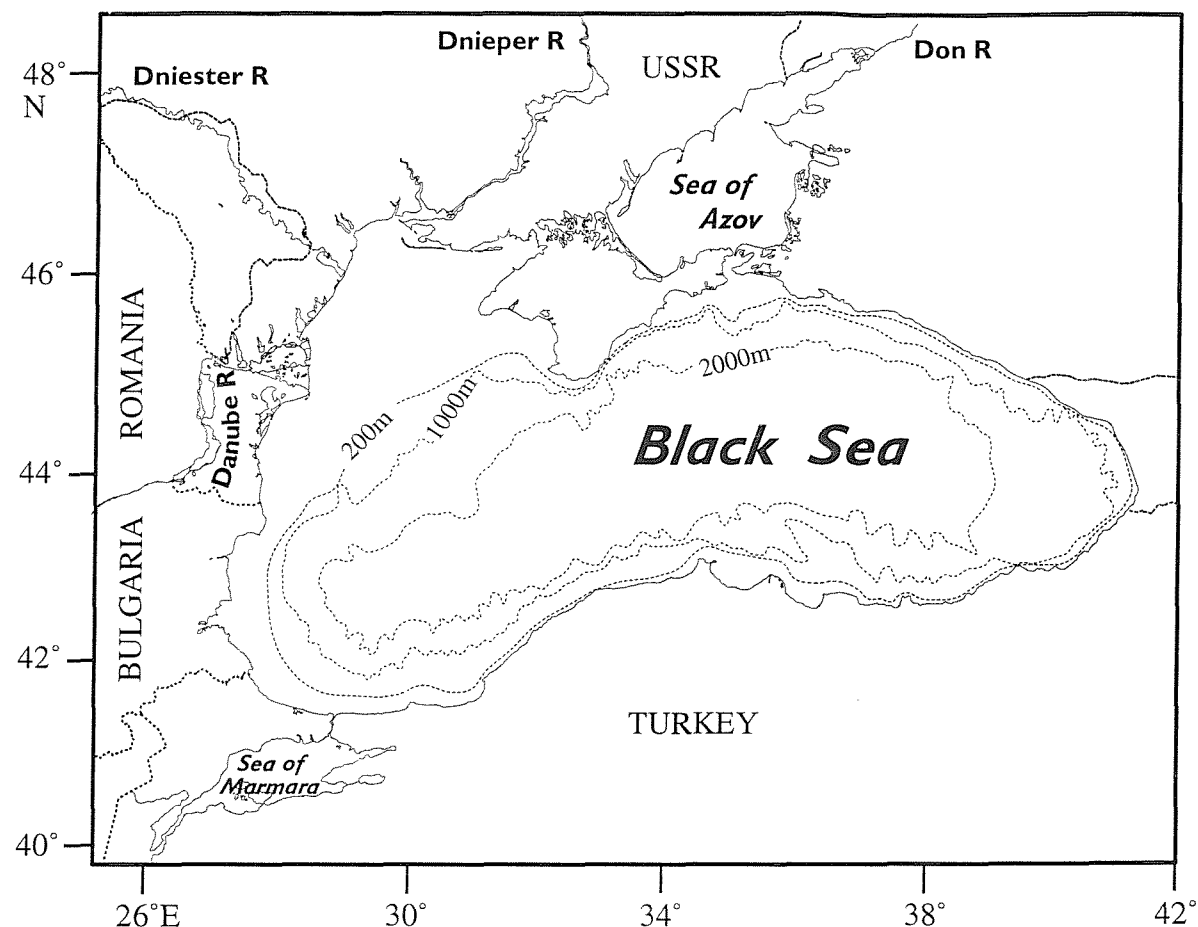


Fig. 6.1a: Topography of the Black Sea

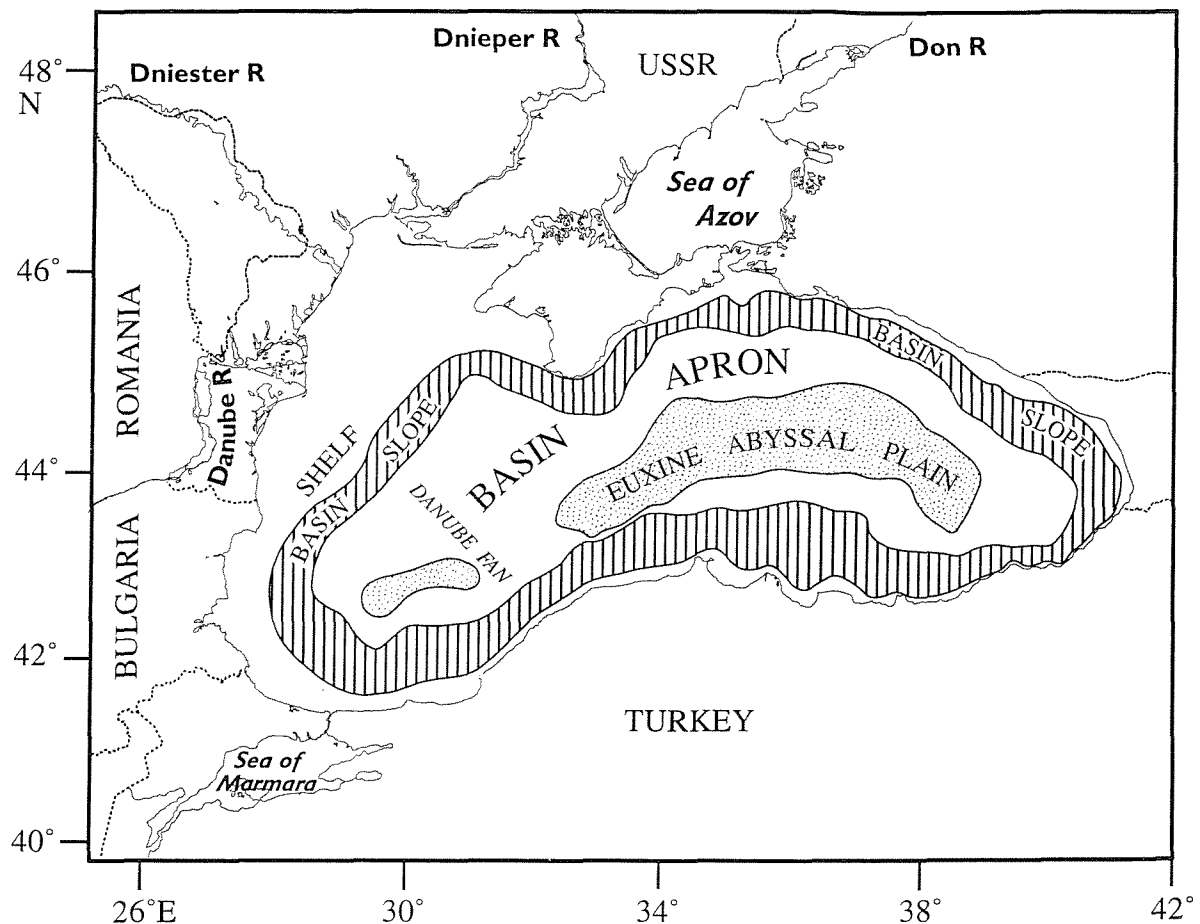


Fig. 6.1b: Physiographic provinces of the Black Sea

by small hill-like features. Different origins can be ascribed to these topographic highs: slumping, levee formation, and formation by bottom currents. The abyssal plain in the centre of the basin reaches a maximum observed depth of 2,206 m. This plain is best developed in the east, where turbidity-current deposition is more prevalent.

6.1.2 Anoxia in the Black Sea

The Black Sea is the largest anoxic basin in the world. Investigation of sediments from the deep parts of the Black Sea basin has indicated that the Black Sea was an aerated brackish-water or a freshwater body during the late Pleistocene and early Holocene. The condition for oxygen depletion in the Black Sea was established 9,000 years ago, when significant influx of Mediterranean water through the Bosphorus began to develop a density stratification in the basin (Deuser, 1974). This influx was caused by a rise of world sea level to the sill depth in that strait. The important consequence of the addition of saline water to the basin was the gradual establishment of a density stratification. After passing the sill, much of the inflowing, denser salt water sank and spread across the deep parts of the basin. Vertical circulation in the Black Sea was impeded greatly by this stratification, and the supply of dissolved oxygen to the deep water was limited to that brought in with the Mediterranean water. This supply of oxygen (7×10^7 moles/year) was not sufficient to oxidize the carbon introduced into the deep sea (1.7×10^{11} moles) since the oxidation of each mole of carbon in plankton requires 1.3 moles of oxygen (Deuser, 1974). The result of this has been the depletion in oxygen of an ever-increasing portion of the deep water.

The depth of the oxic/anoxic interface is related to the circulation. Studies by Neumann (1943) and Caspers (1957) suggest that the depth of the oxic/anoxic interface is shallowest in the centre of the western gyre and deepest at the margins of the Black Sea. Minimum depths for the 23 μM sulfide isopleth were about 150 m (Fig. 6.2). There is an accumulation of evidence suggesting that the upper boundary of the sulfide zone has been migrating toward the sea surface. Some data suggest that this change began before significant river diversion (Zhorov and Boguslasky, 1985; Bryantsev *et al.*, 1988). Most workers believe that the interface is continuing to rise at a significant rate, and it is possible

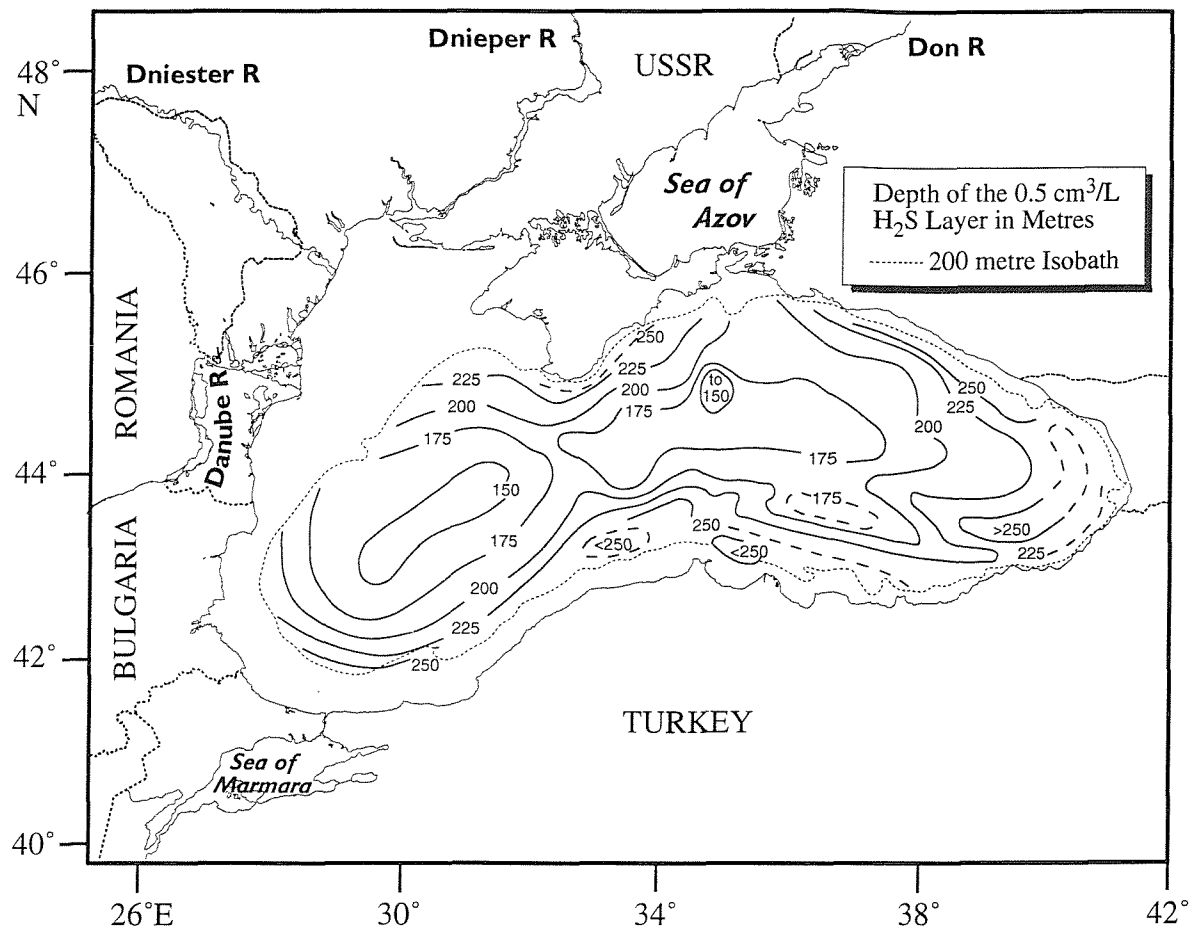


Fig. 6.2: Depths for the $23 \mu\text{M}$ sulfide isopleth in the Black Sea

that riverine diversion is contributing to this change (Zhorov *et al.*, 1984; Fashchuk and Ayzatullin, 1986; Murray *et al.*, 1989). It has also been suggested that the upper boundary of the H₂S zone in the Black Sea oscillates in time with an approximately centenary period (Eremeev *et al.*, 1996). This may possibly be due to a global climatic process free from any permanent unidirectional trend.

Hydrogen sulfide concentrations tend to increase with depth and reach maximum values of approximately 350 µM. Most investigations suggest that there is a zone in the oxic/anoxic interface where significant amounts of oxygen and hydrogen sulfide can co-exist (Karl, 1978; Sorokin, 1983). Grasshoff (1975) disputed the existence of such a layer and suggested that it arose from sampling and analytical artifacts. To investigate this, Codispoti *et al.* (1991) employed a pumping system to generate continuous vertical profiles of sulfide and collected oxygen samples from discrete depths; they did not find regions where both oxygen and sulfide occurred at concentrations > 1 µM.

6.1.3 Hydrography

The Black Sea is strongly stratified. The depth of the halocline reflects the balance between the fresh water and seawater inflows. The overall halo-circulation is estuarine in nature, which is the reverse of that for the Mediterranean. The surface mixed layer has a relatively low salinity that varies from 17.5 to 18.5 depending on the season and the proximity to river input (especially in the northwestern region). Temperature varies seasonally in the surface layer due mainly to solar heating and decreases with depth to a minimum located at a depth of approximately 50 m in the central basin and as deep as 100 m near the margins. This temperature minimum layer is present throughout the Black Sea and has been called the Cold Intermediate Layer (CIL). Tolmazin (1985) summarized evidence suggesting that the water in the CIL originates in an area of intense cooling in the northwestern shelf region and spreads horizontally throughout the Black Sea on an isopycnal surface. Ovchinnikov and Popov (1987) argued that the water of the CIL forms in the winter in the central cyclonic eddies. Spiral outflow of the newly generated CIL water occurs along the dome-shaped isopycnal surfaces. Both mechanisms are in fact of equal importance (Oguz *et*

al., 1991). The process of CIL formation is closely associated with vertical convection in the upper layers of the water column caused by the appropriate combination of meteorological and hydrodynamical conditions. Once the CIL is formed, it is eventually advected around the basin by the general circulation. The isopycnal surfaces above 300 m are dome-shaped and thus shallower in the central parts of the Black Sea reflecting the gyre-like circulation (Fig. 6.3). In the deep water the vertical salinity and potential temperature gradients are small, but both properties increase continuously to their maximum values of about 22.33 and 8.904 °C respectively at the bottom.

The Black Sea's exchange with the Mediterranean Sea and thus ultimately with the world ocean takes place through the narrow and shallow Bosphorus. Tolmazin (1985) and Fonselius (1974) calculated an outflow of $400 \text{ km}^3 \text{y}^{-1}$ through the Bosphorus and an inflow of $230 \text{ km}^3 \text{y}^{-1}$. The actual values of these exchanges are not well known and some recent investigations by Ozsoy *et al.* (cited by Latif *et al.*, 1991) suggest that the previously accepted value for inflow through the Bosphorus should be revised upward to $310 \text{ km}^3 \text{y}^{-1}$.

6.1.4 River inputs to the Black Sea

The major fresh water sources to the Black Sea are the Danube and Dnepr rivers, both flowing into the northern Western Black Sea (Table 6.1). Total river inputs for the northwestern Black Sea have been estimated as $265 \text{ km}^3/\text{y}$ (Cociasu *et al.*, 1996) which represents 86 % of total river inputs into the Black Sea. The other major river sources for the Black Sea are the Don River through the Sea of Azov ($29.3 \text{ km}^3/\text{y}$) and the Kuban river near the Kerch Strait ($11.9 \text{ km}^3/\text{y}$). The large sediment load of the Danube is possibly due to high population density and intensive agriculture.

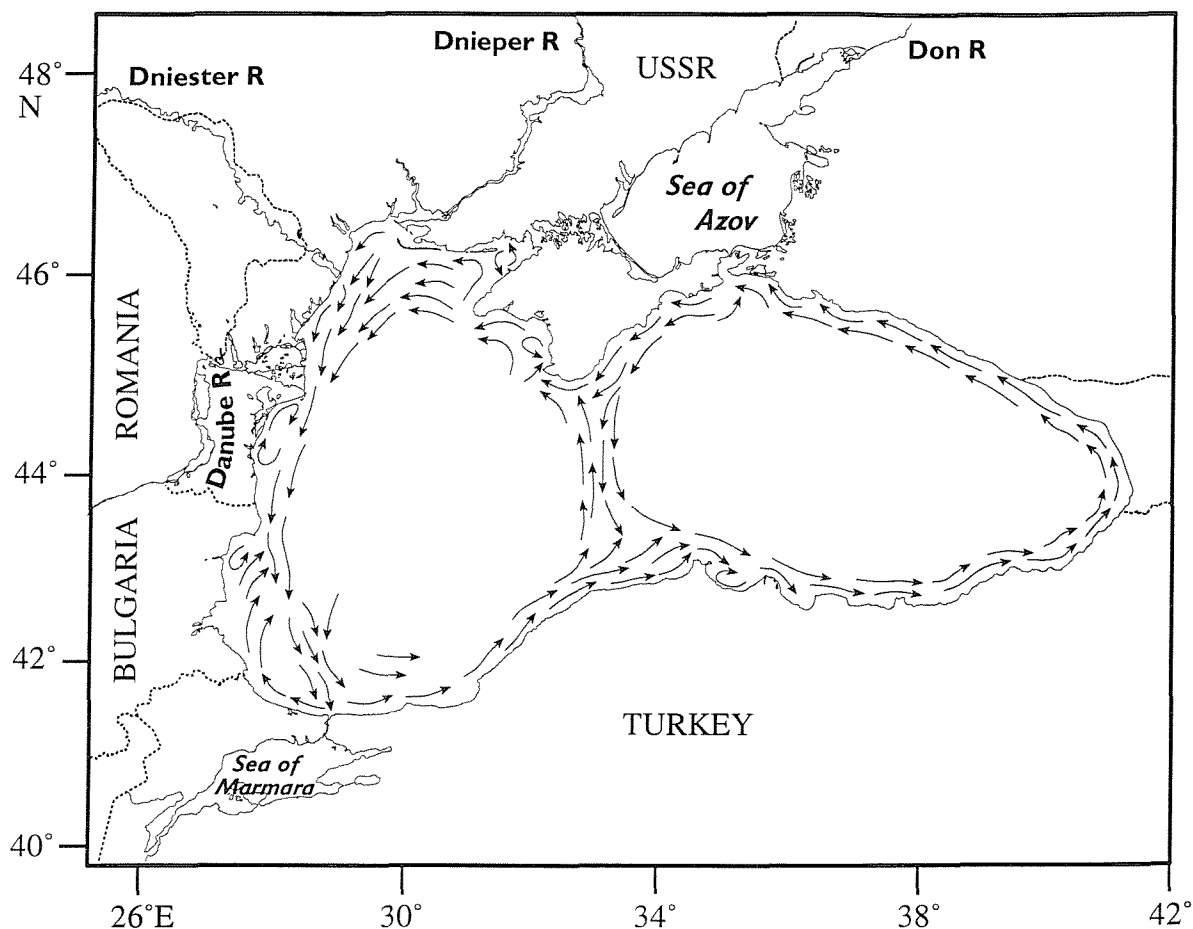


Fig. 6.3: General circulation in the surface layer of the Black Sea

Table 6.1: Major river inputs to the Black Sea

River	Total discharge (km ³ /y)	Catchment area (10 ³ km ²)	Sediment load (10 ⁶ t/y)
Danube	203.4 ^a	817 ^c	67 ^d
Dnestr		77 ^c	2.5 ^e
Bug		65 ^c	0.53 ^e
Dniepr	52.3 ^a	527 ^c	2.1 ^e
Don	29.3 ^a	430 ^c	0.77 ^f
Kuban	11.9 ^b	56 ^c	

^a Czaya (1981); ^b Maltseva (1980); ^c Brockhaus (1952); ^d Milliman and Meade (1983);
^e Hay (1987); ^f Strakhov (1961).

6.2 Database for the study

The EROS 2000 expedition, was conducted in July-August 1995, on board R.V. Professor Vodyanitsky in the Ukrainian, Romanian and Bulgarian exclusive economic zones. The overall objective was to assess and understand the functioning of the northwestern Black Sea continental shelf, under summer conditions, regarding its hydrography and productivity, and the biogeochemical behaviour of nutrients and other constituents including trace metals, with an emphasis on potential pollutants. Investigations were designed to examine the influences of the rivers Danube, Dniestr and Dniepr.

Samples were accordingly taken to cover in detail the water column at one deep Station (Station 3) in the permanently anoxic basin, as well as representative depths at 21 stations in the shelf area adjacent to the Danube inflow (Fig. 6.4).

Samples were analysed for:

- dissolved O₂, H₂S, nutrients, DOC, POC and Chlorophyll *a*, i.e. constituents mostly of importance in relation to productivity, but which also provide useful chemical oceanographic characterisation of the system;

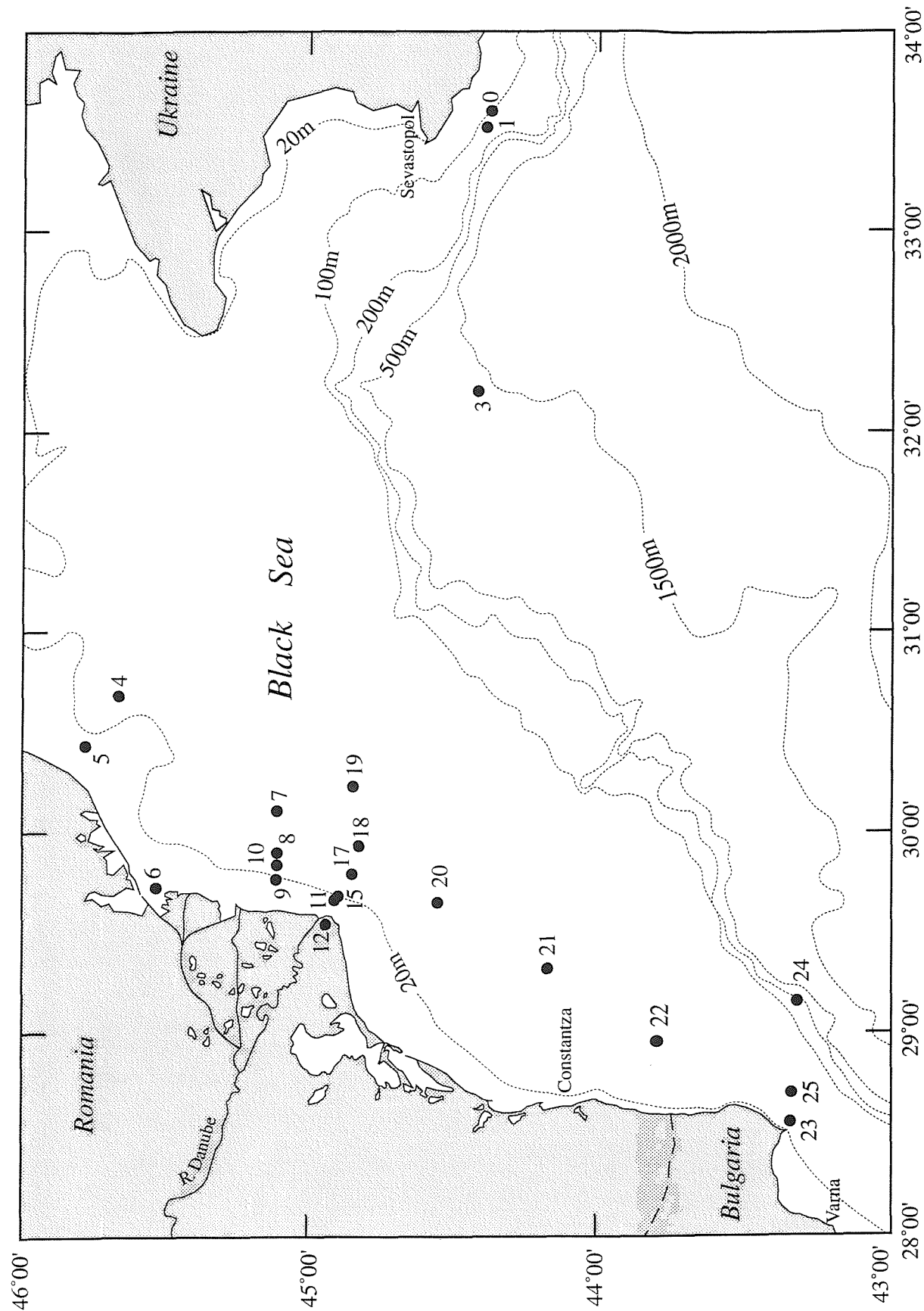


Fig. 6.4: Sampling locations in the north western Black Sea

- trace metals, some chosen for their geochemical importance (Mn, Co and Fe), particularly as indicators of redox processes, others for their potential significance as contaminants (Cu, Ni, Zn, Cd and Pb).

Data for the Black Sea are tabulated in Appendix II.

6.3 Hydrographic and chemical setting

6.3.1 Temperature, salinity, density and fluorescence

Hydrographic data for Stations 0, 1 and 3 are presented in Fig. 6.5. There was strong stratification and little mixing between the surface layer and deep water at the time of the cruise in the North Black Sea. The thermocline is always associated with a maximum in fluorescence which could be due to accumulation of biological debris. The depth of the thermocline varies. For example it appears at 18 m at Station 3, at 43 m at Station 1 and at 35 m at Station 0. In the North Black Sea the thermocline appears deeper near the coast. Higher salinities very near the surface are possibly due to evaporation. The lower temperatures in surface water (at the top one metre) may be due to riverine influence; in summer riverine fresh water tends to be cooler than seawater. The temperature—salinity diagram (Fig. 6.5) shows that there is mixing between 3 different water masses at Station 3: surface water (SW) mixes with cold intermediate layer water (CILW) which mixes with deep Black Sea water (DBSW). The CILW acts as a diffusive barrier between SW and DBSW. At the shallower Stations 0 and 1, the DBSW is not present and mixing occurs only between SW and CILW.

Hydrographic data for Stations 4, 5 and 6 are presented in Fig. 6.6. Surface water salinities are lower than in deeper water suggesting stratification of the water column. Stations 4, 5 and 6 are mostly influenced by the Dnepr, Bug and Dnestr rivers which supply a total fresh water inflow of $61.6 \text{ km}^3/\text{y}$. Stations 5 and 6 are near the coast and the lower surface salinities, compared with those at Station 4, show that they are more influenced by fresh water inputs (Dnestr River). This is also associated with higher fluorescence values. At

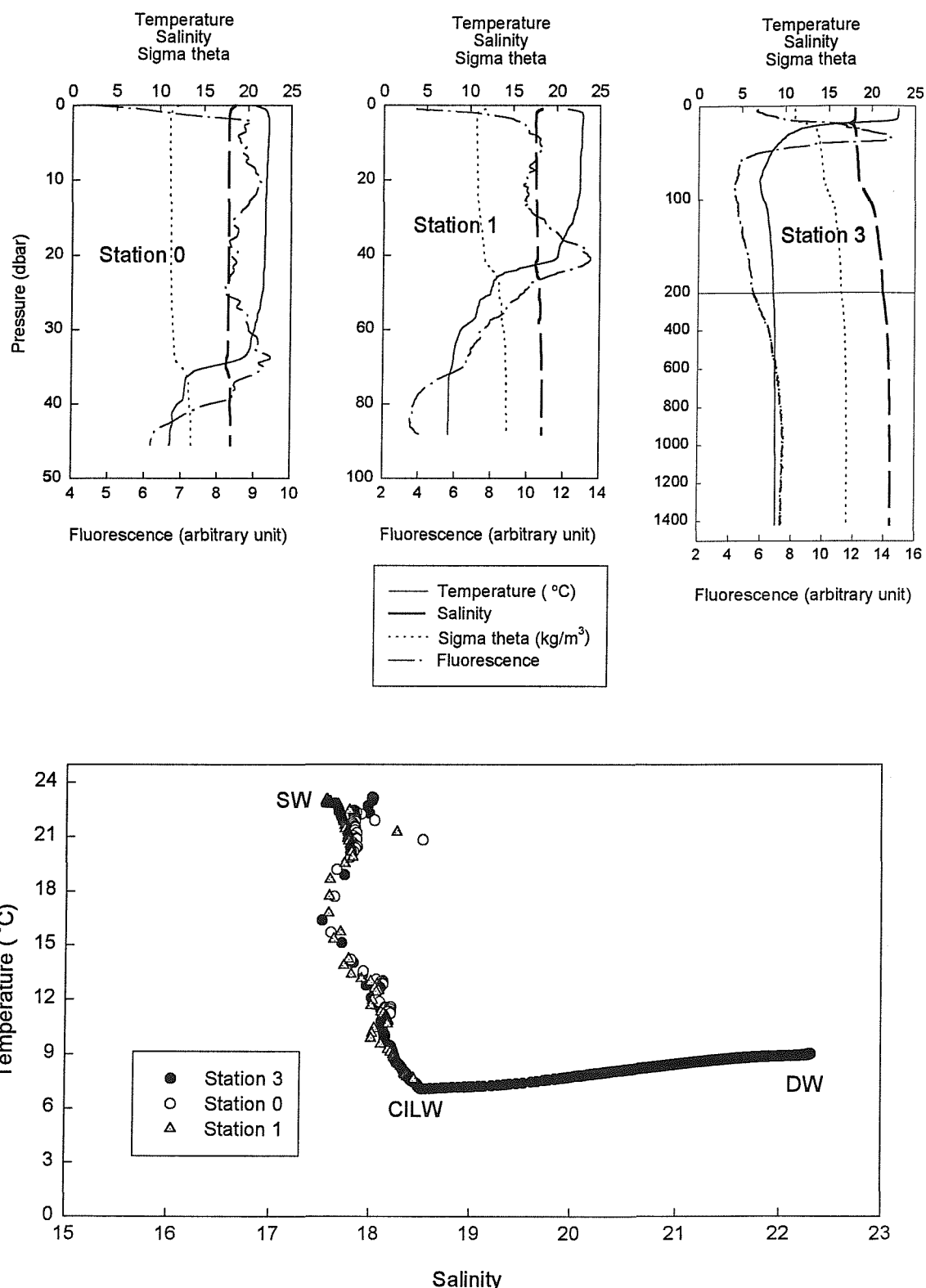


Fig. 6.5: Hydrographic data for Stations 0, 1 and 3

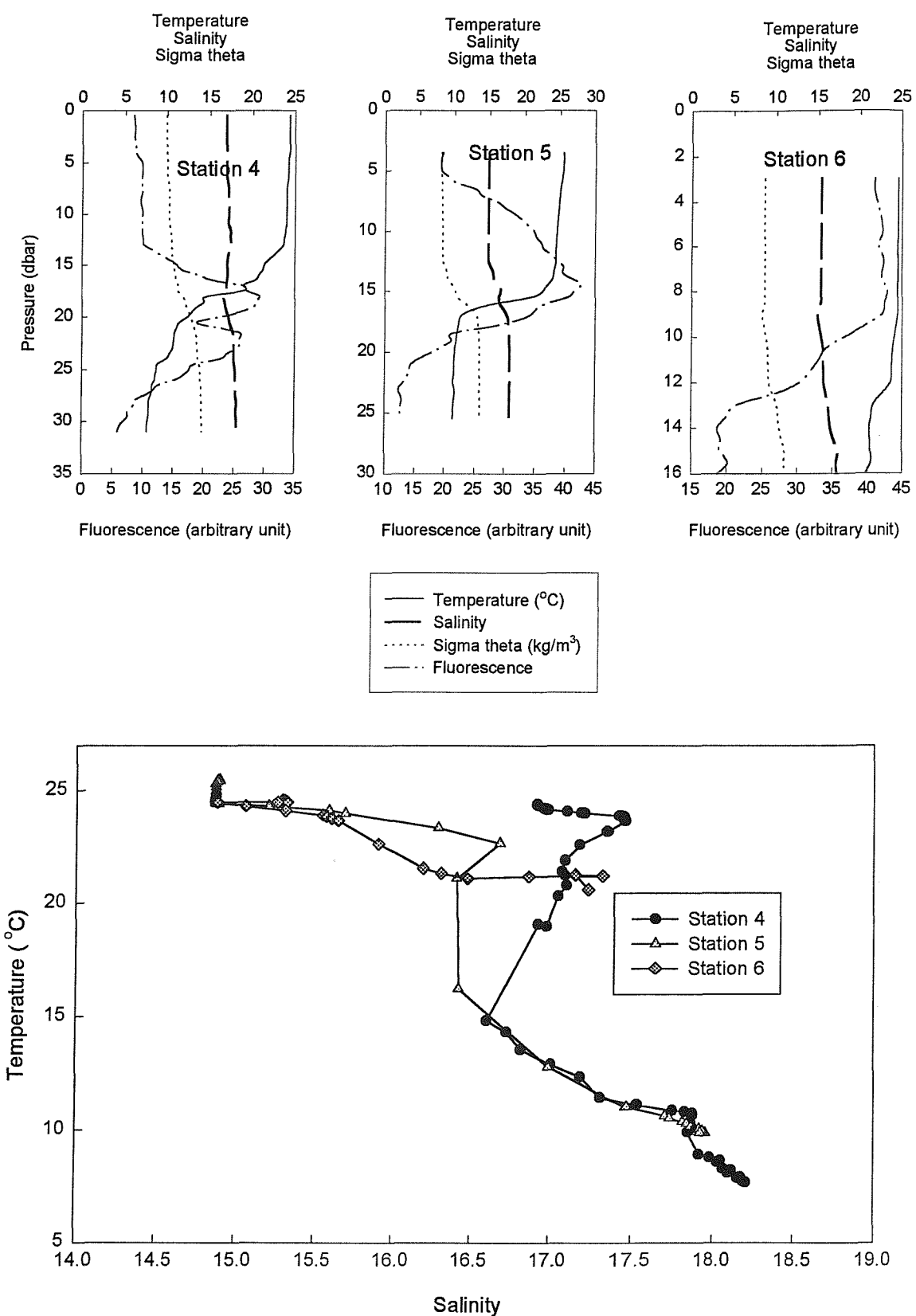


Fig. 6.6: Hydrographic data for Stations 4, 5 and 6

Stations 4 and 5, the thermocline coincides with a maximum in fluorescence and a minimum in salinity. Stations 4 and 5 show similar temperature—salinity diagrams (Fig. 6.6) where Black Sea water mixes with low salinity surface water. The low salinity values at 25 °C reflect the strong riverine influence. Salinity minima above 15 °C reflect downwelled water. At Station 6 the thermocline is much less sharp, temperature varies between 24.6 and 20.6 °C.

Hydrographic data for Stations 7, 8, 10 and 9 are presented in Figs. 6.7 and 6.8. Stations 7, 8, 10 and 9 represents a transect from the second branch of the Danube towards the open sea. Station 9 is adjacent to the Danube delta. Fluorescence is high in the surface layer and decreases below the pycnocline, due to transport of sediments from the Danube. Riverine input of terrestrial humic materials is the dominant source of DOM fluorescence in estuarine areas (Duursma, 1974; Berger *et al.*, 1984; Coble *et al.*, 1990; Coble *et al.*, 1991). The salinity distribution indicates partially mixed estuarine characteristics with low salinity in the surface layer (10) which increases towards the bottom (15). At Station 9, which is shallow, there is no thermocline, and the temperature is nearly constant at 25 °C. Stations 10, 8 and 7 have similar T-S diagrams which are characteristic of a stratified estuary. When going in the offshore direction, the surface layer salinity increases and the depth of the thermocline decreases showing the weaker influence of the Danube river. Below the thermocline, salinity is constant at 18. At Stations 7 and 10, the density increases by steps. These steps could represent individual layers of water, mixed internally but separated from the adjoining layers by sharp density gradients. At Station 7, the fluorescence profile is more akin to those at Stations 4 and 5 than to Stations directly influenced by the Danube (Stations 8, 10, 9).

Hydrographic data for Stations 20, 21, 22, 23, 25 and 24 are presented in Figs. 6.9 and 6.10. Station 20, which is south of the Danube plume, has low salinity suggesting strong influence from fresh water inputs. Above the thermocline, salinity increases from 13.5 to 14.6, while below the thermocline it is constant at 15. The temperature—salinity diagram is indicative of intense stratification with little mixing between surface and deep water. A maximum in fluorescence is observed at the thermocline due to accumulation of biological material. At Stations 21 and 22, fluorescence is higher in the surface water than at Station

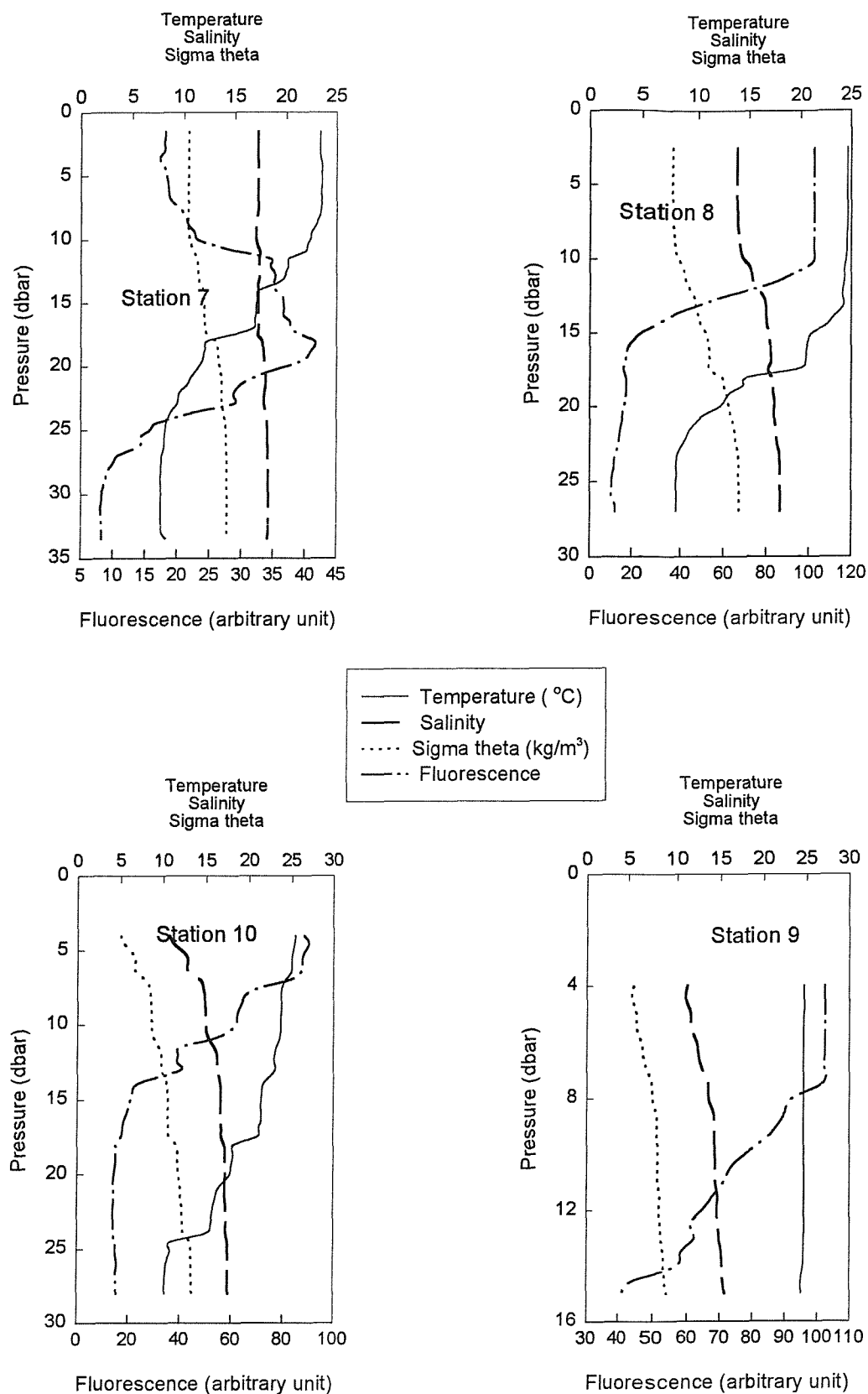


Fig. 6.7: Hydrographic data for Stations 7,8,9 and 10

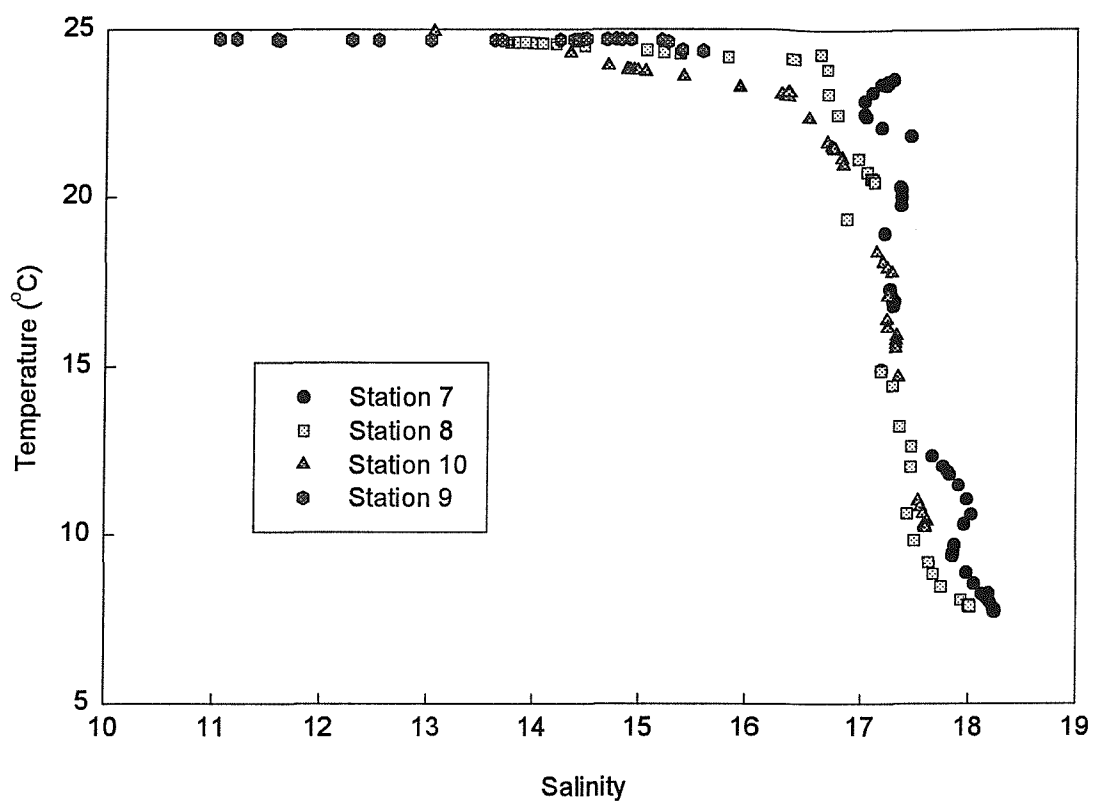


Fig. 6.8: Temperature-salinity plots for Stations 7, 8, 9 and 10

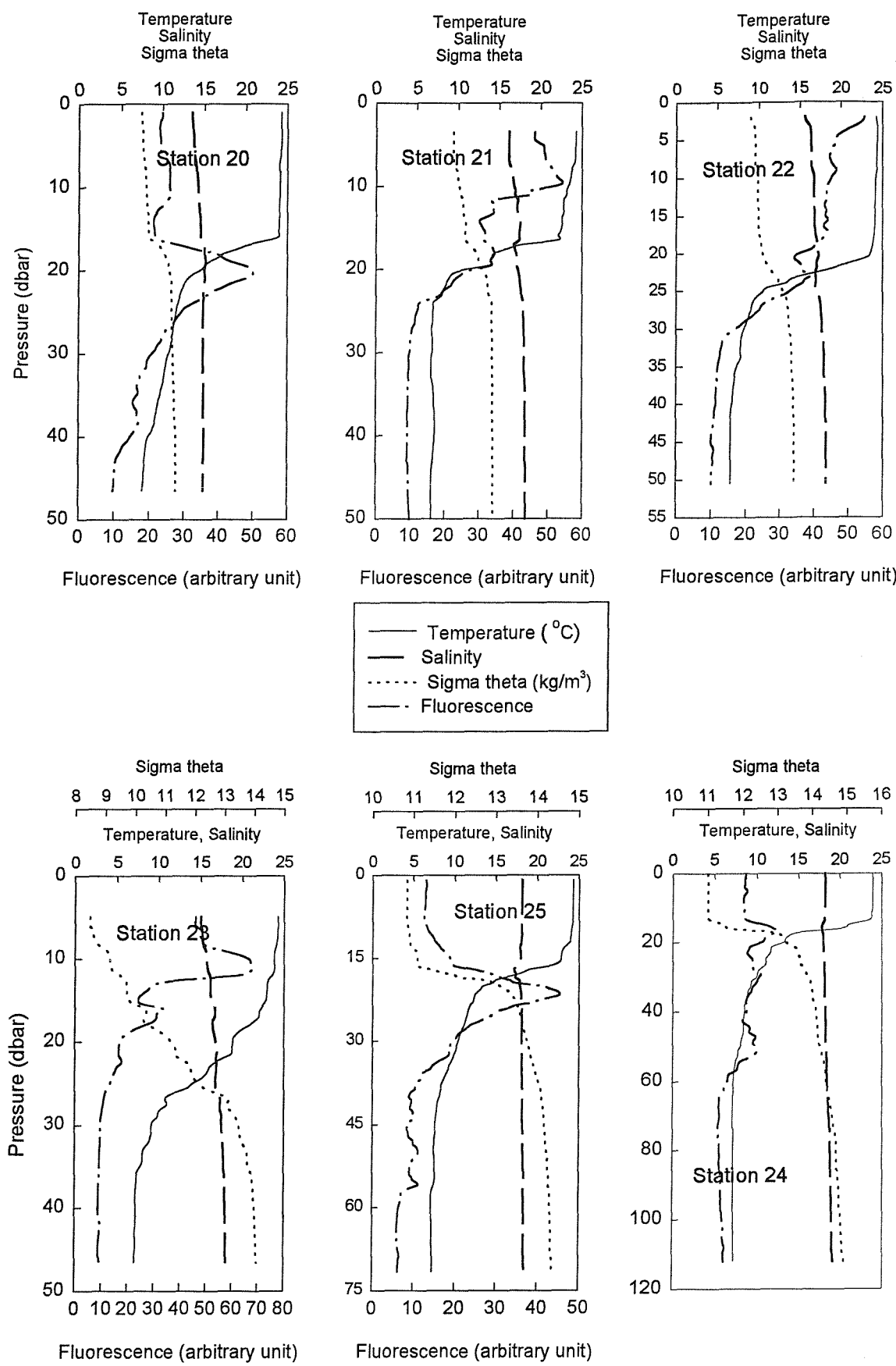


Fig. 6.9: Hydrographic data for Stations 20, 21, 22, 23, 25 and 24

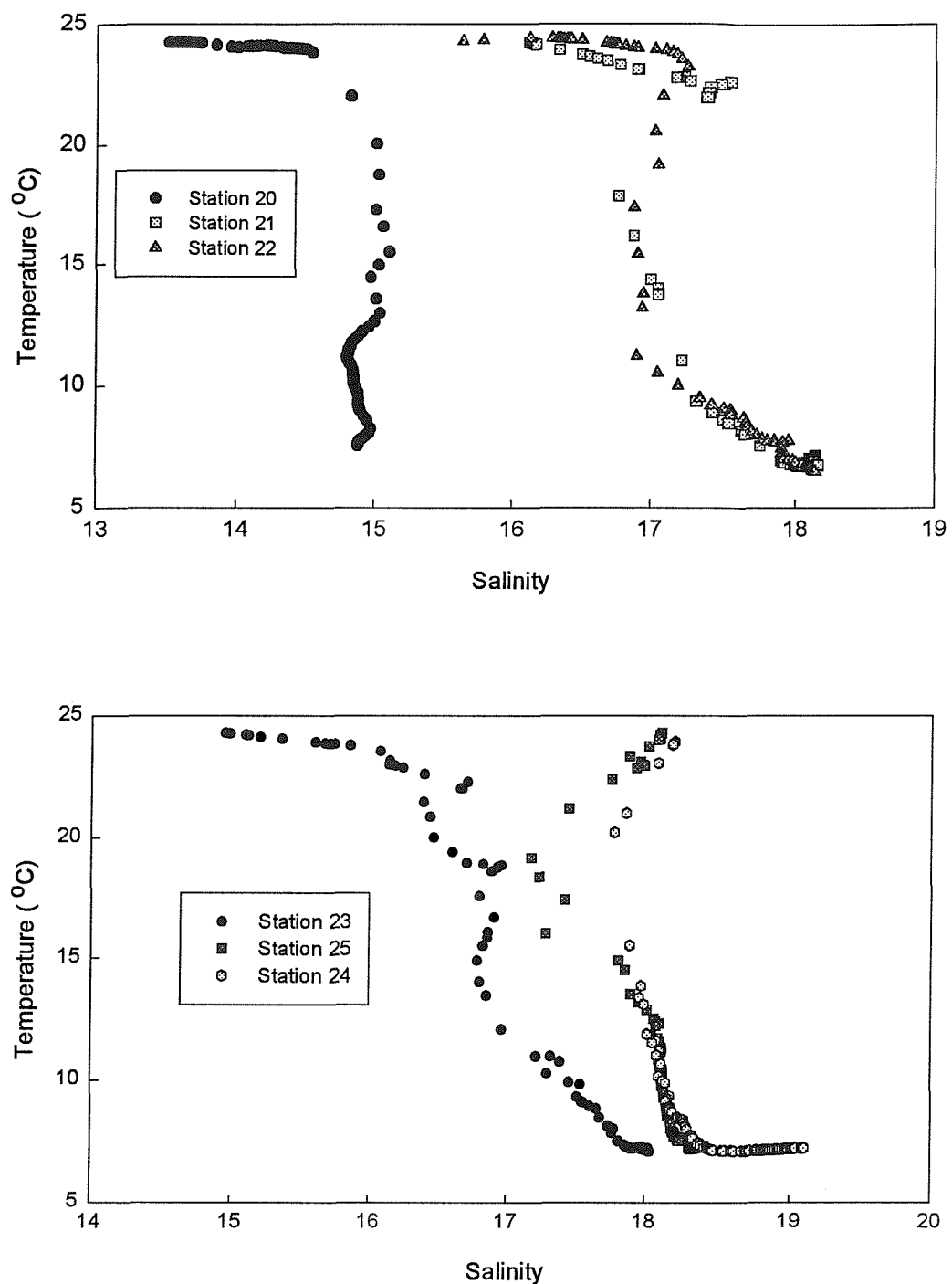


Fig. 6.10: Temperature - salinity plots for Stations 20, 21, 22, 23, 24 and 25

20 and decreases below the thermocline, suggesting high levels of primary production in surface water in this area. For these Stations, temperature—salinity diagrams are different from Station 20. Salinity increases from 15.5 to 17.5 above the thermocline. There is a salinity minimum at the inflection point of the thermocline. Below the thermocline salinity increases up to 18.2. The low salinity at the thermocline may be due to downwelled water. The higher salinity in the surface water probably results from enhanced evaporation.

Stations 23, 25 and 24 define a transect from the coastal zone south of the Danube to the shelf break. The thermocline is deeper and less sharp at Station 23 (25 m) than at Stations 25 and 24 (17 m). The fluorescence signal tends to decrease from the coast towards the open sea, biological material being more abundant in the coastal area. The water column is stratified with different density layers. Such lamination could also explain the distribution of fluorescence with up to 3 individual peaks at Station 24 (11 m, 17 m and 23 m).

Hydrodynamic advective transport may be more important to explain the accumulation of biological material at different levels through the water column than biological processes governed by cell partition rates. The temperature—salinity diagram at Station 23 is more akin to Stations 21 and 22 than to Stations 25 and 24 (Fig. 6.10). Station 23 is influenced by fresh water inputs and consequently salinity is relatively low in surface water (15) and increases up to 18 in deeper water column by mixing with CIL water. The temperature—salinity diagram at Station 25 shows 3 different water masses: surface water ‘salinity 18’ mixes with a water mass of lower salinity (17); the latter may be downwelled water which has been advected from the coastal area; deeper water has the characteristics of the CIL water; evaporation is probably responsible for the high salinity values in the surface layer. At Station 24, the upper part of the temperature—salinity diagram is similar to that of Station 25. The influence of the low salinity water mass below the surface layer is weaker. Near the bottom, CIL water mixes with DBS water.

6.3.2 Dissolved oxygen and chl α

At Station 3, dissolved O₂ concentrations are highest in the surface layer and decrease to near depletion below 200 m (Fig. 6.11.b). The small maxima at 130 m and 182 m are possibly due to contaminations. The hydrographic regime of the Black Sea is characterised by low salinity surface water of river origin overlaying high salinity deep water of

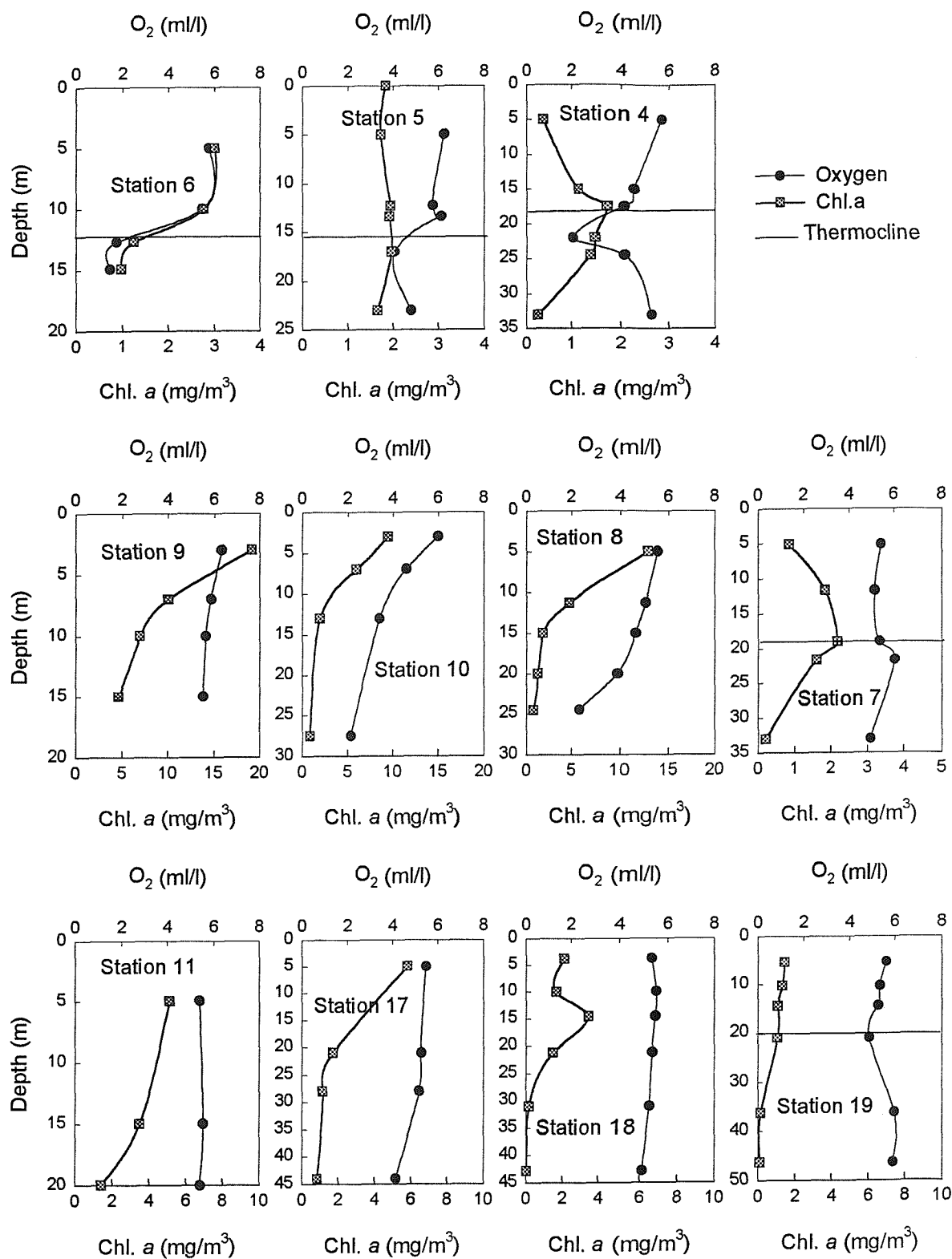


Fig. 6.11.a: Distributions of dissolved O_2 and Chlorophyll a at Stations 6, 5, 4, 9, 10, 8, 7, 11, 17, 18 and 19

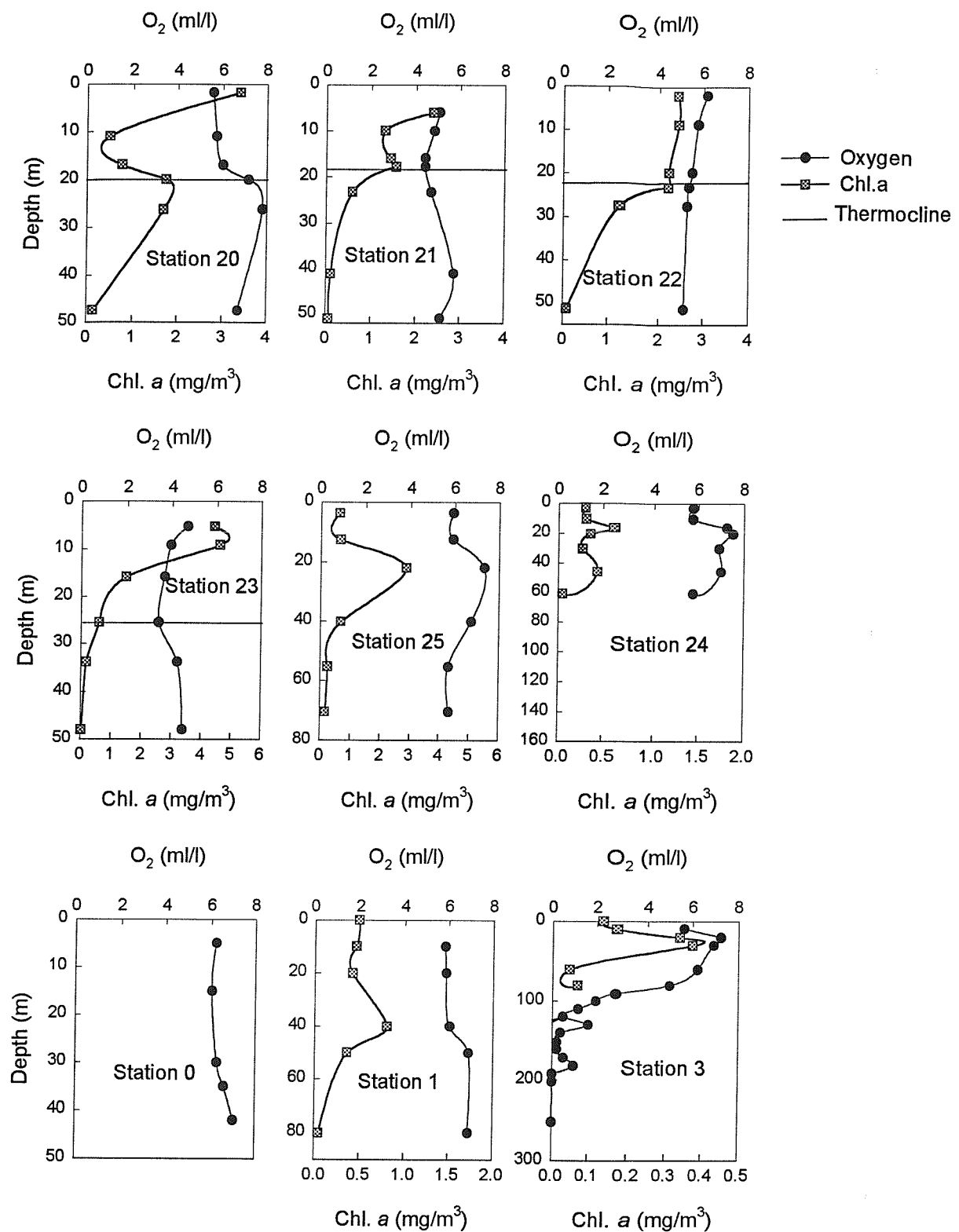


Fig. 6.11.b: Distributions of dissolved oxygen and chlorophyll a at Stations 20, 21, 22, 23, 25, 24, 0, 1 and 3

Mediterranean origin. In the absence of major lateral inputs of oxygenated water, the marked permanent pycnocline leads to the formation of a marked redoxcline (Caspers, 1957; Brewer, 1971, Deuser, 1974). Chl *a* concentrations have been measured in the first 100 m. The Chl *a* profile shows a maximum at 40 m associated with a maximum in dissolved O₂ concentrations suggesting the occurrence of a bloom at this depth.

At Stations directly influenced by fresh water inputs (Stations 6, 9, 10, 8, 17) maxima of dissolved O₂ and Chl *a* are observed in surface water suggesting high levels of primary production (Fig. 6.11.a). Below the thermocline, dissolved O₂ concentrations decrease markedly. This is possibly due to mineralization at the sediment-water interface. Minima of dissolved O₂ are also observed at the thermocline at some stations (Stations 4, 5, 7, 19, 21, 23), indicating remineralization within the water column (Figs. 6.11 a and b). This phenomena has also been observed in the Northern Adriatic Sea (Ott and Herndl, 1995). These minima of dissolved O₂ are associated with maxima in Chl *a* which are possibly due to accumulation of phytoplankton at the thermocline. The phytoplankton is probably under stress due to large imbalance in the P/N ratio. It produces large amounts of organic matter which decay at the thermocline as stratification of the water column increases the residence time at the thermocline. Minima of dissolved O₂ may also be supported by advection of low dissolved O₂ concentration water originating from shallow water where it was in contact with the sediment (Kempe *et al.*, 1991). At some other stations (20, 22, 25, 24) maxima of dissolved O₂ and Chl *a* are found to coincide at the thermocline. This is possibly due to deeper light penetration, i.e. to a level where primary production may be further stimulated by the supply of nutrients diffusing upward from below the thermocline.

6.3.3 Nitrogen, ammonia, phosphorus and silicate

Distributions of nitrogen, ammonia, phosphorus and silicate are presented in Figs. 6.12.a and 6.12.b. At Station 3, which is situated mid-way across the continental slope west of the Crimea peninsula, ammonium concentrations above the redoxcline (150 m) are relatively low (in the range 0.08–0.45 µM). Concentrations rise to high values in anoxic waters. The increase is more or less monotonic with depth and leads up to maximum values of

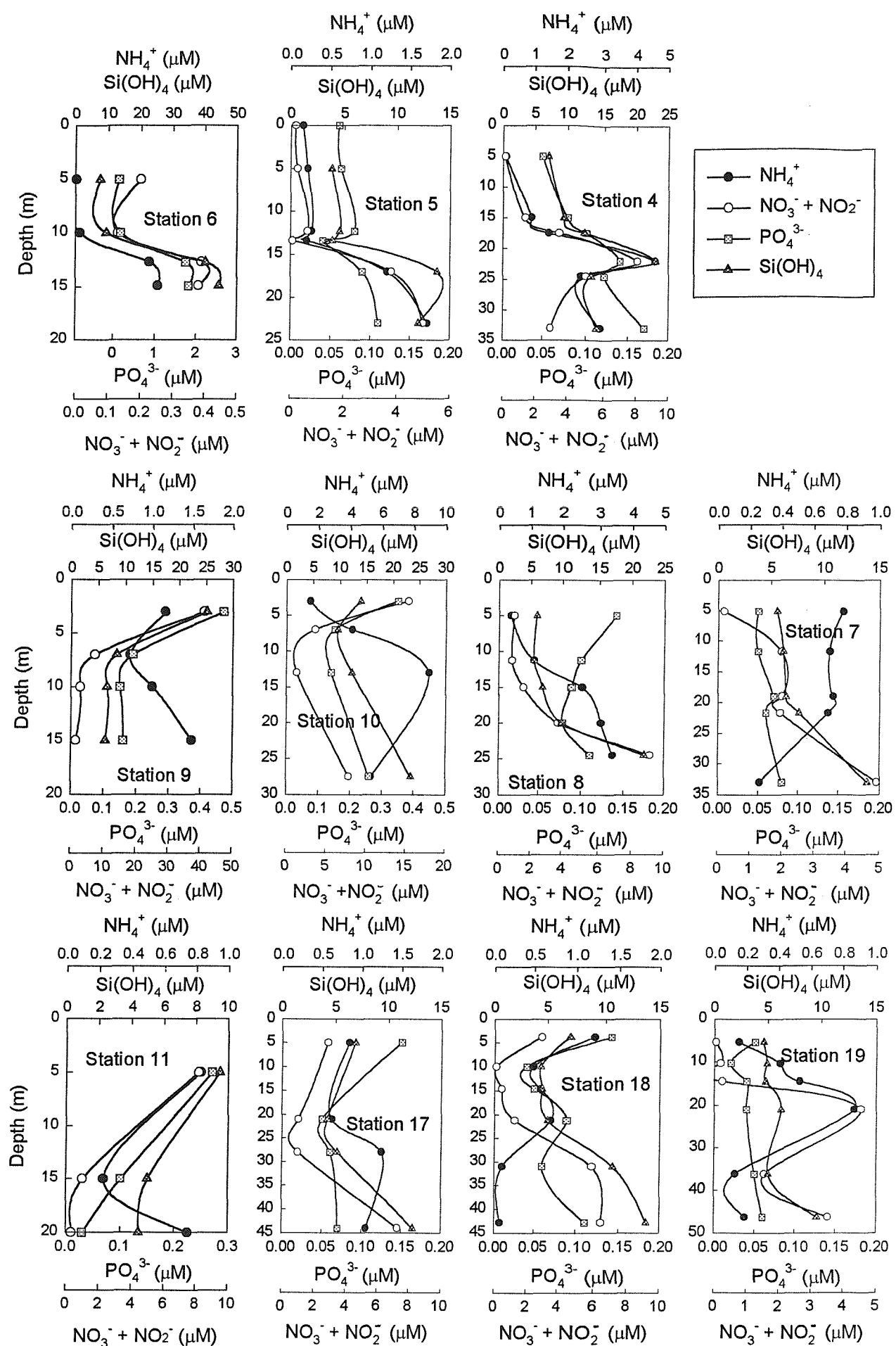


Fig. 6.12.a: Distributions of nutrients at stations influenced by the Danube river

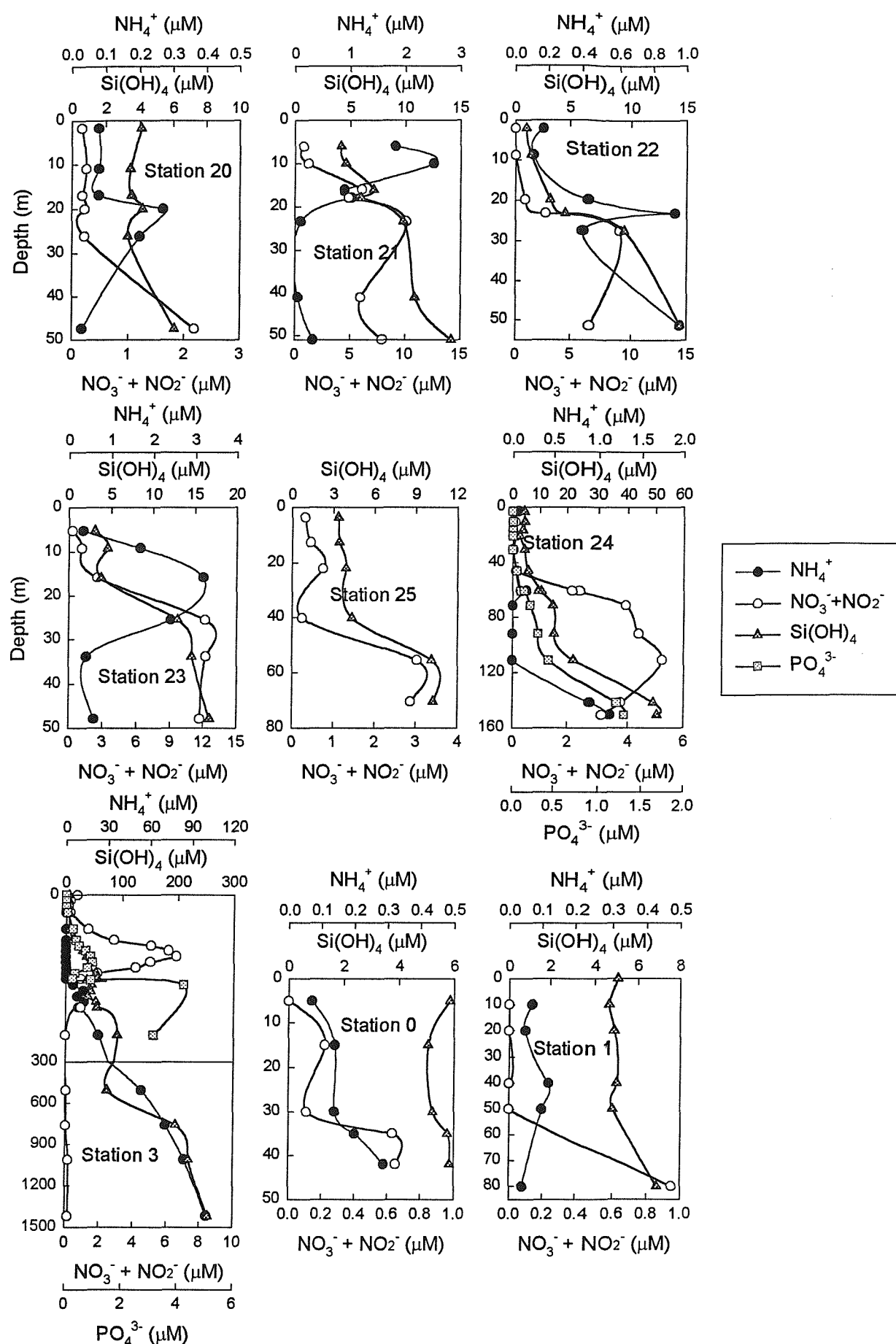


Fig. 6.12.b: Distributions of nutrients at stations on the shelf and on the slope

approximately 100 μM . Phosphate was measured in the top 200 m and the profile displays a double maxima. This feature has also been observed by Brewer and Murray (1973), Fonselius (1974) and Shaffer (1986). The upper maximum arises from the regenerative and respiratory processes that typically occur in oxygenated water. The intervening minimum and lower maximum is thought to arise from redox processes involving iron and perhaps manganese (e.g. Brewer and Spencer, 1974; Mayer *et al.*, 1982; Shaffer, 1986). Reduced iron (II) and manganese (II) diffuse upwards into an oxygenated layer where they form oxides, which in the case of iron and possibly manganese incorporate phosphate. These particles then sink into anoxic layer where they redissolve and liberate the scavenged phosphate. The lower maximum is formed by dissolution of these particles and the minimum by the scavenging of phosphate during the formation of these iron and manganese oxyhydroxides. Silicate uptake and regeneration processes in the Black Sea are similar to the open ocean cycle. Silicate consumption by phytoplankton occurs in surface waters and there is regeneration at depth. Because of the long residence time of anoxic waters in the Black Sea, silicon concentrations can reach values of more than 300 μM (Sorokin, 1983). Here at Station 3, silicon concentrations increase more or less monotonically with depth and reach 255 μM . Nitrate is depleted in surface water due to biological uptake. There is a nitrate maximum between the photic and anoxic zones which arises from oxidative regeneration of sinking biomass. Nitrite concentrations are very low ($< 1.0 \mu\text{M}$) but show a maximum below the nitrate maximum. In deep water, denitrification removes both nitrate and nitrite from the water column, once dissolved O_2 is at sub oxic levels.

At Station 24, which is situated in the slope region off the Bulgarian coast, ammonium concentrations are low in surface waters and increase between 110 and 150 m. Near the bottom, concentrations increase to 1.1 μM suggesting the existence of anoxic conditions. There is a nitrate maximum at 110 m. In the surface layer nitrate is heavily depleted by biological uptake. The removal of nitrate is also clearly visible in the anoxic bottom layer. Silicate and phosphate show similar distributions. Concentrations increase respectively from 4 μM and 0 μM in surface water to 10 μM and 0.3 μM at 90 m; below 110 m concentrations increase more quickly and reach respectively 51 μM and 1.3 μM near the

bottom. The low concentrations in the surface waters reflect the uptake by biological activity whereas the increase near the bottom reflects regeneration from the sinking biomass. There could potentially also be release of phosphate from iron oxyhydroxide phases undergoing reduction when conditions become anoxic in overlying water.

In the coastal zone, the stratification of the water column plays an important role in the distribution of nutrients. Above the thermocline nutrients (nitrate and phosphate) tend to be depleted by biological uptake and are associated with soft tissues; silicate is also depleted but is incorporated into the shells of organisms. Below the thermocline, concentrations of nitrate, phosphate and silicate increase rapidly with depth due to their regeneration from the sinking biomass. At the time of the cruise, regeneration of ammonium was higher than the assimilation of nitrogen by the phytoplankton throughout the northwestern Black Sea. Ammonium regeneration rates were exceeding uptake rates by an average factor of 30 % (Goeyens and Verlimmeren, 1996). Phosphate fluxes across the sediment–water interface were measured using benthic chambers and were generally found to be high at stations close to the coast with an average value of $0.05 \text{ mmol P m}^{-2} \text{ d}^{-1}$ (Zehnder *et al.*, 1996). Nixon (1981) found that phosphate can be released very rapidly from the organic matter relative to nitrogen and carbon in coastal marine environments (Narragansett Bay). Fluxes in aerobic waters may be mainly driven by biological activities in the top few mm of oxidised sediment. Under anoxic conditions inorganic phosphorus chemically bound to iron becomes soluble and is released into the overlying water (Nixon, 1981). Benthic fluxes of silica near the coast were also high ($6.0 \text{ mmol m}^{-2} \text{ d}^{-1}$), although comparable to fluxes determined in other estuaries such as Narragansett Bay and Chesapeake Bay (Callender and Hammond, 1982; Elderfield *et al.*, 1981).

During the summer period the well developed pycnocline can delay the sinking of particles creating a “false benthos”. Particles aggregate and create a viscous mucus referred to as “mucilage” in the Adriatic Sea. Due to the highly viscous nature of these mucoid aggregates, gas produced by the metabolism of marine snow-attached organisms remains entrapped in the matrix and influences the buoyancy of the aggregate. The “false benthos” can act as an efficient trap for sinking particles and consequently is associated with maxima of fluorescence at the pycnocline. This accumulation of flocculent material results in a

noticeable O_2 consumption, indicating enhanced biological and/or chemical activity (Smith, 1978). Maxima in $Si(OH)_4$, NO_3^- , NH_4^+ and PO_4^{3-} can also be observed and may be due to microbial regeneration. Mineralisation at the pycnocline has been observed at Station 4, which is mainly influenced by the Dniestr, Dniepr and Bug rivers and at Stations south of the Danube plume (Stations 19, 20, 21, 22, 23). At stations directly influenced by the Danube river (Stations 9, 10, 11, 17, 18 situated near the mouth of the river) nitrogen, phosphate and silicate concentrations are highest in surface water and decrease rapidly with distance away from the coast. Concentrations decrease from 72.5 to 10 μM for nitrate, from 55 to 10 μM for silicate and from 2.4 to 0.15 μM for phosphate. Mixing between river water and Black Sea water is clearly non conservative for phosphate reflecting removal by biological activity whereas this is far less clear for nitrate and silicate (Fig. 6.13). For nitrate, there is possibly some removal at low salinity (0.5-3).

6.3.4 DOC and POC

DOC and POC distributions are presented in Figs 6.14.a and 6.14.b. DOC concentrations vary between 180 $\mu mol\ C/l$ and 325 $\mu mol\ C/l$ in the northwestern Black Sea. These concentrations are relatively high compared to those in the Adriatic Sea (90-200 $\mu mol\ C/l$) and to the typical marine values (100-120 $\mu mol\ C/l$). Highest values are generally found above the thermocline. Small maxima can be observed at the thermocline at some stations (Stations 4, 5, 7, 20, 25). High DOC concentrations can be due to a high level of primary productivity. Indeed, it has been demonstrated in laboratory and field experiments that phytoplankton exude considerable amount of DOC (Moller-Jensen, 1963; Myklestad *et al.*, 1989). It has also been demonstrated that extracellular releases were higher in conditions of unfavorable nutrient ratios (Myklestad, 1977; Lancelot, 1984). For example, a high N/P ratio leads to elevated release rates of polymers (Myklestad and Haug, 1972; Myklestad *et al.*, 1972; Myklestad, 1974, 1977). Fogg (1983, 1990) interpreted this as an overflow reaction of phytoplankton photosynthesis under conditions when phosphorus is no longer available for nucleic acid synthesis while carbon fixation still continues. The carbohydrates produced in excess are then released into the ambient water leading to exceptionally high release rates by phytoplankton under such conditions. The DOC profile of Station 3 shows

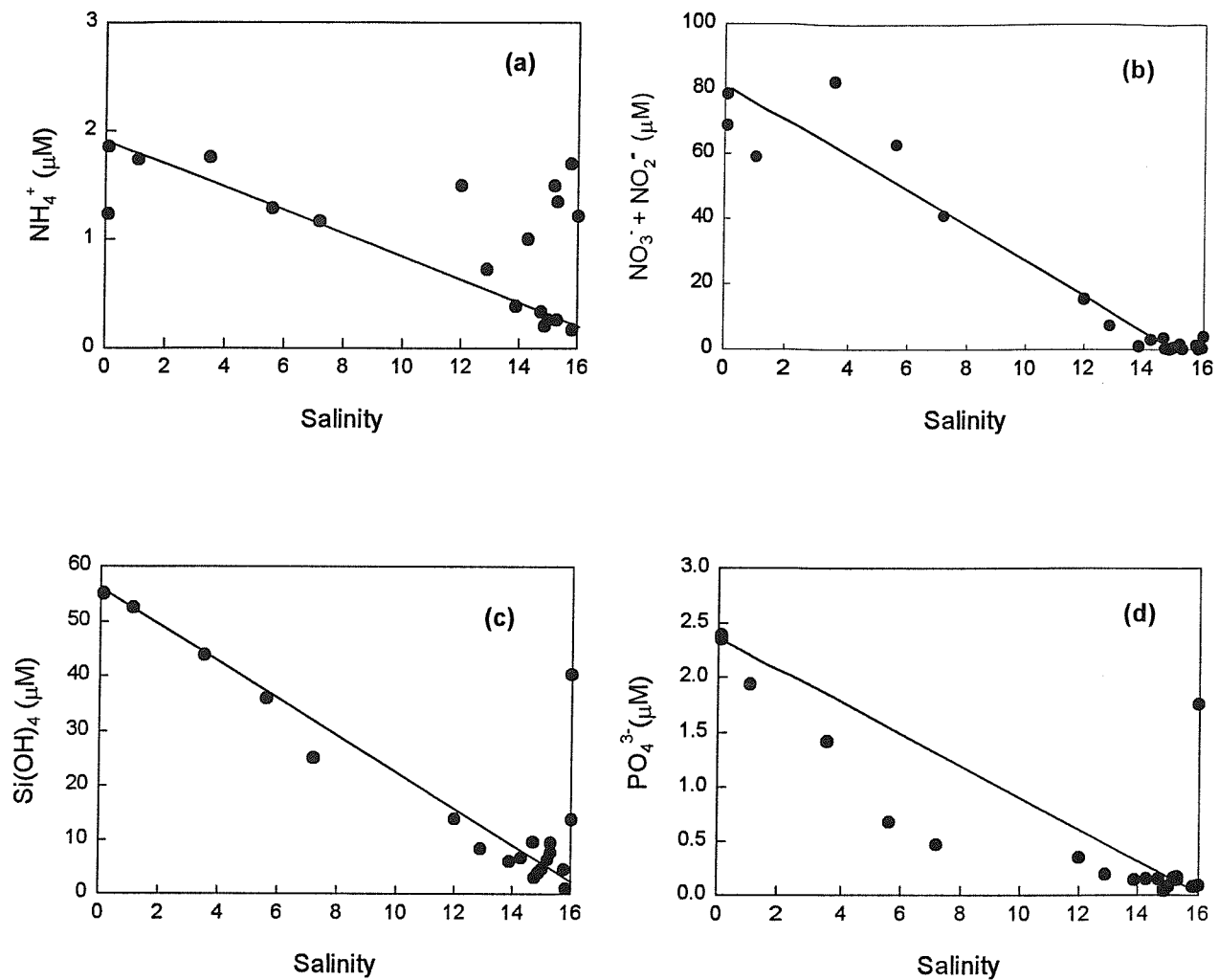


Fig. 6.13: NH_4^+ (a), $\text{NO}_3^- + \text{NO}_2^-$ (b), Si(OH)_4 (c) and PO_4^{3-} (d) plotted versus salinity

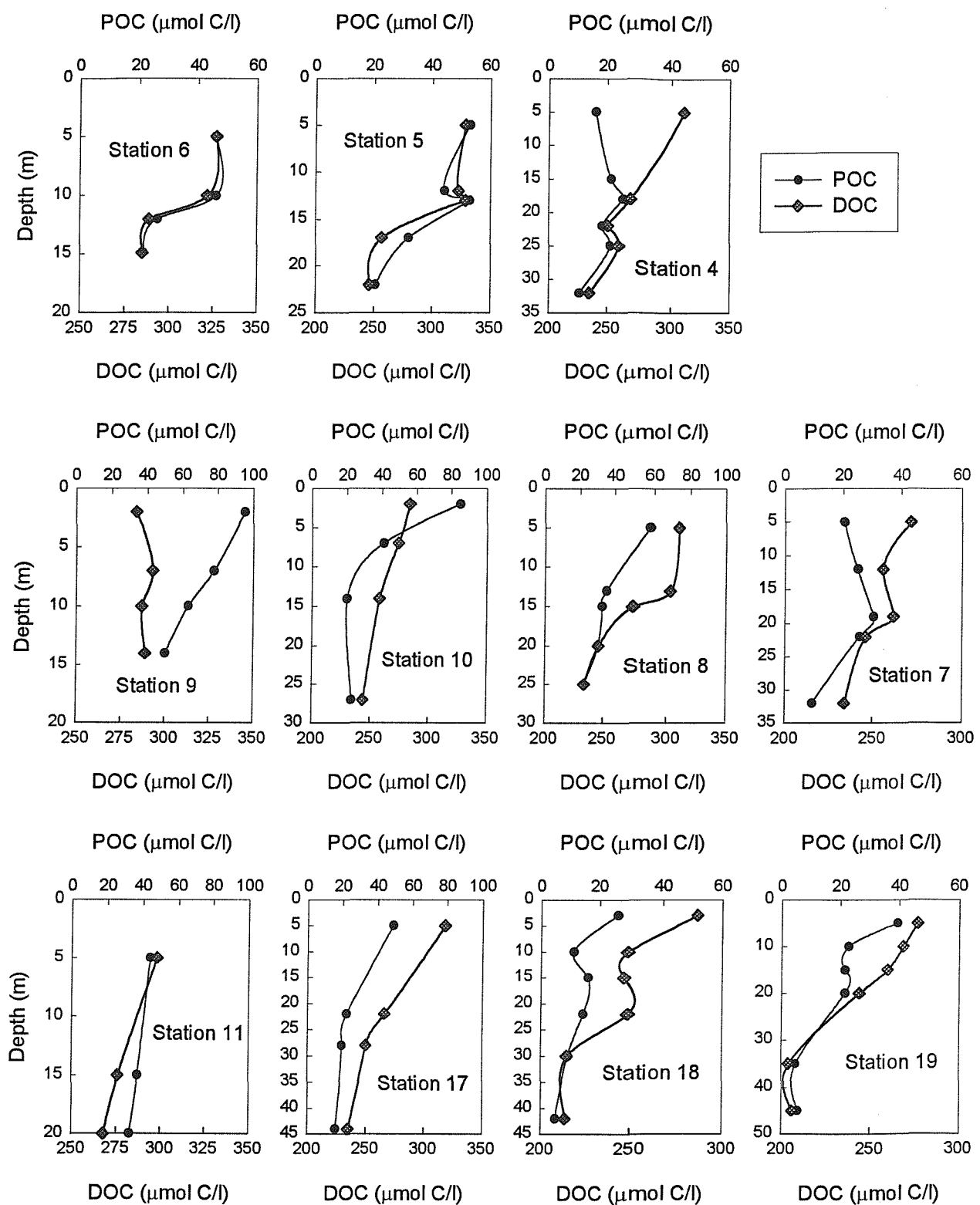
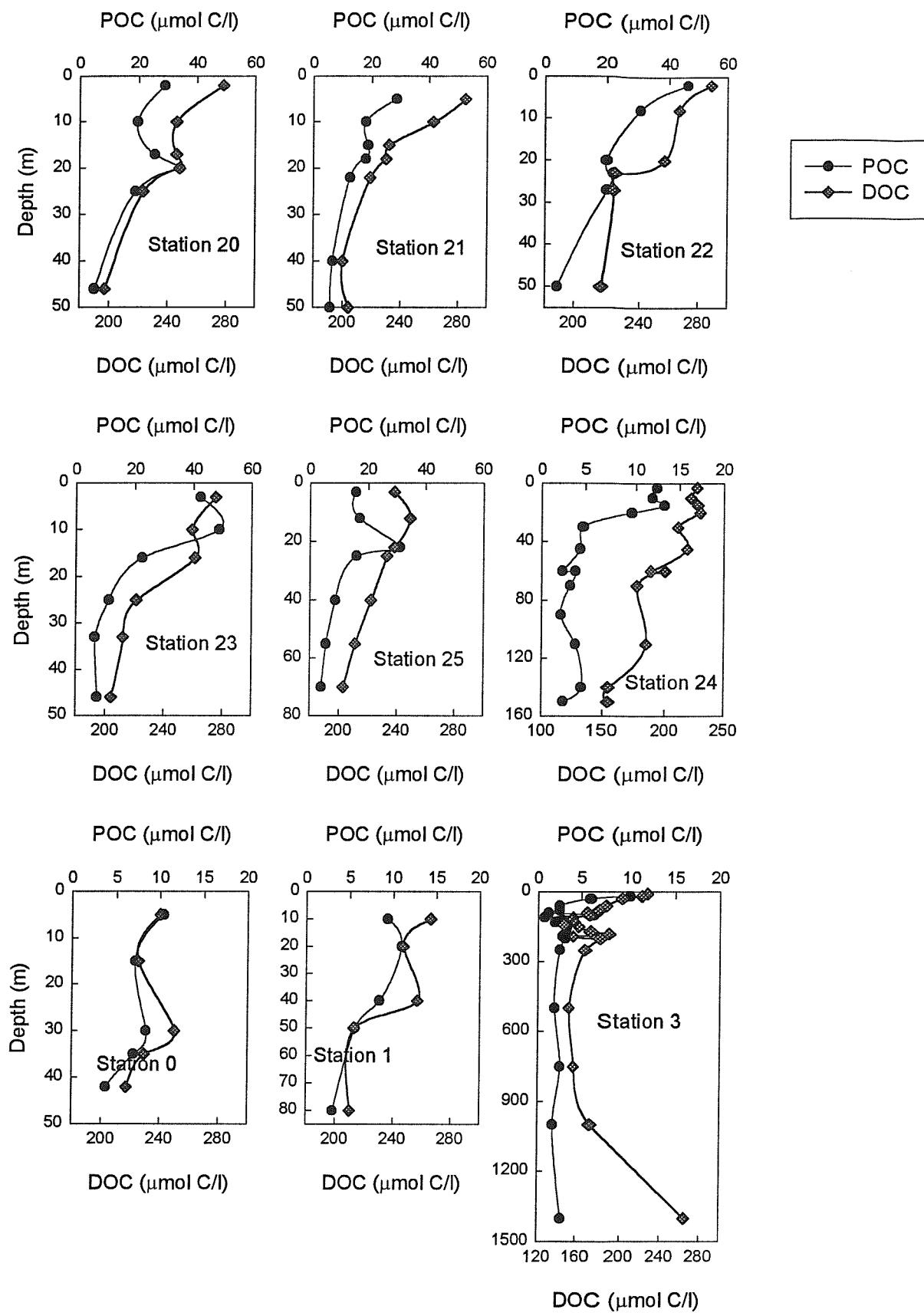


Fig. 6.14.a: Distributions of DOC and POC at Stations 6, 5, 4, 9, 10, 8, 7, 11, 17, 18 and 19



a different feature brought about by the presence of anoxic conditions. Concentrations decrease from 200 to 160 $\mu\text{mol C/l}$ through the surface layer then increase to 200 $\mu\text{mol C/l}$ between 250 and 600 m. Below 600 m concentrations increase to reach 280 $\mu\text{mol C/l}$ at the bottom.

POC concentrations vary between 1 and 100 $\mu\text{mol C/l}$. The highest values are found in surface waters, particularly at Stations strongly influenced by the Danube plume. At most stations (Stations 4, 5, 7, 18, 19, 20, 21, 22, 23, 25) a POC maximum was observed at the thermocline. During summer, stratification of the water column increases the residence time of particles at the thermocline, which enhances also the probability of random collision of aggregates and other POM (Alldredge *et al.*, 1987; Alldredge and Mc Gillivray, 1991) thus potentially enhancing a POC maximum at the thermocline. The POC and Chl *a* profiles are qualitatively similar to one another but the two properties are not strongly linearly correlated (correlation coefficient = 0.521) suggesting that they have different sources. Cauwet *et al.* (1996) found that there was a good correlation between POC and PON with a C/N ratio varying between 10 and 15. However high C/N ratios (up to 20) have been found at Stations 5, 22 and 26 and are possibly due to larger terrestrial inputs. At Stations 7 and 24, lower C/N ratios (7-8) have been found suggesting intense primary productivity in the area.

6.4 Trace metals in the Danube river

The river Danube was sampled at Station 12 (salinity 0.1), which is situated at the mouth of the river, in July 1995. Particulates were not homogeneously distributed and consequently triplicate samples were collected for the particulate phase to provide information on estuarine variability as well as analytical error; only one sample was collected for the dissolved phase. Particulate samples were leached using acetic acid (25%) then the residue was digested with concentrated nitric acid (see Chapter 3). Results for dissolved and particulate trace metals are presented in Table 6.2 and compared with the average trace metal concentrations for the Rhône and Ebro rivers and for the world rivers.

Table 6.2: Trace metal concentrations in the Danube river. Comparison with mean values for the Rhône and Ebro rivers and with the world rivers average.

		Mn	Fe	Co	Pb	Cd	Zn	Ni	Cu
Danube river	Dissolved (nM)	14	36	0.3	0.159	0.132	5.9	15	28
	Leachable particulate (µg/g)	1392	5943	5.4	31	0.6	78	16	33
	Total particulate (µg/g)	1663	33100	14	50	0.8	159	62	68
Average Rhone and Ebro [1]	Dissolved (nM)	61	184	10	0.375	0.265	18.6	25	34
	Total particulate (µg/g)	1037	33100	—	43	1.6	200	48	47
Average world rivers [2]	Dissolved (nM)	150	720	1.7	0.150	0.090	9.0	8	23
	Total particulate (µg/g)	1050	48000	—	35	1.2	250	90	100

[1] Guieu *et al.* (1997)

[2] Martin and Windom (1991)

Total particulate metal concentrations for the Danube river are quite similar to those reported for the Rhône and Ebro rivers (Guieu *et al.*, 1997) and for the world rivers average (Martin and Windom, 1991). Similar observations apply for some of the dissolved trace metals (Pb, Cd, Zn, Ni, Cu). However much lower concentrations of dissolved Mn, Fe and Co have been found in the Danube river compared to the world rivers average. This may be due to precipitation of manganese and iron oxides within the catchment area. The percentages of leachable metals in the SPM (compared with the total metal) are relatively high with the exception of Fe and Ni: Mn (84 %), Cd (75 %), Pb (62 %), Zn (49 %), Co (39 %), Cu (38 %), Ni (26 %) and Fe (18 %).

6.5 Trace metals in the north western Black Sea shelf

6.5.1 Manganese

Manganese distributions (Figs. 6.15.a and 6.15.b) are affected by the mineralization processes and associated changes in redox conditions which occur in the water column and at the sediment water interface (see § 2.2.1).

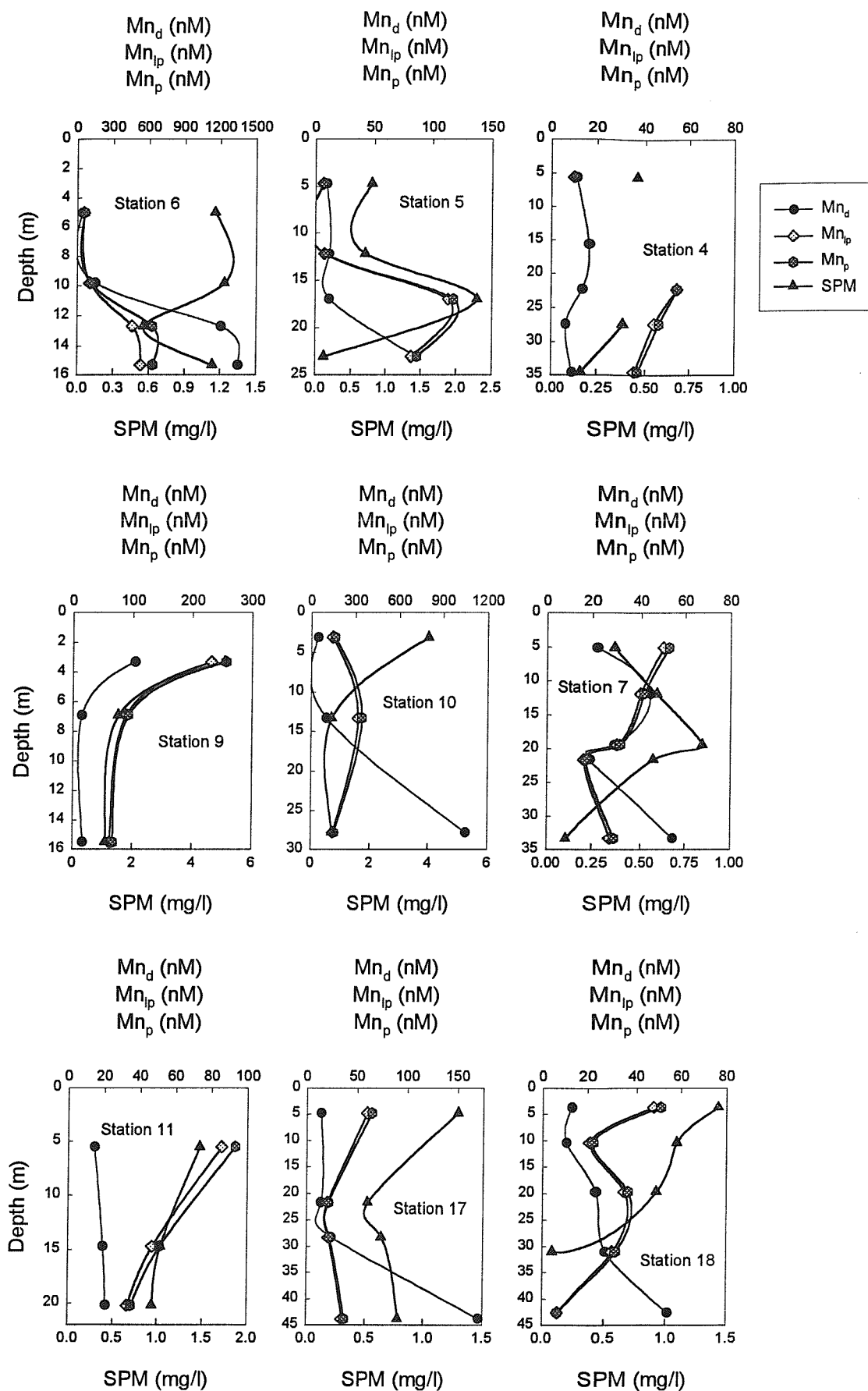


Fig. 6.15.a: Distributions of dissolved Mn (Mn_d), leachable particulate Mn (Mn_{lp}) and total particulate Mn (Mn_p) at Stations 6, 5, 4, 9, 10, 7, 11, 17 and 18

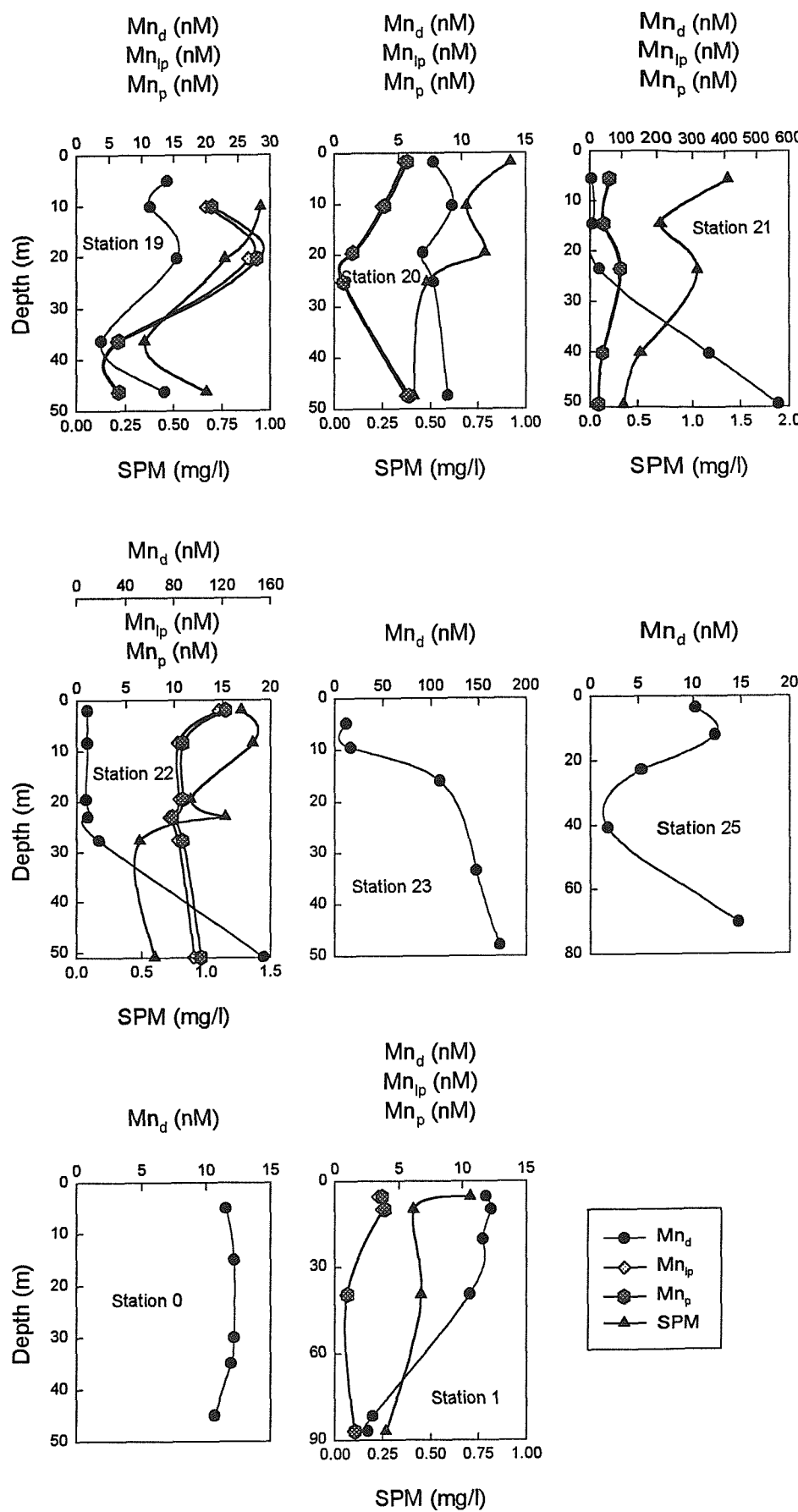


Fig. 6.15.b: Distributions of dissolved Mn (Mn_d), leachable particulate Mn (Mn_{lp}) and total particulate Mn (Mn_p) at Stations 19, 20, 21, 22, 23, 25, 0 and 1

Station 6 is close to the coast and mainly influenced by the Dnepr, Bug and Dniestr rivers. Dissolved and total particulate Mn concentrations are relatively low above the thermocline (respectively 30 and 60 nM) and increase sharply below to reach maxima near the sediment–water interface. Near the bottom, dissolved Mn concentrations (1300 nM) are higher than total particulate Mn concentrations (650 nM). At this station there is a maximum in organic carbon at the surface of the core suggesting deposition of fresh organic inputs (Herman and Wijsman, 1996). Remineralization of this organic carbon uses most of the MnO₂ available as there is a minimum in the solid phase content of Mn at the surface of the core (Herman and Wijsman, 1996). Manganese oxides are reduced to dissolved Mn (II) which diffuses from the sediment into the water column. The dissolved Mn which emanates from the sediment quickly re-precipitates as MnO₂ at the interface of the oxic and anoxic layers, which is close to the bottom, thus inducing high concentrations of particulate Mn. The correspondingly high values of SPM near the bottom may partly be due to resuspension but may also be enhanced by precipitation of manganese and iron oxides (the mass of total particulate Mn and Fe represents 10 % of the SPM mass). The concentration of total Mn in SPM is lower near the bottom (31 mg/g) than at the thermocline (63 mg/g). This suggests that the high concentrations of total particulate Mn in the water near the bottom are mainly due to resuspension since there is a minimum in the solid phase content of Mn at the surface of the core.

Stations 5, 10 and 17 have similar distributions to Station 6 but at Stations 5 and 10 the maximum in particulate (total and leachable) Mn is at the thermocline; at Station 5 this also coincides with a maximum in SPM. These features are characteristic of the Fine Particle Layer (FPL) described by Kempe *et al.* (1991) in the southern part of the Black Sea. The Mn particles may originate from resuspension in shallow water and may have been advected towards the open sea. The density stratification of the Black Sea increases the residence time of these Mn particles at the thermocline. Kempe *et al.* (1991) analysed particles collected in the FPL: their EDX analyses showed that particulate Mn was present on all the filters; using high resolution SEM they found that Mn was mostly concentrated in macroflocs of rather uniform size (around ca. 0.5 µm) and shape which could have derived from bacteria. At Stations 5 and 17 dissolved and total particulate Mn concentrations are an order of magnitude lower than at Station 6, mineralization processes being less intense.

Stations 9 and 11 are located at the mouth of the Danube river in 2 separate branches. Total particulate Mn concentrations are higher than dissolved Mn concentrations; this is mainly due to the relatively high oxygen concentrations which range from 5-7 ml/l. The distributions show in both cases higher concentrations in surface water which decrease towards the bottom. This is mainly due to the Danube influence. The SPM concentrations are relatively high in surface water (5 mg/l, Station 9; 1.5 mg/l, Station 11), reflecting the high particulate load of the Danube river (35-38 mg/l). This limits the light penetration into the water column which thus limits primary productivity. Consequently at those stations sedimentation of organic carbon is less intense and the degradation of this organic load does not lead to any anoxia around the sediment-water interface.

At Stations 4, 7, 18, 19, 20 and 25, Mn concentrations are relatively low and vary between 1 and 60 nM for both dissolved and total particulate phases. The profiles show maxima in dissolved Mn at the thermocline and at the sediment—water interface suggesting that reduction of Mn oxides occurs in both the water column and near the sediment. The dissolution of Mn from particles may involve the use of the MnO_x phase in the oxidation of organic matter but may also be a more general consequence of the influence of low O_2 concentrations on redox states of other constituents. However O_2 concentrations are not markedly low (4–6 ml/l), consequently it is not likely that bulk water conditions favour the release of Mn by either process. It could be that some reduction is occurring in microenvironments (for example decomposing organics within the aggregates) in the dominantly oxic medium. Tebo (1991) demonstrated that Mn(IV) reduction can occur in the presence of oxygen. They measured by radioactive incubation experiments a strong potential for microbial Mn(IV) reduction throughout the suboxic zone in the Black Sea. In their experiments, the rate of Mn(IV) dissolution was only partially inhibited in samples either prefiltered to remove the bacteria or exposed to oxygen, suggesting Mn(IV) reduction is mediated by both dissolved chemical constituents and microbial activity.

The dissolved Mn distribution may also be influenced by the presence of dissolved organic matter. Some of the dissolved organic matter produced during organic matter decomposition is unsaturated and is also a potential oxidant for Mn(II). Richert *et al.*

(1988) demonstrated that organic ligands can undergo electrochemical oxidation. The Mn(II) bound to this oxidized organic ligand can transfer an electron directly on the bond axis to the oxidized ligand which in turn becomes reduced. The overall result is the formation of Mn(III) which is soluble. In sea water systems, soluble Mn(III) complexes can diffuse or be mixed by tides or internal waves throughout the anoxic zone (Luther *et al.*, 1994).

At the thermocline dissolved Mn maxima are associated with higher total particulate Mn concentrations. These relatively high total particulate Mn concentrations may possibly be due to precipitation of dissolved Mn in the presence of oxygen. Tebo (1991) demonstrated that the oxidation of Mn(II) or Mn(III) can be microbially catalysed even at low oxygen concentrations. Particulate Mn maxima may also be enhanced by the accumulation of SPM at the thermocline which is mainly due to strong stratification of the water column.

Maxima in dissolved Mn concentrations near the bottom are associated with a depletion in total particulate Mn. The latter probably reflects more a lower sedimentation from surface water than the dissolution of MnO_x since dissolved Mn concentrations are not particularly high and O₂ concentrations indicate oxic conditions in bottom water; the higher dissolved Mn concentrations are probably due to influx across the diffusive sediment—water interface.

Stations 21 and 23 show higher dissolved Mn concentrations at the bottom (600 and 200 nM respectively) than at Stations 20 and 22 (10 and 20 nM respectively) suggesting that reduction of MnO_x is more intense at Stations 21 and 23. This is also associated with higher POC concentrations in the water column suggesting a high level of primary productivity which is possibly due to larger localised nutrients inputs from the coast. The degradation of this organic carbon at the sediment-water interface is possibly increasing the oxygen demand and thus increasing the reduction of MnO_x.

Stations 0 and 1 are situated in the North and are not directly influenced by riverine inputs. Manganese concentrations are relatively low. They vary between 12 and 14 nM for the dissolved phase and between 1 and 4 nM for the total particulate phase. Concentrations in

both dissolved and total particulate phase tend to be higher in surface water, perhaps as a result of atmospheric inputs. Dissolved Mn maxima in surface waters elsewhere (e.g. Mediterranean Sea) were attributable to eolian inputs (Tankéré *et al.*, 1995; Guieu *et al.*, 1997). Chester (1993) reported average concentrations of particulate trace metals in the atmosphere over the Mediterranean Sea and the Black Sea. Atmospheric Mn inputs were generally higher in the Black Sea than in the Mediterranean Sea.

In areas affected by suboxic or anoxic conditions in the north-western Black Sea, particulate Mn is primarily associated with the acetic acid leachable fraction (95 %), but less so in surface coastal waters elsewhere (80 %). This may reflect the difference in particle origin. In particular, it suggests that Mn in suboxic or anoxic waters may be in a state of dynamic exchange between the dissolved and the particulate phases.

6.5.2 Iron

The distribution of Fe is remarkably similar to that of Mn (Figs 6.16.a and 6.16.b). This result may perhaps seem surprising, especially if one considers the diversity and complexity of the profiles together with the large difference between the oxidation kinetics of Fe(II) and Mn(II). It suggests that the maxima in both dissolved and particulate concentrations are caused by the same in situ processes for Fe as for Mn. It is argued below that these processes are largely driven by the decomposition of organic matter. Lateral advection alone would, over time, lead to a decoupling between Fe and Mn and is therefore not likely to be important in explaining the close similarity in their distribution. Particulate Fe concentrations do tend to be higher than particulate Mn concentrations. This is simply because Fe is more abundant in typical lithogenous material than Mn; particulate Fe concentrations may also be enhanced by the formation of authigenic Fe by spontaneous oxidation of ferrous iron in neutral environments where most of the bacteria occur.

Higher concentrations in dissolved and total particulate Fe are found near the sediment-water interface (Stations 6, 4, 10, 7, 17, 18, 19, 21, 22, 25). Very high concentrations are found near the bottom at Station 6 (175 nM for the dissolved phase and 1437 nM for the

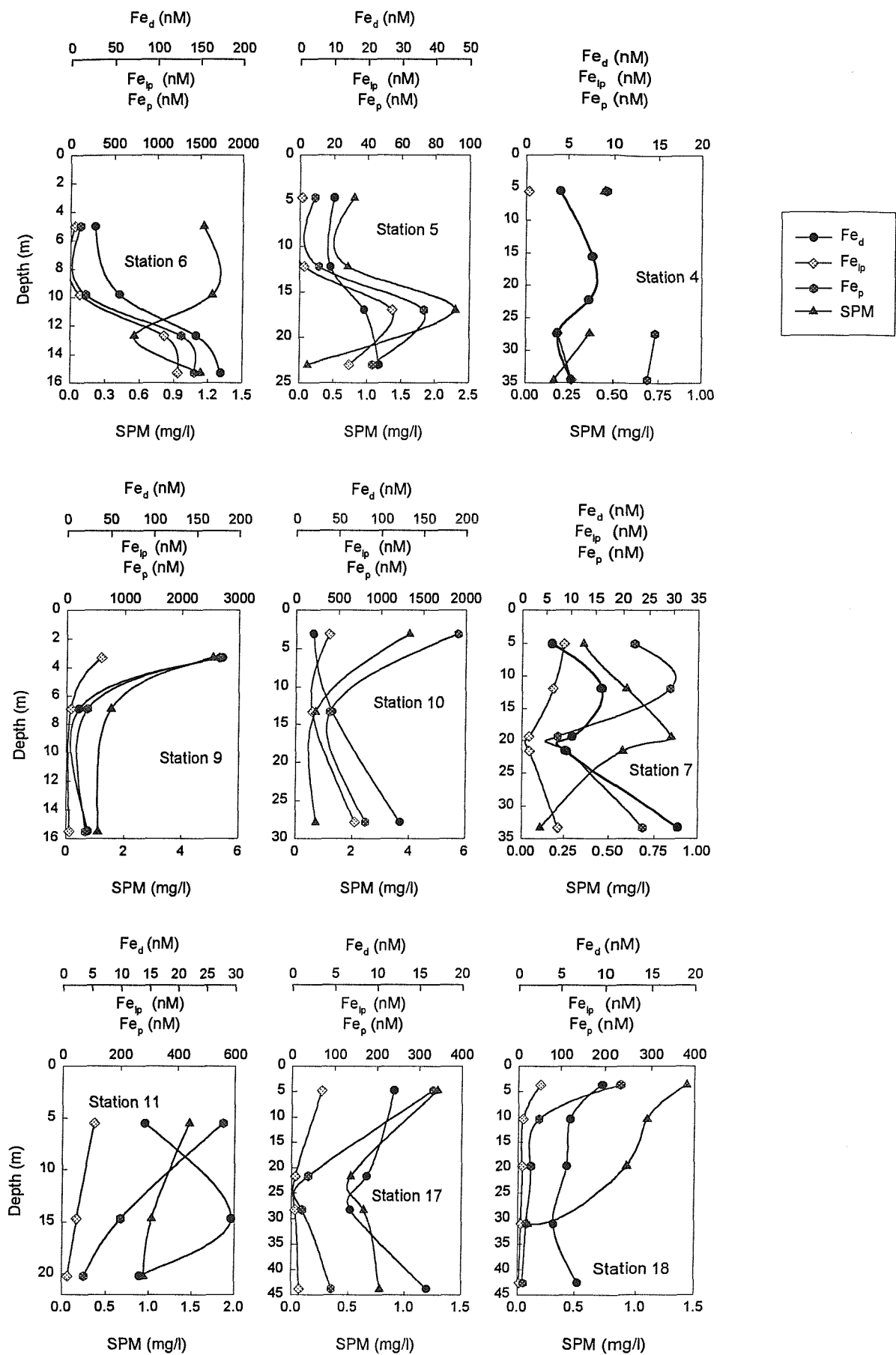


Fig. 6.16.a: Distributions of dissolved Fe (Fe_d), leachable particulate Fe (Fe_{ip}) and total particulate Fe (Fe_p) at Stations 6, 5, 4, 9, 10, 7, 11, 17 and 18

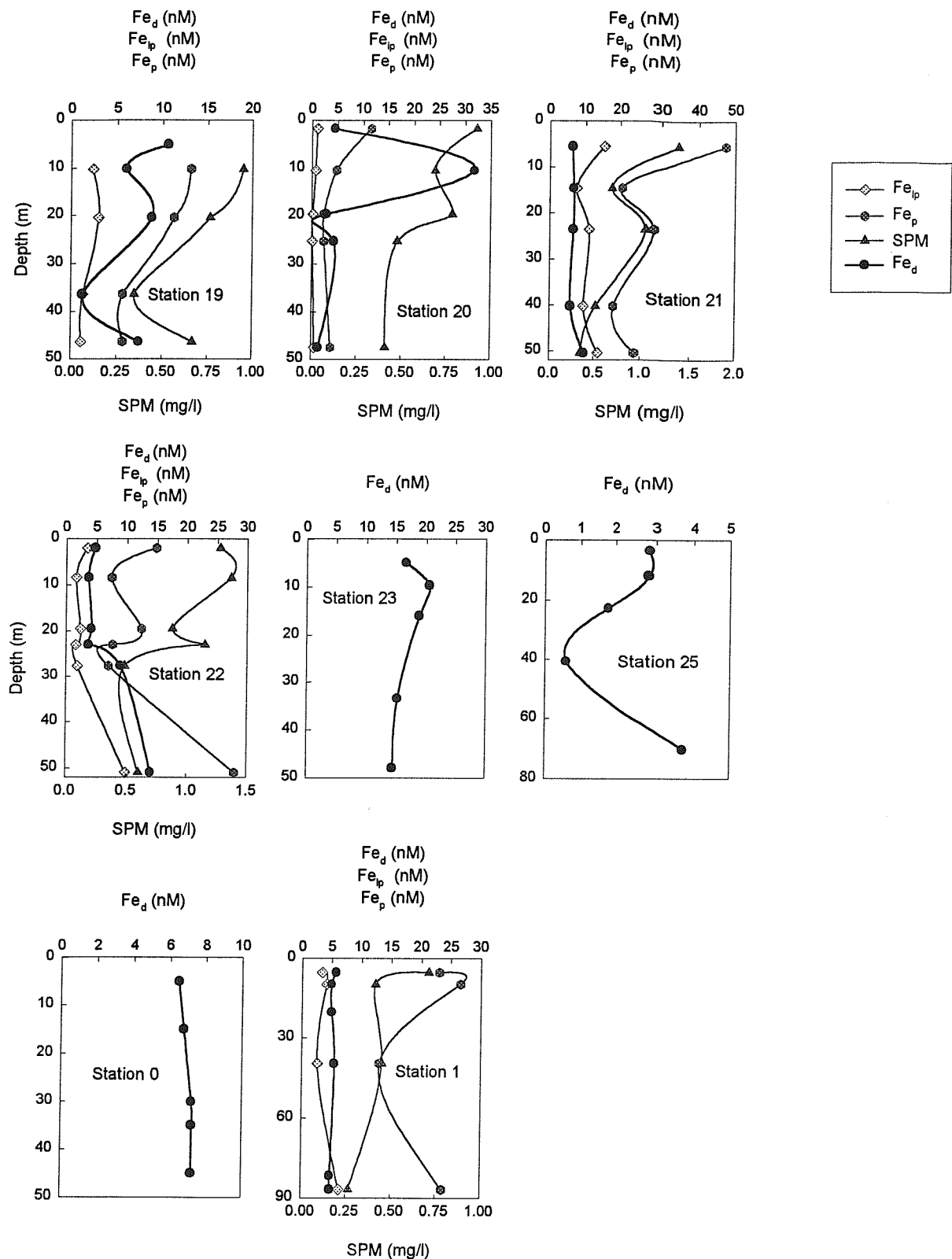


Fig. 6.16.b: Distributions of dissolved Fe (Fe_d), leachable particulate Fe (Fe_{lp}) and total particulate Fe (Fe_p) at Stations 19, 20, 21, 22, 23, 25, 0 and 1

total particulate phase) and at Station 10 (123 nM for the dissolved phase and 824 nM for the total particulate phase). This is mainly attributed to reduction of Fe-oxides by bacteria during mineralization of organic carbon. More evidence is accumulating that bacteria can grow anaerobically by coupling organic carbon oxidation to reduction of Fe(III) oxides (Nealson, 1982; Arnold *et al.*, 1986; Lovley and Phillips, 1988; Nealson and Myers, 1990). The experimental evidence suggests that certain microorganisms act as agents for the oxidation of organic matter coupled to the reduction of Fe(III) oxides; the latter can be used as the sole or major electron acceptor (Mn(IV), NO_3^- or O_2 can be used as alternative electron acceptor). The percentage of total particulate Fe which is leachable is relatively high near the bottom at Stations 6 and 10: 87% and 85% respectively. This reflects the dynamic nature of the Fe redox cycle; the high leachable particulate Fe concentrations may be attributed to the spontaneous oxidation of Fe(II) in the presence of oxygen (Stumm and Sulzberger, 1992). Maxima in dissolved and total particulate Fe are also found at some locations at the thermocline where there is accumulation of organic carbon (Stations 4, 5, 7, 19). At those locations Fe(III) is probably reduced by microbial activity to Fe(II) which has a tendency to form very strong organic complexes with certain ligands released by microorganisms. Luther *et al.* (1994) also concluded that Fe(II) could be complexed by organic ligands in environments rich in organic matter (this applies particularly where O_2 does not reach significant concentrations). The maxima in total particulate Fe may be due to oxidation of Fe(II) in presence of dissolved O_2 . At the thermocline the percentage of total particulate Fe which is leachable is not particularly high for Stations 4, 7, 19, and varies between 17 and 40 %, whereas a maximum of 74 % is observed at Station 5. Stations within the region of direct influence of the Danube river (Stations 9, 10, 11, 17, 18) present high concentrations in both dissolved and total particulate phases in surface water. For example at Station 9, concentrations reach 190 nM for the dissolved phase and 2800 nM for the total particulate phase. This is mainly due to riverine inputs. In the surface plume, high Fe concentrations in the dissolved phase may be further enhanced by the photoreductive dissolution of Fe(III)-oxides, Fe colloids and organically chelated Fe (Waite and Morel, 1984; Rich and Morel, 1990). The total Fe composition of SPM in surface water varies between 2033 $\mu\text{g/g}$ and 6550 $\mu\text{g/g}$. These high Fe concentrations are a reflection of the terrestrial origin of the particles. At stations least influenced by riverine inputs or by remineralisation of large quantities of organic material (Stations 19, 20, 21,

22, 23, 25), dissolved Fe concentrations vary between 4 and 35 nM and total particulate Fe concentrations vary between 5 and 50 nM. In the North (Stations 0 and 1) concentrations are relatively low and vary between 5 and 7 nM for the dissolved phase, between 9 and 22 nM for the total particulate phase.

6.5.3 Cobalt

Dissolved Co concentrations vary between 150 and 400 pM at most stations on the North Western Black Sea shelf (Figs 6.17.a and 6.17.b). Higher concentrations are found at some locations, for example near the bottom at Stations 6 and 10 (1600 pM and 1797 pM, respectively) where remineralization processes are intense and in surface waters at Stations 9, 10 and 11 (689 pM, 478 pM and 470 pM respectively) which are influenced by the Danube inflow. Available particulate Co concentrations are relatively low compared to the dissolved phase and vary between 0 and 150 pM. These concentrations are similar to those in the Western Mediterranean Sea (Tankéré *et al.*, 1995) and in the North Sea (Tappin *et al.*, 1995). Dissolved Co concentrations have been plotted against dissolved Mn and Fe concentrations in Fig. 6.18. The relationship is closer with Mn ($r^2=0.73$) than with Fe ($r^2=0.49$). The closer relationship to Mn may be due to the influence of organic matter. Marchand (1974) found that in the presence of organic matter, Mn^{2+} and Co^{2+} form soluble ionic forms in seawater whereas the organic matter affects the physicochemical equilibrium of Fe by forming anionic, neutral or cationic organo-metallic complexes. However, concentrations of dissolved Co broadly increase with those of dissolved Fe and dissolved Mn up to about 400 pM. An association of Co with the Mn cycle has been observed in marine environments as different as the permanently anoxic Drammensfjord in Norway (Oeztuerk and Murat, 1995) and the North Sea (Kremling *et al.*, 1987; Kremling and Hydes, 1988; Tappin *et al.*, 1995). Then allowing for the scatter, dissolved Co concentrations remain similar with further increases in dissolved Fe and Mn. These results indicate that Co^{2+} concentrations are possibly limited by CoS precipitation while Fe^{2+} and Mn^{2+} concentrations in anoxic waters are controlled by fluxes across the sediment-water interface. Consequently the concentrations of the latter two metals are expected to increase with prolonged stagnation of the deeper water body. Similar findings have also been reported in anoxic Baltic waters by Kremling (1983).

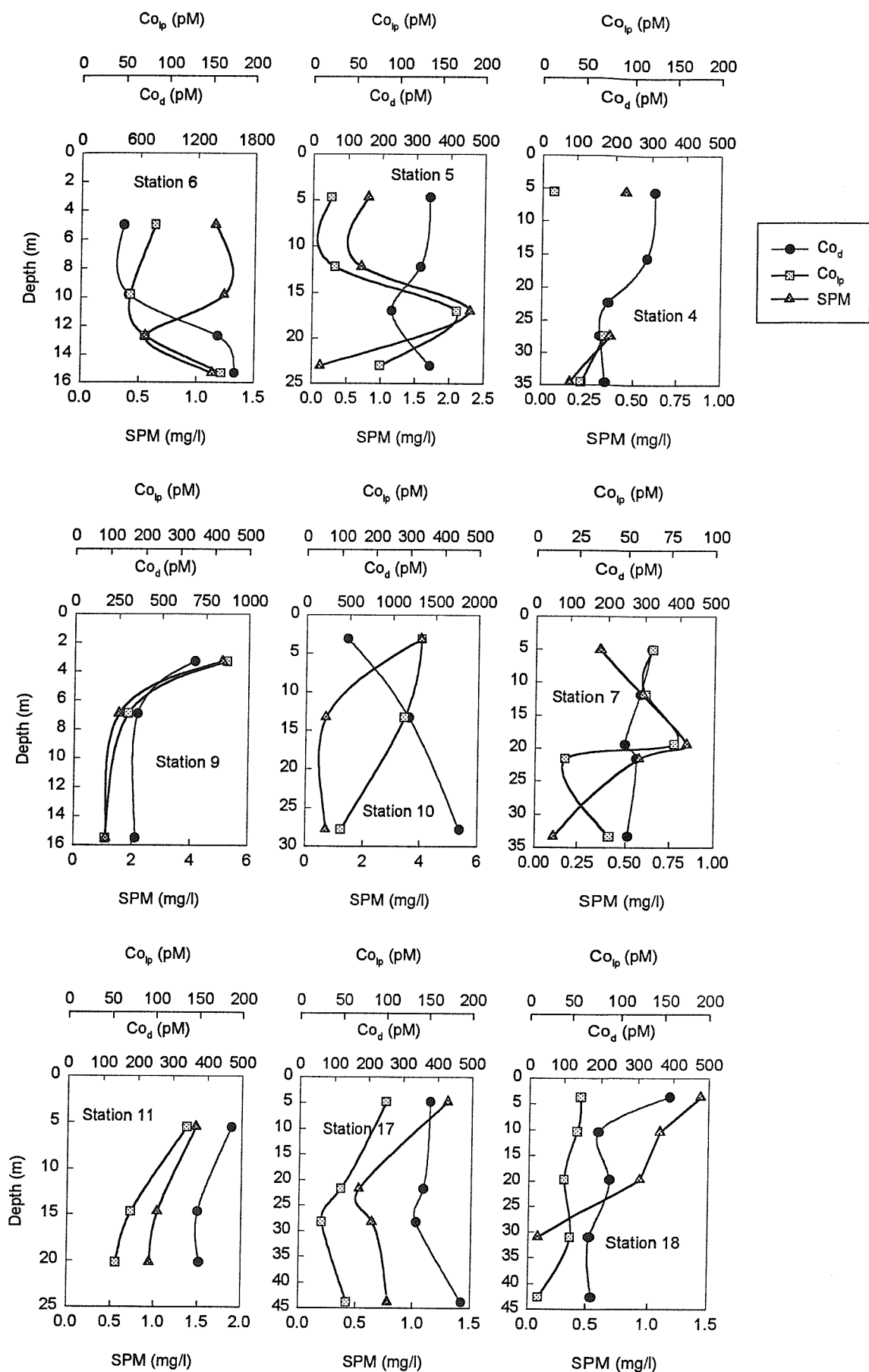


Fig. 6.17.a: Distributions of dissolved Co (Co_d) and leachable particulate Co (Co_{lp}) at Stations 6, 5, 4, 9, 10, 7, 11, 17 and 18

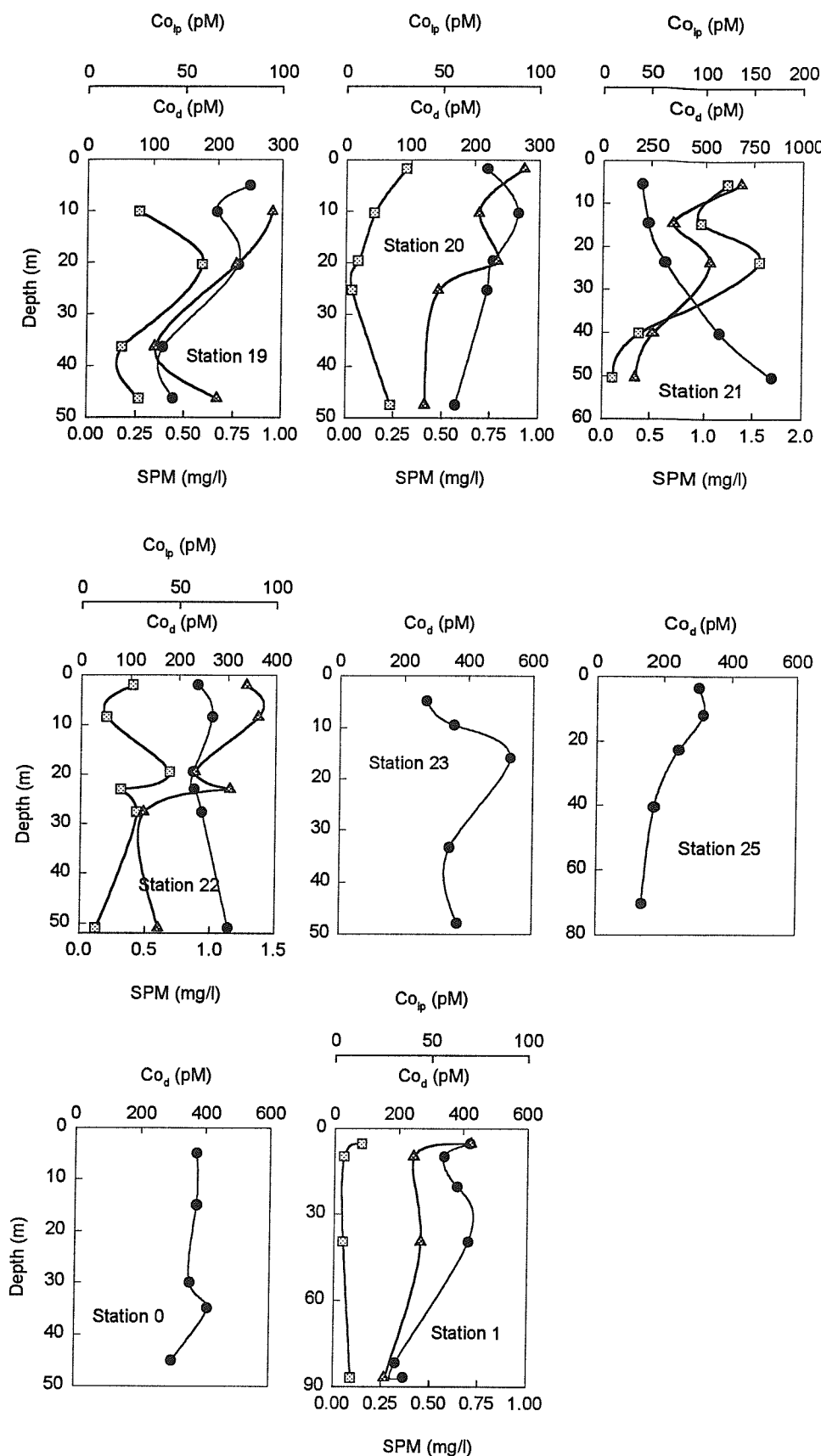


Fig. 6.17.b: Distributions of dissolved Co (Co_d) and leachable particulate Co (Co_{lp}) at Stations 19, 20, 21, 22, 23, 25, 0 and 1

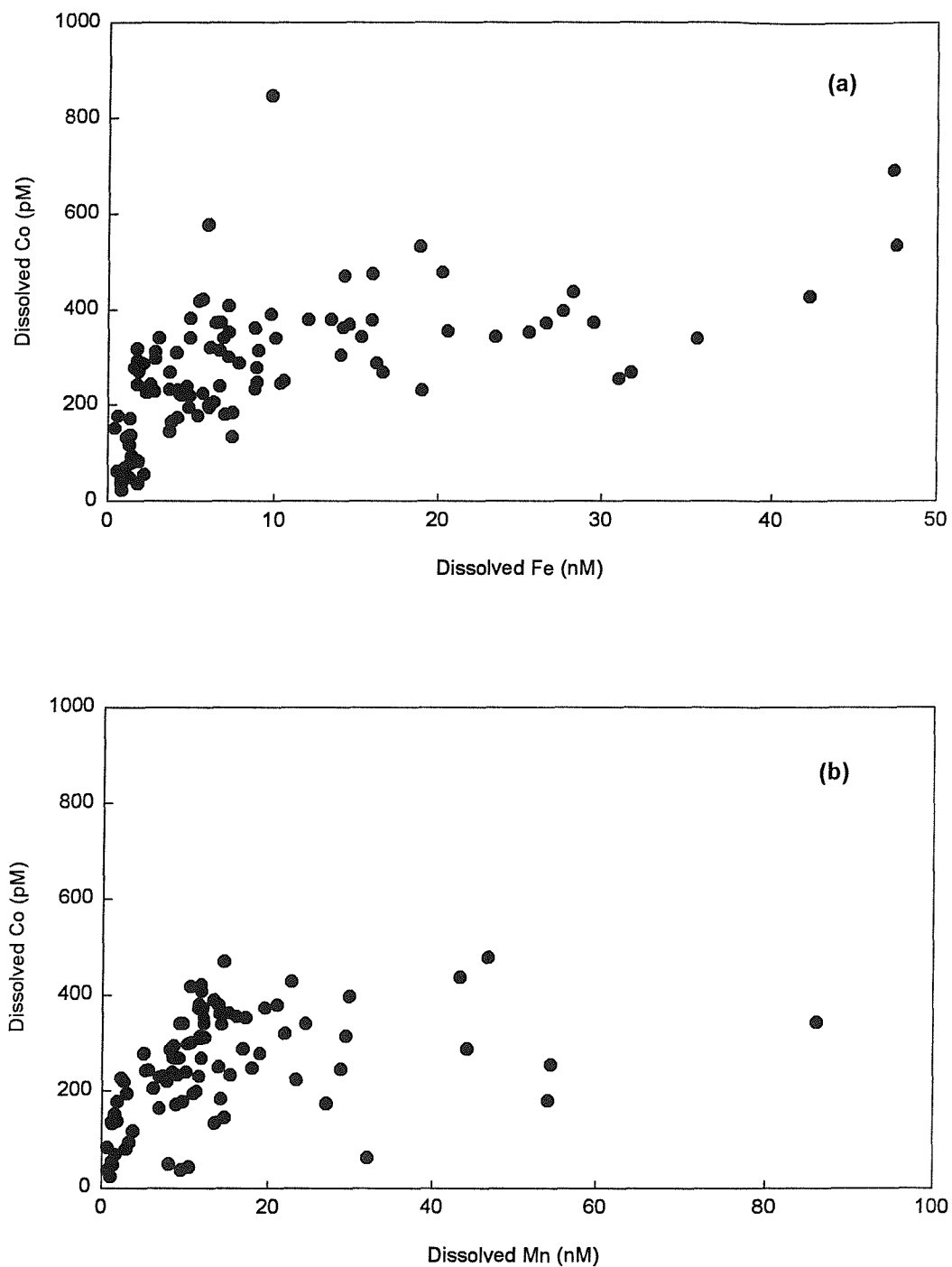


Fig. 6.18: Dissolved Co plotted versus dissolved Fe (a) and dissolved Mn (b)

6.5.4 Lead

Dissolved Pb concentrations vary generally between 0.025 and 0.13 nM (Figs. 6.19.a and 6.19.b). Higher concentrations (0.61 nM) are found in the Danube plume at Station 9. Available particulate Pb concentrations vary between 3 and 120 µg/g. These concentrations are lower than the values reported by Tappin *et al.* (1995) for the North Sea (dissolved Pb: 0.066-0.45 nM; available particulate Pb: 8-844 µg/g) but similar to the values reported by Tankéré *et al.* (1995) for the Western Mediterranean Sea (dissolved Pb: 0.045-0.13 nM; available particulate Pb: 1.4-22 µg/g).

At Station 6 dissolved Pb concentrations are low in surface water (0.025 nM) and increase to reach a maximum at the thermocline (0.075 nM). Near the bottom dissolved Pb concentrations decrease markedly. These low concentrations of dissolved Pb have been ascribed to efficient scavenging of Pb from solution onto particles (Mart *et al.*, 1982; Balls, 1985, 1988). Dissolved Pb follows a similar trend to dissolved Mn and Fe to 13 m, but then unlike them, decreases towards the bottom. Higher dissolved Pb concentrations at the thermocline may be due to release from the dissolution of Mn and Fe oxides on which Pb was previously adsorbed. Available particulate Pb concentrations are relatively constant between 6 and 15 µg/g, with a small increase at the pycnocline.

Station 7 shows typical effects of remineralization processes which occur above the thermocline and at the sediment-water interface. Above the thermocline, dissolved Pb distribution shows a minimum (0.024 nM) which coincides with a maximum in available Pb in SPM (20 µg/g), suggesting some transfer between phases. At the thermocline, where SPM is highest, available Pb in SPM shows no further increase with depth. This is possibly due to the increased plankton content of SPM. Below the thermocline, dissolved and available particulate Pb concentrations are similar (0.020 nM). The decrease in dissolved Pb suggests uptake of dissolved Pb by settling particles.

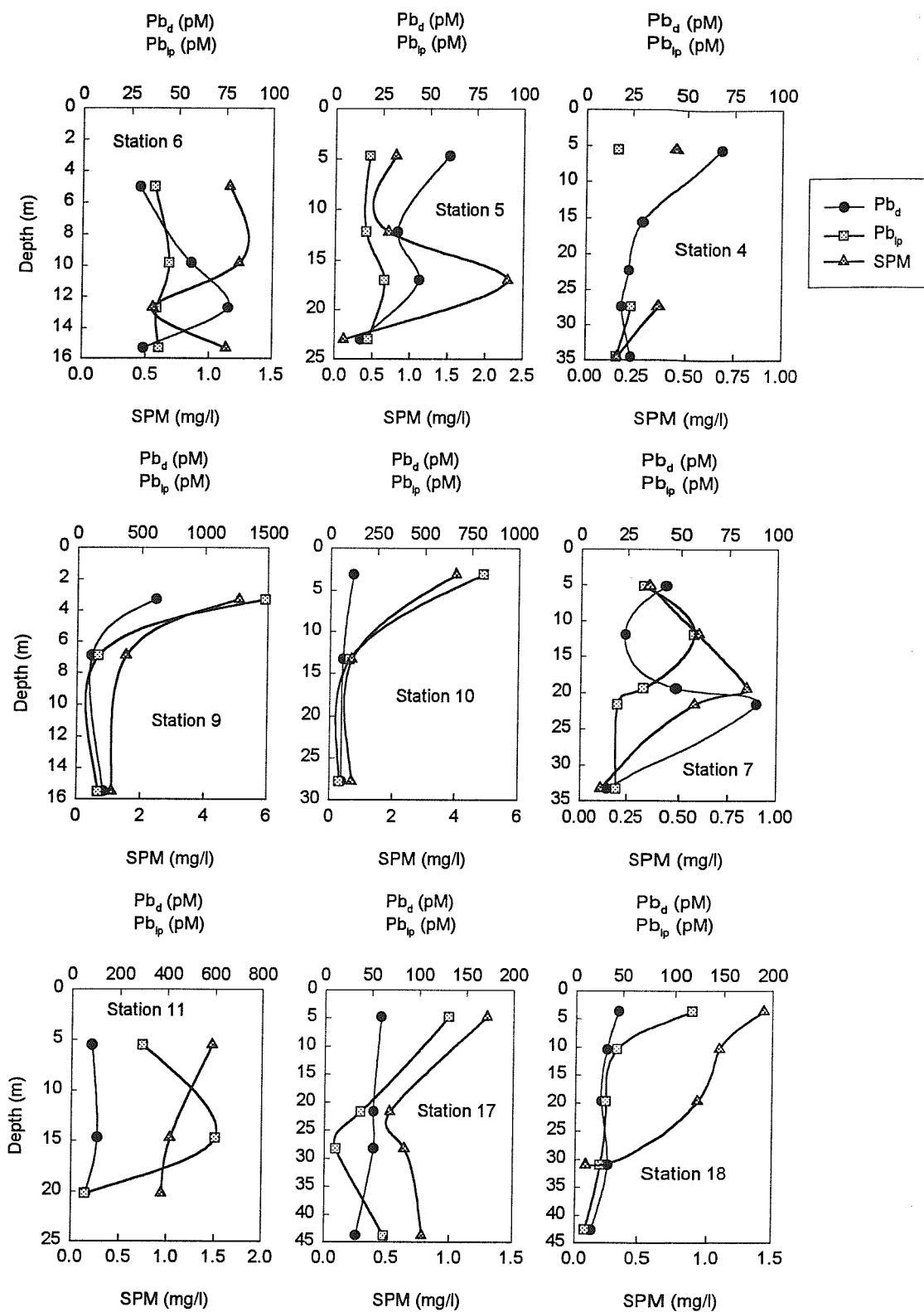


Fig. 6.19.a: Distributions of dissolved Pb (Pb_d) and leachable particulate Pb (Pb_{lp}) at Stations 6, 5, 4, 9, 10, 7, 11, 17 and 18

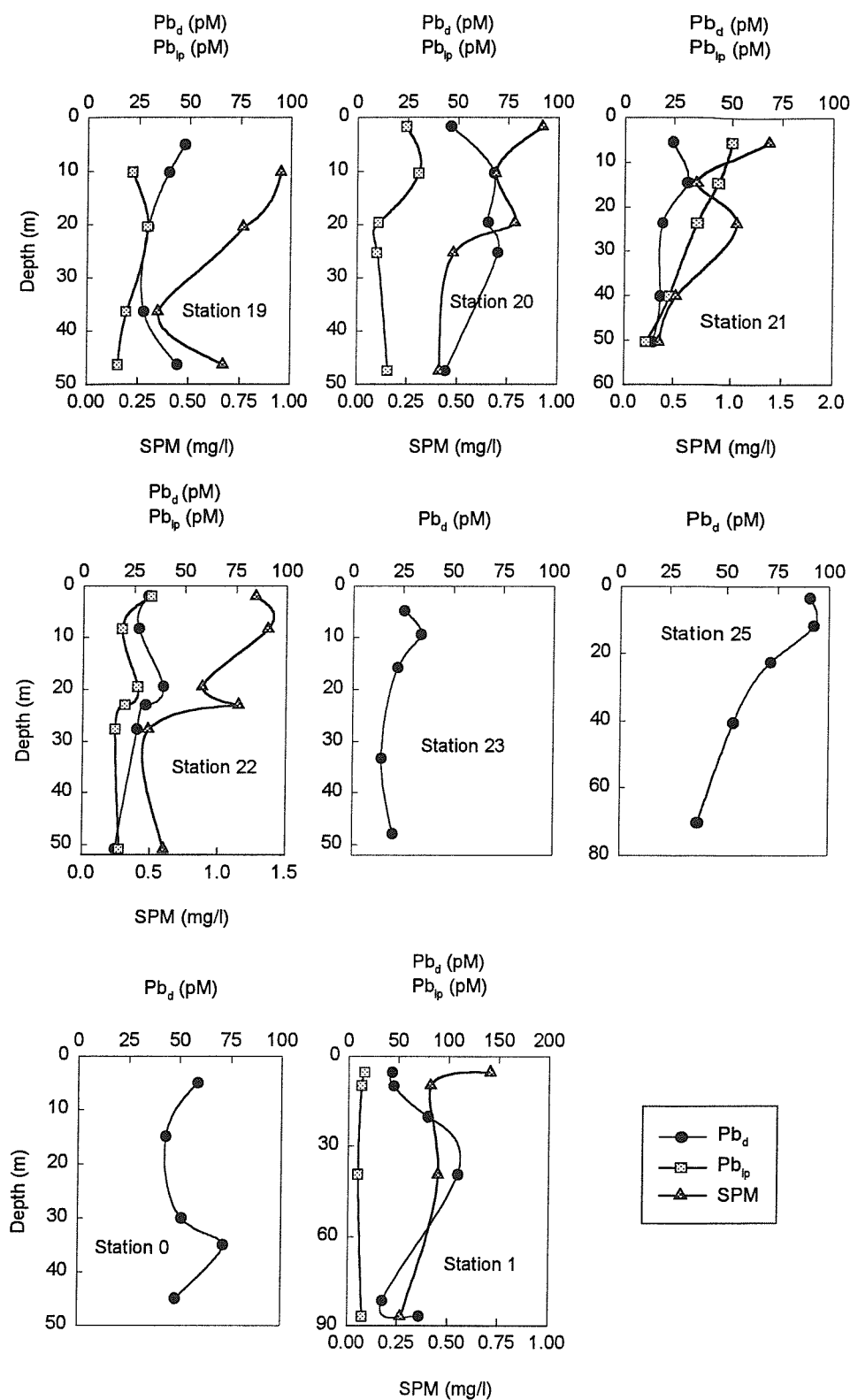


Fig. 6.19.b: Distributions of dissolved Pb (Pb_d) and leachable particulate Pb (Pb_{ip}) at Stations 19, 20, 21, 22, 23, 25, 0 and 1

Stations 9 and 10 present elevated concentrations of dissolved and available particulate Pb in surface waters (at Station 9, dissolved Pb: 0.614 nM and available particulate Pb: 1.500 nM) which reflect the fresh water contribution from the Danube River. Lead is mainly in the particulate phase in surface water whereas there is about equal partitioning between the dissolved and available particulate phases deeper in the water column.

Station 20 shows higher concentrations in dissolved Pb (44–70 pM) than Stations 19, 21, 22 and 23 (15–48 pM) suggesting possible sources. Station 25 is deeper and away from direct riverine influence, therefore the higher concentrations in dissolved Pb observed in surface water (91–93 pM) may be attributable to atmospheric inputs. The lowest concentrations of dissolved Pb are found at inshore stations and coincide with the highest SPM concentrations. By the same token, high concentrations of dissolved Pb occur where SPM values are correspondingly low. Due to lower SPM concentrations offshore, scavenging is less efficient so that the diffuse atmospheric inputs can sustain higher dissolved Pb concentrations. Similar observations have been made in the North Sea (Althaus, 1992; Tappin *et al.*, 1995).

At Stations 0 and 1, dissolved Pb concentrations vary between 35 and 110 pM. At Station 1, the relatively low dissolved Pb concentrations in surface water coincide with relatively high SPM values which may increase the scavenging efficiency. Available particulate Pb concentrations are relatively constant at circa 0.020 nM, with slightly higher concentrations in surface waters.

6.5.5 Copper

Dissolved Cu concentrations vary between 7 and 13 nM for the most part (Figs. 6.20.a and 6.20.b). Higher concentrations are found at stations situated at the mouth of the Danube river (29 nM, Station 9; 22 nM, Station 10; 15 nM, Station 11). Overall, dissolved Cu concentrations in the North Western Black Sea are much higher than in the open waters of the Western Mediterranean Sea, where they are reported to be around 1.5 nM (Tankéré *et al.*, 1995; Morley *et al.*, 1997), but are similar to those in the Rhône outflow area (Morley

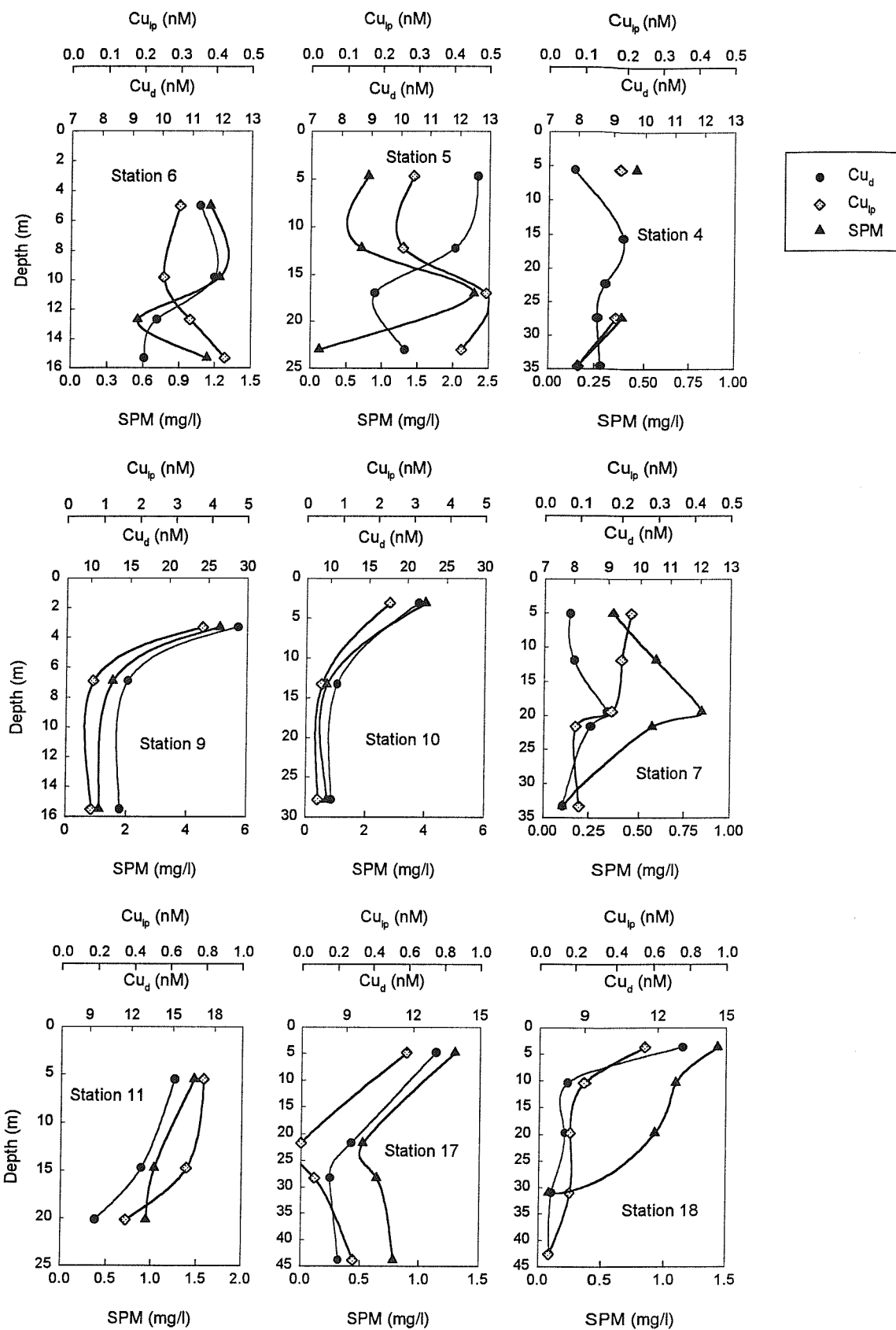


Fig. 6.20.a: Distributions of dissolved Cu (Cu_d) and leachable particulate Cu (Cu_{lp}) at Stations 6, 5, 4, 9, 10, 7, 11, 17 and 18

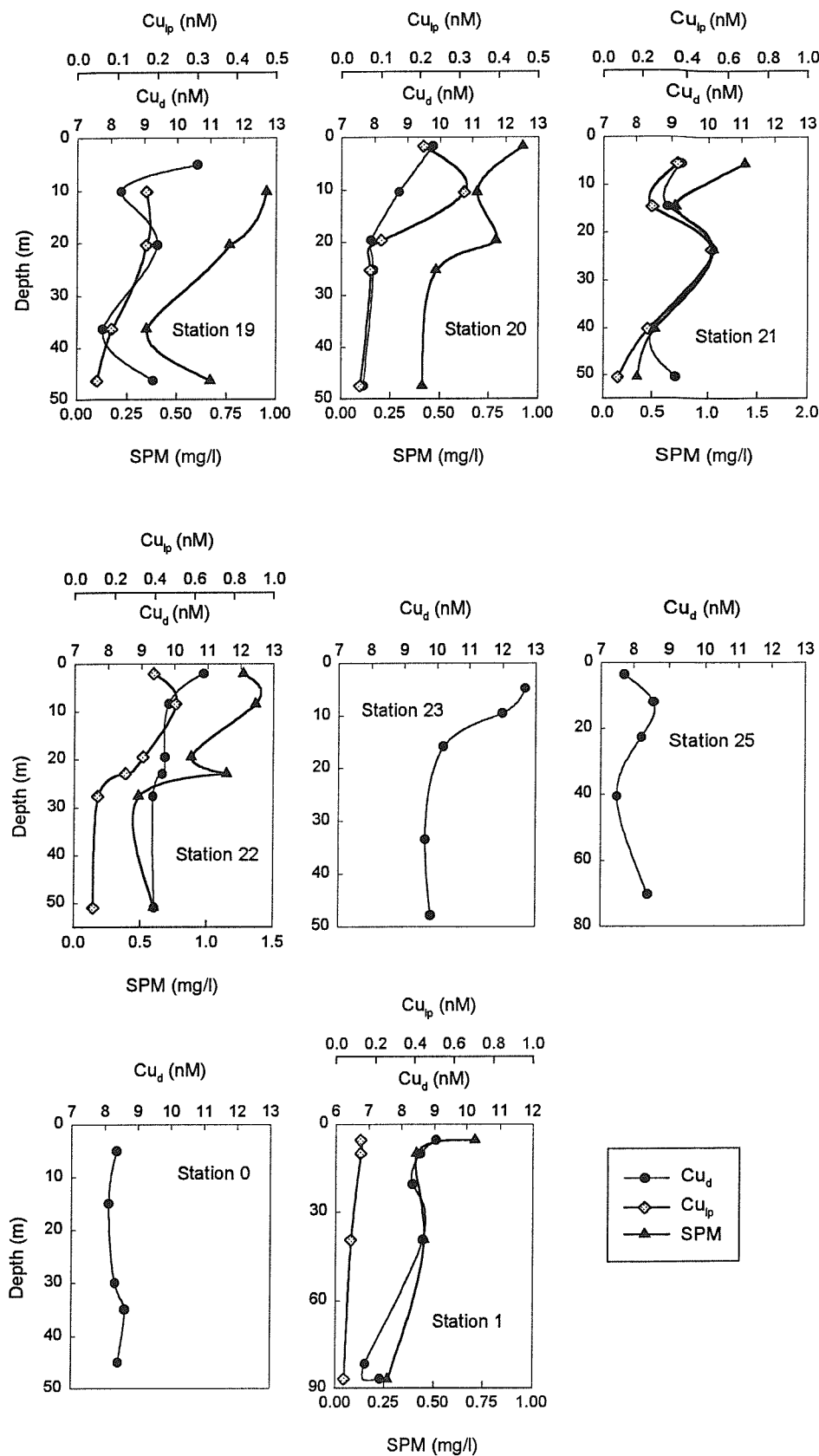


Fig. 6.20.b: Distributions of dissolved Cu (Cu_d) and leachable particulate Cu (Cu_{lp}) at Stations 19, 20, 21, 22, 23, 25, 0 and 1

et al., 1990). Similar concentrations to those in the North Western Black Sea have also been reported in the Northern Adriatic Sea (Tankéré and Statham, 1996). Available particulate Cu concentrations are low compared to the dissolved phase and vary between 0.05 nM and 1 nM. The residual fraction was below detection limit. Higher Cu concentrations in the available particulate phase are found at the mouth of the Danube river (2–4 nM). Available particulate Cu concentrations in the North Western Black Sea are similar to those in the North Sea (Tappin *et al.*, 1995) higher than in the Western Mediterranean Sea (Tankéré *et al.*, 1995).

The dissolved Cu–salinity diagram (Fig. 6.21) shows essentially conservative mixing between surface water and deeper water at salinities between 13 and 19 in the northwestern Black Sea. The intercept from the linear regression (29 nM) is similar to the value measured at zero salinity in the Danube river suggesting conservative mixing between Danube river water and coastal Black Sea water. This is in agreement with the results of several authors who described a nearly conservative behaviour for Cu in low salinity regions of a number of estuaries (Duinker *et al.*, 1980; Boyle *et al.*, 1982; Danielsson *et al.*, 1983; Edmond *et al.*, 1985; Shiller and Boyle, 1991; Althaus, 1992). Only three points deviate from the regression line by more than $\pm 2\sigma$, and all three correspond to surface samples taken within the region of freshwater influence of the Danube river. Variations in river source concentrations may have contributed to the deviations, particularly if they occurred over time scales shorter than the mixing time of water in the Danube surface plume. River source variations can induce curvature into otherwise conservative profiles (Officer and Lynch, 1981; Cifuentes *et al.*, 1990) but in practice the deviations are both smaller and more systematic than the ones seen here (Kaul and Froelich, 1984). Thus, in situ processes leading to input (Stations 9 and 10) or removal (Station 15) are likely to be involved here. At Station 15 (salinity 3.5) the observed depletion may be due to incorporation in particulate organic matter (Paulson *et al.*, 1994) or to aggregation with colloidal Fe and humic substances (Sholkovitz and Copeland, 1981). At Stations 9 and 10 inputs of dissolved Cu to the surface waters are the likely explanation for the two high values observed. Two types of addition processes for copper are possible. One relates to the increasing copper solubility with increasing pH; the second one relies on

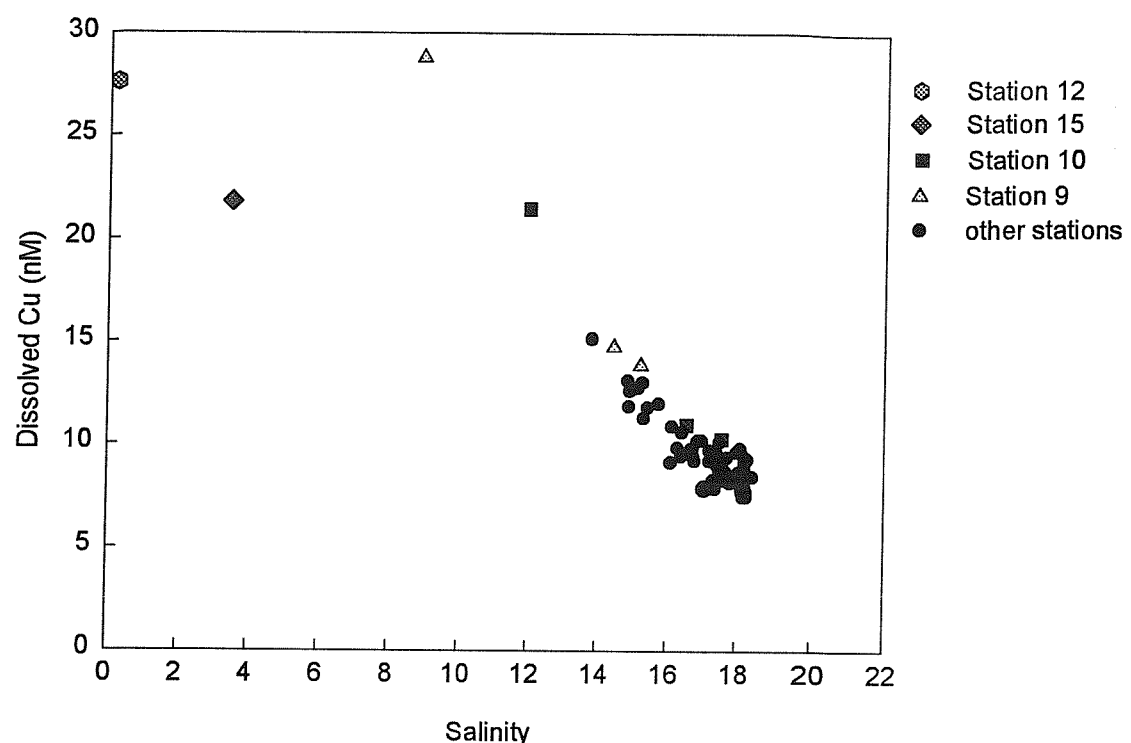


Fig. 6.21: Dissolved Cu plotted versus salinity

the desorption of the large fraction of exchangeable Cu associated with high river discharge as a result of dilution, ionic strength, and cation competition (Windom *et al.*, 1983). The second mechanism is likely to be dominant in the lower salinity region, and hence contribute significantly to the mid-estuary addition. SPM concentrations vary with the Danube river flow and 50 % of total particulate Cu in the Danube River (17 nM) belongs to the available fraction and may potentially be desorbed during mixing with Black Sea water. Photoreduction of Mn- and Fe- oxides in surface water may also release adsorbed Cu. At Station 9, other metals (Co, Pb, Ni, Cd, Zn) show higher concentrations in surface water and may also be affected by dissolution of oxides.

On the northwestern Black Sea shelf, Cu is mainly in the dissolved phase. A similar observation has been made in the Adriatic Sea at the end of the summer period (Chapter 4). There is also a good correlation between dissolved Cu and DOC ($r^2=0.992$), (Fig. 6.22). Kuwabara *et al.* (1989) observed a similar correlation in South San Francisco Bay and suggested the trend was a result of organic complexation. The dissolved Cu in South San Francisco Bay was subsequently found to exist predominantly as organic complexes (80–92 %), (Donat *et al.*, 1994). However, this good correlation could also be coincidental, reflecting that both constituents have the same riverine source and behave conservatively in the mixing zone. Copper concentrations show interesting spatial variations. At Stations 5 and 6, dissolved Cu concentrations tend to be higher above the thermocline, and this feature is associated with lower available particulate Cu concentrations and higher DOC concentrations. At Stations 4, 7, 19, 21 and 25 there are maxima in dissolved Cu concentrations at the thermocline, i.e. where remineralization of organic carbon has been shown to occur at the microscale level. Copper adsorbed on Mn- and Fe- oxides is likely to be released during dissolution of the host phase by remineralization processes. These maxima provide evidence that microbial or chemical degradation processes taking place at a molecular level can influence bulk concentrations of copper sufficiently as to produce a signal at a macroscopic level. At Stations 9, 10, 11, 17, 18 Cu concentrations in dissolved and available particulate phases are highest in surface water and decrease with depth. This reflects the strong riverine inputs. A major fraction of the total Cu (58 %) is delivered to the northwestern Black Sea coastal environment in the particulate form. Around 25 % of the

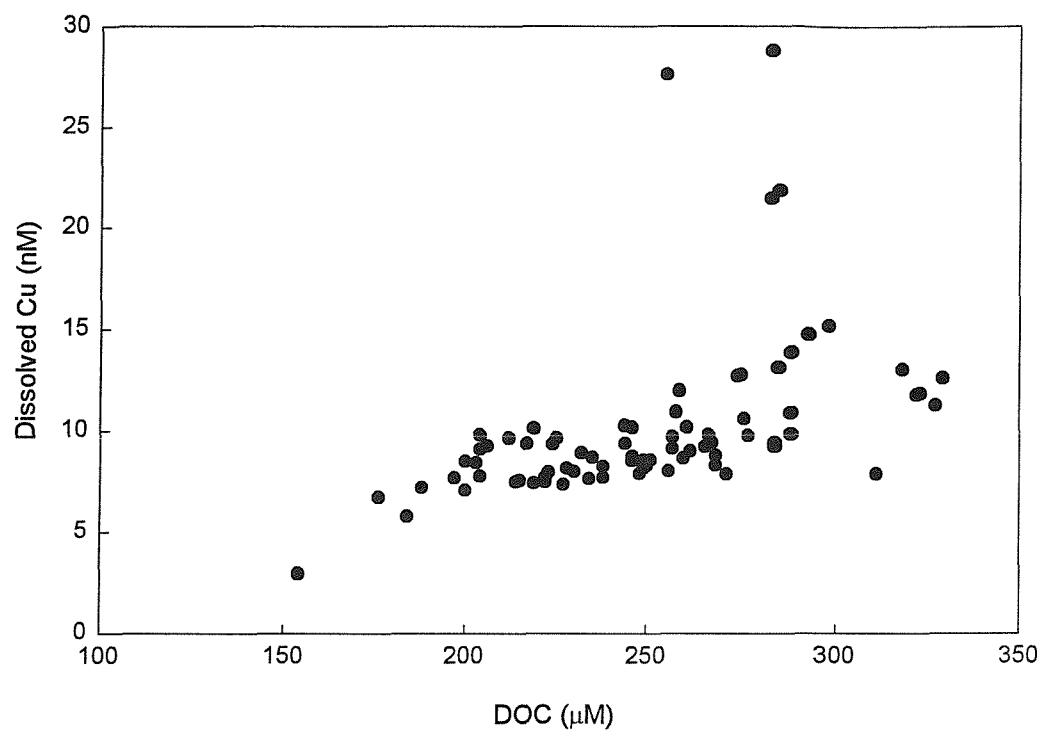


Fig. 6.22: Dissolved Cu plotted versus DOC

total Cu pool is present in the reactive particulate fraction and may be released to the dissolved phase by desorption during mixing with seawater or by dissolution of Mn- and Fe- oxides. Concentrations of Cu at the northern limit of the study area (Stations 0 and 1) are lower than in the area of direct riverine influence and vary between 8 and 9 nM for the dissolved phase and between 0.05 and 0.10 nM for the available particulate phase.

6.5.6 Nickel

Dissolved Ni concentrations in the North Western Black Sea shelf vary between 11 and 16 nM (Figs. 6.23a and 6.23b). The concentrations are generally higher than in the Western Mediterranean Sea (2 - 4 nM), (Tankéré *et al.*, 1995) and the Northern Adriatic Sea (6 - 22 nM) (Tankéré and Statham, 1996). Available particulate Ni concentrations in the North Western Black Sea vary between 3 and 36 µg/g. The residual fraction was below the detection limit. These concentrations tend to be higher than in the Western Mediterranean Sea (0.8 - 22 µg/g).

At a majority of stations dissolved Ni concentrations tend to be lower in surface water than in deeper water whereas available particulate Ni concentrations show the reverse. Available particulate Ni is significantly correlated to total particulate Fe ($r^2=0.81$) and the higher concentrations in surface water reflect riverine inputs. Higher dissolved Ni concentrations near the bottom may be due to benthic inputs. Westerlund *et al.* (1986) found enrichment of Ni in pore waters relative to ambient seawater in Gullmarsfjorden (Sweden) whereas a depletion was observed for Cu, Cd and Zn. Previous studies have shown that dissolved Ni tends to be one of the most conservative metals during estuarine mixing (Windom *et al.*, 1988; Shiller and Boyle, 1991; Althaus; 1992). The Ni-salinity plot (Fig. 6.24) is linear over the salinity range 0 to 14 suggesting conservative mixing between Danube River Water and Black Sea Water in surface layer. This relationship breaks down at salinities higher than 15 where it gives way to a highly diffuse data swarm. Although scattered, most of the data points lie above the mixing line suggesting inputs of dissolved Ni to the water column. Just as nickel may be adsorbed onto Mn- and Fe- oxides, it may equally be transferred from the particulate to the dissolved phase when reduction of Mn- and Fe-

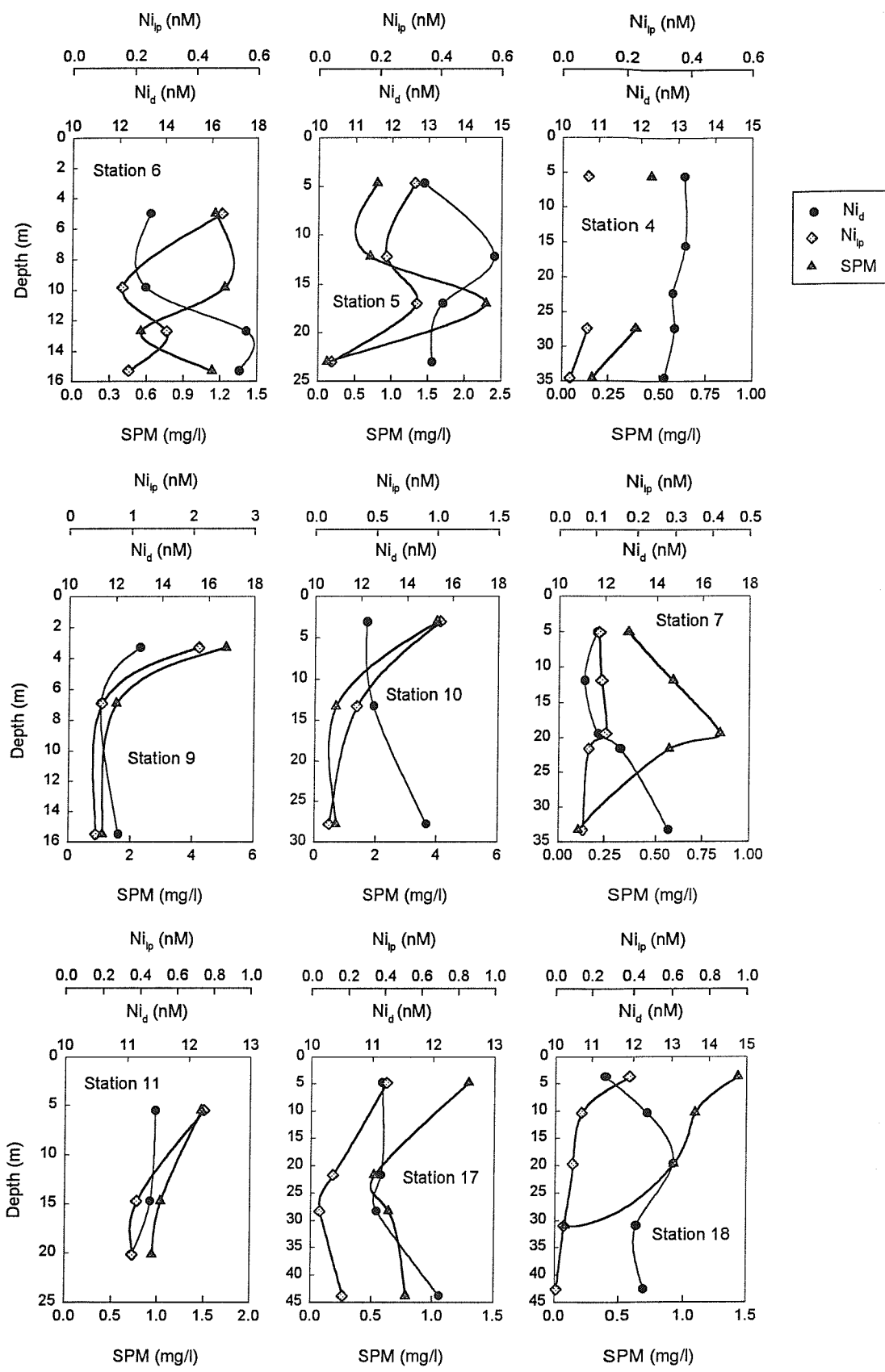


Fig. 6.23.a: distributions of dissolved Ni (Ni_{d}) and leachable particulate Ni (Ni_{lp}) at Stations 6, 5, 4, 9, 10, 7, 11, 17 and 18

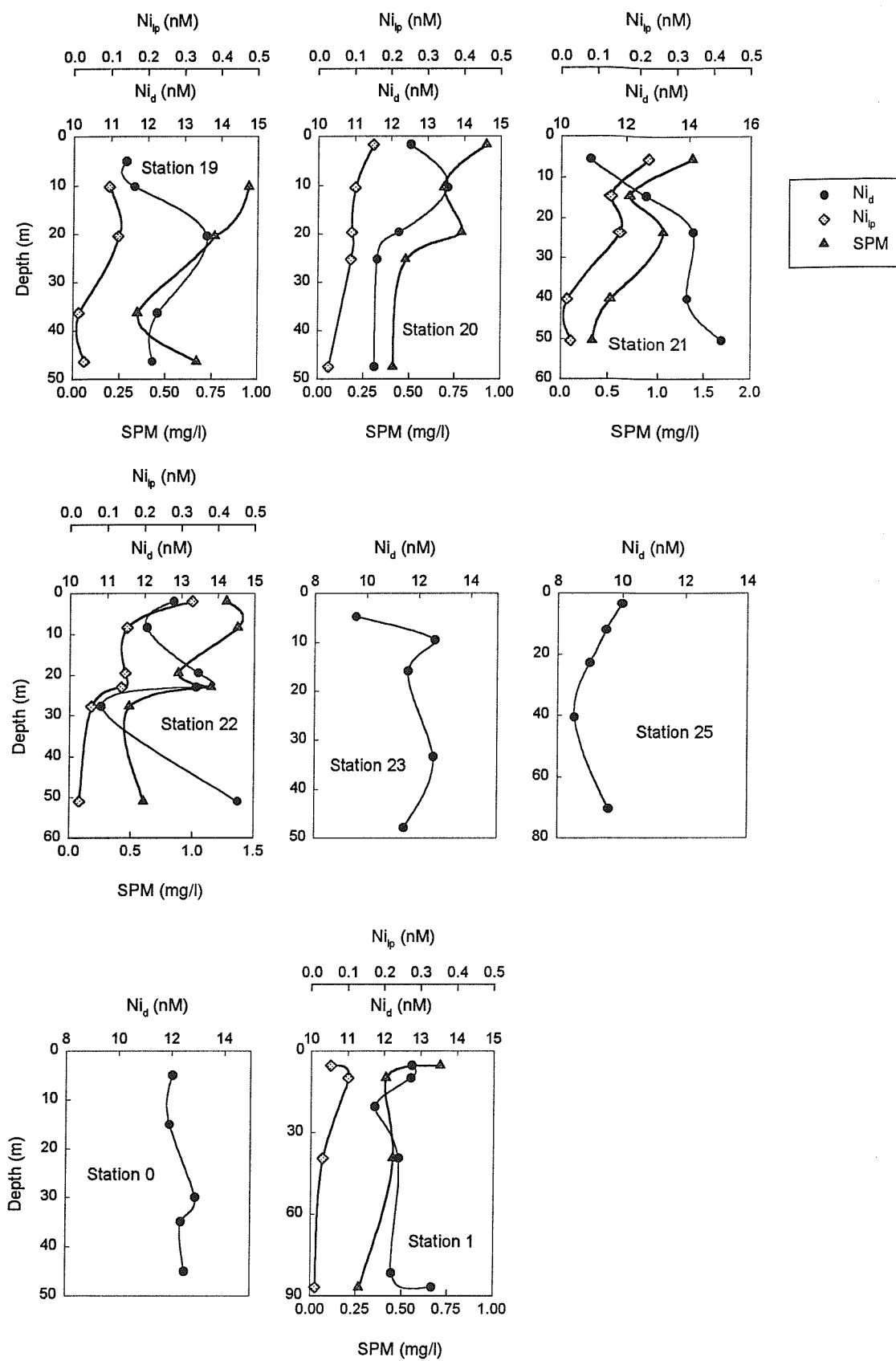


Fig. 6.23.b: Distributions of dissolved Ni (Ni_d) and leachable particulate Ni (Ni_{lp}) at Stations 19, 20, 21, 22, 23, 25, 0 and 1

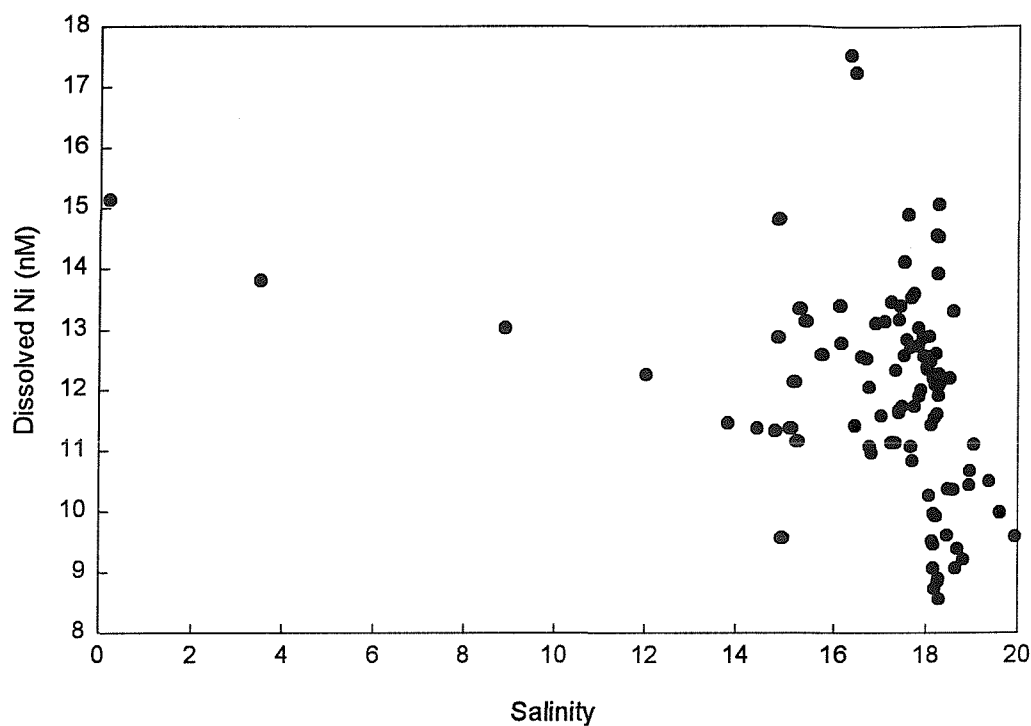


Fig. 6.24: Dissolved Ni plotted versus salinity

oxides occurs under suboxic conditions at the sediment-water interface. In the northwestern Black Sea, $98.5 \pm 1.2\%$ of total Ni is in the dissolved forms. The partitioning between dissolved and particulate forms in the North Western Black Sea is different from that in the Danube River water where 71 % of total Ni is present in the particulate phase. The available fraction of Ni in river particles represents 18 % of the total and could be transferred to the dissolved phase by desorption upon mixing between fresh water and Black Sea water although the conservative behaviour for Ni during mixing between the Danube River water and the Black Sea water suggests only small effects of this process on concentrations.

6.5.7 Cadmium

Dissolved Cd concentrations in the North Western Black Sea vary between 0.033 and 0.165 nM; available particulate Cd concentrations vary between 0.48 and 6.27 $\mu\text{g/g}$ (Figs. 6.25.a and 6.25.b). These concentrations are higher than those reported by Tankéré *et al.* (1995) for the Mediterranean Sea (dissolved Cd: 0.27-0.078 nM; particulate Cd: 0.09-2.64 $\mu\text{g/g}$) but lower than those reported by Tappin *et al.* (1995) for the North Sea (dissolved Cd: 0.095-0.661 nM; particulate Cd: 0.77-7.75 $\mu\text{g/g}$).

Dissolved Cd concentrations tend to be lower in surface water than in deeper water at nearly all Stations, in line with the known 'recycled element' behaviour of Cd. Dissolved Cd is depleted in surface waters through active uptake by phytoplankton and/or adsorption onto particles. The concentrations increase with depth as sinking detrital particles undergo microbial decomposition of their organic phases, and/or dissolution of their inorganic mineral phases. Removal of Cd by plankton from shelf seawaters has been documented by Martin and Knauer (1973) and Jickells (1986). A seasonal depletion of dissolved Cd and phosphate in the euphotic zone in Funka Bay was accompanied by a simultaneous increase in the concentration of Cd in the flagellate phytoplankton present in this zone (Noriki *et al.*, 1985; Abe and Matsunaga, 1988; Abe *et al.*, 1990). The Cd increase with depth may also be enhanced by benthic inputs. Westerlund *et al.* (1986) show that Cd can have a benthic source not directly related to the degradation of organic matter. Whatever the

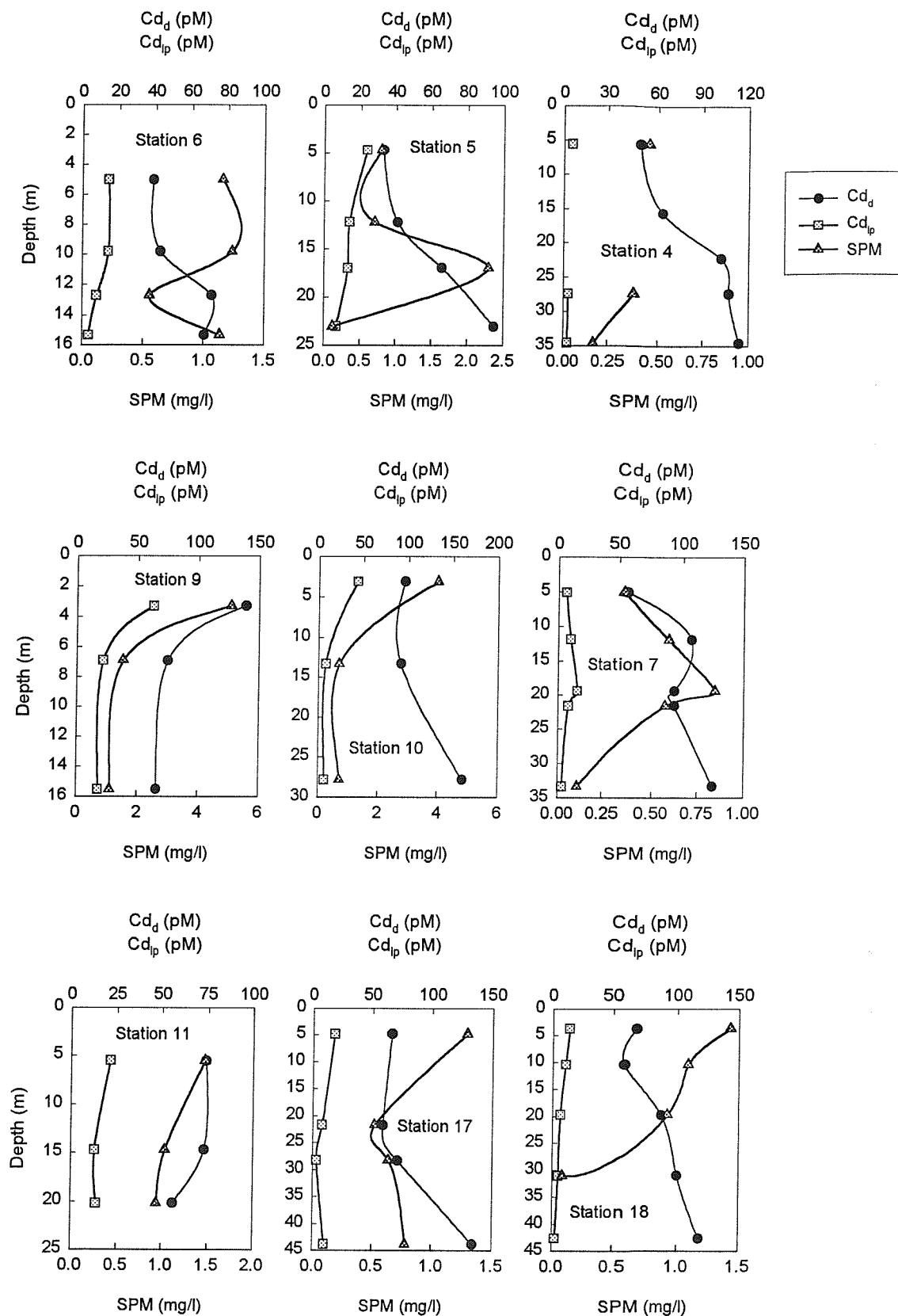


Fig. 6.25.a: Distributions of dissolved Cd (Cd_d) and leachable particulate Cd (Cd_{lp}) at Stations 6, 5, 4, 9, 10, 7, 11, 17 and 18

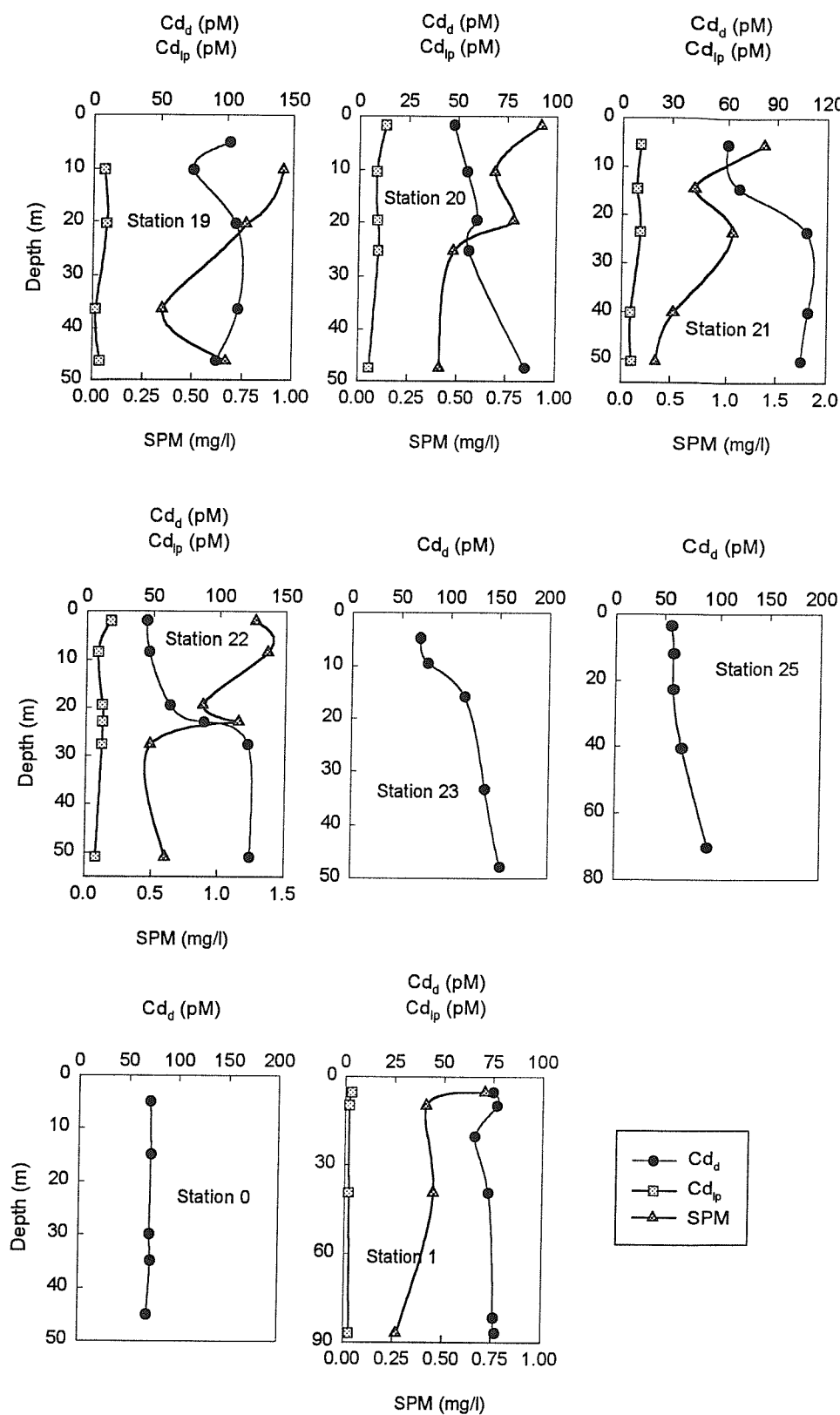


Fig. 6.25.b: Distributions of dissolved Cd (Cd_d) and leachable particulate Cd (Cd_{lp}) at Stations 19, 20, 21, 22, 23, 25, 0 and 1

source, the solubilization of Cd mainly depends on the oxygen flux across a thin oxic layer covering the sediment surface. Available particulate Cd concentrations in water tend to be higher in surface water. This probably reflects sorption/surface complexation of the metal at sites on the outer surface of biological cells.

At Stations 9, 11 and 7 the dissolved Cd distribution differs from above. At Stations 9 and 11, dissolved Cd concentrations tend to be higher in surface water. This is mainly due to riverine inputs from the Danube River and to atmospheric inputs. Chester and Murphy (1990) compiled reports showing that the atmospheric flux of some metals (Cd, Zn, Pb) to surface coastal waters can equal or exceed their riverine flux. At Station 7, there is a maximum above the thermocline which is possibly related to mineralization processes. This maximum is associated with maxima in dissolved Mn and Fe, $\text{NO}_2^- + \text{NO}_3^-$, NH_4^+ . Cadmium which have been adsorbed onto Mn– and Fe– oxides, will be released along side Mn and Fe following reduction of Mn– and Fe– oxides.

The Cd–salinity diagram (Fig. 6.26) shows a maximum at low salinity (3.5); this is possibly due to mobilization from riverine particulate matter when river water mixes with seawater (Edmond *et al.*, 1985; Elbaz-Poulichet *et al.*, 1987; Comans and Van Dijk, 1988). The scatter at high salinity (18-21) reflects inputs from sinking detrital particles which undergo microbial decomposition of their organic phases and/or dissolution of their inorganic mineral phases, and benthic inputs.

In some studies, the vertical distribution of Cd correlates closely with that of phosphate (Bruland, 1980; Frew and Hunter, 1992), suggesting that Cd follows the cycle of the formation and decomposition of organic soft tissues. A good correlation between Cd and phosphate has been observed at most stations. However, at some locations (Stations 10, 11, 17, 18), the distribution of Cd does not show such a correlation. High concentrations of phosphate in surface waters could be due to some local riverine inputs; and processes other than recycling (such as benthic inputs) may also affect the distribution of Cd.

6.5.8 Zinc

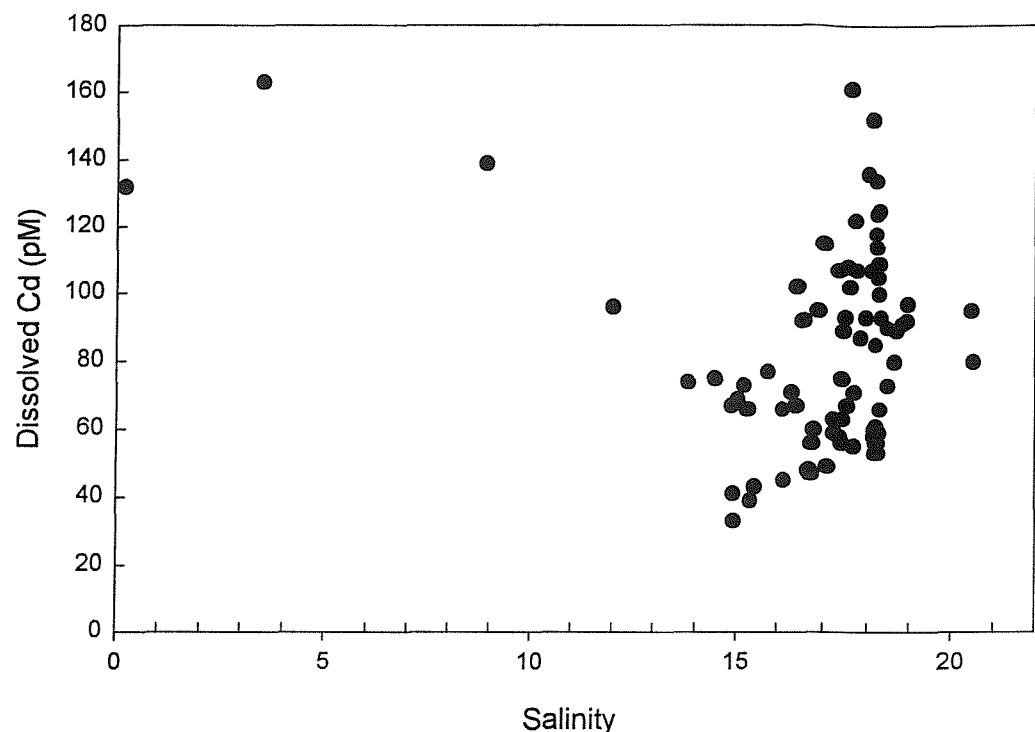


Fig. 6.26: Dissolved Cd plotted versus salinity

Dissolved Zn concentrations in the North Western Black Sea vary between 1 and 8 nM (Figs. 6.27.a and 6.27.b). These concentrations are similar to those reported by Tankéré *et al.* (1995) for the Western Mediterranean Sea (1-8 nM) but are lower than those reported for the North Sea by Tappin *et al.* (1995). Available particulate Zn concentrations in the North Western Black Sea vary between 13 and 358 µg/g and are higher than those reported by Tankéré *et al.* (1995) for the Western Mediterranean Sea (10-103 µg/g) but similar to those reported by Tappin *et al.* (1995) for the North Sea.

The vertical distribution of Zn is generally similar to that of Cd and correlates well with Si. Common trends include lower dissolved concentrations in surface water than in deeper water, combined with higher available particulate concentrations in surface water than in deeper water. When taken in combination, these trends indicate the nutrient-like behaviour of Cd and Zn. As with Cd, the higher available particulate Zn concentrations in surface water are again attributed to active uptake by phytoplankton (Hudson and Morel, 1993) and/or adsorption onto biogenic particles. Removal of dissolved Zn by plankton from shelf sea waters has been documented by Bruland and Frank (1983). The vertical distribution of Zn correlates closely with that of silicate (Fig. 6.28). Bruland *et al.* (1978) suggested that Zn is involved in a regeneration cycle of the kind that affects opal (silicate) and calcium carbonate. The higher concentrations in the dissolved phase near the bottom are also thought to be caused by benthic inputs (Westerlund *et al.*, 1986); however, at some stations, there is a depletion near the bottom which is possibly due to adsorption of Zn onto resuspended bottom sediments. A slight increase in dissolved Zn in surface water was observed at some stations (6, 5, 4, 9, 19, 21, 1) and may be due to riverine or atmospheric inputs (Donat and Bruland, 1995).

6.6 Trace metals in the slope region of the north western Black Sea

6.6.1 Manganese

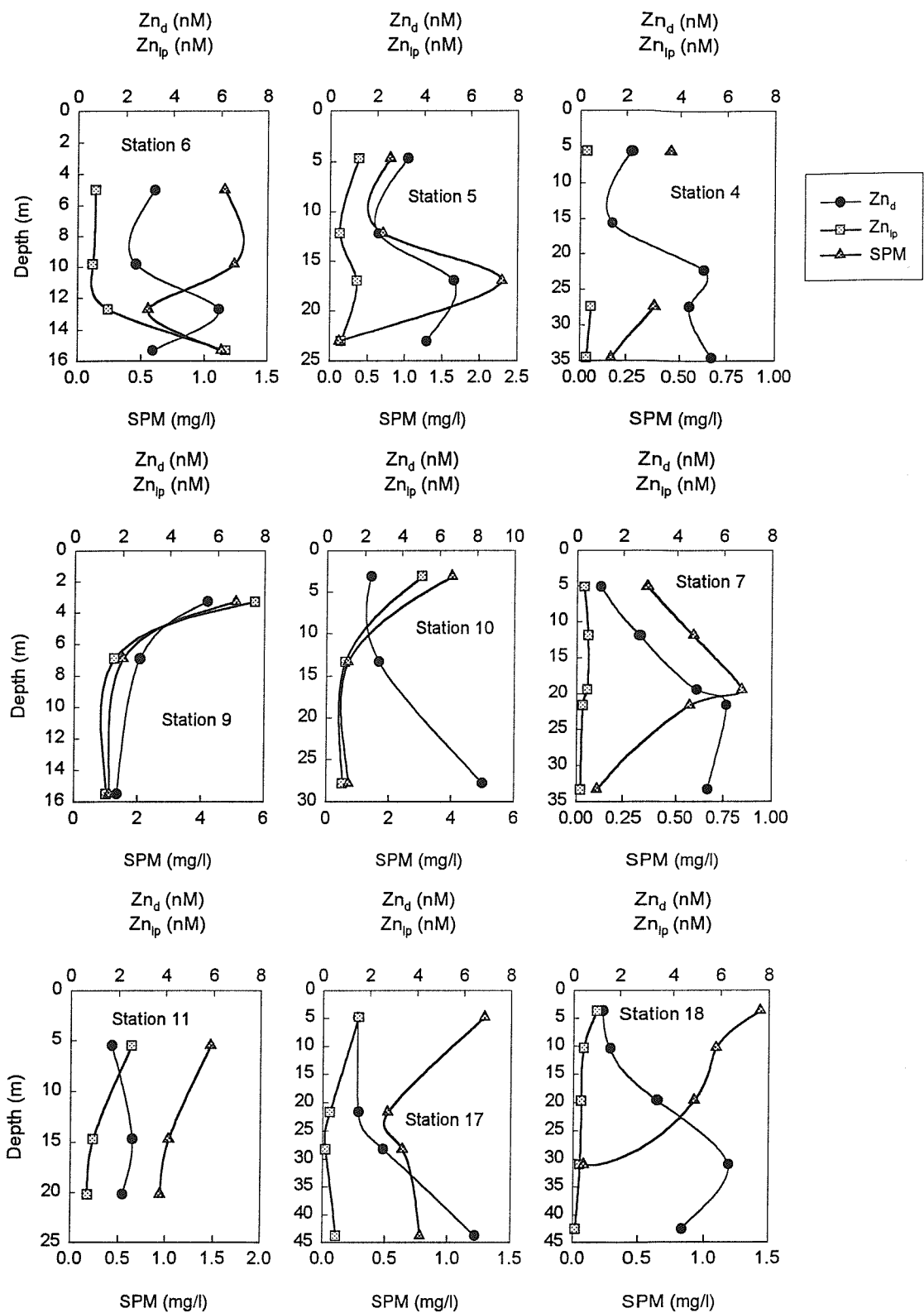


Fig. 6.27.a: Distributions of dissolved Zn (Zn_d) and leachable particulate Zn (Zn_{lp}) at Stations 6, 5, 4, 9, 10, 7, 11, 17 and 18

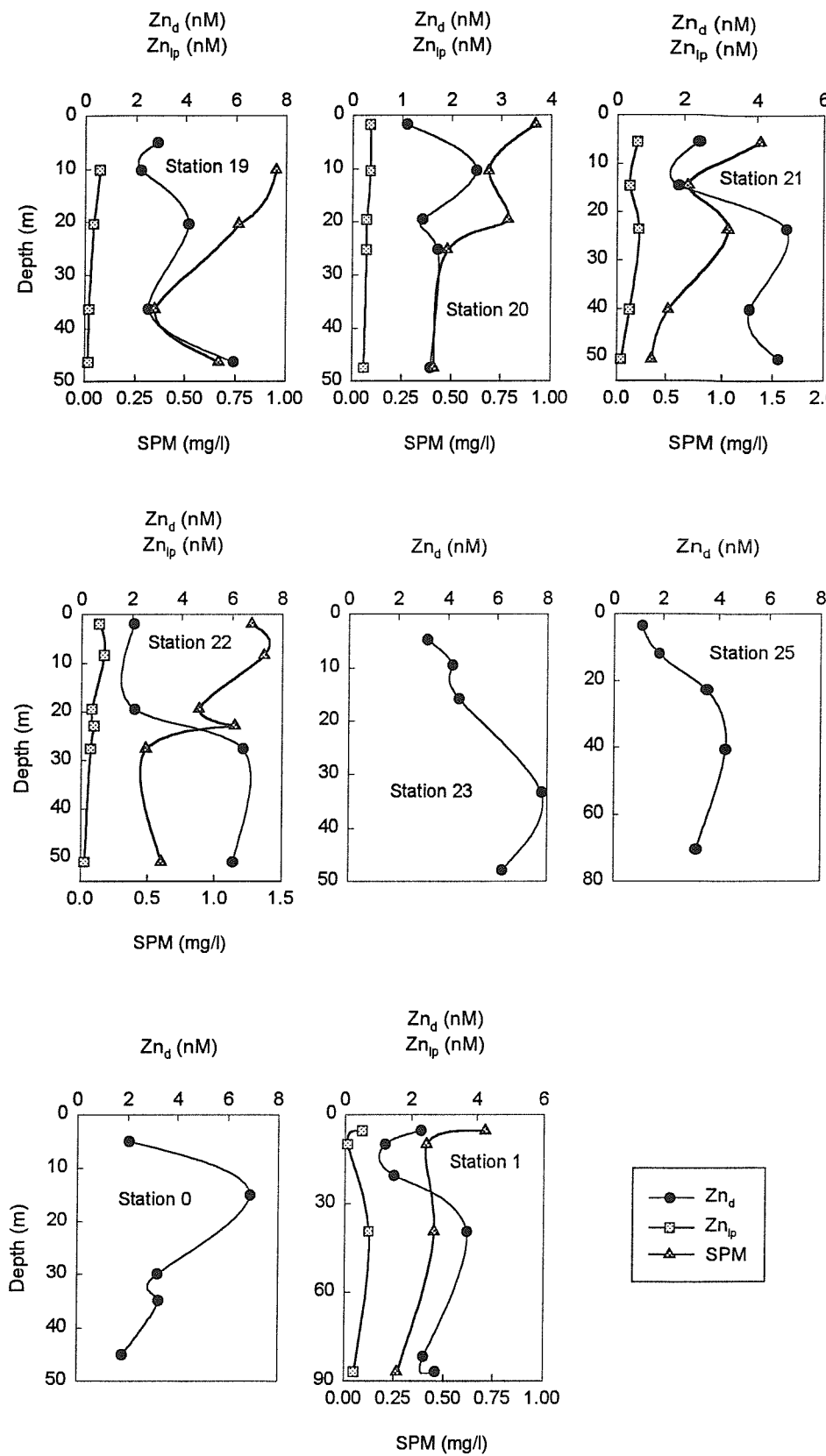


Fig. 6.27.b: Distributions of dissolved Zn (Zn_d) and leachable particulate Zn (Zn_{lp}) at Stations 19, 20, 21, 22, 23, 25, 0 and 1

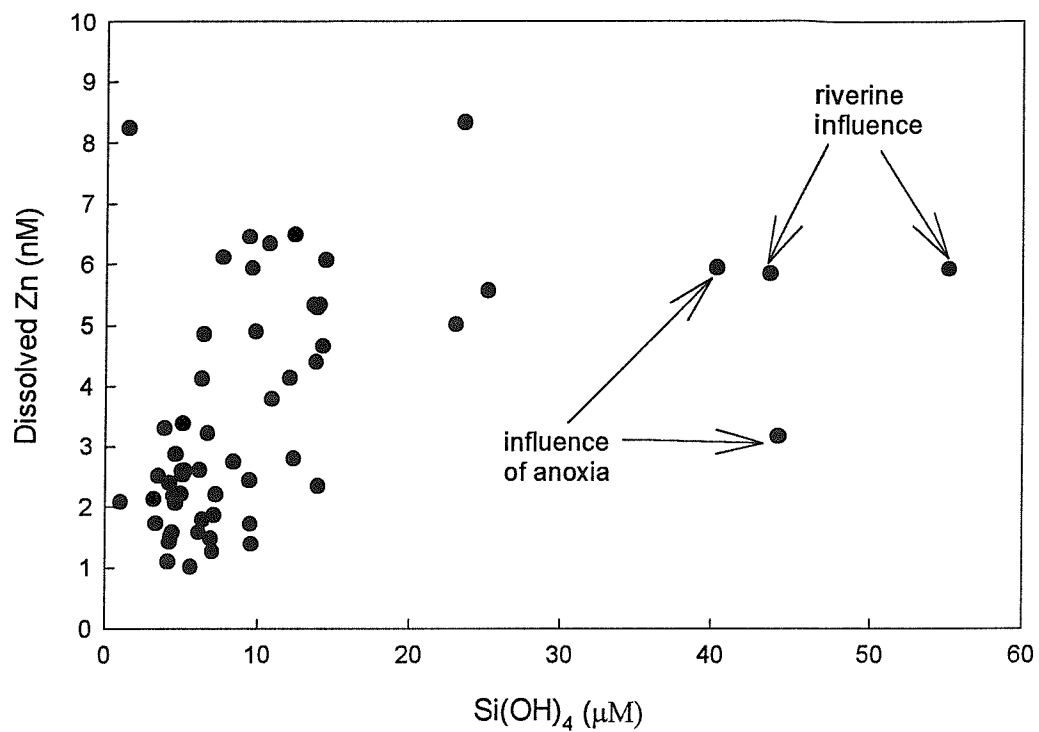


Fig. 6.28: Dissolved Zn plotted versus silicate

At Station 3, relatively high dissolved Mn concentrations (10 nM) are found in surface water and are possibly due to atmospheric inputs (Fig. 6.29). The concentrations decrease to reach a minimum of 1 nM between 60 and 110 m. Below 110 m, which is the upper limit of the redoxcline, dissolved Mn concentrations increase rapidly to reach a maximum at 190 m (8746 nM). Below 200 m, dissolved Mn concentrations decrease again with depth. At present, there is some uncertainty as to how much of the decrease is due to an inorganic control on the solubility of Mn and how much is due to a removal from the water column by sinking particles. The shape of the Mn maximum is controlled by a dynamic balance between the rates of diffusion and oxidation of Mn(II) and the rates of sinking and redissolution of solid phase MnO_x . Lewis and Landing (1991) found a similar vertical distribution for Mn in the central Black Sea but at a different depth, the redoxcline appearing at 70 m. When the data are plotted against density, the Mn maximum appears at the isopycnal 16.4 as found by Lewis and Landing (1991). Available and total particulate Mn was measured in the top 200 m of the water column. The profile shows a maximum in total particulate Mn (30 nM) at 130 m, above the dissolved Mn maximum. This distribution differs from the one reported by Lewis and Landing (1991) and Tebo (1991) who found 2 particulate maxima of similar magnitude coinciding with maxima in Mn(II) binding capacity. More than 90 % of the total particulate Mn occurs in the acetic acid leachable fraction. The removal of Mn(II) from solution is catalysed by microbial processes (e.g. Emerson *et al.*, 1982; Rosson *et al.*, 1984; Tebo and Emerson, 1986). Lewis and Landing (1991) established a vertical mixing model for dissolved Mn in the central basin of the Black Sea which yields removal rates consistent with measured bacterial Mn oxidation rates.

At Station 24, which is closer to the shelf, dissolved Mn concentrations vary between 8.2 and 8.6 nM in surface water. Below 16 m, concentrations decrease to a minimum. A maximum appears at 71 m, which may be due to lateral transport from the coast. Near the bottom, concentrations increase to 32 nM, this is possibly due to reduction of MnO_x . Total particulate Mn concentrations are below 10 nM in the upper 90 m then increase to reach a maximum near the bottom. The magnitude of this maximum (260 nM for the leachable fraction and 1100 nM for total particulate Mn) is much higher than those observed at Station 3 or at the shelf stations. Tebo (1991) found that the Mn(II) oxidation rates were 1–

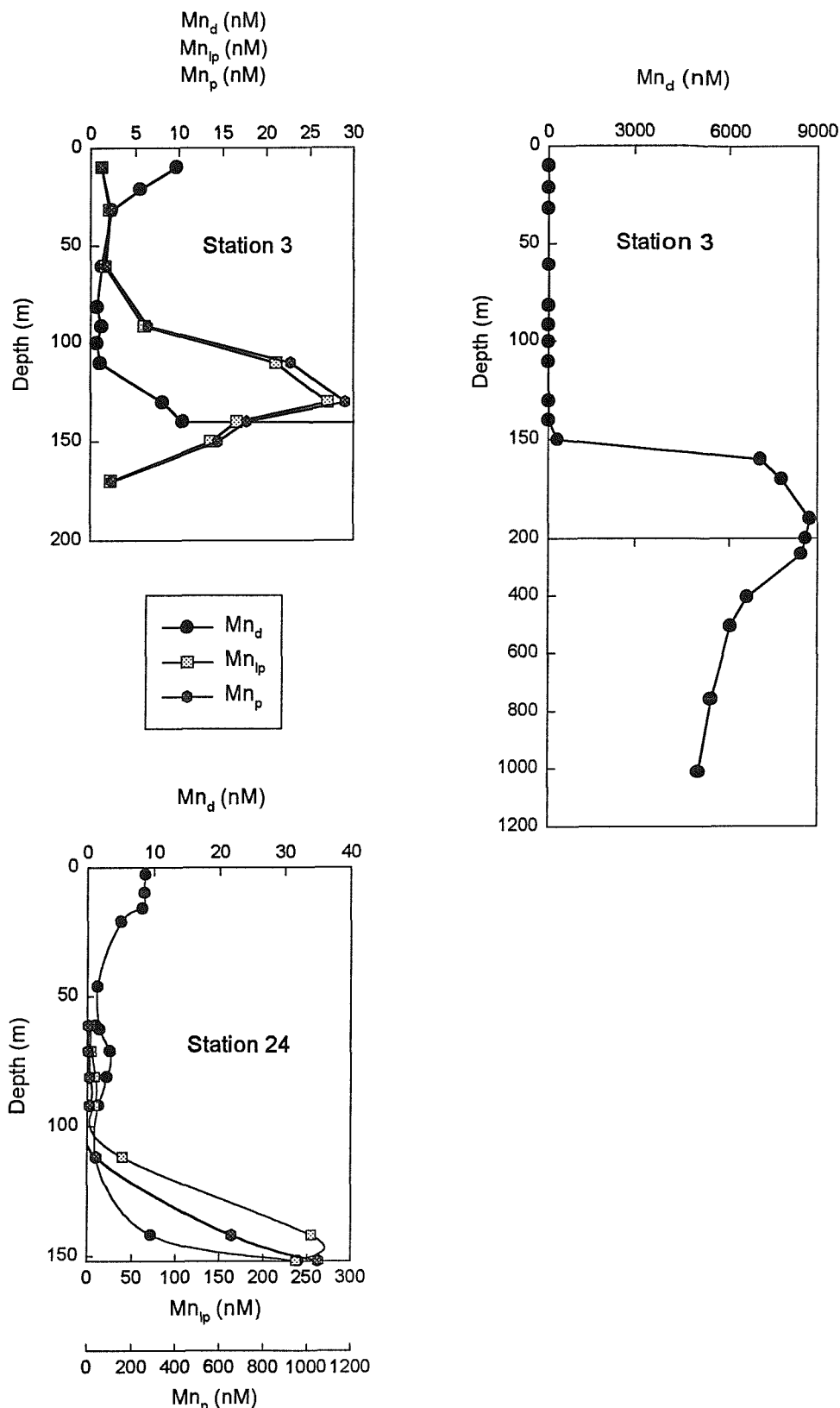


Fig. 6.29: Distributions of dissolved Mn (Mn_d), leachable particulate Mn (Mn_{lp}) and total particulate Mn (Mn_p) at Stations 3 and 24

2 orders of magnitude higher at a nearshore station than at a station in the central Black Sea. Variations in the rates with depth were due to differences in the biological (e.g. numbers and types of bacteria) and chemical (e.g. presence or absence of inorganic surfaces or reductants) components present in the water; rapid rates were generally a good indication of microbial catalysis.

Kempe *et al.* (1991) suggested that a “ manganese pump ” was operating in the Black Sea coastal waters to explain the transport process which produces vertically highly structured Mn-rich particle layers with intensities decreasing from the coast. A similar model was proposed to explain Mn export from the St Lawrence estuary (Yeats *et al.*, 1979). The argument runs as follows: Seasonal variability of the depth of the pycnocline and the associated chemocline causes the surface sediments found at the same depth to be exposed to fluctuating redox conditions. One of the consequence of these fluctuations is that they periodically expose sediments to more reducing and higher saline water. This water replaces the more oxidizing pore waters of surface sediments, mobilizing whatever oxidized manganese is present or has recently been deposited by settling macroflocs. In the second part of this seasonal cycle, which is typical of the winter regime, the pycnocline dips down and the surficial sediments of the sea bed are once again exposed to oxic conditions. Upon mixing with the more oxic ambient water, particles of MnO_x are formed which are subject to lateral transport by the coastal current. Since these fine-grained particles settle very slowly they can spread considerably downcurrent from their coastal source.

6.6.2 Iron

At Station 3, the controls on the concentration of Fe are qualitatively similar to those for Mn and, not surprisingly, result in a similar distribution. However, a deeper maximum is observed for dissolved Fe (292 nM at 253 m) as a consequence of the more rapid oxidation of Fe in the redoxcline combined with the high degree of insolubility of FeS below the redoxcline (Fig. 6.30). In surface water dissolved Fe concentrations are relatively low and vary between 0.8 and 3.0 nM. Lewis and Landing (1991) found that colloidal and organically-complexed Fe species can account for 10–30% of the total dissolved Fe in the

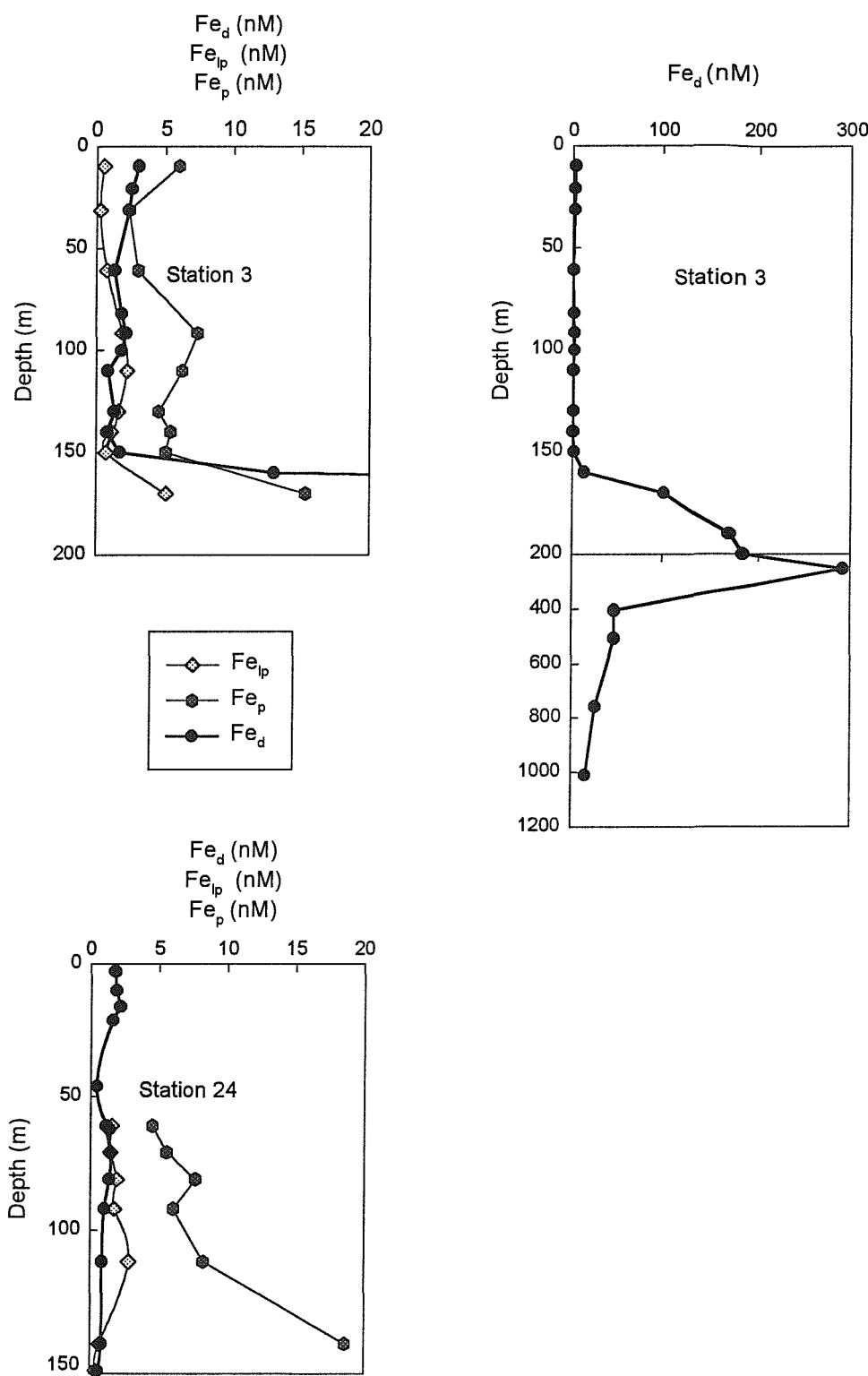


Fig. 6.30: Distributions of dissolved Fe (Fe_d), leachable particulate Fe (Fe_{lp}) and total particulate Fe (Fe_p) at Stations 3 and 24

oxic zone while colloidal Fe-sulfides account for 30–60% of the total in the mid depth dissolved Fe(II) maximum. Total and available particulate Fe concentrations were measured in the top 170 m. Total concentrations vary between 2.3 nM and 15.3 nM with a maximum at 110 m (7.4 nM) and a steady increase to a value of 15.3 nM at 170 m. The available fraction represents 9 % of total particulate in surface water; this percentage varies between 14 and 35 % in deeper water. The maximum in total particulate Fe concentration at 100 m –possibly the result of advective transport from the coast – corresponds to the FPL described by Kempe *et al.* (1991). The increase in total particulate Fe at 170 m and the relatively high concentrations (5.0–6.2 nM) between 100 and 150 m compared to the subsurface water (2.3 nM) are possibly due to the spontaneous oxidation of Fe which diffuses from anoxic waters. The distribution of Fe at Station 3 is similar to that of Lewis and Landing (1991) in the central Black Sea, but maxima in dissolved and particulate Fe appear in deeper water due to the deeper redoxcline nearshore than in the central basin caused by sloping isopycnal surfaces.

At Station 24, dissolved Fe concentrations are relatively low and vary between 0.42 and 2.12 nM. Total particulate Fe concentrations vary between 4.5 and 24.6 nM. A maximum is observed at 80 m that may be due to advective transport from the shelf. Near the bottom, the sharp increase is possibly due to resuspension of bottom sediments and/or precipitation of Fe(II) which diffuses from the sediment–water interface. The available fraction varies between 25 and 35 % of total particulate Fe between 60–110 m and decrease to 2–4 % near the bottom suggesting that the high particulate Fe concentration near the bottom is likely due to resuspension.

6.6.3 Trace elements: Co, Pb, Cu, Ni, Cd and Zn

At Station 3, concentrations of dissolved Co, Pb, Cu and Ni in the oxic layer are lower than those reported in the northwestern Black Sea (Table 6.3). The Cd concentrations are similar throughout the Black Sea. Compared to the Mediterranean Sea, dissolved metals (Cd, Ni, Cu, Pb and Co) have generally higher concentrations in the oxic layer at Station 3, although concentrations of Co and Pb can also be lower in some cases. This probably

reflects the strong influence of river water in the Black sea surface water. Dissolved Zn concentrations at Station 3 are similar to the concentrations reported for the Mediterranean Sea.

Table 6.3: Concentrations (nM) of dissolved Co, Pb, Cu, Ni, Cd and Zn in Black Sea surface waters (Station 3) and comparison with Mediterranean surface waters and northwestern Black Sea.

Metal	northwestern Black Sea	Black Sea (Station 3)	Mediterranean Sea (*)
Co	0.04–1.89	0.024–0.340	0.040–0.146
Pb	0.03–0.61	0.024–0.186	0.073–0.100
Cu	2.9–28.8	1.64–7.87	1.2–1.9
Ni	8.6–17.5	8.6–11.9	2.1–4.0
Cd	0.033–0.161	0.071–0.158	0.036–0.076
Zn	1–45	0.9–6.9	1.50–7.05

* (Tankéré *et al.*, 1995)

At Station 3, the distribution of Co closely resembles that of Mn throughout the upper water column and redoxcline, probably reflecting coupling through scavenging although an independent redox behaviour of Co is also possible; the marked decrease in concentration in the anoxic layer reflects efficient removal by scavenging or insoluble sulphide formation (Fig. 6.31). For Cu, Zn, Cd and Pb, dissolved concentrations are very low in the anoxic layers as a result of control of solubility by formation of, or association with, solid sulphide phases (Fig. 6.31). In the oxic layers, the concentrations of Zn, Cd and Pb show features characteristic of open sea profiles observed elsewhere but the increase in concentration of Zn and Cd with depth is sharply reversed around the top of the redoxcline through the existence of the sink in the anoxic layers. For Cu, the upper water column distribution shows that there is less of a recycled behaviour for Cu than for Cd and Zn and the distribution appears to be governed primarily by this sink function. Average concentrations of dissolved Ni are similar in the oxic and anoxic layers but there is evidence of removal within the redoxcline (Fig. 6.31). These observations are similar to those of Brewer and Spencer (1974), Haraldsson and Westerlund (1988) and Lewis and Landing (1991).

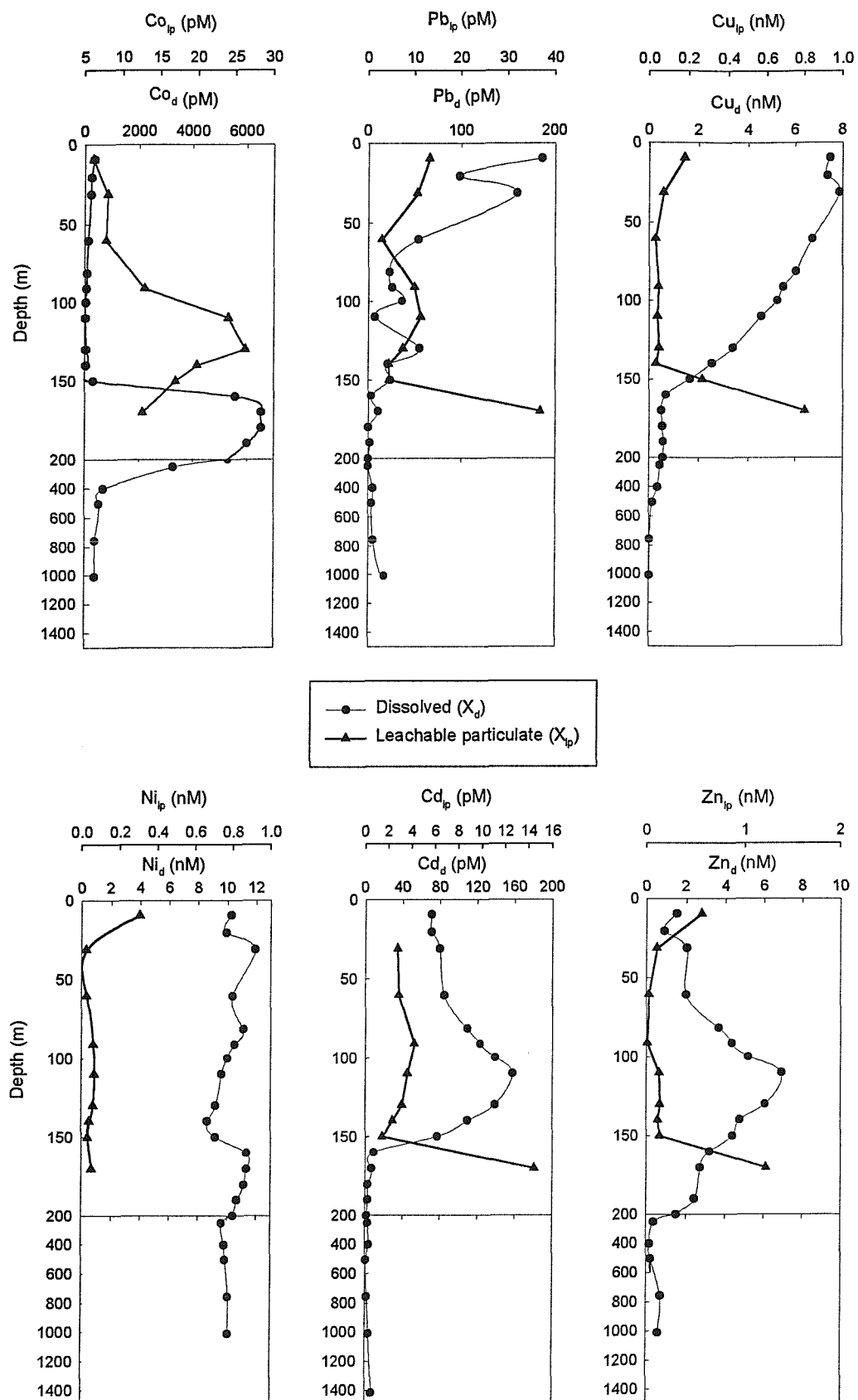


Fig. 6.31: Distributions of dissolved and leachable particulate Co, Pb, Cu, Ni, Cd and Zn at Station 3

Available particulate Co and Pb concentrations are lower at Station 3 than in the northwestern Black Sea (Table 6.4). Cobalt and Pb are particulate reactive metals and these observations reflect the low SPM concentrations at Station 3. Biological uptake is the main process which could affect the particulate distribution of Cu, and the higher available particulate Cu concentrations in the northwestern Black Sea than Station 3 reflect the relatively high rate of primary production in the northwestern Black Sea shelf waters. Available particulate Cd concentrations are similar throughout the Black Sea. Available particulate Zn and Ni concentrations are higher in surface water at station 3 than in the northwestern Black Shelf reflecting atmospheric inputs. Particulate trace elements (Co, Ni, Cu, Zn and Cd) have generally higher concentrations in the Black Sea (Station 3) than in the Mediterranean Sea, although bottom end of range is lower in the case of Zn.

Table 6.4: Concentrations (µg/g) of leachable particulate Co, Ni, Cu, Zn, Cd and Pb in Black Sea surface waters (Station 3) and comparison with the Mediterranean surface waters and the northwestern Black Sea. (* Tankére et al., 1995)

Metal	Black Sea (Station 3)	Northwestern Black Sea	Mediterranean Sea (*)
Co	1.6–8.7	0.38–39	1.33–1.91
Ni	7–78	2–36	2.6–11.2
Cu	12–49	5–225	4–32
Zn	6–600	12–359	53–77
Cd	1.4–6.1	0.34–6.3	0.17–1.28
Pb	10–16	2.4–121	1.4–15.2

At Station 3, available particulate trace elements were measured throughout the top 170 m only. Cobalt, Ni, Pb and Cd, generally show a maximum concentration just above the redoxcline –which may be due to adsorption onto Mn– and Fe– oxides– and a minimum at the redoxcline. For Pb and Cd, there is a sharp increase below this minimum. For Cu and Zn, available particulate concentrations are low in the oxic layer and increase at the redoxcline. Increases in available particulate Pb, Cd, Cu and Zn at the redoxcline probably reflect the enrichment of these metals in biological matter (Haraldsson and Westerlund, 1991). Copper and Zn are essential elements for most organisms while Cd can be taken up by analogy with essential elements, with the consequence that its nutrient-like cycling resembles that of phosphate. A significant amount of particulate Pb can also be bound to bacteria (Haraldsson and Westerlund, 1991)

At Station 24, dissolved Co, Pb, Cd, Cu, Zn and Ni show similar distributions to those in the oxic layer of Station 3 (Fig.6.32). Differences are more pronounced in the particulate fraction whose trace element composition was measured between 60 m depth and the bottom. For Ni, Cu and Zn, available particulate concentrations increase below 110 m to reach maxima near the bottom. These maxima could be due to resuspension and/or adsorption onto Mn- and Fe- oxides since total particulate Mn and Fe have relatively high concentrations. Available particulate Co shows a similar distribution to that of Station 3 in the oxic layer, with a maximum which coincides with that of total particulate Mn suggesting coupling between the two elements. Available particulate Pb and Cd profiles show maxima between 60 and 110 m, with a depletion near the bottom. The maxima at 80 m could be due to adsorption onto Mn- and Fe- oxides which have been advected from the shelf.

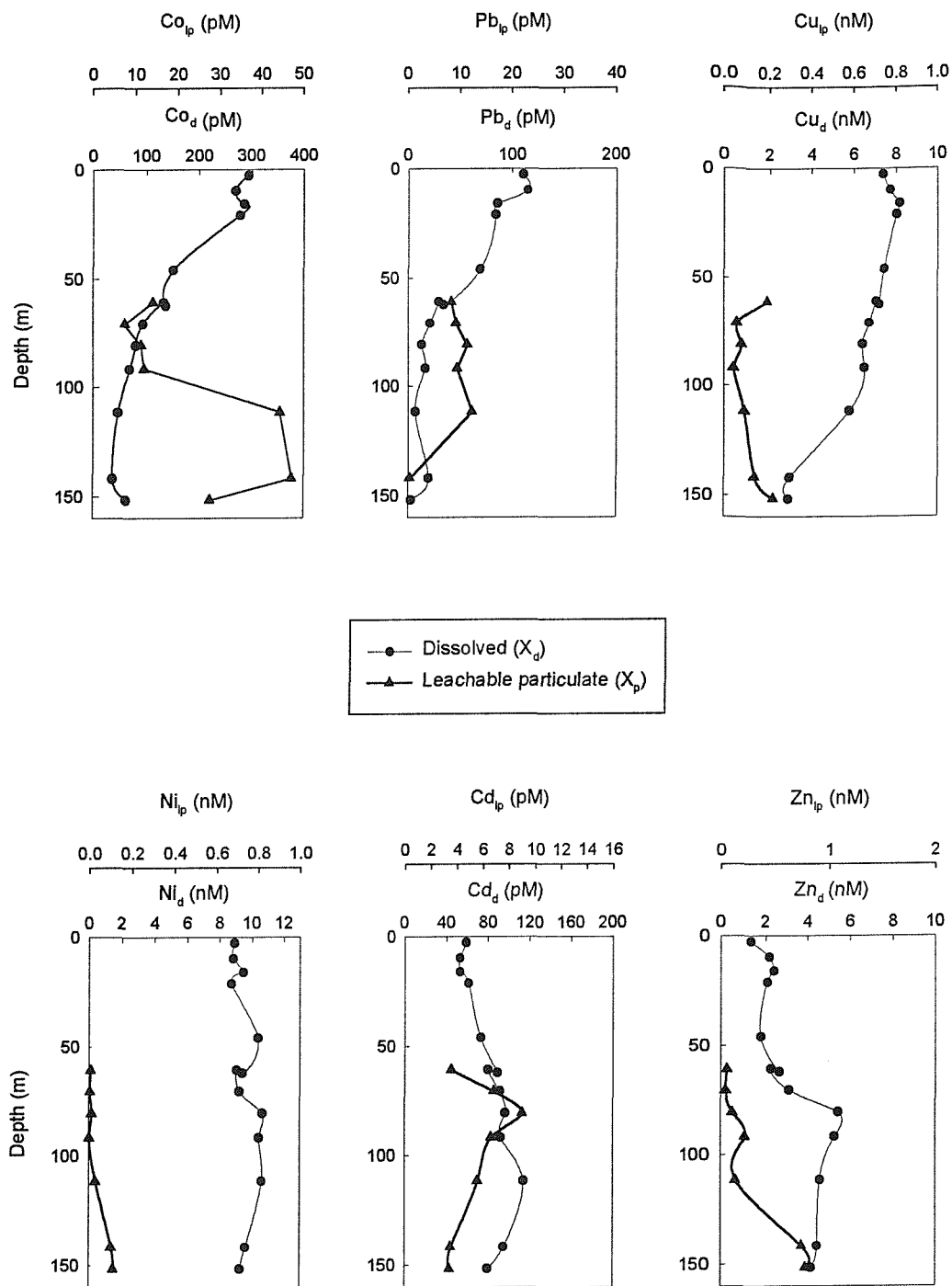


Fig. 6.32: Distributions of dissolved and leachable particulate Co, Pb, Cu, Ni, Cd and Zn at Station 24

CHAPTER 7

SUMMARY AND CONCLUSIONS

7.1 Introduction

The principal aims of this work were to study the distributions and geochemical behaviour of trace metals in the Adriatic Sea and the Black Sea. The findings for the Adriatic and Black Sea system have been described and evaluated in Chapters 4 and 6 respectively. In Chapter 5, a mass balance of trace metals for the Adriatic has been presented. In the present chapter, the more important aspects of the behaviours of trace metals in both environments are summarised. A comparison of metal concentrations and loadings between the Adriatic and the Black Sea has been made. Suggestions are made for further work which can provide a fuller understanding of the biogeochemical cycles of trace metals in the Adriatic and Black Sea regions.

7.2 The Adriatic Sea

Dissolved and total particulate Mn, Fe, Pb, Zn, Cu and Ni, and dissolved Co and Cd were measured on samples collected at 3 stations in the northern Adriatic Sea during 4 surveys representing 4 different seasons in 1994 and 1995, and at 2 stations in the central Adriatic Sea in June 1994. Pore water samples were also collected and analysed for Mn and Fe. This work was carried out within the EUROMARGE-AS project (1994–1996).

In the northern Adriatic Sea, the distribution of Mn and Fe vary seasonally and depends on the reduction-oxidation potential in the water column. Fluctuations of the reduction-potential in the water column are related to the biodegradation of the organic matter produced during bloom periods. Deposition of the spring bloom, although the largest organic carbon input event of the year, does not cause substantial water column anoxia, partly because of winter ventilation and the high oxygen concentrations in cold winter water. In spring, dissolved Mn and Fe concentrations were slightly higher than winter

concentrations. Particulate Mn and Fe concentrations were high (2-100 nM, 500-4000 nM respectively) particularly near the bottom due to resuspension. In summer, the stratification of the water column increased leading to accumulation of biological material at the thermocline and a decline in oxygen concentrations below the thermocline. Dissolved Mn and Fe concentrations were increasing (respectively 10-200 nM, 1-20 nM) particularly at the thermocline where reduction occurred at a microscale level within the “marine snow”, and near the bottom where reduction of Mn- and Fe- solid phases occurred during remineralization of organic carbon at the sediment-water interface. Particulate Mn and Fe were also high near the bottom due to reprecipitation of Mn(II) and Fe(II) in presence of oxygen and to resuspension. In Autumn, some storms broke down the stratification of the water column, leading to inputs of fresh organic matter from the autumn bloom to the bottom which reduced oxygen levels significantly. Dissolved Mn and Fe concentrations in interstitial waters were highest at the surface of the core in September 1994. Particulate Mn and Fe concentrations were also high near the bottom due to precipitation, in the presence of oxygen, of Mn(II) and Fe(II) diffused from the sediment-water interface. In winter, mixing aerates the water column and sediment inducing relatively low concentrations of dissolved Mn and Fe. Particulate Mn and Fe concentrations were relatively high due to adsorption, resuspension and advective transport.

Trace metals (Co, Pb, Cu, Ni, Cd, Zn) were influenced by Mn and Fe cycling. The dissolved Co distribution was similar to that of Mn suggesting some coupling between the two elements. Lead was mainly associated with the particulate phase, possibly adsorbed on Mn- and Fe- oxides (dissolved Pb: 0.04-0.75 nM; particulate Pb: 0.1-3.5 nM). Dissolved Cu and Ni had essentially conservative behaviour during mixing between the river Po and the Northern Adriatic Water. Dissolved Cu and Ni concentrations were higher during the summer period when the water column was enriched in organic material. Particulate Cu and Ni were also high near the bottom, possibly due to resuspension. The Cd distribution was influenced by riverine, atmospheric and benthic inputs. Removal of Cd through the water column was observed in the summer period and was attributed to biological uptake and/or scavenging by Fe- and Mn- oxides. Dissolved and particulate distributions of zinc were affected by riverine inputs in surface water and by benthic inputs. The relatively low

dissolved Zn concentrations in surface water during the summer period was attributed to biological uptake.

In the central Adriatic Sea, dissolved and particulate Mn and Fe concentrations were generally lower than in the northern Adriatic Sea (Mn, 0.8-33, 0.2-58; Fe, 0.2-5.3, 10-1200 respectively). The distributions of Mn and Fe were influenced by riverine and atmospheric inputs in surface water, by advective transport and by benthic inputs and resuspension near the bottom. Dissolved Co concentrations were relatively high in surface water reflecting riverine and atmospheric inputs and benthic inputs advected from the shelf. Relatively high particulate Pb concentrations were found in surface waters reflecting atmospheric and riverine inputs and near the bottom reflecting resuspension. While dissolved Cd showed a recycled behaviour, Zn distribution did not have any link to the cycle of biological utilization and regeneration of nutrients and was more influenced by boundary inputs. Particulate Zn concentrations correlated well with those of Fe suggesting some association with Fe-oxides.

Samples were collected in the Strait of Otranto on one occasion in November 1994, as part of the OTRANTO project. Distributions of dissolved trace metals (Mn, Fe, Co, Pb, Cd, Zn, Cu and Ni) reflect the presence of different water masses: the East Surface Water (ESW), the West Surface Water (WSW), the Mixed Adriatic Water (MAW), the Mixed Levantine Intermediate Water (MLIW) and the South Adriatic Water (SAW).

Concentrations of metals in the WSW were generally higher than the ESW reflecting riverine inputs flowing along the Italian coast and through the Strait of Otranto. The MAW which is a mixture of MLIW and North Adriatic Water, is formed in the central Adriatic Sea and is influenced by riverine inputs from the Northern Adriatic Sea whereas the SAW is formed in the South Adriatic Pit during winter due to air-sea heat exchanges and has relatively low dissolved metals concentrations. For Mn, Co, Ni and Cu mixing between the different water masses was essentially conservative, reflecting the low SPM content of the water column. The metal-salinity diagrams for Mn, Fe, Pb and Zn show the presence of inputs in surface waters possibly due to atmospheric and riverine inputs; for Fe, Mn, Zn, Cu and Cd relatively high concentrations at around 38.7 salinity have been attributed to benthic sources.

In Chapter 5, a first order mass balance of 6 different trace metals (Mn, Fe, Pb, Zn, Cu, Ni) has been presented for a one year period for the different compartments of the Adriatic Sea: compartment 1 (northern Adriatic Sea), compartment 2 (central Adriatic Sea and surface layer of the southern Adriatic Sea) and compartment 3 (deep water of the southern Adriatic Sea). The Adriatic Sea appears to be a source of dissolved Cu, Mn, Co, Cd and Fe for the Mediterranean Sea whereas for dissolved Zn and Pb the Adriatic Sea appears to be a net sink. Dissolved Zn and Pb are imported into the system through the Strait of Otranto and subsequently trapped in the sediment. The residence time of all metals in compartment 1 are significantly shorter than that of water indicating significant removal. In compartments 2 and 3, residence times of Mn and Fe are relatively short suggesting removal from the water column whereas for the other metals their residence times are similar to that of water. Calculations of turnover time of metals with respect to different processes show that in compartments 1 and 2, sedimentation is the main process which affect the content of the reservoirs whereas in compartment 3, the water flux exchanges play an important role for Zn, Cu and Ni.

Most of the metals clearly undergo a very dynamic cycle of sedimentation/remobilization particularly in the Northern Adriatic Sea. In the northern Adriatic Sea, most of the Mn and Fe in deposited sediment is remobilized. This is related to diagenetic processes involving the utilization and solubilisation of Mn and Fe oxides which occur in the surface of the sediment in the northern Adriatic Sea. In the central Adriatic Sea, remobilization of Mn and Fe is less than in the northern Adriatic Sea, suggesting that diagenesis processes appear deeper in the sediment. For Cu, Ni and Zn, which are recycled elements, remobilization from the sediment is attributed to oxidation of organic matter carrier phases via oxidants such as O₂, nitrate, MnO₂, Fe₂O₃. Pb and Zn show little remobilization in the central. Advective transport of sediment is a major source of metals for the deep basin. As much as 80 % of the sediments in the South Adriatic Pit might have been advected from the shelf. Remobilization fluxes in the South Adriatic Pit are significantly less than in the Northern and Central Adriatic Sea reflecting hemi-pelagic sediments.

7.3 The Black Sea

Measurements of dissolved and leachable particulate trace metals (Mn, Fe, Co, Pb, Cd, Zn, Cu and Ni) and total particulate Mn and Fe were made on samples collected in the Northwestern Black Sea during the EROS 2000 expedition conducted in July-August 1995. At stations on the shelf, Mn and Fe distributions were influenced by suboxic and/or anoxic conditions related to the biodegradation of organic matter, which occurred below the thermocline or at the sediment-water interface, and by riverine inputs. Dissolved concentrations were high in some cases mainly due to the reduction of Mn- and Fe-oxides which occurred in microenvironments in the dominantly oxic medium at the thermocline or in low O₂ zones near the bottom. Dissolved Mn and Fe concentrations varied between 1.2 and 1348 nM and between 0.4 and 181 nM, respectively. Particulate concentrations of Mn and Fe were high, due to reprecipitation of Mn²⁺ and Fe²⁺ in presence of oxygen, riverine inputs and advective transport. Total particulate concentrations of Mn and Fe were 0.7-1052 nM and 2.3-2653 nM respectively. Particles of Mn and Fe oxides produced in large quantities on the continental shelf margin by precipitation of Mn²⁺ and Fe²⁺ near the bottom, are subject to lateral transport by coastal currents and feed the “Fine Particle Layer” which spreads all over the Black Sea basin with intensities decreasing from the coast.

Trace metal distributions (Co, Pb, Cu, Ni, Cd, Zn) were influenced by the Mn and Fe cycling, especially the “particulate reactive” metals (Co, Pb) and by riverine inputs. Relatively high dissolved and available particulate concentrations were generally found in surface waters at stations directly influenced by the Danube river. High dissolved metal concentrations were found at the thermocline or near the sediment-water interface where dissolution of Fe- and Mn-oxides, on which metals were adsorbed, occurs under suboxic or anoxic conditions. Cd and Zn had generally similar distributions reflecting their “nutrient like” behaviour. Cu and Ni were mainly in the dissolved phase. In the oxic layer, at the deep station on the slope, the suspended fractions of Mn and Fe were a major part of the total concentrations reflecting the presence of the “Fine Particle Layer”. Dissolved and total particulate concentrations were respectively: Mn, 0.69-9.6, 1.2-29; Fe, 0.79-3.03,

2.3-7.4 nM. Dissolved trace metal (Co, Pb, Cu, Ni, Cd, Zn) concentrations were higher than in the Mediterranean Sea, reflecting the stronger influence of river water in the Black Sea.

7.4 Comparison between the Adriatic Sea and the Black Sea

The Adriatic and Black seas are two European closed seas connected to the Mediterranean Sea. The Black Sea is connected with only a 1-5 km wide channel (the Bosphorus) whereas the Adriatic is connected to the Mediterranean Sea by the Strait of Otranto which is 80 km wide. The Adriatic and the Black seas differ significantly in physical, chemical and biological characteristics but their common characteristics are relative confinement and huge drainage areas carrying great amounts of waters. The drainage areas are $230 \cdot 10^3 \text{ km}^2$ for the Adriatic Sea and $245 \cdot 10^4 \text{ km}^2$ for the Black Sea. The areas most affected by terrestrial waters of both anthropogenic and natural origins are the northwestern Black Sea via the River Danube with an outflow of $203.4 \text{ km}^3/\text{y}$ which represents 68 % of the total riverine inputs for the Black Sea, and the northern Adriatic Sea via the River Po with an outflow of $67.8 \text{ km}^3/\text{y}$ which represents 49 % of the total riverine inputs for the Adriatic Sea.

The SPM concentration in the River Po (206 mg/l) is much higher than in the Danube (38 mg/l), although the Danube value does not represent a mean value over a year period as with the value for the River Po. However, the particulate load depends very much on the dynamics of the flow regime and since during the 1995 Black Sea expedition, the average discharge of the Danube River for July ($7400 \text{ m}^3/\text{s}$) was equivalent to the 40 years mean established between 1931 and 1970 by Stancik et al. (1988), the extrapolation of the data from one sampling trip to an annual cycle seems a valid assumption (Guieu *et al.*, 1998). The low sediment discharge of the River Danube is possibly due to the influence of the Iron Gate dams (Milliman, 1997). As a consequence, particulate metal concentrations are much lower in the River Danube than in the River Po. The Iron Gate dams could have a significant effect not only on the particulate metal loads of the Danube river but also on its dissolved metal loads. Dissolved trace metal concentrations are lower in the mouth of the Danube River than in the River Po for Mn and Fe by a factor of 2, for Co and Ni by a

factor of 3, for Pb by a factor of 4 and for Zn by a factor of 7. As for silicate, the reservoir lakes could retain large quantities of Zn (Humborg *et al.*, 1997). Dissolved concentrations of Cu and Cd are similar in the Danube and Po rivers.

The metal loadings in the River Po and the River Danube over a year period have been calculated and can be compared to atmospheric inputs for the Adriatic and Black sea estimated using Mediterranean Sea data (Guieu *et al.*, 1997; Chester *et al.*, 1993a and b), and to “natural” loadings for the entire Adriatic and Black Sea, estimated by Sekulic and Vertacnik (1997), see Table 7.1. In “natural” waters Sekulic and Vectacnik (1997) took into account precipitation, rivers, groundwaters and direct runoff. There is a significant anthropogenic impact on natural waters and Sekulic and Vectacnik (1997) estimated that the sewage contribution to natural waters represents 0.3 % and 0.1 % of natural waters for the Adriatic and Black seas respectively. The metal loadings in the River Po are significantly higher for Fe, Pb, Cd, Zn and Ni than in the River Danube. This is related to the high SPM concentrations in the River Po. For Mn, Co and Cu, this is reverse, the metal loadings in the Danube river are higher than the River Po and this can be attributed to the high river outflow of the River Danube. The comparison of riverine fluxes from the Po and Danube rivers with atmospheric inputs indicate the predominance of riverine inputs for most metals (Mn, Fe, Co, Cu and Ni). For Zn there is a predominance of riverine inputs in the Adriatic although a predominance of atmospheric inputs is indicated in the Black Sea. The atmospheric inputs dominates the total external inputs in the case of elements originating from pollution sources such as Pb and Cd. This has also been observed in the Mediterranean Sea (Guieu *et al.*, 1997). The Mn loadings estimated in this study for the Po and Danube rivers are about twice the Mn loadings estimated for the entire Adriatic Sea and Black Sea by Sekulic and Vertacnik (1997) which suggest that their estimation for Mn is possibly underestimated, since sediments fluxes from small mountainous rivers have not been taken into account in the estimation of this study and are possibly important (Milliman and Syvitski, 1992). When River Po and River Danube metal loadings are combined with atmospheric inputs of the Adriatic and Black Sea respectively, and compared with the “natural” loading estimated by Sekulic and Vertacnik (1997), the two estimations appear similar for Cd and Pb for both the Adriatic and Black Sea whereas for Ni and Cu this is only the case for the Adriatic. Metal loadings given by Sekulic and

Table 7.1: Comparison of metal loadings in the Rivers Po and Danube, in the Adriatic Sea and in the Black Sea

	This study			This study			^a Sekulic and Vertacnik (1997)	This study		
	The River Po (1)			The River Danube (2)				The Adriatic Sea		
	Dissolved concentrations (nM)	Total particulate concentrations ($\mu\text{g/l}$)	metal loading t/y	Dissolved concentrations (nM)	Total particulate concentrations ($\mu\text{g/l}$)	metal loading t/y		Atmospheric inputs t/y	“Natural” loading ^a t/y	
Mn	39	75.2	5060	14	48.1	9940	1850	2060	2480	3750
Fe	69	2260	152,000	36	213	43,700	6050	—	4060	—
Co	1.1	—	1.8<	0.3	0.189	42	1.8	—	6	—
Pb	0.610	7.61	493	0.159	1.06	223	508	985	1130	1900
Cd	0.146	0.233	16	0.132	0.021	7	40	65	113	155
Zn	42.3	23.0	1740	5.9	3.71	832	323	9100	992	29,200
Cu	27	4.96	494	28	1.18	602	197	1650	271	5620
Ni	45	17.9	1390	15	0.613	304	73	1800	226	3750

(1) Mean values of data collected monthly over a year period (1993-1994)

(2) Mean values of data collected in one cruise in July 1995

Vertacnik (1997) for Zn in the Adriatic and Black Sea and for Cu and Ni in the Black Sea seem overestimated, since their estimations appear much higher than the estimation of external inputs (riverine and atmospheric inputs) calculated in this study. The data used by Sekulic and Vertacnik in their study were from the early 80's (UNEP/ECE/UNIDO/FAO/UNESCO/WHO/IAEA (1984)). At that time, it was possible that contaminations and the lack of sufficiently precise analytical techniques have led to reported concentration data that for some trace elements were artificially too high.

In the northern Adriatic and northwestern Black Sea, high concentrations of nutrients and advanced eutrophication have been registered. As discussed in this thesis, eutrophication processes influence the distribution of metals, and particularly Mn, Fe and Co which are redox sensitive elements. Dissolved Mn, Fe and Co concentrations are much higher in the northwestern Black Sea than in the northern Adriatic Sea (Table 7.2), suggesting that diagenetic reactions involving the destruction of organic carbon are more intense in the northwestern Black Sea (reduction of Fe-oxides) than in the Adriatic Sea (reduction of Mn-oxides). This is related to larger organic carbon inputs on the seafloor in the Black Sea (90–685 mg/m²/d; Von Bodungen and Humborg, 1996) than in the Adriatic (96–456mg/m²/d; Giordani *et al.*, 1996). This elevated “carbon rain” in the northwestern Black Sea can be explained by high primary production rates which are induced by increased vertical nutrient fluxes into the photic zone and by flocculation of the dissolved organic matter at the seawater-fresh water interface (Von Bodungen and Humborg, 1996). Dissolved concentrations of Pb, Cd, Cu, Ni and Zn are generally similar in the northern Adriatic Sea and the northwestern Black Sea.

Particulate Mn concentrations are generally higher in the Black sea than in the northern Adriatic Sea (Table 7.2). This is possibly due to precipitation of Mn²⁺ into MnO₂ in presence of oxygen since dissolved Mn²⁺ concentrations are also higher in the Black Sea. Particulate Fe, Pb, Cu, Ni, Cd and Zn concentrations are higher in the northern Adriatic Sea than in the Black Sea. In the Po River, metals are essentially associated with the particulate phase, and the relatively high particulate metals concentrations in the northern Adriatic sea reflect the strong influence of riverine inputs on the shallow northern part of

the Adriatic where depth hardly ever exceeds 40 m. Resuspension and advective transport may also influence the distribution of particulate metals.

Table 7.2: Dissolved and total particulate metal concentrations in the northern Black Sea and the northern Adriatic Sea

	Northern Black Sea		Northern Adriatic Sea	
	Dissolved (nM)	Particulate (nM)	Dissolved (nM)	Particulate (nM)
Mn	1.2–1348	0.7–1052	6.7–192	0.73–253
Fe	0.4–181	2.3–2653	0.05–25.03	29–4709
Co	0.04–1.89	0.003–2.89	0.235–1.071	–
Pb	0.03–0.61	0.37–1.47	0.039–0.750	0.05–7.16
Cu	2.9–28.8	0.00–3.7	3.14–24.4	0.26–38
Ni	8.6–17.5	0.002–2.096	6.09–21	0.16–9.4
Cd	0.033–0.161	0.002–0.063	0.071–0.220	–
Zn	1–45	0.04–7.58	2.29–22	1.37–48

7.5 Recommendations for further work

In this work, the cycling and fate of metals were studied separately from the direct effects of eutrophication. Undoubtedly the two must be linked in the Adriatic Sea and Black Sea coastal environments, not least because of the very high organic enrichment of the water column and sediments. Organic substances and metals are likely to take part in reciprocal interactions. One fundamental aspect of metal reactivity and transport concerns the extent to which it becomes combined with organic sequestering entities present in natural waters. Conversely, metal speciation and metal concentration gradients can influence plankton production, bacterial growth and ecosystem structure. Another such feedback loop may well control the flux of trace metals from estuarine and shelf sediments, given the known influence of bacterial exopolymers on sediment stability and resuspension combined with the recent hypothesis that bacterial exopolymers are excreted in different quality and quantity according to metal concentration gradients in sediments (Heisse, 1995). An understanding of these metal/bacteria interactive influences would be highly relevant to the question of the coupling between surface active organic substances produced by eutrophication and trace metal cycles. Finally, there is indirect evidence that these interactive influences between metals and microorganisms take place in microenvironments

(pycnocline, particle/water interface, microbial mats....) so that their understanding requires microtechniques capable of probing these interactions.

In summary, more work needs to be done:

- To investigate the dynamic properties of natural organic matter and their relevance to the transformation and exchange of metals (Fe, Mn, Cu, Pb, Zn) across key interfaces (pycnocline, benthic boundary layer, particle/water interface) in the northwestern Black Sea and the northern Adriatic Sea.
- To explore the biotic and abiotic factors that control metal remobilization from the sediments under the anoxic conditions produced by eutrophication and water column stratification.

This will enable to better understand the biogeochemical cycle of trace metals in eutrophic areas.

REFERENCES

Abe, K., Kuma, K., Kudo, I. And Matsunaga, K. (1990) Residence times for Cd and PO₄ in Funka Bay, Japan. *Marine Chemistry*, 28, 325-331.

Abe, K. and Matsunaga, K. (1988) Mechanism controlling Cd and PO₄ concentrations in Funka Bay, Japan. *Marine Chemistry*, 23, 145-152.

Ali, W., O'Melia, C.R. and Edzwald, J.K. (1985) Colloid stability of particles in lakes-measurements and significance. *Water Science and Technology*, 17, 701-712.

Alldredge, A.L., Gotschalk, C. and MacKintyre, S. (1987) Evidence for sustained residence of microcrustacean fecal pellets in surface waters off southern California. *Deep-Sea research*, 34, 1641-1652.

Alldredge, A.L. and McGillivray, P. (1991) The attachment probabilities of marine snow and their implications for particle coagulation in the ocean. *Deep-Sea research*, 38, 431-443.

Alldredge, A.L. and Gotschalk, C.C. (1989) Direct observations of the mass flocculation of diatoms blooms: characteristics, settling velocities and formation of diatom aggregates. *Deep-Sea Research*, 36, 159-171.

Althaus, M. (1992) Dissolved trace metals in the estuarine plumes of the Humber, Thames and Rhine rivers. Ph D thesis, University of Southampton, UK, 329 pp.

Anderson, L. (1979) Simultaneous spectrophotometric determination of nitrate plus nitrite by flow injection analysis. *Analytica Chimica Acta*, 110, 123-126.

Arnold, R.G., Di Christina, T.J. and Hoffmann, M.R. (1986) Dissimilative Fe(III) reduction by *Pseudomonas* sp. 200-inhibitor studies. *Applied Environmental Microbiology*, 52, 281-294.

Artegiani, A. and Salusti E. (1987) Field observations of the flow of dense water on the bottom of the Adriatic Sea during the winter of 1981. *Oceanologica Acta*, 10(4), 387-391.

Artegiani, A., Azzolini, R. and Salusti, E. (1989) On dense water in the Adriatic Sea. *Oceanologica Acta*, 12, 151-160.

Artegiani, A., Gacic, M., Michelato, A., Kovacevic, V., Russo, A., Pascini, E., Scarazzato, P. and Smircic, A. (1993) The Adriatic Sea hydrology and circulation in spring and autumn (1985-1987). *Deep-Sea Research*, 40(6), 1143-1180.

Balls, P.W. (1985) Copper, Lead and Cadmium in coastal waters of the western North sea. *Marine Chemistry*, 15, 363-378.

Balls, P.W. (1988) The control of trace metals distributions in coastal seawater through partition onto suspended particulate matter. *Netherlands Journal of Sea Research*, 22, 213-218.

Balls, P.W. (1989) The partition of trace metals between dissolved and particulate phases in European coastal waters: a compilation of field data and comparison with laboratory studies. *Netherlands Journal of Sea Research*, 23, 7-14.

Barale, V., Malanotte-Rizzoli, P. and Hendershott, M.C. (1984) Remotely sensing the surface dynamics of the Adriatic Sea. *Deep-Sea Research*, 31, 1433-1459.

Bender, M.L. and Heggie, D.T. (1984) Fate of organic carbon reaching the deep sea floor: a status report. *Geochimica and Cosmochimica Acta*, 48, 977-986.

Berger, P., Laane, R.W.P.M., Ilahude, A.G., Ewald, M. and Courtot, P. (1984) Comparative study of dissolved fluorescent matter in four West-European estuaries. *Oceanologica Acta*, 7, 309-314.

Bethoux, J-P. (1980) Mean water fluxes across sections in the Mediterranean Sea, evaluated on the basis of water and salt budgets and of observed salinities. *Oceanologica Acta*, 3, 79-88.

Bewers, J.M. and Yeats, P.A. (1989) Transport of river-derived trace metals through the coastal zone. *Netherlands Journal of Sea Research*, 23, 359-368.

Bignami, F., D'Archino, R., Montebello, O. and Salusti, E. (1991) New observations on bottom currents in the Southern Adriatic and Ionian Seas (Eastern Mediterranean Sea). *Annales Geophysicae*, 9, 227-232.

Bochdansky, A.B. and Herndl, G.J. (1996) Ecology of amorphous aggregations (marine snow) in the Northern Adriatic Sea: III. Zooplankton interactions with marine snow. *Marine Ecology Progress Series*, 87.

Bodeanu, N. (1989) Algal blooms and development of the main phytoplankton species at the Romanian Black Sea littoral under eutrophication conditions. *Cercetari Marine*, 22, 107-125.

Bolin, B., Bjorkstrom, A. and Holmen, K. (1983) The simultaneous use of tracers for ocean circulation studies. *Tellus*, 35B, 206-236.

Boyle, E.A., Slater, F. and Edmond, J.M. (1977) The distribution of dissolved copper in the Pacific. *Earth and Planetary Science Letters*, 37, 38-54.

Boyle, E.A., Huested, S.S. and Grant, B. (1982) The chemical mass balance of the Amazon plume-II: Copper, nickel and cadmium. *Deep Sea Research*, 29, 405-419.

Brand, L.E., Sunda, W.G. and Guillard, R.R.L. (1983) Limitation of marine phytoplankton reproductive rates by zinc, manganese and iron. *Limnology and Oceanography*, 28, 1182-1198.

Brand, L.E., Sunda, W.G. and Guillard, R.R.L. (1986) Reduction of marine phytoplankton reproduction rates by copper and cadmium. *Journal of Experimental Marine Biology and Ecology*, 96, 225-250.

Brewer, P.G. (1971) Hydrographic and chemical data from the Black Sea. *Woods Hole Oceanographic Institution Technical Report*, 71, 65 pp.

Brewer, P.G. and Murray (1973) Carbon, nitrogen and phosphorus in the Black Sea. *Deep-Sea Research*, 20, 803-818.

Brewer, P.G. and Spencer, D.W. (1974) Distribution of some trace elements in Black Sea and their flux between dissolved and particulate phases. In: The Black Sea: Geology, Chemistry and Biology, Degens, E.T. and Ross, D.A. (eds.), American Association of Petroleum Geologists, Tulsa, Oklahoma, USA, pp. 137-143.

Brewer, P.G. (1975) Minor elements in seawater. In: Chemical Oceanography, 2nd edition, vol. 1, Riley, J.P. and Skirrow, G. (eds.), Academic Press, London, UK, pp. 415-491.

Brockhaus (1952) Der Große Brockhaus, 12 Vol. 16th edn., E. Brockhaus, Wiesbaden.

Bruland, K.W., Knauer, G.A. and Martin, J.H. (1978) Zinc in north-east Pacific water. *Nature*, 271, 741-743.

Bruland, K.W. (1980) Oceanographic distributions of cadmium, zinc, nickel and copper in the North Pacific. *Earth and Planetary Science Letters*, 47, 176-198.

Bruland, K.W. (1983) Trace elements in seawater. In: Chemical oceanography, 8, Riley, J.P. & Chester, R. (eds.), Academic Press, London, pp. 157-220.

Bruland, K.W. and Franks, R.P. (1983) Manganese, nickel, copper, zinc and cadmium in the western north Atlantic. In: Trace Metals in Seawater, Wong, C.S., Boyle, E., Bruland, K., Burton, J.D. and Goldberg, E.D. (eds.), Plenum Press, New York, pp. 395-413.

Bryan, K.W. (1984) Pollution due to heavy metals and their compounds. *Marine Ecology*, 5, 1289-1431.

Bryantsev, V.A., Fashchuk, D. Ya, Ayzatullin, T.A. Bagotskiy, S.V. and Leonov, A.V. (1988) Variation in the upper boundary of the hydrogen sulfide zone in the Black Sea: analysis of field observations and modelling results. *Oceanology*, 28, 180-185.

Burton, J.D. and Statham, P.J. (1990) Trace metals in sea water. In: Heavy metals in the marine environment. Rainbow, P.S. and Furness, R.W. (eds.), CRC Press, Boca Raton, FL, USA, pp. 5-27.

Burton, J.D., Althaus, M., Millward, G.E., Morris, A.W., Statham, P.J., Tappin, A.D. and Turner, A. (1993) Processes influencing the fate of trace metals in the North Sea. *Philosophical Transactions of the Royal Society of London*, 343, 557-568.

Callender, E. and Hammond, D.E. (1982) Nutrient exchange across the sediment-water interface in the Potomac river estuary. *Estuarine, Coastal and Shelf Science*, 15, 395-413.

Cameron, W.M. and Pritchard, D.W. (1963) In: The sea, vol. 2, Hill, M.N. (ed.), John Wiley & Sons, New-York.

Caspers, H. (1957) Black Sea and sea of Azov. In : Treatise on marine ecology and paleoecology, Hedgpeth, J.W. (ed.), Geological Society of America, memoir 67, 801-890, New York.

Cauwet, G., Oriol, L., Déliat, G. (1996) In: EROS 2000 report; the interactions between the river Danube and the north-western Black Sea, pilot phase (1994-1996).

Cavazzoni Galaverni, S. (1972) Distribuzione costiera delle acque dolci continentali nel mare Adriatico (fino alla trasversale Tremiti-Curzola). Rapp. Tecn. Lab. Studio Dinamica Grandi Masse CNR, Venezia, 44, pp. 18.

Chester, R. (1990) Marine Chemistry. Unwin Hyman Ltd, London, UK, pp. 698

Chester, R. and Murphy, K.J.T. (1990) Metals in the marine atmosphere. In: Heavy Metals in the Marine Environment, Rainbow, P.S. and Furness, R.W. (eds.), CRC Press, Boca Raton, FL, 27-49.

Chester, R., Murphy, K.J.T., Lin, F.J., Berry, A.S., Bradshaw, G.A. and Corcoran, P.A. (1993a) Factors controlling the solubilities of trace metals from non-remote aerosols deposited to the sea surface by "dry" deposition mode. *Marine Chemistry*, 42, 107-126.

Chester, R., Nimmo, M., Alarcon, M., Saydam, C., Murphy, K.J.T., Sanders, G.S. and Corcoran, P. (1993b) Defining the chemical character of aerosols from the atmosphere of the Mediterranean Sea and surrounding regions. *Oceanologica Acta*, 16, 231-246.

Chiffolleau, J.F., Cossa, D., Auger, D. and Truquet, I. (1994) Trace metal distribution, partition and fluxes in the Seine estuary (France) in low discharge regime. *Marine Chemistry*, 47, 145-158.

Civitarese, G., Gacic, M., Vetrano, A., Boldrin, A., Bregant, D., Rabitti, S., Souvermezoglou, E. (1998) Biogeochemical fluxes through the Strait of Otranto (Eastern Mediterranean). *Continental Shelf Research*, 18, 773-789.

Cifuentes, L.A., Schemel, L.E. and Sharp, J.H. (1990) Qualitative and Numerical Analyses of the Effects of River Inflow Variations on Mixing Diagrams in Estuaries. *Estuarine, Coastal and Shelf Science*, 30, 411-427.

Coble, P.G., Green, S.A., Blough, N.V. and Gagosian, R.B. (1990) Characterization of dissolved organic matter in the Black Sea by fluorescence spectroscopy. *Nature*, 348, 432-435.

Coble, P.G., Gagosian, R.B., Codispoti, L.A., Friederich, G.E. and Christensen, J.P. (1991) Vertical distribution of dissolved and particulate fluorescence in the Black Sea. *Deep-Sea Research*, 38, S985-S1001.

Cociasu, A., Dorogan, L., Humborg, C. and Popa, L. (1996) Long-Term Ecological Changes in Romanian Coastal Waters of the Black Sea. *Marine Pollution Bulletin*, 32, 32-38.

Codispoti, L.A., Friederich, G.E., Murray, J.W. and Sakamoto, C.M. (1991) Chemical variability in the Black Sea: implications of continuous vertical profiles that penetrated the oxic/anoxic interface. *Deep-Sea Research*, 38, S691-S710.

Collier, R. and Edmond, J. (1983) Plankton composition and trace element fluxes from the surface ocean. In: Trace metals in Seawater, Wong, C.S., Boyle, E.A., Bruland, K.W., Burton, J.D. and Goldberg, E.D. (eds.), Plenum Press, New-York, pp. 789-809.

Comans, R.N.J. and Van Dijk, C.P.J. (1988) Role of complexation processes in cadmium mobilization during estuarine mixing. *Nature*, 336, 151-154.

Copin-Montegut, G., Courau, P. and Nicolas, E. (1986) Distribution and transfer of trace elements in the Western Mediterranean. *Marine Chemistry*, 18, 189-195.

Cruzado, A. and Velasquesz, Z.R. (1989) Nutrient distribution in the Gulf of Lions (NW Mediterranean). *Continental Shelf Research*, 10, 931-942.

Czaya, E. (1981) Ströme der Erde. Aulis Verlag Deubner & Co KG, Köln, 247 pp.

Dal Cin, R. (1983) I litorali del delta del Po e alle foci dell'Adige e del Brenta: Carratteri tessiturali e dispersioni sull'evoluzione futura. *Boll. Soc. Geol. It.*, 102, 9-56.

Danielsson, L.G., Magnusson, B. and Westerlund, S. (1978) An improved metal extraction procedure for the determination of trace metals in seawater by atomic absorption spectrometry with electrothermal atomization. *Analytica Chimica Acta*, 98, 45-57.

Danielsson, L.G., Magnusson, B., Westerlund, S. and Zhang, K. (1983) Trace metals in the Göta river estuary. *Estuarine, Coastal and shelf Science*, 17, 73-85.

Davis, W.J. (1993) Contamination of coastal versus open ocean surface waters. A brief meta-analysis. *Marine Pollution Bulletin*, 26(3), 128-134.

Degobbis, D. and Gilmartin, M. (1990) Nitrogen, phosphorus and biogenic silicon budgets for the northern Adriatic Sea. *Oceanologica Acta*, 13(1), 31-45.

Deuser, W.G. (1974) Evolution of Anoxic Conditions in Black Sea during Holocene. In: The Black Sea: Geology, Chemistry and Biology, Degens, E.T. and Ross, D.A. (eds.), American Association of Petroleum Geologists, Tulsa, Oklahoma, USA, pp. 133-136.

Deuser, W.G. and Ross, E.H. (1980) Seasonal changes in the flux of organic carbon in the deep Sargasso Sea. *Nature*, 283, 364-365.

Donat, J.R. and Bruland, K.W. (1995) Trace elements in the oceans. In: Trace elements in natural waters, Salbu, B. and Steinnes, E. (eds.), CRC Press, USA, pp. 247-281.

Donat, J.R., Lao, K.A. and Bruland, K.W. (1994) Speciation of dissolved copper and nickel in South San Francisco Bay: a multi-method approach. *Analytica Chimica Acta*, 284, 547-571.

Duinker, J.C. and Nolting, R.F. (1977) Dissolved and particulate trace metals in the Rhine estuary and the Southern Bight. *Marine Pollution Bulletin*, 8, 65-71.

Duinker, J.C. and Nolting, R.F. (1978) Mixing, removal and mobilization of trace metals in the Rhine estuary. *Netherlands Journal of Sea Research*, 12, 205-223.

Duinker, J.C., Wollast, R. and Billen, G. (1979) Behaviour of manganese in the Rhine and Scheldt estuaries. *Estuarine and Coastal Shelf Science*, 9, 727-738.

Duinker, J.C., Hillebrand, M.T.J. and Nolting, R.F. (1980) The river Varde Å: processes affecting the behaviour of metals and organochlorines during estuarine mixing. *Netherlands Journal of Sea Research*, 15(2), 170-195.

Duursma, E.K. (1974) The fluorescence of dissolved organic matter in the sea. In: Optical aspects of oceanography, Jerlov, N.G. & Steemann Nielsen, E. (eds.), Academic Press, New York, pp. 237-256.

Dyrssen, D. (1985) Metal complex formation in sulphidic seawater. *Marine Chemistry*, 15, 285-293.

Dyrssen, D. and Kremling, K. (1990) Increasing hydrogen sulfide concentration and trace metal behavior in the anoxic Baltic waters. *Marine Chemistry*, 30, 193-204.

Edmond, J.M., Von Damm, K.L., McDuff, R.E. and Measures, C.I. (1982) Chemistry of hot springs on the East Pacific Rise and their effluent dispersal. *Nature*, 297, 187-191.

Edmond, J.M., Spivack, A., Grant, B.C., Hu, M.H., Chen, Z., Chen, S. and Zeng, X. (1985) Chemical dynamics of the Changjiang estuary. *Continental Shelf Research*, 4, 17-36.

Elbaz-Poulichet, F., Martin, J.M., Huang, W.W. and Zhu, J.X. (1987) Dissolved Cd behaviour in some selected French and Chinese Estuaries. Consequences on Cd supply to the ocean. *Marine Chemistry*, 22, 125-136.

Elderfield, H., Luedtke, N., McCaffrey, R.J. and Bender, M. (1981) Benthic flux studies in Narragansett Bay. *American Journal of Science*, 281, 768-787.

Emerson, S., Kalhorn, S., Jacobs, L., Tebo, B.M., Nealson, K.H. and Rosson, R.A. (1982) Environmental oxidation rate of manganese(II): bacterial catalysis. *Geochimica et Cosmochimica Acta*, 46, 1073-1079.

Eremeev, V.N., Suvorov, A.M., Khaliulin, A.K. and Godin, E.A. (1996) On the correspondence of the upper boundary of the hydrogen sulfide zone in the Black Sea to a certain isopycnic surface from multi year data. *Oceanology*, 36, 216-221.

Fang, T.H. (1995) Studies of the behaviour of trace metals during mixing in some estuaries of the Solent region. Ph. D. Thesis, University of Southampton, UK, 350 pp.

Fashchuk, D. Y. and Ayzatullin, T.A. (1986) A possible transformation of the anaerobic zone of the Black Sea, *Oceanology*, 26, 171-178.

Ferentinos, G. and Kastanos, N. (1988) Water circulation patterns in the Otranto Straits, Eastern Mediterranean. *Continental Shelf Research*, 8, 1025-1041.

Filella, M. and Buffle, J. (1993) Factors controlling the stability of submicron colloids in natural waters. *Colloids and Surfaces A: Physicochemical and Engineering Aspects*, 73, 255-273.

Fisher, N.S. and Wente, M. (1993) The release of trace elements by dying marine phytoplankton. *Deep-Sea Research*, 40, 671-694.

Fogg, G.E. (1983) The ecological significance of extracellular products of phytoplankton photosynthesis. *Bot. Marina*, 26, 3-14.

Fogg, G.E. (1990) Massive phytoplankton gel production. In: Eutrophication-related phenomena in the Adriatic Sea and other Mediterranean coastal zones, Barth, H. and Fegan, L. (eds.). Water pollution research report 16, Commission of the European Communities, Brussels, pp. 207-212.

Fonselius, S.H (1974) Phosphorus in Black Sea: In: The Black Sea: Geology, Chemistry and Biology, Degens, E.T. and Ross, D.A. (eds.) American Association of Petroleum Geologists, Tulsa, Oklahoma, USA, pp. 144-150.

Förstner, U., Calmano, W., Conradt, K., Jacksch, H., Schimkus, C. and Schoer, J. (1981) Chemical speciation of heavy metals in waste materials (sewage sludge, mining waste, dredge materials, polluted sediments) by sequential extraction. Procedures of the International

Conference on Heavy metals in the Environment, Amsterdam, CEP Consultants Eds., Edinburgh, UK, pp. 698-704.

Frew, R.D. and Hunter, K.A. (1992) Influence of Southern Ocean waters on the cadmium-phosphate properties of the global ocean. *Nature*, 360, 144-146.

Frignani, M. and Langone, L. (1991) Accumulation rates and ¹³⁷Cs distribution in sediments off the Po River delta and the Emilia-Romagna coast (north-western Adriatic Sea, Italy). *Continental Shelf Research*, 11, 525-542.

Frignani, M., Langone, L., Beks, J., Alvisi, F. (1996) Sediment accumulation rates from cores collected in the central and southern Adriatic Sea. In: Transfer pathways and fluxes of organic matter and related elements in water and sediments of the northern Adriatic Sea and their importance on the eastern Mediterranean Sea, Final report EUROMARGE-AS Project, EU/MAST2, pp. 148-156.

Froelich, P.N., Klinkhammer, G.P., Bender, M.L., Luedtke, N.A., Heath, G.R., Cullen, D., Dauphin, P., Hammond, D., Hartman, B. and Maynard, V. (1979) Early oxidation of organic matter in pelagic sediments of the eastern equatorial Atlantic: suboxic diagenesis. *Geochimica and Cosmochimica Acta*, 43, 1075-1090.

Garrels, R.M. and Mackenzie, F.T. (1971) In: Evolution of the sedimentary rocks, Norton W.W. (ed.), New-York, pp. 317.

Gilmartin, M. and Revelante, N. (1983) The phytoplankton of the Adriatic Sea: standing crop and primary production. *Thalassia Jugoslavia*, 19, 173-188.

Giordani, P., Miserocchi, S., Balboni, V., Moodley, L., Frignani, M. and Langone, L. (1994) Fluxes of particles and nutrients at the benthic boundary layer. In: Extended Abstracts, First workshop of the Mediterranean Targeted Project (Barcelona, November 21-23, 1994), Tesys, Barcelona, Spain, pp. 157-163.

Giordani, P., Balboni, V., Hammond, D.E., Miserocchi, S., Malaguti, A., Sorgente, D., Vitale, F., Seritti, A. and Tankéré, S.P.C. (1996) Benthic mineralisation: temporal variability and coupling to water column production. In: Transfer pathways and fluxes of organic matter and related elements in water and sediments of the northern Adriatic Sea and their importance on the eastern Mediterranean Sea, Final report EUROMARGE-AS Project, EU/MAST2, pp. 208-219.

Goeyens, L. and Vervlimmeren, J. (1996) In: EROS 2000 report; the interactions between the river Danube and the north-western Black Sea, pilot phase (1994-1996).

Gomoiu M.T. (1985) Problemes concernant l'eutrophisation marine. *Cercetari marine*, 18, 59-95.

Gomoiu, M.T. and Tiganus, V. (1990) Elements pour connaissance de l'état et de l'évolution des communautés benthiques de l'ouest de la mer Noire. Rapport de la Commission Internationale sur la Mer Méditerranée, 32(1), 24.

Grasshoff, K (1975) The hydrochemistry of landlocked basins and fjords. In: Chemical oceanography, 2, Riley, J.P. and Skirrow, G. (eds), Academic Press, New York, USA, pp. 455-597.

Guerzoni, S., Quarantotto, G., Molinaroli, E. and Rampazzo, G. (1995) More data on source signature and seasonal fluxes to the central Mediterranean Sea of aerosol dust originated in desert area. In: European River Ocean System, Fifth Workshop on the North-West Mediterranean Sea, Hamburg (Germany), 28-30 March 1994, Martin, J-M and Barth, H. (eds.), Water Pollution Research Report 32, Commission of the European Communities, Brussels, pp. 267-274.

Guerzoni, S., Landuzzi, W., Lenaz, R., Quarantotto, G., Cesari, G., Rampazzo, G. and Molinaroli, E. (1991) Mineral atmospheric particulate from south to NW Mediterranean: seasonal variations and characteristics. In: European River Ocean System, Third Workshop on the North-West Mediterranean Sea, Den Burg/Texel (The Netherlands), 21-25 October 1991, Martin, J-M and Barth, H. (eds.), Water Pollution Research Report 28, Commission of the European Communities, Brussels, pp. 483-493.

Guieu, C., Martin, J.M., Thomas, A.J. and Elbaz-Poulichet, F. (1991) Atmospheric versus river input of metals to the Gulf of Lions: total concentrations, partitioning and fluxes. *Marine Pollution Bulletin*, 22(4), 176-183.

Guieu, C., Chester, R., Nimmo, M., Martin, J-M, Guerzoni, S., Nicolas, E., Mateu, J. and Keyse, S. (1997) Atmospheric input of dissolved and particulate metals to the North-Western Mediterranean. *Deep-Sea Research*, 44, 655-674.

Guieu, C., Martin, J.-M., Tankéré, S., Mousty, F., Trincherini, P. and Bazot, M. (1998) On trace metal geochemistry in the western Black Sea: Danube and shelf area. *Estuarine and Coastal Shelf Science*, 47, 471-485.

Hall, I.R. (1993) Cycling of Trace Metals in Coastal Waters: Biogeochemical Processes Involving Suspended Particles. Ph.D. Thesis, University of Southampton, U.K., 329 pp.

Hamrud, M. (1983) Residence time and spatial variability for gases in the atmosphere. *Tellus*, 35B, 295-303.

Haraldsson, C. and Westerlund, S. (1988) Trace metals in the water columns of the Black Sea and Framvaren Fjord. *Marine Chemistry*, 23, 417-424.

Haraldsson, C. and Westerlund, S. (1991) Total and suspended cadmium, cobalt, copper, iron, lead, manganese, nickel and zinc in the water column of the Black Sea. In: Black Sea Oceanography, Izdar, E. and Murray, W. (eds.), NATO/ASI Series, Kluwer Academic Publishers, Netherlands, pp. 161-172.

Hartmann, M. and Muller, P.J. (1982) Trace metals in interstitial waters from central Pacific Ocean sediments. In: The dynamic environment of the ocean floor, Fanning, K.A. and Manheim, F. (eds.), Lexington Books, Lexington, MA.

Hay, B.J. (1987) Particle flux in the western Black Sea in the present and over the last 5000 years: temporal variability, source, and transport mechanisms: Ph.D. thesis, WHOI-MIT, Cambridge, MA, 201 pp.

Heise, S. (1995) Der Einfluß von Umweltfaktoren auf die Bildung von exopolymerer Substanz (EP) durch ein marines Bakterium. Ph.D. Thesis, Christian-Albrechts-University, Kiel, Germany, 136 pp.

Herman, P. and Wijsman, J. (1996) In: EROS 2000 report; the interactions between the river Danube and the north-western Black Sea, pilot phase (1994-1996).

Heussner, S., Monaco, A., Kerhervé, P., Carbonne, J., Charriere, B., Delsaut, N., Nyfeller, F., Godet, C-H., Miserocchi, S., Langone, L. and Faganelli, J. (1995) Biogeochemical fluxes in the mid-Adriatic basin: results from the first EUROMARGE-AS trap deployment (April - August 1994). In: 2nd Annual report of the EUROMARGE-AS Project, EU/MAST2, pp. 140-169.

Honeyman, B.D. and Santschi P.H. (1989) A Brownian-pumping model for oceanic trace metal scavenging: Evidence from Th isotopes. *Journal of Marine Research*, 47, 951-992.

Hopkins, T.S. (1978) Physical processes in the Mediterranean basins. In: Estuarine Transport Processes, B. Kjerfve (ed.), University of South Carolina Press, Columbia, 269-309.

Howard, A.G and Statham, P.J. (1993) Inorganic traces analysis, philosophy and practice. Wiley, Chichester, UK, 182 pp.

Hudson, R.J.M. and Morel, F.M.M. (1993) Trace metal transport by marine micro-organisms: implications of metal coordination kinetics. *Deep-Sea Research*, 40, 129-150.

Humborg, C., Ittekkot, V., Cociasu, A. and Bodungen, B.V. (1997) Effect of Danube River dam on Black Sea Biogeochemistry and ecosystem structure. *Nature*, 386, 385-388.

IAEA (1996) The Black sea 1995 contaminant screening project. Preliminary report, Monaco.

Jackson, G.A. and Williams, P.M. (1985) Importance of dissolved organic nitrogen and phosphorus to biological nutrient cycling. *Deep-Sea Research*, 32, 223-235.

Jacobs, L., Emerson, S. and J. Skei (1985) Partitioning and transport of metals across the O₂/H₂S interface in a permanently anoxic basin: Framvaren Fjord, Norway. *Geochimica et Cosmochimica Acta*, 49, 1433-1444.

James, R.H., Statham, P.J., Morley, N.H. and Burton, J.D. (1993) Aspects of the geochemistry of dissolved and particulate Cd, Cu, Ni, Co and Pb in the Dover Strait. *Oceanologica Acta*, 16, 553-564.

Jenkinson I.R. (1989) Increase in viscosity may kill fish in some blooms. In: *Red Tides: Biology, Environmental Science, and toxicology*, Okaichi, T., Anderson, D.M. and Nemoto, T. (eds.), Elsevier Science Publishing, New York, pp. 435-438.

Jickells, T.D. (1986) Studies of trace elements in the Sargasso Sea and the Mid-Atlantic Bight. Ph. D. Thesis, University of Southampton, U.K., 268 pp.

Johnson, K.S., Berelson, W.M., Coale, K.H., Coley, T.L., Elrod, V.A., Fairey, W.R., Iams, H.D., Kilgore, T.E., Nowicki, J.L. (1992) Manganese Flux from Continental Margin Sediments in a Transect Through the Oxygen Minimum. *Science*, 257, 1242-1245.

Junge, C.E. (1974) Residence time and variability of tropospheric gases. *Tellus*, 26, 477-488.

Justic (1987) Long-term Eutrophication of the Northern Adriatic Sea. *Marine Pollution Bulletin*, 18(6), 281-284.

Justic, D., Legovic, T. and Rottini-Sandrini, L. (1987) Trends in Oxygen content 1911-1984 and occurrence of benthic mortality in the Northern Adriatic Sea. *Estuarine, Coastal and Shelf Science*, 25, 435-445.

Justic, D. (1991) Hypoxic conditions in the northern Adriatic Sea: historical development and ecological significance. In: *Modern and Ancient Continental Shelf Anoxia*, Tyson, R.V. and Pearson, T.H. (eds.), Geological Society Publication, 58, pp. 95-105.

Justic, D., Rabalais N.N., Turner, R.E. and Wiseman, W.J. (1993) Seasonal coupling between riverborne nutrients, net productivity and hypoxia. *Marine Pollution Bulletin*, 26(4), 184-189.

Justic, D., Rabalais, N.N., and Turner, R.E. (1994) Riverborne nutrients, hypoxia and coastal ecosystem evolution: biological responses to long-term changes in nutrient loads carried by the Po and the Mississippi Rivers. In: *Changes in fluxes in estuaries, Implications from Science to Management*, Dyer, K.R. and Orth, R.J. (eds.), International Symposium Series, Olsen & Olsen, Fredensborg, pp. 161-166.

Kaltenböck, E. and Herndl, G.L. (1995) Ecology of amorphous aggregations (marine snow) in the Northern Adriatic Sea: IV. Dissolved nutrients and the autotrophic component associated with marine snow. *Marine Ecology Progress Series*, 87.

Karl, D.M. (1978) Distribution, abundance and metabolic states of microorganisms in the water column and sediments of the Black Sea. *Limnology and Oceanography*, 23, 936-949.

Kempe, S., Diercks, A.-R., Liebezeit, G. and Prange, A. (1991) Geochemical and structural aspects of the pycnocline in the Black Sea (R/V Knorr 134-8 leg 1, 1988). In:

Black Sea Oceanography, Izdar, E. and Murray, J.W. (eds.), NATO/ASI Series, Kluwer Academic Publishers, Netherlands, pp. 161-172.

Kevder, S., Revelante, N., Smolak, N. and Skrivanic, A. (1971) Some characteristic of phytoplankton and phytoplankton productivity in the Northern Adriatic. *Thalassia Jugoslavia*, 7, 151-158.

Kideys, A.E. (1994) Recent dramatic changes in the Black Sea ecosystem: The reason for the sharp decline in Turkish anchovy fisheries. *Journal of marine Systems*, 5, 171-181.

Klinkhammer, G.P. and Bender, M.L. (1980) The distribution of manganese in the Pacific Ocean. *Geochimica and Cosmochimica Acta*, 46, 361-384

Klinkhammer, G.P. and Bender, M.L. (1981) Trace metal distributions in the Hudson river estuary. *Estuarine, coastal and Shelf Science*, 12, 629-643.

Klinkhammer, G., Elderfield, H., Grieves, M., Rona, P. and T. Nelson (1986) Manganese geochemistry near high temperature vents in the Mid-Atlantic Ridge rift valley. *Earth and Planetary Science Letters*, 80, 230-240.

Knauss J.A. (1978) Introduction to physical oceanography. Prentice Hall, Inc., Englewood Cliffs, pp. 338.

Kremling, K. (1983) The behaviour of Zn, Cd, Cu, Ni, Co, Fe and Mn in anoxic Baltic waters. *Marine Chemistry*, 13, 87-108.

Kremling, K. and Hydes, D. (1988) Summer distribution of dissolved Al, Cd, Co, Cu, Mn and Ni in surface waters around the British Isles. *Continental Shelf Research*, 8, 89-105.

Kremling, K., Wenck, A. and Pohl, C. (1987) Summer distributions of dissolved Cd, Co, Cu, Mn and Ni in central North Sea waters. *Deutsche Hydrographische Zeitschrifte*, 40, 103-114.

Kuwabara, J.S., Chang, C.C.Y., Cloern, J.E., Fries, T.L., Davis, J.A. and Luoma, S.N. (1989) Trace metal associations in the water column of South San Francisco Bay, California. *Estuarine and Coastal Shelf Science*, 28, 307-325.

Lancelot C. (1984) Extracellular release of small and large molecules by phytoplankton in the Southern Bight of the North Sea. *Estuarine and Coastal Shelf Science*, 18, 65-77.

Lascaros, A. (1993) Estimation of deep and intermediate water mass formation rates in the Mediterranean Sea. *Deep-Sea Research II*, 40(6), 1327-1332.

Laslett, R.E. (1995) Concentrations of dissolved and suspended particulate Cd, Cu, Mn, Ni, Pb and Zn, in surface waters around the coasts of England and Wales and in adjacent seas. *Estuarine, Coastal and Shelf Science*, 40, 67-85.

Latif, M.A., Özsoy, E., Oguz, T. and Ünlüata, Ü (1991) Observations of the Mediterranean inflow into the Black Sea. *Deep-Sea Research*, 38, S711-S723.

Lewis, B.L. and Landing, W.M. (1991) The biogeochemistry of manganese and iron in the Black Sea. *Deep-Sea Research*, 38, S773-S803.

Lewis, B.L. and Landing, W.M. (1992) The investigation of dissolved and suspended-particulate trace metal fractionation in the Black Sea. *Marine Chemistry*, 40, 105-141.

Liss, P.S. (1976) Conservative and non-conservative behaviour of dissolved constituents during estuarine mixing. In: *Estuarine Chemistry*, Burton, J.D. and Liss, P.S. (eds.), Academic Press, London, UK, pp. 93-130.

Loring, D.H., Rantala, R.T.T., Morris, A.W., Blake, A.J. and Howland, R.J.M. (1983) Chemical composition of suspended particles in an estuarine turbidity maximum zone. *Canadian Journal of Fisheries and Aquatic Sciences*, 40, Supp. No 1, 201-206.

Loring, D.H. and Rantala, R.T.T. (1990) Sediments and suspended particulate matter: Total and partial methods of digestion. *Techniques in Marine Environmental Science*, No. 9, International Council for the exploration of the Sea (Copenhagen, DK), pp. 16.

Lovley, D.R. and Phillips, E.J.P. (1988) Novel mode of microbial energy metabolism: Organic carbon oxidation coupled to dissimilatory reduction of iron and manganese. *Applied Environmental Microbiology*, 54, 1472-1480.

Luther III, G.W., Nuzzio, D.B. and Wu, J. (1994) Speciation of manganese in Chesapeake Bay waters by voltammetric methods. *Analytica Chimica Acta*, 284, 473-480.

Malo, B.A. (1977) Partial extraction of trace metals from aquatic sediments. *Environmental Science and Technology*, 11, 277-282.

Maltseva, A.V. (1980) Mean perennial discharge of organic substances from the territory of the USSR and its temporal variation. *Gidrokhimicheskive Marteriali*, Leningrad. Gidrometeoizdat, 68, 14-21.

Marchand, M. (1974) Physicochemical forms of cobalt, manganese, zinc, chromium, and iron in a seawater with and without organic material. *Journal du Conseil, Conseil International de l' Exploration de la Mer*, 35(2), 130-142.

Marchetti, R., Provini, A. and Crosta, G. (1989) Nutrient load carried by the river Po into the Adriatic Sea 1968-1987. *Marine Pollution Bulletin*, 20, 168-172.

Mart, L., Rützel, H., Klare, P., Sipos, L., Platzek, U., Valenta, P. and Nürnberg, H.W. (1982) Comparative studies on the distribution of trace metals in the oceans and coastal waters. *The Science of the Total Environment*, 26, 1-7.

Martin, J.H. and Knauer, G.A. (1973) The elemental composition of plankton. *Geochimica et Cosmochimica Acta*, 37, 1639-1653.

Martin, J.H. and Knauer, G.A. (1985) Lateral transport of Mn in the north-east Pacific Gyre oxygen minimum. *Nature*, 314, 524-526.

Martin, J.H., Knauer, G.A. and Broenkow, W.W. (1986) VERTEX: the lateral transport of Manganese in the Northeast Pacific. *Deep-Sea Research*, 32, 1405-1427.

Martin, J.H. and Fitzwater, S.E. (1988) Iron deficiency limits phytoplankton growth in the north-east Pacific subarctic. *Nature*, 331, 341-343.

Martin, J.H. and Gordon, R.M. (1988) Northeast Pacific iron distributions in relation to phytoplankton productivity. *Deep-Sea research*, 35, 177-196.

Martin, J.H., Gordon, R.M., Fitzwater, S. and Broenkow, W.W. (1989) VERTEX: phytoplankton/iron studies in the Gulf of Alaska, *Deep-Sea Research*, 36, 649-680.

Martin, J-M. and Whitfield, M. (1983) The significance of the river input of chemical elements to the ocean. In: Trace metal in Seawater, Wong, C.S., Boyle, E.A., Bruland, K.W., Burton, J.D. and Goldberg, E.D. (eds.), Plenum Press, New-York, pp. 265-296.

Martin. J.-M., Nirel, P. and Thomas, A.J. (1987) Sequential extraction techniques: Promises and problems. *Marine Chemistry*, 28, 159-182.

Martin, J-M., Elbaz-Poulichet, F., Guieu, C., Loyer-Pilot. M.D. and Han, G.C. (1989) River versus atmospheric input of material to the Mediterranean Sea. *Marine Chemistry*, 28, 159-182.

Martin, J-M and Windom, H.L. (1991) Present and future roles of ocean margins in regulating marine biogeochemical cycles of trace elements. In: Ocean Margin Processes in Global Change, Mantoura, R.F.C., Martin, J-M, and Wollast, R. (eds.). John Wiley & Sons Ltd, pp. 45-67.

Martin, J-M., Huang, W.W. and Yoon, Y.Y. (1994) Level and fate of trace metals in the lagoon of Venice (Italy). *Marine Chemistry*, 46, 371-386.

Martin, J-M. and Thomas, A.J. (1994) The global insignificance of telluric inputs of dissolved trace metals (Cd, Cu, Ni and Zn) to the ocean margins. *Marine Chemistry*, 46, 165-178.

Martin, J.-M., Dai, M.-H and Cauwet, G. (1995) Significance of colloids in the biogeochemical cycling of organic carbon and trace metals in the Venice Lagoon (Italy). *Limnology and Oceanography*, 40, 119-131.

Mayer, L.M., Liotta, F.P. and Norton, S.A. (1982) Hypolimnetic redox and phosphorus cycling in hypereutrophic Lake Sebasticook, Maine. *Water Research*, 16, 1189-1196.

Meade, R.H. (1992) River-sediment inputs to major deltas. In: Rising Sea Level and Subsiding Coasts, Milliman, J.D. (ed.), Wiley, New-York.

Milliman J.D. and Meade, R.H. (1983) World-wide delivery of river sediment to the oceans. *Journal of Geology*, 91, 1-21.

Milliman, J.D. and Syvitski, J.P.M. (1992) Geomorphic/Tectonic control of sediment discharge to the ocean: the importance of small mountainous rivers. *Journal of Geology*, 100, 525-544.

Milliman, J.D. (1997) Blessed dams or damned dams? *Nature*, 386, 325-327.

Moller Jensen L. (1983) Phytoplankton release of extracellular organic carbon, molecular weight composition, and bacterial assimilation. *Marine Ecology Progress Series*, 11, 39-48.

Moore, R.M., Burton, J.D., Williams, P.J. and Young, M.L. (1979) The behaviour of dissolved organic material, iron, manganese in estuarine mixing. *Geochimica et Cosmochimica Acta*, 43, 919-926.

Morel, F.M.M., Dzombak, D.A. and Price, N.M. (1991) Heterogeneous reactions in coastal waters. In: Ocean Margin Processes in Global Change, Mantoura, R.F.C., Martin, J.M., Wollast, R. (eds.), John Wiley & Sons, London, pp. 165-180.

Morgan, J.J. (1967) Chemical equilibria and kinetic properties of manganese in natural waters. In: Principles and Applications of Water and Chemistry, Faust, S.D. and Hunter, J.V. (eds.), Wiley, New York, pp. 561-624.

Morley, N.H., Fay, C.W. and Statham, P.J. (1988) Design and use of a clean shipboard handling system for seawater samples. *Advances in Underwater Technology, Ocean Science and Offshore Engineering*, 16, 283-289.

Morley, N.H., Burton, J.D. and Statham, P.J. (1990) Observations on dissolved trace metals in the Gulf of Lions. In: European River Ocean System, 2nd workshop on the North-West Mediterranean Sea, Blanes (Spain), 6-9 February 1990, Martin, J-M and Barth, H. (eds.), Water Pollution Research Report 20, Commission of the European Communities, Brussels, pp. 309-328.

Morley, N.H., Statham, P.J. and Burton, J.D. (1993) Dissolved trace metals in the south-western Indian Ocean. *Deep-Sea Research*, 40, 1043-1062.

Morley, N.H., Burton, J.D., Tankéré, S.P.C., and Martin, J.-M. (1997) Distribution and behaviour of some dissolved trace metals in the western Mediterranean Sea. *Deep-Sea Research*, 44, 675-692.

Morris, A.W. and Bale, A.J. (1979) Effect of rapid precipitation of dissolved Mn in river water on estuarine Mn distributions. *Nature*, 279, 318-319.

Morris, A.W., Bale, A.J. and Havland, R.J.M. (1982) The dynamics of estuarine manganese cycling. *Estuarine, Coastal and Shelf Science*, 14, 175-192.

Mosetti, R., Zavatarelli, M. and Price, N.B. (1996) Horizontal budgets on the shelf and Otranto Strait. In: Transfer pathways and fluxes of organic matter and related elements in water and sediments of the northern Adriatic Sea and their importance on the eastern Mediterranean Sea, Final report EUROMARGE-AS Project, EU/MAST2, pp. 144-148.

Mowbray, S.R., Rabbi, E. and Price, N.B. (1995) Temporal variability and fluctuations in biogeochemical associations of suspended particulate matter and water from the river Po at Pontelagoscuro. In: 2nd Annual report of the EUROMARGE-AS Project, EU/MAST2, pp. 10-23.

Muller, F.L.L., Tranter, M. and Balls, P.W. (1994) Distribution and transport of chemical constituents in the Clyde estuary. *Estuarine, Coastal and Shelf Science*, 39, 105-126.

Murphy, M. and Riley, J.P. (1962) A modified single solution method for the determination of phosphate in natural waters. *Analytica Chimica Acta*, 27, 31-36.

Murray, J.W., Spell, B. and Paul, B. (1983) The contrasting geochemistry of manganese and chromium in the eastern tropical Pacific Ocean. In: Trace metals in seawater, C.S. Wong, E. Boyle, K.W. Bruland, J.D. Burton and E.D. Goldberg (eds.), Plenum Press, New York, pp. 643-669.

Murray, J.W., Jannasch, H.W., Honjo, S., Anderson, R.F., Reeburgh, W.S., Top, Z., Friederich, G.E., Codispoti, L.A. and E. Izdar (1989) Unexpected changes in the oxic/anoxic interface in the Black Sea. *Nature*, 338, 411-413.

Myers, C.R. and K.H. Nealson (1988a) Bacterial Manganese Reduction and Growth with Manganese Oxide as the Sole Electron Acceptor. *Science*, 240, 1319-1321.

Myers, C.R. and K.H. Nealson (1988b) Microbial reduction of manganese oxides: Interactions with iron and sulfur. *Geochimica et Cosmochimica Acta*, 52, 2727-2732.

Myklestad, S. (1974) Production of carbohydrates by marine planktonic diatoms. I. Comparison of nine different species in culture. *Journal of Experimental Marine Biology and Ecology*, 15, 261-274.

Myklestad, S. (1977) Production of carbohydrates by marine planktonic diatoms. II. Influence of the N/P ratio in the growth medium on the assimilation ratio, growth rate, and production of cellular and extracellular carbohydrates by *Chaetoceros affinis* var. *willei* (Gran) Hustedt and *Skeletonema coatum* (Grev.) Cleve. *Journal of Experimental Marine Biology and Ecology*, 29, 161-179.

Myklestad, S. and Haug, A (1972) Production of carbohydrates by the marine diatom *Chaetoceros affinis* var. *willei* (Gran) Hustedt. I. Effect of the concentration of nutrients in the culture medium. *Journal of Experimental Marine Biology and Ecology*, 9, 125-136.

Myklestad, S., Haug, A and Laersen, B. (1972) Production of carbohydrates by the marine diatom *Chaetoceros affinis* var. *willei* (Gran) Hustedt. II. Preliminary investigation of the extracellular polysaccharide. *Journal of Experimental Marine Biology and Ecology*, 9, 137-144.

Myklestad, S., Holm-Hansen, O., Varum, K.M. and Volcani, B.E. (1989) Rate of release of extracellular amino acids and carbohydrates from the marine diatom *Chaetoceros affinis*. *Journal of Plankton Research*, 11, 763-773.

Nealson, K.H. (1982) Microbiological oxidation and reduction of Iron. In: Mineral Deposits and Evolution of the biosphere, Dahlem Konferenzen, Holland, H.D. and Schidlowski, M. (eds.), Springer-Verlag, pp. 51-56.

Nealson, K.H. and Myers, C.R. (1990) Iron reduction by bacteria: A potential role in the genesis of banded iron formation. *American Journal of Science*, 290A, 35-45.

Neas, E.D. and Collins, M.J. (1988) Theoretical concepts and equipment design. In: Introduction to Microwave Samples Preparation: Theory and Practise, Kingston, H.M. and Jassie, L.B. (eds.), American Chemical Society Professional Reference Book, Washington DC, USA, pp. 7-32.

Neumann, G. (1943) Über den Aufbau und die Frage der Tiefenzirculation des Scharzen Meeres. *Annalen der Hydrographie und Maritimen Meteorologie*, 71, 1-20.

Nicolas, E., Migon, C., Leblond, N. and Journel, B. (1995) Seasonality of dry and wet depositions of trace metals in the Ligurian Sea. In: European River Ocean System, Fifth Workshop on the North-West Mediterranean Sea, Hamburg (Germany), 28-30 March 1994, Martin, J-M and Barth, H. (eds.), Water Pollution Research Report 32, Commission of the European Communities, Brussels, pp. 275-285.

Nimmo, M., van den Berg, C.M.G. and Brown, J. (1989) The chemical speciation of dissolved nickel, copper, vanadium and iron in Liverpool Bay, Irish sea. *Estuarine and Coastal Shelf Science*, 29, 57-74.

Nixon, S.W. (1981) Remineralisation and nutrient cycling in coastal marine ecosystems. In: Nutrient Enrichment in Estuaries, Neilson, B. and Cronin, L.E. (eds.), Humama Press, Clifton, pp. 111-138.

Noriki, S., Ishimori, N., Harada, K. and Tsunogai, S. (1985) Removal of trace metals from seawater during a phytoplankton bloom as studied with sediment traps in Funka Bay, Japan. *Marine Chemistry*, 17, 75-89.

Oeztuerk and Murat (1995) Trends of trace metals (Mn, Fe, Co, Ni, Cu, Zn, Cd and Pb) distributions at the oxic-anoxic interface and in sulphidic water of the Drammensfjord. *Marine Chemistry*, 48, 329-342.

Officer, C.B. and Lynch, D.R. (1981) Dynamics of mixing in estuaries. *Estuarine, Coastal and Shelf Science*, 12, 525-533.

Oguz, T., Latif, M.A., Özsoy, E., Sur, H.I. and Unluata, U. (1991) On the dynamics of the Southern Black Sea. In: Black Sea Oceanography, E. Izdar and J.W. Murray (eds.), NATO/ASI Series, Kluwer Academic Publishers, The Netherlands, pp. 43-63.

Orlic, M., Gacic, M. and La violette, P. (1992) The currents and circulation of the Adriatic Sea. *Oceanologica Acta*, 15(2), 109-124.

Orlic, M., Kuzmic and Pasaric, Z. (1994) Response of the Adriatic Sea to the Bora and Sirocco forcing. *Continental Shelf Research*, 14(1), 91-116.

Ott, J.A. and Herndl, G.J. (1995) Marine snow, mucus aggregates and bottom anoxia: consequences for benthic-pelagic coupling. *Bulletin de l'Institut Océanographique*, Monaco, S15, 133-147.

Ovchinnikov, I.M., Zats, V.I., Krivosheya, V.G. and Udodov, A.I. (1985) A forming of deep eastern Mediterranean water in the Adriatic Sea. *Okeanologija*, 25(6), 911-917.

Ovchinnikov, I.M. and Popov, Y.I. (1987) Evolution of the cold intermediate layer in the Black Sea. *Oceanology*, 27, 555-560.

Passow, U. (1991) Species-specific sedimentation and sinking velocities of diatoms. *Marine Biology*, 108, 449-455.

Paulson, A.J., Curl, H.C. and Gendron, J.F. (1994) Partitioning of Cu in estuarine waters, II. Control of partitioning by the biota. *Marine Chemistry*, 45, 81-93.

Pedersen, T.F. (1985) Early diagenesis of copper and molybdenum in mine tailings and natural sediments in Rupert and Holberg inlets, British Columbia. *Canadian Journal of Earth Science*, 22, 1474-1484.

Pettine, M. (1991) La qualita delle acque del fiume Po negli anni 90. Conference report, CNR Ferrara 1991.

Poniz, P., Malaguti, A., Lippolini, E., Lorenzelli, R., Milandri, A., Ceredi, A. and Honsell, G. (1996) Plankton taxonomy, biomass and primary production: temporal variations as related to salinity and nutrients. In: Transfer pathways and fluxes of organic matter and related elements in water and sediments of the northern Adriatic Sea and their importance on the eastern Mediterranean Sea, Final report EUROMARGE-AS Project, EU/MAST2, pp.69-76

Poulain, P.-M., Gacic, M. and Vetrano, A. (1996) Current measurements in the Strait of Otranto Reveal Unforseen Aspects of its Hydrodynamics. *EOS*, 77 (issue 36), 3-5.

Price, N.B., Mowbray, S., Giordani, P., Frignani, M. and Thompson, R. (1993) Transfer pathways of iron and related elements in the Northern Adriatic sea. Final report for the EUROMARGE-AS MAST1 Project (contract 00018C).

Price, N.B., Mowbray, S., Wilkinson, M., Lindsay, F.S., Stewart, H.R. (1995) Geochemical variations of sediment composition in cores from the western Adriatic shelf, with particular reference to the deposition of anthropogenic heavy metals (Zn, Pb and Cu). In: Transfer pathways and fluxes of organic matter and related elements in water and sediments of the northern Adriatic Sea and their importance on the eastern Mediterranean Sea, 2nd Annual Report for the EUROMARGE-AS Project, EU/MAST2, pp. 172-213.

Price, N.B., Mowbray, S., Rabbi, E. and Pates, J. (1996) Biogeochemistry of trace metals in the River Po. In: Transfer pathways and fluxes of organic matter and related elements in water and sediments of the northern Adriatic Sea and their importance on the eastern Mediterranean Sea, Final report EUROMARGE-AS Project, EU/MAST2, pp.55-63.

Rabitti, S., Boldrin, A., De Lazzari, A. and Turchetto, M. (1994) Suspended matter distribution and dynamics in the Otranto Strait (February-May 1994). In: Extended Abstracts, First workshop of the Mediterranean Targetted Project (Barcelona, November 21-23, 1994), Canals, M. and Lipiatou, E. (eds.), Tesys, Barcelona, Spain, pp. 133-139.

Rantala, R.T.T. and Loring, D.H. (1985) Partition and determination of cadmium, copper, lead and zinc in marine suspended particulate matter. *International Journal in Environmental and analytical Chemistry*, 19, 165-173.

Revelante, N. and Gilmartin, M. (1991) The phytoplankton composition and population enrichment in gelatinous "macroaggregates" in the Northern Adriatic during summer of 1989. *Journal of experimental marine Biology and Ecology*, 146(2), 217-233.

Rich, H.W. and Morel, F.M.M. (1990) Availability of well-defined colloids to the marine diatom *Thalassiosira weissflogii*, *Limnology and Oceanography*, 35, 652-662.

Richert, S.A., Tsang, P.K.S. and Sawyer, D.T. (1988) Ligand-Centered oxidation of manganese II complexes. *Inorganic Chemistry*, 27, 1814-1818.

Roether, W. and Schlitzer, R. (1991) Eastern Mediterranean deep water renewal on the basis of CFM and tritium data. *Dynamics of Atmosphere and oceans*, 15, 333-354.

Ross, D.A., Degens, E.T. and J. MacIlvaine (1970) Black Sea: recent sedimentary history, *Science*, 170, 163-165.

Ross, D.A., Uchupi, E., Prada, K.E. and MacIlvaine, J.C. (1974) Bathymetry and Microtopography of Black Sea. In: The Black Sea: Geology, Chemistry and Biology, Degens, E.T. and Ross, D.A. (eds.), American Association of Petroleum Geologists, Tulsa, Oklahoma, USA, pp. 1-10.

Rosson, R.A., Tebo, B.M. and Nealson, K.H. (1984) Use of poisons in the determination of microbial manganese binding rates in seawater. *Applied and Environmental Microbiology*, 47, 740-745.

Ruiz-Pino, D.P., Nicolas, E., Bethoux, J-P. and Lambert, C.E. (1991) Zinc budget in the Mediterranean Sea: a Hypothesis for non-steady-state behaviour. *Marine Chemistry*, 33, 145-169.

Saager, P.M. (1994) On the relationships between dissolved trace metals and nutrients in seawater. Ph D Thesis, University of Amsterdam, Netherlands, 240 pp.

Salomons, W. (1978) Release of trace metals from anoxic sediments resuspended in oxygenated seawater. Delft Hydraulics Laboratory Report R 1024.

Santschi, P.H. and Honeyman, B.D. (1991) Radioisotopes as tracers for the interactions between trace elements, colloids and particles in natural waters. In: Heavy metals in the environment, Vernet, J.P. (eds.), Elsevier, pp. 229-246.

Sawlan, J.J. and Murray, J.W. (1983) Trace metal remobilization in the interstitial waters of red clay and hemipelagic marine sediments. *Earth and Planetary Science Letters*, 64, 213-230.

Schlemmer, G. and Welz, B. (1986) Palladium and magnesium nitrates, a more universal matrix modifier for graphite furnace atomic absorption spectrometry. *Spectrochimica Acta*, 41B, 1157-1166.

Scoullos, M.J. (1983) Trace metals in a landlocked intermittently anoxic basin. In: Trace metals in seawater, Wong, C.S., Boyle, E., Bruland, K., Burton J.D. and Goldberg, E.D. (eds.), Plenum Press, 351-366.

Sekulic, B. and Vertacnik, A. (1997) Comparison of anthropological and “natural” input of substances through waters into Adriatic, Baltic and Black Sea. *Water research*, 31, 3178-3182.

Shaffer, G. (1986) Phosphate pumps and shuttles in the Black Sea. *Nature*, 321, 515-517.

Shaw, T.J., Gieskes, J.M. and Jahnke, R.A. (1990) Early diagenesis in differing depositional environments: The response of transition metals in pore water. *Geochimica et Cosmochimica Acta*, 54, 1233-1246.

Shiller, A.M. and Boyle, E.A. (1985) Dissolved zinc in rivers. *Nature*, 317, 49-52.

Shiller, A.M. and Boyle, E.A. (1991) Trace elements in the Mississippi River delta outflow region: Behavior at high discharge. *Geochimica et Cosmochimica Acta*, 55, 3241-3251.

Sholkovitz, E.R. and Copeland, D. (1981) The coagulation, solubility and adsorption property of Fe, Mn, Cu, Ni, Cd, Co and humic acids in a river water. *Geochimica et Cosmochimica Acta*, 45, 181-189.

Sigleo, A.C., Hoering, T.C. and Helz, G.R. (1982) Composition of estuarine colloidal material: Organic components. *Geochimica and Cosmochimica Acta*, 46, 1619-1626.

Sigleo, A.C. (1985) Stable isotope and amino-acid composition of estuarine dissolved colloidal material. In: Marine and estuarine geochemistry, A.C. Sigleo and A. Hattori (eds.), Lewis, pp. 29-46.

Smith, K.L., Jr. (1978) Benthic community respiration in the N.W. Atlantic Ocean: in situ measurements from 40-5200 m. *Marine Biology*, 47, 333-347.

Sorokin, Y.I. (1983) The Black Sea. In: Ecosystems of the world: estuaries and enclosed seas, 26, Ketchum, B.H. (ed.), Elsevier, New York, pp. 253-292.

Søndergaard, M. and Jensen, L.M. (1986) Phytoplankton. In: Carbon dynamics in eutrophic, temperate lakes, Riemann, B. and Søndergaard, M. (eds.), Elsevier, pp. 27-126.

Sposito, G. (1985) Sorption of trace metals by humic material in soils and natural waters. CRC Critical Reviews in Environmental Control, 16(2).

Stachowitsch, M. (1984) Mass mortality in the Gulf of Trieste: the course of community destruction. *Marine Ecology*, 5, 243-264.

Stachowitsch, M., Fanuko, N. and Richter, M. (1990) Mucus aggregates in the Adriatic Sea, an overview of stages and occurrences. *Marine Ecology*, 11(4), 327-350.

Stancik, A., Iovanovic, S., Sikora, A., Urge, L. and Miklos, D. (1988) Hydrology of the River Danube, Bratislava, Priroda Publ. House, 272 pp.

Staresinic, N., Zvonaric, T. and Benovic, A. (1983) Particulate organic matter sedimentation in the middle Adriatic Sea. *Thalassia Jugoslavia*, 19, 343-349.

Statham, P.J. (1985) The determination of dissolved manganese and cadmium in seawaters at low nM concentrations by chelation and extraction followed by electrothermal atomic absorption spectrometry. *Analytica Chimica Acta*, 169, 149-159.

Stoyanov, A. (1991) Features of 0-200 m layer in the Western deep water zone of the Black Sea. C.R. Acad. Bulg. Sci., 44, 70-73.

Strakhov, N.M. (1961) Onekotroykh zakonomemostiakh denudatsii i perenosa osadochnogo materiala na ploshchadyakh gymidnykh klimatov. In: Sovremennye osadki moei i oceanov, Strakov, N.M., Bezrykov, P.L and Yablokov, V.S. (eds.), Izdatelstvo Akademii Nauk SSSR, Moscow, pp. 5-27.

Strickland J.D.H. and Parsons, T.R. (1977) A practical handbook of seawater analysis. *Bulletin of Fisheries Research*, 167, 2nd Edition, pp. 310.

Stumm, W. and Sulzberger, B. (1992) The cycling of iron in natural environments: Considerations based on laboratory studies of heterogeneous redox processes. *Geochimica et Cosmochimica Acta*, 56, 3233-3257.

Stumm, W. (1993) Aquatic colloids as chemical reactants: surface structure and reactivity. *Colloids and Surfaces A: Physicochemical and Engineering Aspects*, 73, 1-18.

Stumm, W. and Morgan, J.J. (1996) Aquatic chemistry: Chemical equilibria and rates in Natural Waters. J. Wiley & Sons, New York, pp. 1022.

Sunda, W.G., Huntsman, S.A. and Harvey, G.R. (1983) Photoreduction of manganese oxides in seawater and its geochemical and biological implications. *Nature*, 301, 234-236.

Sunda, W.G. and Huntsman, S.A. (1987) Microbial oxidation of manganese in a North Carolina estuary. *Limnology and Oceanography*, 32, 552-564.

Sunda, W.G. and Huntsman, S.A. (1988) Effect of sunlight on redox cycles of manganese in the south-western Sargasso Sea, *Deep-Sea Research*, 35, 1297-1317.

Sunda, W.G. and Huntsman, S.A. (1994) Photoreduction of manganese oxides in seawater. *Marine Chemistry*, 46, 133-152.

Sundby, B., Andersson, L.G., Hall, P.O.J., Iverfeld, A., Rutgers van der Loeff, M.M. and Westerlund, S.F.G. (1986) The effect of oxygen on release and uptake of cobalt, manganese, iron and phosphate at the sediment-water interface. *Geochimica et Cosmochimica Acta*, 50, 1281-1288.

Sung, W. (1995) Some observations on surface partitioning of Cd, Cu and Zn in estuaries. *Environmental Science and Technology*, 29, 1303-1312.

Sur, H.İ., Özsoy, E., Ilyin, Y.P. and Ünlüata, Ü. (1996) Coastal/deep ocean interactions in the Black Sea and their ecological/environmental impacts. *Journal of Marine Systems*, 7, 293-320.

Tankéré, S.P.C., Morley, N.H. and Burton, J.D. (1995) Spatial and temporal variations in concentrations of trace metals in the regions of the Strait of Sicily and Gibraltar. In: European River Ocean System, Fifth Workshop on the North-West Mediterranean Sea, Hamburg (Germany), 28-30 March 1994, Martin, J-M and Barth, H. (eds.), Water Pollution Research Report 32, Commission of the European Communities, Brussels, pp. 205-219.

Tankéré, S.P.C. and Statham, P.J. (1996) Distribution of dissolved Cd, Cu, Ni and Zn in the Adriatic Sea. *Marine Pollution Bulletin*, 32, 623-630.

Tappin, A.D., Millward, G.E., Statham, P.J., Burton, J.D. and Morris, A.W. (1995) Trace Metals in the Central and Southern North Sea. *Estuarine, Coastal and Shelf Science*, 41, 275-323.

Tebo, B.M. and Emerson, S. (1986) Microbial manganese (II) oxidation in the marine environment: a quantitative study. *Biogeochemistry*, 2, 149-161.

Tebo, B.M. (1991) Manganese(II) oxidation in the suboxic zone of the Black Sea. *Deep-Sea Research*, 38, S883-S905.

Tessier, A., Campbell, P.G.C. and Bisson, M. (1979) Sequential extraction procedure for the speciation of particulate trace metals. *Analytical Chemistry*, 51, 844-851.

Tiller, C.L. and O'Melia, C.R. (1993) Natural organic matter and colloidal stability: models and measurements. *Colloids and Surfaces A: Physicochemical and Engineering Aspects*, 73, 89-102.

Tipping, E. and Ohnstad, M. (1984) Colloid stability of iron particles from fresh water lake. *Nature*, 308, 266-268.

Tipping, E. and Higgins, D.C. (1982) The effect of adsorbed humic substances on the colloid stability of hematite particles. *Colloids Surfaces*, 5, 85-92.

Tolmazin, D. (1985) Changing coastal oceanography of the Black Sea I: North-western Shelf. *Progress in Oceanography*, 15, 217-276.

Turekian, K.K. (1977) The fate of metals in the ocean. *Geochimica et Cosmochimica Acta*, 41, 1139-1144.

Turner, A., Millward, G.E., Bale, A.J. and Morris, A.W. (1992) The solid-solution partitioning of trace metals in the southern North Sea - in situ radiochemical experiments-. *Continental Shelf Research*, 12, 1311-1329.

UNEP/ECE/UNIDO/FAO/UNESCO/WHO/IAEA (1984) Pollutants from Land-Based Sources in the Mediterranean. *UNEP Regional Seas Reports and Studies*, 32, UNEP.

Van den Berg, C.M.G. and Nimmo, M. (1987) Determination of interactions of nickel with dissolved organic material in seawater using cathodic stripping voltammetry. *Science of the Total Environment*, 60, 185-195.

Vasiliu F.L. (1980) La production des espèces d' *Enteromorpha* du littoral roumain de la mer Noire. *Cercetari marine*, 13, 147-161.

Von Bodungen, B. and Humborg, C. (1996) In: EROS 2000 report; the interactions between the river Danube and the north-western Black Sea, pilot phase (1994-1996).

Waite, T.D. and Morel F.M.M. (1984) Photoreductive dissolution of colloidal iron oxides in natural waters. *Environmental Science and Technology*, 18, 860-868.

Weilenmann, U., O'Melia, C.R. and Stumm, W. (1984) Particle transport in lakes: Models and measurements. *Limnology and Oceanography*, 34, 1-18.

Westerlund, S.F.G., Anderson, L.G., Hall, P.O., Verfeldt, A.I., Van der Looff, M.M.R. and Sundby, B. (1986) Benthic fluxes of cadmium, cobalt, nickel, zinc and lead in the coastal environment. *Geochimica et Cosmochimica Acta*, 50, 1289-1296.

Windom, H., Wallace, G., Smith, R., Dudek, N., Maeda, M., Dulmage, R. and Storti, F. (1983) Behaviour of copper in south-eastern United States estuaries. *Marine Chemistry*, 12, 183-193.

Windom, H., Smith, R., Rawlinson, C., Hungspreugs, M., Dharmvanij, S. and Wattayakom, G. (1988) Trace metal transport in a tropical estuary, *Marine Chemistry*, 24, 293-305.

Windom, H., Byrd, J., Jr. Smith, R., Hungspreugs, M., Dharmvanij, S., Thumtrakul, W. and Yeats, P. (1991) Trace metal-nutrient relationships in estuaries. *Marine Chemistry*, 32, 177-194.

Wollast, R. (1981) Redox processes in estuaries. In: River inputs to Ocean System, Martin, J-M., Burton, J.D. and Eisma, D. (eds.), UNEP and UNESCO, pp. 211-222.

Yeats, P.A., Sundby, B. and Bewers, J.M. (1979) Manganese recycling in coastal waters, *Marine Chemistry*, 8, 43-55.

Yoon, Y.Y., Martin, J.-M. Martin and Cotte, M.H. (1995) Dissolved trace metals in the western Mediterranean Sea: total concentration and speciation. In: European River Ocean System, Fifth Workshop on the North-West Mediterranean Sea, Hamburg (Germany), 28-30 March 1994, Martin, J-M and Barth, H. (eds.), Water Pollution Research Report 32, Commission of the European Communities, Brussels, pp. 235-251.

Zaitsev Y. (1979) Problèmes biologiques de la partie nord-ouest de la mer Noire. *Cercetari marine*, 12, 7-32.

Zehnder, A.J.B., Wehrli, B., Friedl, G. and Dinkel, C. (1996) In: EROS 2000 report; the interactions between the river Danube and the north-western Black Sea, pilot phase (1994-1996).

Zhorov, V.A. and Boguslavky (1985) Tendentsii nekotorykh gidrologo-gidrokhimicheskikh protsessov Chernogo Morya (Trends of certain hydrologic-hydrochemical processes of the Black Sea), *Meteorologiya I Gidrologiya*, 11, 63-69.

Zhorov, V.A., Eremeyev, V.N., Boguslasky, S.G. and Kalashnikova, Y.S. (1984) Osebennosti raspredeleniya i prostranstvenno-vremennaya izmenchivost polya

serovodoroda v Chernom More (distribution and spatial-temporal variability of the hydrogen sulfide zone in the Black Sea), *Geokhimiya*, 3, 421-429.

Zoccolotti, L. and Salusti, E. (1987) Observations of a vein of very dense marine water in the southern Adriatic Sea. *Continental Shelf Research*, 7, 535-551.

Zore-Armanda, M. (1963) Les masses d'eau de la mer Adriatique. *Acta Adriatica*, 10, 3, 5-88.

APPENDIX I

EUROMARGE-AS DATA BASE

Description of some parameters:

Code: code number for each sample

Type: M = samples have been collected manually

Kv = samples have been collected with clean Go-Flo bottles deployed on a Kevlar line

CTD = samples have been collected with Go-Flo bottles deployed on a rosette fitted with CTD instrumentation

EDIN = river Po samples which have been collected by the Edinburgh group

SOTON = river Po samples which have been collected manually by the Southampton group

Station: name of the station

TM bottle: bottle number for trace metal samples

Date: sampling date for each sample

Tables AI1a and AI1b: May cruise 11/5/1994 - 16/5/1994 in the Northern Adriatic Sea

Samples were collected for trace metals, nutrients and salinity on board N/O Daphne II at stations: 1 and 2 (see Fig. 4.1). A small CTD instrumentation system giving salinity, temperature, oxygen, Chl α and pH was deployed. Density has been calculated from salinity and temperature with tables (Knauss, 1978).

Samples were collected at stations 3 (see Fig. 4.1) on board N/O Salvatore Lo Bianco. CTD instrumentation giving salinity, temperature and oxygen was deployed. Density has been calculated from salinity and temperature with tables (Knauss, 1978).

Tables AI2a and AI2b: June cruise 25/6/1994 - 3/7/1994 in the Adriatic Sea

Samples were collected for trace metals and salinity on board N/O URANIA at stations: 1, 2, 3, 4, 5, 10 (see Fig. 4.1). CTD instrumentation, giving the following parameters: salinity, temperature, density, chl a and turbidity, was deployed.

Tables AI3a and AI3b: July cruise 7/7/1994 - 8/7/1994 in the Northern Adriatic Sea

Samples were collected for trace metals and salinity on board N/O DAPHNE II at stations 1A and 2A (see Fig. 4.1). The CTD instrumentation was giving the following parameters: salinity, temperature, oxygen, Chl α and pH.

Tables AI4a and AI4b: September cruise 27/9/1994 - 1/10/1994 in the Northern Adriatic Sea

Sampling strategy was the same as in May cruise. The only difference was that the CTD for station 3 was giving the following parameters: salinity, temperature and density.

Tables AI5a and AI5b: November cruise 11/11/1994 - 25/11/1994 in the Strait of Otranto

Samples were collected for trace metals and salinity on board RV AEGAIO in the Strait of Otranto at different stations (Fig. 4.2). CTD instrumentation was giving the following parameters: salinity, temperature and density. During this cruise, it was not possible to pressurise the Go-Flo bottles with nitrogen gas. Consequently those samples were collected in 1l cleaned polyethylene bottles from the Go-Flo bottles and filtered through Nuclepore filters with a Teflon filter holder fitted on a chamber which was connected to a vacuum pump.

Tables AI6a and AI6b: February cruise 15/2/1995 - 17/2/1995 in the Northern Adriatic Sea

The sampling strategy was the same as in September cruise.

Tables AI7a and AI7b: River Po sampling

River Po samples were collected monthly. The Southampton group collected the samples manually (see chapter 3) from a bridge at Pontelagoscuro whereas the Edinburgh group collected them in cleaned polyethylene bottles using a pump from a boat. The flow rates were given by the Azendia Regionale per la Navigazione Internale (ARNI).

Tables AI8, AI9, AI10, AI11: Pore water sampling

Pore water samples were collected in February 1994 and June 1994 on board URANIA at stations 1, 2, 3, 4, and 5. They were collected in September 1994 and February 1995 on board DAPHNE II for stations 1 and 2 and on board N/O Salvatore Lo Bianco for station 3.

Table A1a: General sample parameters (Cruise May 1994)

Code	Type	Station	Depth m	TM bottle	Date d/m/y	Latitude °N	Longitude °E	Salinity psu	Temperature °C	Sigma theta kg/m ³	O ₂ %	pH	Chl. a µg/l
EM 1	M	1	0	9	05/11/94	44.5442	12.4506						
EM 2	Kv	1	0	8	05/11/94	44.5442	12.4506						
EM 3	Kv	1	3	7	05/11/94	44.5442	12.4506	31.33	17.19	22.69	102.8	8.37	1.94
EM 4	Kv	1	6	6	05/11/94	44.5442	12.4506	31.29	17.19	22.65	103.2	8.37	3.26
EM 5	Kv	1	9	3	05/11/94	44.5442	12.4506	31.96	16.20	23.39	105.3	8.36	5.88
EM 6	Kv	1	12	5	05/11/94	44.5442	12.4506	34.18	13.28	25.73	106.1	8.31	5.54
EM 7	Kv	1	16	4	05/11/94	44.5442	12.4506	34.75	12.11	26.40	90.0	8.17	2.24
EM 8	M	2	0	12	13/5/94	44.3070	12.5782						
EM 9	Kv	2	3	19	13/5/94	44.3070	12.5782	30.22	17.43	21.78	107.8	8.38	1.52
EM 10	Kv	2	6	14	13/5/94	44.3070	12.5782	30.05	17.41	21.66	108.0	8.38	2.46
EM 11	Kv	2	9	13	13/5/94	44.3070	12.5782	31.24	15.73	22.94	107.3	8.34	3.79
EM 12	Kv	2	12	11	13/5/94	44.3070	12.5782	31.73	15.34	23.41	114.2	8.33	3.67
EM 13	Kv	2	15	18	13/5/94	44.3070	12.5782	32.41	14.47	24.12	111.9	8.29	4.18
EM 14	Kv	2	18	16/17	13/5/94	44.3070	12.5782	32.86	12.07	24.94	92.6	8.11	2.69
EM 15	M	3	0	70	16/5/94	43.7175	13.4347						
EM 16	Kv	3	1	74	16/5/94	43.7175	13.4347	36.35	16.38	26.73	143.6		
EM 17	Kv	3	3	72	16/5/94	43.7175	13.4347	36.36	16.37	26.73	143.7		
EM 18	Kv	3	6	55	16/5/94	43.7175	13.4347	36.36	16.37	26.73	143.3		
EM 19	Kv	3	9	75	16/5/94	43.7175	13.4347	37.34	15.31	27.72	144.7		
EM 20	Kv	3	12	23	16/5/94	43.7175	13.4347	37.65	14.39	28.18	147.4		
EM 21	Kv	3	15	22	16/5/94	43.7175	13.4347	37.94	14.27	28.42	146.2		
EM 22	Kv	3	18	20	16/5/94	43.7175	13.4347	37.92	14.01	28.46	140.3		

Table A11b: Dissolved trace metals and other parameters (Cruise May 1994)

Code	MnD Nm	FeD nM	CoD nM	PbD nM	CdD nM	ZnD nM	NiD nM	CuD nM	Salinity (measured)	PO ₄ ³⁻ μM	NO ₃ ⁻ +NO ₂ ⁻ μM
EM 1	22.78	1.05	1.034	0.248	0.173	10.42	14.70	12.97	32.917		
EM 2	22.02	10.65	1.018	0.184	0.160	22.19	15.62	14.29	32.917	0.03	10.22
EM 3	24.65	10.97	1.071	0.204	0.172	9.95	16.67	11.36	32.931	0.05	10.75
EM 4	24.46	3.55	0.902	0.280	0.186	25.67	13.95	11.44	32.931	0.14	10.32
EM 5	22.98	8.23	0.854	0.135	0.141	6.95	14.41	11.60	33.035	0.04	9.89
EM 6	20.18	4.65	0.625	0.145	0.131	6.47	11.16	8.30	34.852	0.47	7.20
EM 7	54.04	15.15	0.749	0.053	0.149	13.17	10.12	7.53	36.659	0.15	4.30
EM 8	20.38	1.53	0.956	1.701	0.169	7.92	14.50	10.99		0.16	8.60
EM 9	20.46	1.62	0.971	0.095	0.160	10.47	14.58	10.70	33.222	0.15	8.71
EM 10	20.03	1.59	0.967	0.121	0.146	10.25	15.38	11.41	33.247	0.24	8.92
EM 11	15.26	1.32	0.825	0.080	0.132	8.64	12.99	8.82	34.103	0.16	7.31
EM 12	13.16	1.14	0.628	0.090	0.109	7.17	10.81	6.89	34.898	0.24	6.66
EM 13	13.62	1.59	0.485	0.091	0.094	6.83	8.88	5.26	35.900	0.20	3.60
EM 14	57.67	5.33	0.805	0.041	0.149	9.81	9.90	6.92	36.683	0.17	4.19
EM 15	42.26	2.72	0.543	0.096	0.102	3.67	7.59	5.39	36.275	0.07	1.93
EM 16	32.26	1.60	0.481	0.062	0.116	3.80	10.54	6.37	36.975	0.02	1.07
EM 17	40.63	3.03	0.401	0.104	0.087	10.06	9.47	5.57	36.819	0.08	1.29
EM 18	39.39	3.20	0.470	0.085	0.087	6.35	9.71	5.28	36.837	0.12	1.29
EM 19	20.86	2.17	0.297	0.087	0.075	7.23	7.55	3.62	37.448	0.06	0.43
EM 20	17.20	1.86	0.235	0.069	0.075	4.92	7.03	3.14	37.606	0.08	0.22
EM 21	37.26	5.12	0.285	0.072	0.087	7.72	7.55	3.48	37.769	0.05	0.22
EM 22	45.53	6.39	0.320	0.060	0.077	6.18	7.08	3.54	37.825	0.06	0.11

Table AI2a: General sample parameters (Cruise June 1994)

Code	Type	Station	Depth	TM bottle	Date	Latitude	Longitude	Salinity	Temperature	Sigma theta	Turbidity	Chl. a
			m		d/m/y	°N	°E	psu	°C	kg/l	mFTU	µg/l
EM 23	CTD	1	2	80	07/03/94	44.5433	12.4514	32.60	24.06	21.81	3789	2.20
EM 24	CTD	1	5	86	07/03/94	44.5433	12.4514	33.36	23.35	22.59	2908	4.54
EM 25	CTD	1	7	81	07/03/94	44.5433	12.4514	33.69	22.35	23.12	4745	1.12
EM 26	CTD	1	10	96	07/03/94	44.5433	12.4514	35.47	19.07	25.36	3934	4.22
EM 27	CTD	1	12	83	07/03/94	44.5433	12.4514	35.98	18.52	25.89	1317	3.01
EM 28	CTD	1	14	84	07/03/94	44.5433	12.4514	36.17	18.39	26.07	656	1.35
EM 29	CTD	1	17	85	07/03/94	44.5433	12.4514	37.47	17.40	27.32	717	0.43
EM 30	CTD	2	2	54	07/02/94	44.3079	12.5792	32.96	24.73	21.88	2279	3.42
EM 31	CTD	2	5	2860	07/02/94	44.3079	12.5792	33.11	23.86	22.26	2776	4.86
EM 32	CTD	2	7	2857	07/02/94	44.3079	12.5792	34.13	21.91	23.58	2421	5.26
EM 33	CTD	2	10	2858	07/02/94	44.3079	12.5792	35.12	20.12	24.83	1769	3.37
EM 34	CTD	2	14	2850	07/02/94	44.3079	12.5792	35.86	19.51	25.55	589	1.00
EM 35	CTD	2	17	2856	07/02/94	44.3079	12.5792	36.49	18.67	26.25	2624	0.49
EM 36	CTD	3	2	50	07/01/94	43.7152	13.4460	34.47	23.42	23.41	1494	1.99
EM 37	CTD	3	7	51	07/01/94	43.7152	13.4460	35.12	23.33	23.93	1492	2.15
EM 38	CTD	3	10	52	07/01/94	43.7152	13.4460	36.15	23.67	24.61	1099	1.33
EM 39	CTD	3	12	53	07/01/94	43.7152	13.4460	36.21	23.42	24.73	926	1.51
EM 40	CTD	3	15	2851	07/01/94	43.7152	13.4460	36.55	20.78	25.74	673	1.24
EM 41	CTD	3	17	2852	07/01/94	43.7152	13.4460	36.58	20.73	25.77	644	1.43
EM 42	CTD	10	5	49	29/6/94	42.8396	14.7413	38.04	23.59	26.07	467	0.14
EM 43	CTD	10	25	48	29/6/94	42.8396	14.7413	38.11	14.59	28.47	591	0.22
EM 44	CTD	10	50	47	29/6/94	42.8396	14.7413	38.23	13.11	28.88	538	0.76
EM 45	CTD	10	75	46	29/6/94	42.8396	14.7413	38.37	12.97	29.01	148	0.51
EM 46	CTD	10	100	45	29/6/94	42.8396	14.7413	38.52	12.96	29.13	136	0.18
EM 47	CTD	10	150	44	29/6/94	42.8396	14.7413	38.51	12.26	29.27	362	0.04
EM 48	CTD	10	200	43	29/6/94	42.8396	14.7413	38.44	11.44	29.37	801	0.04
EM 49	CTD	10	240	42	29/6/94	42.8396	14.7413	38.42	11.31	29.38	3614	0.04
EM 50	CTD	4	5	39	27/6/94	42.2339	14.9203	36.24	23.71	24.67	535	0.36
EM 51	CTD	4	11	37	27/6/94	42.2339	14.9203	37.86	21.72	26.48	352	0.15
EM 52	CTD	4	20	38	27/6/94	42.2339	14.9203	37.77	18.70	27.22	751	0.37
EM 53	CTD	4	26	36	27/6/94	42.2339	14.9203	37.85	16.15	27.91	440	0.30

Code	Type	Station	Depth	TM bottle	Date	Latitude	Longitude	Salinity	Temperature	Sigma theta	Turbidity	Chl. a
			m		d/m/y	°N	°E	psu	°C	kg/m ³	mFTU	µg/l
EM 54	CTD	4	29	35	27/6/94	42.2339	14.9203	38.00	15.43	28.19	428	0.27
EM 55	CTD	4	43	34	27/6/94	42.2339	14.9203	38.03	13.54	28.63	412	0.52
EM 56	CTD	4	56	41	27/6/94	42.2339	14.9203	38.08	13.08	28.76	311	0.85
EM 57	CTD	4	66	28	27/6/94	42.2339	14.9203	38.12	12.91	28.83	350	0.55
EM 58	CTD	4	71	40	27/6/94	42.2339	14.9203	38.15	12.77	28.88	1432	0.48
EM 59	CTD	5	7	31	25/6/94	41.8698	17.3933	38.02	21.71	26.60	330	0.08
EM 60	CTD	5	42	32	25/6/94	41.8698	17.3933	38.54	13.79	28.97	505	0.44
EM 61	CTD	5	44	29	25/6/94	41.8698	17.3933	38.55	13.74	28.99	501	0.47
EM 62	CTD	5	45	25	25/6/94	41.8698	17.3933	38.55	13.69	29.00	478	0.48
EM 63	CTD	5	54	24	25/6/94	41.8698	17.3933	38.59	13.41	29.09	676	1.43
EM 64	CTD	5	55	30	25/6/94	41.8698	17.3933	38.60	13.40	29.10	647	1.54
EM 65	CTD	5	200	27	25/6/94	41.8698	17.3933	38.70	13.40	29.18	89	0.04
EM 66	CTD	5	900	33	25/6/94	41.8698	17.3933	38.61	12.70	29.26	79	0.03
EM 67	CTD	5	950	26	25/6/94	41.8698	17.3933	38.60	12.63	29.26	82	0.04

Table AI2b: Dissolved trace metals and other parameters (Cruise June 1994)

Code	MnD nM	FeD nM	CoD nM	PbD nM	CdD nM	ZnD nM	NiD nM	CuD nM	Salinity (measured)
EM 23	12.88	0.27	0.577	0.116	0.135	7.35	11.29	24.40	32.615
EM 24	18.49	0.15	0.617	0.101	0.122	3.58	10.07	9.84	33.849
EM 25	35.36	0.27	0.710	0.071	0.124	3.67	9.51	8.47	34.845
EM 26	133.02	4.32	1.023	0.072	0.139	6.86	9.98	8.26	35.745
EM 27	127.48	3.38	0.995	0.078	0.131	6.63	9.81	8.21	35.687
EM 28	113.91	4.03	0.948	0.066	0.121	7.05	10.79	8.24	35.936
EM 29	192.27	16.36	0.770	0.051	0.102	5.66	8.66	6.52	37.250
EM 30	20.69	0.11	0.740	0.102	0.094	4.10	11.95	17.56	33.011
EM 31	19.64	0.18	0.668	0.083	0.086	2.33	13.01	10.49	33.186
EM 32	24.64	0.09	0.506	0.098	0.079	2.87	8.42	7.31	34.511
EM 33	32.94	0.23	0.447	0.080	0.077	3.34	7.70	6.56	35.214
EM 34	36.44	1.81	0.426	0.117	0.071	4.58	7.26	5.76	35.848
EM 35	101.10	15.39	0.535	0.076	0.079	4.00	7.14	6.06	36.430
EM 36	21.32	0.05	0.577	0.099	0.079	4.82	9.11	7.52	34.044
EM 37	22.25	0.17	0.699	0.093	0.082	2.63	10.60	7.30	33.776
EM 38	22.18		0.617	0.103	0.084	3.07	8.56	6.65	34.374
EM 39	29.30	0.30	0.620	0.095	0.085	3.56	8.91	7.32	34.610
EM 40	45.39	1.88	0.696	0.092	0.084	3.05	8.92	7.24	34.697
EM 41	104.00	5.46	0.705	0.092	0.083	4.98	8.29	6.81	36.323
EM 42	9.14	1.95	0.265	0.088	0.065	2.57	5.90	4.61	38.075
EM 43	4.82	0.14	0.209	0.054	0.065	1.98	5.98	2.99	38.108
EM 44	2.92	0.48	0.121	0.049	0.062	4.62	5.39	2.74	38.222
EM 45	1.86	0.43	0.091	0.037	0.061	2.79	5.54	2.67	38.315
EM 46	0.88	0.67	0.005	0.033	0.065	3.72	5.71	2.52	38.536
EM 47	0.77	0.68	0.029	0.028	0.076	2.68	6.06	2.94	38.516
EM 48	1.04	0.30	0.023	0.022	0.086	2.82	6.65	3.53	38.445
EM 49	6.19	1.25	0.034	0.018	0.090	2.91	6.51	3.68	38.413
EM 50	32.65	1.77	0.485	0.149	0.071	3.99	6.28	4.83	36.369
EM 51	25.56	5.29	0.347	0.057	0.065	6.21	6.09	3.74	37.824
EM 52	20.54	3.28	0.314	0.081	0.063	4.16	6.00	3.45	37.814
EM 53	12.72	2.53	0.256	0.075	0.067	3.73	6.04	3.54	37.984

Code	MnD	FeD	CoD	PbD	CdD	ZnD	NiD	CuD	Salinity
	nM	nM	nM	nM	nM	nM	nM	nM	(measured)
EM 54	9.65	1.88	0.160	0.042	0.061	3.24	6.45	3.35	38.019
EM 55	8.81	1.06	0.192	0.041	0.066	2.18	5.99	3.28	38.058
EM 56	5.59	1.11	0.124	0.026	0.052	4.04	5.41	2.34	38.108
EM 57	5.18	1.47	0.162	0.033	0.069	2.62	6.55	3.19	38.144
EM 58	16.50	0.66	0.154	0.040	0.058	4.72	6.19	3.12	38.118
EM 59	9.80	1.21	0.219	0.072	0.057	2.48	6.05	3.23	38.106
EM 60	1.10	0.50	0.027	0.046	0.065	14.95	5.68	2.53	38.570
EM 61	1.41	0.89	0.072	0.099	0.058	3.68	5.16	2.12	38.574
EM 62	0.54	0.67	0.024	0.043	0.058	5.13	5.38	2.29	38.580
EM 63	0.56	0.50	0.024	0.041	0.057	4.38	5.49	2.42	38.607
EM 64	1.50	0.55	0.050	0.134	0.053	1.63	5.46	1.99	38.628
EM 65	0.29	0.36	0.019	0.049	0.047	2.63	5.10	1.74	38.712
EM 66	0.44	0.30	0.041	0.043	0.053	18.14	5.94	2.19	38.638
EM 67	1.08	1.11		0.069	0.070	10.81	5.16	2.85	38.628

Table A13a: General sample parameters (Cruise July 1994)

Code	Type	Station	Depth	TM bottle	Date	Latitude	Longitude	Salinity	Temperature	Sigma theta	O ₂	Chl. a	pH
			m	d/m/y		°N	°E	psu	°C	kg/m ³	%	µg/l	
EM 68	M	1A	0	105	07/07/94	44.7448	12.4383						
EM 69	Kv	1A	3	109	07/07/94	44.7448	12.4383	32.87	26.29	21.37	129.7	8.26	8.78
EM 70	Kv	1A	6	103	07/07/94	44.7448	12.4383	35.13	23.09	24.03	135.2	6.53	8.65
EM 71	Kv	1A	9	107	07/07/94	44.7448	12.4383	35.19	20.17	24.89	128.3	5.31	8.60
EM 72	Kv	1A	12	104	07/07/94	44.7448	12.4383	35.80	19.11	25.63	109.9	8.52	8.60
EM 73	Kv	1A	15	118	07/07/94	44.7448	12.4383	36.83	18.78	26.50	105.8	7.07	8.55
EM 74	Kv	1A	18	123	07/07/94	44.7448	12.4383	37.50	17.01	27.46	63.5	4.17	8.14
EM 75	M	2A	0	119	07/08/94	44.1142	12.7776						
EM 76	Kv	2A	3	111	07/08/94	44.1142	12.7776	33.09	25.64	21.74	126.9	1.60	8.53
EM 77	Kv	2A	6	112	07/08/94	44.1142	12.7776	33.56	25.22	22.22	130.6	1.76	8.53
EM 78	Kv	2A	9	116	07/08/94	44.1142	12.7776	34.61	22.22	23.88	138.2	1.90	8.50
EM 79	Kv	2A	12	115	07/08/94	44.1142	12.7776	35.73	19.95	25.37	136.5	2.89	8.47
EM 80	Kv	2A	15	113	07/08/94	44.1142	12.7776	36.71	18.78	26.41	111.7	5.31	8.38
EM 81	Kv	2A	17	114	07/08/94	44.1142	12.7776	36.73	18.79	26.42	95.9	5.25	8.36

Table A13b: dissolved trace metals and other parameters (Cruise July 1994)

Code	MnD nM	FeD nM	CoD nM	PbD nM	CdD nM	ZnD nM	NiD nM	CuD nM	Salinity (measured)
EM 68	141.81	0.54	1.672	0.168	0.114	3.46	31.84	18.78	17.512
EM 69	27.25	0.96	0.752	0.149	0.112	3.49	14.52	8.88	30.448
EM 70	15.76	0.96	0.544	0.142	0.113	7.05	8.86	6.45	34.600
EM 71	14.07	0.86	0.564	0.111	0.118	5.31	10.70	6.49	35.089
EM 72	9.33	0.23	0.425	0.178	0.097	3.66	8.89	5.34	35.510
EM 73	80.42	10.57	0.502	0.101	0.102	5.53	9.12	5.50	36.568
EM 74	1393.68	55.41	1.677	0.096	0.094	11.96	13.31	6.90	37.190
EM 75	24.55	0.24	0.727	0.134	0.108	5.15	12.71	14.16	32.774
EM 76	19.48	0.47	0.650	0.136	0.106	7.19	12.85	8.63	32.824
EM 77	14.98	0.05	0.569	0.112	0.099	4.69	13.71	7.77	33.216
EM 78	10.28	0.08	0.493	0.084	0.099	4.20	10.69	6.45	34.197
EM 79	11.78	0.86	0.482	0.073	0.097	4.98	8.31	5.33	35.252
EM 80	22.09	4.77	0.540	0.043	0.102	7.45	8.73	5.74	36.055
EM 81	23.22	3.47	0.586	0.075	0.128	6.15	9.21	5.86	36.174

Table A14a: General sample parameters (Cruise September 1994)

Code	Type	Station	Depth	TM bottle	Date	Latitude	Longitude	Salinity	Temperature	Sigma theta	O ₂	Chl. a	pH
			m		d/m/y	°N	°E	psu	°C	kg/m ³	%	µg/l	
EM 82	M	1	0	97	27/9/94	44.5442	12.4506						
EM83	M	1	1	200	27/9/94	44.5442	12.4506	26.59	21.38	18.05	139.0	15.64	8.65
EM 84	Kv	1	3	95	27/9/94	44.5442	12.4506	33.26	21.16	23.16	140.6	23.68	8.48
EM 85	Kv	1	6	94	27/9/94	44.5442	12.4506	35.43	21.34	24.76	118.9	11.28	8.38
EM 86	Kv	1	9	89	27/9/94	44.5442	12.4506	35.85	20.98	25.17	103.7	6.90	8.34
EM 87	Kv	1	12	92	27/9/94	44.5442	12.4506	36.20	20.95	25.44	94.0	7.12	8.32
EM 88	Kv	1	15	93	27/9/94	44.5442	12.4506	36.41	21.15	25.55	86.8	4.50	8.30
EM 89	Kv	1	18	88	27/9/94	44.5442	12.4506	36.68	20.53	25.93	75.3	3.04	8.19
EM 90	M	2	0.5	203	28/9/94	44.3070	12.5782						
EM 91	Kv	2	3	206	28/9/94	44.3070	12.5782	34.59	21.51	24.08	116.1	11.07	8.45
EM 92	Kv	2	6	205	28/9/94	44.3070	12.5782	36.16	21.58	25.24	107.4	5.85	8.35
EM 93	Kv	2	9	202	28/9/94	44.3070	12.5782	36.44	21.49	25.49	94.2	3.98	8.33
EM 94	Kv	2	12	204	28/9/94	44.3070	12.5782	36.52	21.36	25.59	90.4	3.54	8.32
EM 95	Kv	2	15	207	28/9/94	44.3070	12.5782	36.66	20.74	25.85	87.9	2.98	8.28
EM 96	Kv	2	18	208	28/9/94	44.3070	12.5782	36.71	20.50	25.95	77.3	1.99	8.25
EM 97	M	3	0	218	10/01/94	43.7175	13.4347						
EM 98	M	3	1	219	10/01/94	43.7175	13.4347	34.58	21.73	23.97			
EM 99	Kv	3	3	212	10/01/94	43.7175	13.4347	35.45	20.72	24.91			
EM 100	Kv	3	6	213	10/01/94	43.7175	13.4347	35.53	20.67	24.99			
EM 101	Kv	3	9	214	10/01/94	43.7175	13.4347	36.05	20.97	25.30			
EM 102	Kv	3	12	215	10/01/94	43.7175	13.4347	36.70	21.28	25.71			
EM 103	Kv	3	15	216	10/01/94	43.7175	13.4347	36.99	20.71	26.09			
EM 104	Kv	3	18	217	10/01/94	43.7175	13.4347	37.90	19.33	27.15			

Table A14b: Dissolved trace metals and other parameters (Cruise September 1994)

Code	MnD nM	FeD nM	CoD nM	PbD nM	CdD nM	ZnD nM	NiD nM	CuD nM	Salinity (measured)	PO ₄ ³⁻ μM	NO ₃ ⁻ +NO ₂ ⁻ μM
EM 82	12.97	0.53	0.826	0.075	0.135	2.89	12.77	11.85	26.436	0.05	14.22
EM 83	10.72	0.26	0.646	0.083	0.129	2.29	12.31	10.54	26.541	0.10	15.88
EM 84	13.09	0.67	0.714	0.136	0.138	6.72	9.65	10.81	30.763	0.06	7.35
EM 85	10.92	6.66	0.608	0.081	0.111	4.61	8.07	7.47	34.752	0.02	1.53
EM 86	9.25	1.99	0.464	0.097	0.107	4.44	7.30	6.75	35.482	0.00	1.05
EM 87	6.88	5.36	0.481	0.143	0.105	10.19	6.71	5.85	36.266	0.02	0.70
EM 88											
EM 89	138.60	25.03	0.716	0.072	0.106	5.24	7.14	6.39	36.684	0.09	2.95
EM 90	15.47	1.66	0.776	0.047	0.139	4.37	10.78	11.36	31.914	0.12	6.10
EM 91	13.64	0.26	0.665	0.108	0.144	7.13	9.36	8.42	32.833	0.04	2.15
EM 92	11.07	3.79	0.612	0.106	0.108	5.37	7.50	6.70	34.633	0.00	1.92
EM 93	11.38	2.86	0.460	0.073	0.125	5.41	6.88	6.62	35.594	0.00	0.52
EM 94	6.73	1.46	0.378	0.089	0.093	4.45	6.37	5.12	36.407	0.00	0.68
EM 95	6.86	1.11	0.339	0.130	0.090	7.09	6.45	4.95	36.643	0.00	0.38
EM 96	12.55	7.98	0.404	0.039	0.103	5.14	6.73	6.30	36.774	0.01	0.09
EM 97	15.47	1.56	0.580	0.155	0.220	5.77	9.06	7.86	34.828	2.57	1.13
EM 98	15.50	0.87	0.461	0.047	0.097	2.63	8.60	6.85	34.781	0.11	0.56
EM 99	19.43	0.89	0.770	0.052	0.115	5.65	9.35	8.91	35.312	0.00	0.00
EM 100	16.15	1.74	0.622	0.075	0.120	6.09	8.54	8.10	35.322	0.00	0.00
EM 101	6.79	2.09	0.348	0.063	0.095	5.34	7.10	5.95	35.923	0.00	0.00
EM 102	10.32	2.21	0.513	0.053	0.095	5.13	8.01	7.06	36.563	0.00	0.00
EM 103	5.53	1.76	0.358	0.078	0.084	6.72	6.93	5.99	36.826	0.00	0.00
EM 104	12.86	10.86	0.278	0.066	0.078	4.72	6.41	4.77	37.209	0.40	0.00

Table A15a: General sample parameters (Cruise November 1994)

Code	Type	Station	Depth	TM bottle	Date	Latitude	Longitude	Salinity	Temperature	Sigma theta
						°N	°E	psu	°C	kg/m ³
EM 105	CTD	OT 104	3	341	Nov-94	40.1666	18.7750	37.8645	18.4772	27.3614
EM 106	CTD	OT 104	10	351	Nov-94	40.1666	18.7750	37.8111	18.4709	27.3513
EM 107	CTD	OT 104	30	335	Nov-94	40.1666	18.7750	38.2550	14.2418	28.7868
EM 108	CTD	OT 104	50	334	Nov-94	40.1666	18.7750	38.4433	13.6399	29.1487
EM 109	CTD	OT 104	100	337	Nov-94	40.1666	18.7750	38.5995	13.4954	29.5239
EM 110	CTD	OT 104	200	350	Nov-94	40.1666	18.7750	38.6948	13.6476	30.0074
EM 111	CTD	OT 104	300	331	Nov-94	40.1666	18.7750	38.7064	13.5615	30.4758
EM 112	CTD	OT 104	500	332	Nov-94	40.1666	18.7750	38.7065	13.5349	31.3619
EM 113	CTD	OT 104	600	336	Nov-94	40.1666	18.7750	38.6970	13.4816	31.8046
EM 114	CTD	OT 108	2	346	Nov-94	40.1666	19.0750	38.0754	20.8664	26.8873
EM 115	CTD	OT 108	10	345	Nov-94	40.1666	19.0750	38.0608	20.8729	26.9049
EM 116	CTD	OT 108	50	344	Nov-94	40.1666	19.0750	38.2270	15.1329	28.6526
EM 117	CTD	OT 108	100	353	Nov-94	40.1666	19.0750	38.6066	14.0621	29.4077
EM 118	CTD	OT 108	200	343	Nov-94	40.1666	19.0750	38.7447	13.8084	30.0114
EM 119	CTD	OT 108	300	342	Nov-94	40.1666	19.0750	38.7426	13.6918	30.4771
EM 120	CTD	OT 108	500	339	Nov-94	40.1666	19.0750	38.7221	13.5675	31.3696
EM 121	CTD	OT 108	600	352	Nov-94	40.1666	19.0750	38.7116	13.5283	31.8089
EM 122	CTD	OT 108	900	340	Nov-94	40.1666	19.0750	38.6487	13.1161	33.1644
EM 123	CTD	OT 108	955	338	Nov-94	40.1666	19.0750	38.6378	13.0270	33.4143
EM 124	CTD	OT 212	2	354	Nov-94	40.0000	19.3750	38.2795	20.9896	27.008
EM 125	CTD	OT 212	10	347	Nov-94	40.0000	19.3750	38.3101	20.9855	27.0636
EM 126	CTD	OT 212	30	348	Nov-94	40.0000	19.3750	38.5410	21.1738	27.2743
EM 127	CTD	OT 212	50	349	Nov-94	40.0000	19.3750	38.5393	20.8245	27.4574
EM 128	CTD	OT 212	75	355	Nov-94	40.0000	19.3750	38.2616	15.8315	28.6272
EM 129	CTD	OT 212	100	333	Nov-94	40.0000	19.3750	38.4066	14.4142	29.1730
EM 130	CTD	OT 212	200	366	Nov-94	40.0000	19.3750	38.7596	14.0872	29.9604
EM 131	CTD	OT 212	345	361	Nov-94	40.0000	19.3750	38.7705	13.7898	30.6756
EM 132	CTD	OT 208	50	356	Nov-94	40.0000	19.0750	38.1490	14.7339	28.6829
EM 133	CTD	OT 208	100	371	Nov-94	40.0000	19.0750	38.6454	14.0612	29.4384
EM 134	CTD	OT 208	300	367	Nov-94	40.0000	19.0750	38.7685	13.7628	30.4811
EM 135	CTD	OT 208	400	362	Nov-94	40.0000	19.0750	38.7479	13.6693	30.9282

Code	Type	Station	Depth m	TM bottle	Date	Latitude	Longitude	Salinity	Temperature	Sigma theta
						°N	°E	psu	°C	kg/m ³
EM 136	CTD	OT 208	500	357	Nov-94	40.0000	19.0750	38.7260	13.5843	31.3695
EM 137	CTD	OT 208	600	372	Nov-94	40.0000	19.0750	38.7129	13.5367	31.8090
EM 138	CTD	OT 208	700	368	Nov-94	40.0000	19.0750	38.7061	13.5106	32.2451
EM 139	CTD	OT 208	800	363	Nov-94	40.0000	19.0750	38.7034	13.5027	32.6837
EM 140	CTD	OT 208	980	358	Nov-94	40.0000	19.0750	38.6273	12.9716	33.5278
EM 141	CTD	OT 204	2	373	Nov-94	40.0000	18.7750	37.7404	18.7507	27.1901
EM 142	CTD	OT 204	10	369	Nov-94	40.0000	18.7750	37.7411	18.7515	27.2282
EM 143	CTD	OT 204	30	364	Nov-94	40.0000	18.7750	38.0061	17.7182	27.7792
EM 144	CTD	OT 204	50	359	Nov-94	40.0000	18.7750	38.2167	13.3779	29.0343
EM 145	CTD	OT 204	75	374	Nov-94	40.0000	18.7750	38.2714	13.0884	29.2478
EM 146	CTD	OT 204	100	370	Nov-94	40.0000	18.7750	38.2986	13.0387	29.3899
EM 147	CTD	OT 204	200	365	Nov-94	40.0000	18.7750	38.4864	13.1579	29.9542
EM 148	CTD	OT 204	300	360	Nov-94	40.0000	18.7750	38.6635	13.5156	30.4562
EM 149	CTD	OT 204	572	225	Nov-94	40.0000	18.7750	38.7025	13.4819	31.6861
EM 150	CTD	OT 201	2	223	Nov-94	40.0000	18.5500	37.6504	18.8258	27.1064
EM 151	CTD	OT 201	10	227	Nov-94	40.0000	18.5500	37.6505	18.8374	27.1358
EM 152	CTD	OT 201	30	226	Nov-94	40.0000	18.5500	37.9218	18.7151	27.4613
EM 153	CTD	OT 201	50	312	Nov-94	40.0000	18.5500	38.0435	16.9660	28.0803
EM 154	CTD	OT 201	75	303	Nov-94	40.0000	18.5500	38.1998	13.7889	29.0412
EM 155	CTD	OT 201	98	308	Nov-94	40.0000	18.5500	38.3446	13.2547	29.3693
EM 156	CTD	OT 302	3	306	Nov-94	39.8333	18.6000	37.7529	19.2168	27.0859
EM 157	CTD	OT 302	30	301	Nov-94	39.8333	18.6000	38.1204	17.5865	27.9004
EM 158	CTD	OT 302	50	302	Nov-94	39.8333	18.6000	38.1516	14.4247	28.7548
EM 159	CTD	OT 302	75	315	Nov-94	39.8333	18.6000	38.2930	13.1138	29.2592
EM 160	CTD	OT 302	115	310	Nov-94	39.8333	18.6000	38.3785	13.2137	29.4799
EM 161	CTD	OT 305	50	311	Nov-94	39.8333	18.9000	38.1167	15.6611	28.4455
EM 162	CTD	OT 305	100	309	Nov-94	39.8333	18.9000	38.4225	13.4331	29.3997
EM 163	CTD	OT 305	200	317	Nov-94	39.8333	18.9000	38.6986	13.6874	29.9993
EM 164	CTD	OT 305	300	305	Nov-94	39.8333	18.9000	38.7428	13.7025	30.4707
EM 165	CTD	OT 305	500	316	Nov-94	39.8333	18.9000	38.7175	13.5535	31.3676
EM 166	CTD	OT 305	600	307	Nov-94	39.8333	18.9000	38.7013	13.4662	31.8116
EM 167	CTD	OT 305	700	314	Nov-94	39.8333	18.9000	38.6498	13.1220	32.2887

Code	Type	Station	Depth m	TM bottle	Date	Latitude °N	Longitude °E	Salinity psu	Temperature °C	Sigma theta kg/m ³
EM 168	CTD	OT 305	803	304	Nov-94	39.8333	18.9000	38.6264	12.9385	32.7635
EM 169	CTD	OT 307	50	330	Nov-94	39.8333	19.1000	38.1084	15.0775	28.5738
EM 170	CTD	OT 307	100	329	Nov-94	39.8333	19.1000	38.6724	14.1791	29.4305
EM 171	CTD	OT 307	200	328	Nov-94	39.8333	19.1000	38.8031	13.9713	30.0173
EM 172	CTD	OT 307	300	327	Nov-94	39.8333	19.1000	38.7680	13.7640	30.4791
EM 173	CTD	OT 307	500	326	Nov-94	39.8333	19.1000	38.7253	13.5823	31.3663
EM 174	CTD	OT 307	600	325	Nov-94	39.8333	19.1000	38.7146	13.5428	31.8044
EM 175	CTD	OT 307	700	324	Nov-94	39.8333	19.1000	38.7077	13.5204	32.2436
EM 176	CTD	OT 307	800	321	Nov-94	39.8333	19.1000	38.7043	13.5115	32.6790
EM 171	CTD	OT 307	900	322	Nov-94	39.8333	19.1000	38.7039	13.5123	33.1149
EM 172	CTD	OT 307	1005	323	Nov-94	39.8333	19.1000	38.6753	13.3407	33.5931
EM 173	CTD	OT 309	800	320	Nov-94	39.8333	19.3000	38.7060	13.5230	32.6807
EM 174	CTD	OT 309	900	319	Nov-94	39.8333	19.3000	38.7039	13.5202	33.1152
EM 175	CTD	OT 309	1030	318	Nov-94	39.8333	19.3000	38.7092	13.5362	33.6814

Table A15b: Dissolved trace metals and other parameters (Cruise November 1994)

Code	MnD nM	FeD nM	CoD nM	PbD nM	CdD nM	ZnD nM	NiD nM	CuD nM	Salinity (measured)
EM 105	8.01	3.28	0.300	0.162	0.072	2.58	5.64	3.59	37.862
EM 106	6.46	1.89	0.306	0.171	0.111	1.62	4.77	3.77	37.895
EM 107	3.78	0.75	0.106	0.074	0.057	1.93	5.48	2.32	38.248
EM 108	3.24	1.74	0.106	0.084	0.063	4.70	5.19	2.10	38.405
EM 109	1.22	1.41	0.065	0.059	0.081	3.40	4.86	1.91	38.568
EM 110	1.01	1.18	0.059	0.079	0.063	4.42	4.96	1.71	38.676
EM 111	1.05	0.54	0.041	0.064	0.056	3.80	4.38	1.57	38.704
EM 112	0.96	0.53	0.035	0.059	0.053	4.33	4.65	1.28	38.677
EM 113	1.39	0.54	0.012	0.059	0.096	3.17	4.88	1.46	38.668
EM 114	8.60	6.18	0.211	0.179	0.047	2.48	2.56	2.64	38.053
EM 115	6.52	2.24	0.235	0.155	0.059	3.89	4.67	3.52	38.065
EM 116	1.38	1.75	0.153	0.098	0.056	1.79	3.09	2.69	38.286
EM 117	1.22	1.13	0.106	0.128	0.065	3.58	3.59	1.72	38.620
EM 118	2.09	0.69	0.059	0.100	0.051	3.10	3.66	1.52	38.733
EM 119	0.67	0.59	0.047	0.114	0.054	4.08	4.49	1.30	38.733
EM 120	1.41	0.86	0.047	0.074	0.042	3.35	3.91	1.38	38.700
EM 121	0.27	0.45	0.041	0.091	0.042	2.56	4.29	1.44	38.700
EM 122	0.43	0.65	0.035	0.074	0.075	2.18	3.63	2.19	38.622
EM 123	1.87	3.65	0.041	0.074	0.096	3.08	4.91	1.90	38.638
EM 124	7.32	1.99	0.138	0.206	0.054	15.3	4.86	2.17	38.291
EM 125	6.71	1.61	0.159	0.212	0.059	5.60	4.99	2.26	38.313
EM 126	2.97	1.50	0.118	0.154	0.049	4.45	5.42	2.17	38.546
EM 127	5.49	1.83	0.135	0.182	0.048	4.48	5.28	3.47	38.555
EM 128	2.69	1.27	0.077	0.106	0.047	3.30	4.99	2.54	38.294
EM 129	1.54	1.35	0.081	0.140	0.051	2.93	4.92	5.77	38.402
EM 130	0.53	1.02	0.039	0.112	0.052	3.75	4.71	2.07	38.735
EM 131	0.43	0.80	0.033	0.112	0.043	7.79	4.76	3.26	38.738
EM 132	3.38	0.82	0.096	0.078	0.041	4.08	4.69	2.74	38.265
EM 133	0.49	0.89	0.040	0.122	0.053	5.77	4.59	2.15	38.638
EM 134	0.20	0.97	0.023	0.120	0.061	4.99	4.71	3.33	38.768
EM 135	0.13	0.40	0.005	0.182	0.048	6.17	4.88	5.72	38.725

Code	MnD nM	FeD nM	CoD nM	PbD nM	CdD nM	ZnD nM	NiD nM	CuD nM	Salinity (measured)
EM 133	0.49	0.89	0.040	0.122	0.053	5.77	4.59	2.15	38.638
EM 134	0.20	0.97	0.023	0.120	0.061	4.99	4.71	3.33	38.768
EM 135	0.13	0.40	0.005	0.182	0.048	6.17	4.88	5.72	38.725
EM 136	0.20		0.021	0.148	0.058	4.80	5.11	3.02	38.679
EM 137	0.11	0.82	0.034	0.096	0.031	6.46	4.74	2.71	38.803
EM 138	0.37	2.25	0.000	0.108	0.033	4.20	5.07	2.17	38.736
EM 139	1.91	0.45	0.026	0.064	0.046	6.99	4.90	2.44	38.677
EM 140	0.17	0.08	0.040	0.100	0.028	2.04	4.64	2.32	38.614
EM 141	6.88	7.4	0.272	0.100	0.074	4.79	5.19	4.08	37.766
EM 142	8.30		0.243	0.104	0.066	3.22	5.28	3.69	37.806
EM 143	8.82	2.61	0.169	0.114	0.068	3.88	5.77	3.80	38.061
EM 144	4.73	1.62	0.095	0.048	0.060	3.42	5.34	3.79	38.257
EM 145	4.28		0.067	0.056	0.065	3.51	4.87	3.24	38.264
EM 146	3.24	0.88	0.042	0.060	0.052	4.42	5.09	3.51	38.479
EM 147	2.38	0.86	0.038	0.040	0.066	2.50	4.48	2.40	38.460
EM 148	2.48	1.62	0.023	0.085	0.074	3.40	4.50	1.89	38.692
EM 149	1.91	4.28	0.016	0.096	0.057	2.74	4.51	2.19	38.680
EM 150	6.44	2.87	0.253	0.090	0.071	3.54	5.71	4.69	37.630
EM 151	6.57	2.24	0.266	0.185	0.072	3.41	4.45	4.04	37.639
EM 152	5.01	2.82	0.209	0.142	0.060	2.57	4.28	3.58	38.058
EM 153	4.71	1.94	0.159	0.175	0.065	3.67	5.42	4.49	38.068
EM 154	4.88	2.27	0.084	0.206	0.069	5.33	5.10	4.80	38.244
EM 155	6.52	2.31	0.080	0.185	0.076	3.98	5.32	3.79	38.350
EM 156	7.87	1.32	0.273	0.106	0.067	6.75	5.45	4.30	37.819
EM 157	6.31	1.35	0.159	0.094	0.077	2.29	5.08	3.95	38.123
EM 158	4.65	0.78	0.146	0.079	0.077	3.16	5.42	3.84	38.121
EM 159	3.17	1.01	0.090	0.054	0.064	3.66	4.86	3.07	38.270
EM 160	6.07	10.64	0.050	0.071	0.077	3.14	4.65	3.08	38.345
EM 161	5.63	1.12	0.164	0.115	0.066	2.82	4.97	3.66	38.132
EM 162	2.43	1.41	0.069	0.094	0.085	4.48	4.99	3.16	38.434
EM 163	0.91	0.79	0.045	0.100	0.119	4.26	4.41	2.28	38.676
EM 164	0.85	0.74	0.052	0.123	0.086	3.96	4.29	2.33	38.716

Code	MnD nM	FeD nM	CoD nM	PbD nM	CdD nM	ZnD nM	NiD nM	CuD nM	Salinity (measured)
EM 165	1.61	0.92	0.000	0.106	0.053	3.81	4.88	2.53	38.691
EM 166	1.54	0.83	0.042	0.127	0.062	3.54	5.30	2.40	38.678
EM 167	0.48	0.45	0.051	0.083	0.045	2.18	3.12	2.81	38.672
EM 168	2.18	0.74	0.059	0.077	0.053	10.08	3.47	3.21	38.620
EM 169	4.91	0.68	0.136	0.102	0.063	2.70	4.00	2.57	38.213
EM 170	0.99	0.94	0.079	0.108	0.165	4.25	3.86	2.10	38.737
EM 171	0.30	0.55	0.048	0.125	0.074	4.52	3.65	1.84	38.861
EM 172	0.49	0.61	0.030	0.122	0.048	4.12	3.61	1.67	38.743
EM 173	0.16	0.75	0.019	0.182	0.038	4.97	3.79	1.47	38.770
EM 174	0.41	0.63	0.017	0.115	0.043	4.42	4.16	1.68	38.729
EM 175	0.08	0.42	0.004	0.113	0.037	3.30	3.92	1.53	38.681
EM 176	0.08	0.47	0.036	0.117	0.035	2.68	4.05	1.84	38.719
EM 171	0.17	0.26		0.102		2.58	4.43	2.06	38.683
EM 172	0.46	0.31	0.013	0.100	0.041		4.07	2.26	38.648
EM 173	0.20	0.32	0.007	0.103	0.036	4.41	3.82	1.91	38.678
EM 174	0.11	0.22	0.005	0.097	0.032	4.21	3.91	1.91	38.681
EM 175	0.37	0.42	0.005	0.098	0.036	2.90	3.75	1.47	38.671

Table A16a: General sample parameters (Cruise February 1995)

Code	Type	Station	Depth	TM bottle	Date	Latitude	Longitude	Salinity	Temperature	Sigma theta	O ₂	Chl a	pH
			m		d/m/y	°N	°E	psu	°C	kg/m ³	%	µg/l	
EM 176	M	1	0	475	17/2/95	44.5442	12.4506	26.51	7.70		139.9	20.32	8.68
EM 177	Kv	1	1	435	17/2/95	44.5442	12.4506	29.69	7.53		144.1	21.77	8.68
EM 178	Kv	1	3	434	17/2/95	44.5442	12.4506	32.61	7.51	25.50	147.0	14.75	8.56
EM 179	Kv	1	6	497	17/2/95	44.5442	12.4506	35.19	8.04	27.44	133.9	8.02	8.37
EM 180	Kv	1	9	498	17/2/95	44.5442	12.4506	35.64	8.05	27.79	119.6	3.96	8.32
EM 181	Kv	1	12	436	17/2/95	44.5442	12.4506	36.84	8.88	28.60	108.7	1.44	8.20
EM 182	Kv	1	15	430	17/2/95	44.5442	12.4506	37.22	9.06	28.88	93.0	0.30	8.19
EM 183	Kv	1	17	499	17/2/95	44.5442	12.4506	37.25	8.95	28.92	87.1	0.21	8.18
EM 184	Kv	1	18.5	429	17/2/95	44.5442	12.4506	37.26	8.90	28.93	79.9	0.06	8.19
EM 185	M	2	0	477	16/2/95	44.3070	12.5782	32.05	7.60	25.04	102.8	3.06	8.60
EM 186	Kv	2	1	493	16/2/95	44.3070	12.5782	32.17	7.59	25.13	102.7	3.06	8.61
EM 187	Kv	2	3	494	16/2/95	44.3070	12.5782	33.75	7.78	26.35	102.9	5.19	8.56
EM 188	Kv	2	6	491	16/2/95	44.3070	12.5782	35.81	8.19	27.91	101.5	3.44	8.46
EM 189	Kv	2	9	492	16/2/95	44.3070	12.5782	37.10	8.87	28.81	95.5	1.79	8.39
EM 190	Kv	2	12	496	16/2/95	44.3070	12.5782	37.42	9.70	28.93	87.3	0.27	8.30
EM 191	Kv	2	15	495	16/2/95	44.3070	12.5782	37.44	9.73	28.93	77.9	0.22	8.29
EM 192	Kv	2	17	489	16/2/95	44.3070	12.5782	37.45	9.76	28.94	73.6	0.15	8.29
EM 193	Kv	2	18	490	16/2/95	44.3070	12.5782	37.44	9.77	28.93	71.9	0.14	8.29
EM 194	Kv	3	0	487	15/2/95	43.7175	13.4347	36.00	8.56		27.98		
EM 195	Kv	3	1	488	15/2/95	43.7175	13.4347	36.20	8.54		28.13		
EM 196	Kv	3	3	481	15/2/95	43.7175	13.4347	36.30	8.54		28.21		
EM 197	Kv	3	6	482	15/2/95	43.7175	13.4347	36.37	8.53		28.27		
EM 198	Kv	3	9	485	15/2/95	43.7175	13.4347	36.52	8.53		28.39		
EM 199	Kv	3	12	486	15/2/95	43.7175	13.4347	36.62	8.54		28.47		
EM 200	Kv	3	15	483	15/2/95	43.7175	13.4347	36.74	8.59		28.55		
EM 201	Kv	3	18	484	15/2/95	43.7175	13.4347	36.79	8.61		28.58		

Table A16b: dissolved trace metals and other parameters (Cruise February 1995)

Code	MnD nM	FeD nM	CoD nM	PbD nM	CdD nM	ZnD nM	NiD nM	CuD nM	Salinity (measured)	PO ₄ ³⁻ μM	NO ₃ ⁻ +NO ₂ ⁻ μM
EM 176											
EM 177	34.62	0.44	0.661	0.308	0.172	13.48	20.98	11.22	22.474	0.11	75.33
EM 178	17.27	2.36	0.653	0.292	0.158	8.75	13.84	9.20	30.996	0.02	40.08
EM 179	14.42	0.69	0.491	0.240	0.118	7.87	9.21	6.38	31.462	0.01	29.28
EM 180	7.29	0.67	0.462	0.162	0.129	9.85	7.94	5.29	34.958	0.00	30.39
EM 181	5.06	0.71	0.372	0.135	0.140	10.82	7.56	4.90	36.26	0.00	6.77
EM 182	16.41	1.88	0.368	0.227	0.118	7.68	6.36	4.30	36.782	0.00	6.69
EM 183	30.95	6.63	0.385	0.123	0.131	9.75	7.12	4.79	37.082	0.00	6.16
EM 184	29.65	20.68	0.415	0.448	0.123	11.55	6.09	4.27	37.177	0.00	4.60
EM 185	19.28	0.51	0.634	0.214	0.157	6.25	11.22	7.50	32.911	0.16	21.13
EM 186	22.77	1.25	0.700	0.220	0.158	10.68	11.70	7.36	32.543	0.04	23.94
EM 187	15.17	0.00	0.605	0.168	0.133	8.04	9.53	6.87	33.382	0.00	19.39
EM 188	7.42	0.34	0.424	0.172	0.106	6.22	7.43	4.81	35.232	0.00	9.49
EM 189	5.31	1.03	0.301	0.108	0.104	7.31	7.58	4.88	36.360	0.00	6.09
EM 190	21.32	1.18	0.304	0.128	0.091	4.68	6.86	4.82	37.167	0.00	5.04
EM 191	29.27	2.05	0.307	0.052	0.090	7.01	6.50	4.84	37.231	0.00	4.14
EM 192	41.88	3.91	0.328	0.086	0.091	4.82	6.53	4.80	37.467	0.00	4.58
EM 193	50.83	5.26	0.320	0.712	0.091	7.23	6.74	5.23	37.454	0.11	5.70
EM 194	10.08	9.56	0.493	1.700	0.099	21.91	8.39	6.52	35.861	0.02	6.00
EM 195	9.65	7.29	0.466	0.356	0.103	17.88	8.82	6.41	36.001	0.01	4.68
EM 196	7.20	5.71	0.476	0.222	0.094	16.31	8.99	6.24	36.248	0.00	4.65
EM 197	8.73	11.39	0.439		0.094	10.68	8.32	5.86	36.319	0.00	4.76
EM 198	5.08	4.88	0.378	0.320	0.085	3.39	6.84	4.55	36.524	0.03	2.92
EM 199	6.77	19.65	0.364	0.224	0.093	3.64	7.75	5.05	36.694	0.00	2.69
EM 200	8.78	1.34	0.389	0.104	0.090	4.18	6.12	4.68	36.713	0.01	2.97
EM 201	11.31	3.25	0.365	0.054	0.088	4.43	6.17	4.26	36.78	0.00	2.63

Table AI7a: Sampling parameters and dissolved trace metals (River Po)

Code	Type	Date	Julian day	Flow rate	MnD	FeD	CoD	PbD	CdD	ZnD	NiD	CuD
		d/m/y		m ³ /s	nM	nM	nM	nM	nM	nM	nM	nM
EM 202	EDIN	01/10/93	274	6170	36.35		1.188	2.201	0.250		34.12	44.34
EM 203	EDIN	15/10/93	288	6490	18.27	36.78	0.525	2.275	0.778	115.1	44.11	99.73
EM 204	EDIN	03/11/93	307	3060	34.50		2.128	2.085	1.298	77.1	44.16	71.93
EM 205	EDIN	03/12/93	337	1540	120.89	24.69	0.711	1.91	0.497	106.2	53.19	55.51
EM 206	EDIN	15/12/93	349	1250	50.75	25.36	1.159	2.257	0.920	80.2	57.95	62.83
EM 207	EDIN	30/12/93	364	1300	101.48	55.58	0.734	1.678	2.033	101.4	52.94	58.07
EM 208	EDIN	20/1/94	20	2170	35.60	46.55	1.366	1.574	7.287	115.8	56.23	51.04
EM 209	EDIN	24/2/94	55	1310	34.93	66.50	0.653	1.377	1.972	169.4	64.39	44.04
EM 210	EDIN	31/3/94	90	1280	17.55	66.68	5.775	7.403	1.712	143.3	60.45	45.58
EM 211	EDIN	14/4/94	104	981	16.40	47.11	0.969	2.262	1.590	250.2	57.45	55.02
EM 212	EDIN	06/05/94	126	1440	12.23	48.73	0.845	1.801	0.978	111.4	57.16	52.71
EM 213	EDIN	03/06/94	154	2520	10.18	37.38	7.098	3.513	1.100	189.0	48.99	93.48
EM 214	EDIN	24/6/94	175	2730	9.12	31.99	3.02	1.832	1.212	162.5	56.96	92.95
EM 215	SOTON	10/07/94	191		16.13	15.94	0.514	0.221	0.120	11.5	33.63	26.87
EM 216	SOTON	10/07/94	191		18.73	9.14	0.453	0.177	0.112	10.9	30.77	29.46
EM 217	EDIN	21/7/94	202	659	74.09		3.003		1.324	241.2	53.83	122.12
EM 218	EDIN	10/08/94	222	577	70.36	44.22	0.998	2.658	0.711	78.8	43.38	69.18
EM 219	EDIN	05/09/94	248	1940	13.90	210.76	1.198	3.463	1.825	215.6	80.49	118.59
EM 220	EDIN	23/9/94	266	3220	24.80	283.24	1.135	1.71	1.482	184.5	72.00	75.02
EM 221	EDIN	23/9/94	266	3220	48.24	284.00	0.977	0.694	0.142	30.3	34.22	10.50
EM 222	EDIN	23/9/94	266	3220	115.02		2.449	1.222	0.449	45.1	73.15	9.70
EM 223	SOTON	02/10/95			36.72	44.39	0.614	1.073	0.179	86.3	59.71	47.76
EM 224	SOTON	02/10/95			31.10	35.59	0.534	0.97	0.173	69.8	54.06	39.50

Table AI7b: Particulate trace metals and organic carbon (River Po, from Mowbray et al., 1995)

Code	MnP	FeP	AlP	PbP	CdP	ZnP	NiP	CuP	C organic
	µg/l	mg/l	mg/l	µg/l	µg/l	µg/l	µg/l	µg/l	mg/l
EM 202	123.40	3.79	6.09	12.81	0.183	49.7	34.7	9.94	2.75
EM 203	92.30	3.15	5.09	9.20	0.112	22.4	20.9	5.15	3.31
EM 204	54.00	3.15	4.82	8.79	0.244	27.3	23.7	6.04	2.52
EM 205	91.10	1.76	2.79	3.58	0.091	16.2	16.5	4.29	1.24
EM 206	48.50	1.46	2.35	2.71	0.156	11.8	13.6	3.41	1.43
EM 207	37.90	1.24	2.18	2.31	0.107	10.3	11.6	3.10	1.49
EM 208	72.80	3.15	5.00	6.51	0.144	20.7	18.9	5.17	2.54
EM 209	29.70	0.94	1.59	1.87	0.075	16.7	9.0	4.06	1.25
EM 210	31.00	0.56	1.06	1.98	0.059	7.8	7.1	1.94	1.52
EM 211	69.00	1.79	3.20	5.72	0.164	26.8	13.4	4.66	2.01
EM 212	56.00	1.76	3.00	5.50	0.074	20.8	15.0	4.03	2.48
EM 213	71.00	2.60	3.92	7.81	0.120	21.8	26.7	5.24	1.77
EM 214	56.00	1.80	3.20	6.98	0.140	15.5	14.5	3.36	1.68
EM 215									
EM 216									
EM 217	79.00	0.92	1.54	9.49	0.097	13.6	10.4	2.31	2.05
EM 218	93.00	1.02	1.81	8.03	0.078	19.7	11.8	2.36	3.39
EM 219	175.00	6.84	12.35	24.49	1.656	62.7	38.1	14.34	2.21
EM 220	615.00	28.32	55.71	30.50	3.270	104.0	223.0	28.50	
EM 221									
EM 222									
EM 223									
EM 224									

Table A18: Mn and Fe in pore waters (Cruise February 1994)

Station	Depth (cm)	Mn (µM)	Fe (µM)	Station	Depth (cm)	Mn (µM)	Fe (µM)	Station	Depth (cm)	Mn (µM)	Fe (µM)
1	BW	0.22	2.41	3	BW	0.07		5	0.25	0.86	4.33
1	0.25	4.93	0.8	3	BW	0.11		5	1.5	0.67	5.91
1	0.75	28.39		3	BW	0.42	0.87	5	2.5	2.11	28.33
1	1.5	27.66	12.18	3	0.25	4.95	2.02	5	3.5	2.37	33.56
1	2.5	22.02	138.23	3	1.25	64.07	130.46	5	7	0.06	0.79
1	3.5	22.52	141.46	3	2.5	39.32	81.19	5	9	0.18	1.83
1	5	28.4	83.69	3	3.5	32.95	112.09	5	16	0.42	4.28
1	7	35.28	97.05	3	5	64.4	140.44				
1	9	17.4	55.02	3	7	53.59	130.25				
1	12	11.21	24.57	3	9	25.08	63.92				
1	16	8.84	18.48	3	12	14.49	54.68				
2	0.25	0.69	32.23	3	16	11.61	61.42				
2	0.75	21.15	6.77	4	0.25	1.46	3.8				
2	1.25	29.23	55.33	4	0.75	26.76	0.59				
2	1.75	26.57	95.87	4	1.5	30.65	0.54				
2	3.5	45.4	164.56	4	2.5	42.05	4.91				
2	5	28.1	73.77	4	3.5	66.58	3.85				
2	7	26.65	44.94	4	5	81.44	39.05				
2	9	18.35	54.79	4	7	73.5	78.79				
2	16	38.44	56.76	4	9	71.35	166.87				
				4	12	59.88	152.56				
				4	16	99.2	153.45				

Table AI9: Mn and Fe in pore waters (Cruise June 1994)

Station	Depth	Mn	Fe	Station	Depth	Mn	Fe
	cm	µM	µM		cm	µM	µM
1	BW	1.32	6.07	4	0.5	0.09	1.07
1	0.5	63.12	1.17	4	1.5	6.7	0.63
1	1.5	31.05	64.25	4	2.5	61.45	0.95
1	2.5	22.05	79.2	4	4	112.13	10.03
1	4	21.68	118.68	4	9	79.18	96.51
1	9	15.07	37.53	4	16	56.57	256.77
1	16	9.21	18.1	4	23.5	56.24	309.42
1	23.5	7.57	5.35	5	0.5	0.58	3.08
2	BW	0.96	10.13	5	1.5	0.06	2.81
2	0.5	52.13	2.24	5	2.5	0.1	0.95
2	1.5	46.38	40.75	5	4	0.78	3.78
2	2.5	32.33	61.16	5	9	0.34	1.65
2	4	23.59	87.56	5	16	2.85	1.54
2	9	20.02	74.67	5	23.5	58.76	2.45
2	16	16.42	52.12				
2	23.5	15.58	44.66				
3	0.5	141.43	19.09				
3	1.5	98.11	261.43				
3	2.5	85.91	218.81				
3	4	58.79	143.1				
3	9	18.64	117.46				
3	16	9.57	23.3				
3	23.5	7.75	25.01				

Table A110: Mn and Fe in pore waters (Cruise September 1994)

Station	Depth	Mn	Fe	Station	Depth	Mn	Fe
	cm	µM	µM		cm	µM	µM
1	BW	0.51	0.98	3	BW	0.29	0.13
1	0.5	107.44	1.90	3	0.5	162.59	4.33
1	1.5	21.13	105.29	3	1.5	47.45	172.69
1	2.5	13.43	68.40	3	2.5	23.82	138.41
1	4	8.42	47.45	3	4	24.89	128.39
1	9	14.65	22.56	3	9	7.02	15.94
1	16	8.56	6.62	3	16	6.02	41.34
1	23.5	5.84	13.43	3	23.5	7.48	38.14
1	31.5	5.77	13.61	3	31.5	12.07	104.75
1	41.5	10.74	50.85				
2	BW	0.53					
2	0.5	178.75	1.31				
2	1.5	33.31	69.49				
2	2.5	12.92	48.06				
2	4	15.47	25.68				
2	9	22.72	9.65				
2	16	9.50	7.63				
2	23.5	5.02	21.84				
2	31.5	7.79	14.38				
2	41.5	14.74	54.09				

Table A111: Mn and Fe in pore waters (Cruise February 1995)

Station	Depth	Mn	Fe
	cm	µM	µM
1	0.5	22.68	0.91
1	1.5	29.31	50.14
1	2.5	24.57	49.29
1	4	33.86	47.93
1	9	12.54	17.40
1	16	10.48	9.31
1	23.5	19.04	11.28
1	31.5	6.50	13.97
2	0.5	42.21	11.10
2	1.5	24.59	59.63
2	2.5	16.73	10.21
2	4	13.63	27.84
2	9	14.76	18.26
2	16	13.63	68.94
2	23.5	42.03	139.68
2	31.5	15.79	54.17
3	0.5	24.59	1.13
3	1.5	50.97	0.73
3	2.5	55.23	2.63
3	4	49.24	34.56
3	9	22.13	87.38
3	16	10.47	66.43
3	23.5	8.96	89.15
3	31.5	11.45	77.89

APPENDIX II

EROS 2000 DATA BASE

Samples were collected in the north western Black for dissolved and particulate trace metals, nutrients, oxygen and Chl *a* measurements (for sampling locations see Fig. 6.4). Hydrographic data (salinity, temperature, density, fluorescence) were obtained by CTD measurements.

Description of some parameters:

Code: code number for each sample

Station: name of the station

TM bottle: bottle number for trace metal samples

Date: sampling date for each sample

Table AII1: General sample parameters

Code	Station	Depth	Date	Latitude	Longitude	Temperature	Salinity	NH ₄ ⁺	NO ₃ ⁻ +NO ₂ ⁻	Si(OH) ₄	PO ₄ ³⁻	Oxygen	Chl.a
		m				°C		μM	μM	μM	μM	ml/l	mg/m ³
BS1	0	5	19/07/95	44:24:36	33:41:48	22.3	17.83	0.07	0	5.86	<0.05	6.22	
BS2	0	15	19/07/95	44:24:36	33:41:48	22.1	17.84	0.14	0.22	5.07	<0.05	6.04	
BS3	0	30	19/07/95	44:24:36	33:41:48	21.2	17.86	0.14	0.11	5.24	<0.05	6.27	
BS4	0	35	19/07/95	44:24:36	33:41:48	20.3	17.9	0.2	0.63	5.78	<0.05	6.59	
BS5	0	45	19/07/95	44:24:36	33:41:48	11.42	18.2	0.29	0.65	5.86	<0.05	7.02	
BS6	1	5	20/07/95	44:23:12	33:35:15								
BS7	1	10	20/07/95	44:23:12	33:35:15	22.78	17.63	0.07	0	4.64	<0.05	5.83	0.457
BS8	1	20	20/07/95	44:23:12	33:35:15	22.76	17.65	0.05	0	4.89	<0.05	5.89	0.417
BS9	1	40	20/07/95	44:23:12	33:35:15	20.4	17.8	0.12	0	4.99	<0.05	6.05	0.807
BS10	1	82	20/07/95	44:23:12	33:35:15	7.64	18.44	0.04	0.95	6.89	0.06	6.9	0.046
BS11	1	87	20/07/95	44:23:12	33:35:15								
BS12	3	10	22/07/95	44:25:20	32:41:00	23.3	18.04	0.37	0.26	4.24	0	5.59	0.173
BS13	3	21	22/07/95	44:25:20	32:41:00	12.95	18.16	0.45	0.15	3.68	0	7.23	0.339
BS14	3	31	22/07/95	44:25:20	32:41:00	9.35	18.25	0.23	0.24	4.13	0.04	6.92	0.374
BS15	3	61	22/07/95	44:25:20	32:41:00	7.05	18.49	0.21	1.33	6.88	0.24	6.21	0.048
BS16	3	81	22/07/95	44:25:20	32:41:00	7.08	18.9	0.14	2.84	12.61	0.37	4.96	0.07
BS17	3	91	22/07/95	44:25:20	32:41:00	7.27	19.36	0.19	5.06	23.87	0.47	2.73	
BS18	3	100	22/07/95	44:25:20	32:41:00	7.37	19.53	0.07	6.09	29.98	0.7	1.95	
BS19	3	110	22/07/95	44:25:20	32:41:00	7.56	19.79	0.08	6.58	37.19	0.87	1.15	
BS20	3	130	22/07/95	44:25:20	32:41:00	8	20.39	0.06	4.12	39.2	0.75	1.6	
BS21	3	140	22/07/95	44:25:20	32:41:00	8.14	20.6	0.16	1.86	53.78	0.32	0.36	
BS22	3	150	22/07/95	44:25:20	32:41:00	8.25	20.75	0.19	0.91	55.82	0.23	36	
BS23	3	161	22/07/95	44:25:20	32:41:00	8.39	20.97	5.22		45.99	4.2	0.2	
BS24	3	172	22/07/95	44:25:20	32:41:00	8.49	21.11	12.5		44.23		0.49	
BS25	3	182	22/07/95	44:25:20	32:41:00	8.55	23.39	8.39		39.2		0.96	
BS26	3	192	22/07/95	44:25:20	32:41:00	8.59	21.29	13.2		53.78		0	
BS27	3	202	22/07/95	44:25:20	32:41:00	8.61	21.33	9.36	0.91	55.82		0	
BS28	3	252	22/07/95	44:25:20	32:41:00	8.71	21.56	23.5	0	92.02	3.12	0	
BS29	3	403	22/07/95	44:25:20	32:41:00								
BS30	3	505	22/07/95	44:25:20	32:41:00	8.85	22.01	54.2	0.06	74.88		0	

Code	Station	Depth m	Date	Latitude	Longitude	Temperature °C	Salinity	NH ₄ ⁺ μM	NO ₃ ⁻ +NO ₂ ⁻ μM	Si(OH) ₄ μM	PO ₄ ³⁻ μM	Oxygen ml/l	Chl.a mg/m ³
BS31	3	757	22/07/95	44:25:20	32:41:00	8.88	22.19	71.3	0.02	196.51		0	
BS32	3	1011	22/07/95	44:25:20	32:41:00	8.93	22.27	85	0.19	220.34		0	
BS33	3	1417	22/07/95	44:25:20	32:41:00	8.99	22.31	101	0.16	255.14		0	
BS34	4	5	23/07/95	45:40:36	30:44:06	24.2	16.97	0.09	0.14	7.23	0.05	5.67	0.375
BS35	4	15	23/07/95	45:40:36	30:44:06	22	17.32	0.9	1.4	9.56	0.08	4.49	1.157
BS36	4	22	23/07/95	45:40:36	30:44:06	12.05	17.33	4.59	8.07	23	0.14	2.06	1.511
BS37	4	27.4	23/07/95	45:40:36	30:44:06	10.75	17.55	2.38	5.02	13.17	0.12	4.14	1.419
BS38	4	33	23/07/95	45:40:36	30:44:06	7.58	18.22	2.89	3.03	14.01	0.17	5.23	0.263
BS39	5	5	23/07/95	45:49:47	30:27:55	24.95	14.89	0.21	0.25	3.86	0.063	6.24	1.725
BS40	5	12.3	23/07/95	45:49:47	30:27:55	24.4	15	0.26	0.62	4.58	0.08	5.73	1.934
BS41	5	17	23/07/95	45:49:47	30:27:55	23.5	16	1.21	3.8	13.84	0.09	4.05	1.956
BS42	5	23	23/07/95	45:49:47	30:27:55	10.19	17.86	1.72	5	12.06	0.11	4.78	1.654
BS43	6	5	24/07/95	45:29:48	30:00:49	24.9	15.3	0.26	0.2	7.66	0.14	5.76	3.003
BS44	6	10	24/07/95	45:29:48	30:00:49	24.5	15.3	1.34	0.13	9.43	0.17	5.47	2.756
BS45	6	12.7	24/07/95	45:29:48	30:00:49	22.78	15.98	22.7	0.39	40.3	1.76	1.74	1.236
BS46	6	14.9	24/07/95	45:29:48	30:00:49	20.81	17.36	25.3	0.38	44.36	1.82	1.47	0.975
BS47	7	5.1	24/07/95	45:05:90	30:07:23	23.3	17.3	0.78	0.17	5.56	0.05	5.42	0.854
BS48	7	11.7	24/07/95	45:05:91	31:07:23	24.3	17.8	0.7	1.99	6.14	0.05	5.14	1.844
BS49	7	19	24/07/95	45:05:92	32:07:23	17.8	17.3	0.72	2	6.39	0.07	5.34	2.183
BS50	7	21.7	24/07/95	45:05:93	33:07:23	16.8	17.37	0.69	1.95	7.62	0.06	6.02	1.601
BS51	7	33	24/07/95	45:05:94	34:07:23	7.79	18.24	0.26	4.91	13.84	0.08	4.92	0.209
BS52	8	surface	25/07/95	45:05:54	29:52:54								
BS53	8	fond	25/07/95	45:05:54	29:52:54								
BS54	9	3	25/07/95	45:05:54	29:46:30	24.9	7.2	1.16	41.05	25.11	0.47	6.33	19.13
BS55	9	7	25/07/95	45:05:54	29:46:30	24.7	12.9	0.72	7.32	8.37	0.19	5.86	10.03
BS56	9	15	25/07/95	45:05:54	29:46:30	24.2	15.2	1.49	1.55	6.34	0.16	5.52	4.62
BS57	10	3	25/07/95	45:05:04	29:50:03	25.3	12	1.49	15.32	13.94	0.35	5.99	9.42
BS58	10	13	25/07/95	45:05:04	29:50:03	21.6	16.7	8.96	1.28	12.34	0.14	3.41	1.93
BS59	10	27.5	25/07/95	45:05:04	29:50:03	10.4	17.6	5.34	7.86	23.5	0.26	2.14	0.84
BS60	11	5	26/07/95	44:52:38	29:40:22	24.24		0.83	8.15	9.49	0.27	5.39	5.11
BS61	11	15	26/07/95	44:52:38	29:40:22	24.5		0.23	1.02	4.99	0.1	5.55	3.48

Code	Station	Depth m	Date	Latitude	Longitude	Temperature °C	Salinity	NH ₄ ⁺ μM	NO ₃ ⁻ +NO ₂ ⁻ μM	Si(OH) ₄ μM	PO ₄ ³⁻ μM	Oxygen ml/l	Chl.a mg/m ³
BS62	11	20	26/07/95	44:52:38	29:40:22	23.9		0.75	0.34	4.45	0.03	5.41	1.39
BS63	12	surface	26/07/95	St George			0.1	1.85	78.56	55.08	2.39		22.12
BS64	13	surface	26/07/95	St George			0.1	1.23	68.74	55.18	2.35		23.78
BS65	14	surface	26/07/95	St George			1.1	1.73	58.92	52.52	1.94		19.26
BS66	15	surface	26/07/95	St George			3.5	1.75	82.48	43.81	1.42		9.82
BS67	16	surface	26/07/95	St George			5.6	1.28	62.84	35.89	0.68		19.09
BS68	17	5	26/07/95	18:17:29	44:49:25	24.58		0.84	2.85	6.89	0.15	5.47	5.79
BS69	17	21	26/07/95	18:17:29	44:49:25	23.8		0.62	1	4.25	0.05	5.25	1.7
BS70	17	28	26/07/95	18:17:29	44:49:25	23		1.25	0.98	5.18	0.06	5.18	1.14
BS71	17	44	26/07/95	18:17:29	44:49:25	7.27		1.06	7.27	12.35	0.07	4.15	0.84
BS72	18	3.7	27/07/95	44:48:22	29:56:30	24.32		1.2	2.95	7	0.14	5.29	2.11
BS73	18	10.4	27/07/95	44:48:22	29:56:30	23.84		0.49	0.11	4.36	0.04	5.5	1.68
BS74	18	21.2	27/07/95	44:48:22	29:56:30	21.79		0.71	1.26	5.02	0.09	5.32	1.5
BS75	18	31	27/07/95	44:48:22	29:56:30	8.6		0.1	5.89	10.68	0.06	5.19	0.17
BS76	18	42.6	27/07/95	44:48:22	29:56:30	7.2		0.07	6.43	13.78	0.11	4.9	0.04
BS77	19	5.4	27/07/95	44:49:32	30:15:02	24.47		0.15	0.04	4.55	0.05	5.6	1.44
BS78	19	10.3	27/07/95	44:49:32	30:15:02	23.56		0.41	0.19	4.89	0.02	5.32	1.32
BS79	19	21	27/07/95	44:49:32	30:15:02	18.67		0.87	4.55	6.26	0.04	4.85	1.06
BS80	19	36.2	27/07/95	44:49:32	30:15:02	8.36		0.13	1.55	5.02	0.05	5.94	0.15
BS81	19	46.3	27/07/95	44:49:32	30:15:02	7.5		0.19	3.52	9.54	0.06	5.87	0.1
BS82	20	1.7	28/07/95	44:33:29	29:41:46	24.17	16.2	0.08	0.18	4.1		5.57	3.39
BS83	20	10.9	28/07/95	44:33:29	29:41:46	24.05	17.7	0.08	0.25	3.45		5.73	0.49
BS84	20	20	28/07/95	44:33:29	29:41:46	22.47	17.7	0.27	0.23	4.19		7.18	1.74
BS85	20	26.2	28/07/95	44:33:29	29:41:46	12.4	18.12	0.2	0.22	3.29		7.81	1.69
BS86	20	47.4	28/07/95	44:33:29	29:41:46	7.63	18.12	0.03	2.18	6.08		6.72	0.14
BS87	21	6	28/07/95	44:10:54	29:22:24	23.16	16.78	1.82	0.78	4.17		5.08	2.4
BS88	21	14.6	28/07/95	44:10:54	29:22:24	22.28	17.46	0.9	6.08	7.12		4.45	1.43
BS89	21	23.3	28/07/95	44:10:54	29:22:24	12.64	17.57	0.1	10.12	9.8		4.71	0.58
BS90	21	41	28/07/95	44:10:54	29:22:24	6.87	18.19	0.05	5.94	10.88		5.74	0.1
BS91	21	50.9	28/07/95	44:10:54	29:22:24	6.76	18.17	0.33	7.96	14.23		5.13	0.06
BS92	22	2	29/07/95	43:49:59	29:01:52	24.46	15.83	0.17	0	0.99	0.08	6.15	2.42

Code	Station	Depth m	Date	Latitude	Longitude	Temperature °C	Salinity	NH ₄ ⁺ μM	NO ₃ ⁻ +NO ₂ ⁻ μM	Si(OH) ₄ μM	PO ₄ ³⁻ μM	Oxygen ml/l	Chl.a mg/m ³
BS93	22	8.7	29/07/95	43:49:59	29:01:52	24.28	16.54	0.11	0	1.39		5.75	2.44
BS94	22	19.8	29/07/95	43:49:59	29:01:52	23.58	17.14	0.43	0.9	3.17		5.49	2.22
BS95	22	23.2	29/07/95	43:49:59	29:01:52	23	17.37	0.93	2.77	4.61		5.34	2.21
BS96	22	27.5	29/07/95	43:49:59	29:01:52	9.5	17.38	0.4	8.94	9.36		5.27	1.22
BS97	22	51.3	29/07/95	43:49:59	29:01:52	6.42	18.1	0.96	6.54	14.4	0.03	5.13	0.09
BS98	23	5.2	29/07/95	43:21:09	28:33:19	24.4	14.76	0.33	0.29	3.03		4.69	4.41
BS99	23	9.1	29/07/95	43:21:09	28:33:19	23.64	15.76	1.69	1.15	4.54		3.95	4.59
BS100	23	15.8	29/07/95	43:21:09	28:33:19	22.44	16.38	3.2	2.54	3.83		3.67	1.47
BS101	23	33.8	29/07/95	43:21:09	28:33:19	8.84	17.6	0.42	12.22	14.64		4.26	0.17
BS102	23	47.9	29/07/95	43:21:09	28:33:19	7.03	18.04	0.6	11.71	16.75		4.51	0.03
BS103	24	3	30/07/95	43:20:54	29:09:55	23.84	18.2	0.07	0	4.24	0	5.75	0.3
BS104	24	10.4	30/07/95	43:20:54	29:09:55	22.82	18.17	0	0.09	4.24	0	5.73	0.31
BS105	24	16.3	30/07/95	43:20:54	29:09:55	13.86	18.07	0	0	3.57	0	7.25	0.61
BS106	24	20.4	30/07/95	43:20:54	29:09:55	11.62	18.12	0.04	0	2.52	0	7.53	0.36
BS107	24	45.8	30/07/95	43:20:54	29:09:55	7.65	18.41	0.04	0.15	5.69	0.05	7	0.44
BS108	24	60.8	30/07/95	43:20:54	29:09:55	7.06	18.63	0.1	2.41	10.54	0.1	5.77	0.05
BS109	24	60.6	30/07/95	43:20:54	29:09:55	7.1	18.55	0.17	2.17	9.36	0.14		
BS110	24	71.3	30/07/95	43:20:54	29:09:55	7.13	18.76	0	3.91	14.68	0.21		
BS111	24	80.8	30/07/95	43:20:54	29:09:55								
BS112	24	91.8	30/07/95	43:20:54	29:09:55	7.15	18.87	0	4.39	15.19	0.31		
BS113	24	111	30/07/95	43:20:54	29:09:55	7.27	19.2	0	5.23	22.3	0.44		
BS114	24	141.4	30/07/95	43:20:54	29:09:55	8.04	20.39	0.91	3.75	49.12	1.2		
BS115	24	150.5	30/07/95	43:20:54	29:09:55	8.1	20.48	1.13	3.12	50.57	1.29		
BS116	25	3.6	31/07/95	43:21:18	28:41:18	24.25	18.11		0.31	3.35		5.93	0.6
BS117	25	12.5	31/07/95	43:21:18	28:41:18	24	18.08		0.45	3.41		5.94	0.64
BS118	25	22	31/07/95	43:21:18	28:41:18	17.73	17.8		0.75	3.91		7.36	2.86
BS119	25	40.2	31/07/95	43:21:18	28:41:18	8.4	18.19		0.24	4.35		6.76	0.67
BS120	25	70.3	31/07/95	43:21:18	28:41:18	7.32	18.42		2.87	10.27	0.14	5.76	0.16

Table AII2: Dissolved trace metals and other parameters

Code	TM bottle	Salinity (meas.)	MnD	FeD	CoD	PbD	CdD	ZnD	CuD	NiD
			nM	nM	nM	nM	nM	nM	nM	nM
BS1	4	17.867	11.53	6.48	0.372	0.059	0.071	2.04	8.35	12.02
BS2	5	17.826	12.17	6.77	0.373	0.043	0.072	6.89	8.12	11.92
BS3	3	17.915	12.16	7.21	0.353	0.051	0.071	3.20	8.31	12.89
BS4	1	18.003	11.91	7.23	0.408	0.071	0.072	3.24	8.61	12.36
BS5	2	18.076	10.66	7.23	0.300	0.048	0.069	1.81	8.41	12.50
BS6	11	17.805	11.83	5.69	0.421	0.044	0.075	2.29	9.05	12.76
BS7	12	17.636	12.23	4.91	0.341	0.045	0.077	1.21	8.59	12.73
BS8	10	17.721	11.61	4.93	0.381	0.080	0.066	1.48	8.34	11.75
BS9	8	17.998	10.58	5.45	0.418	0.110	0.073	3.70	8.66	12.40
BS10	9	18.495	2.95	4.82	0.194	0.035	0.076	2.40	6.91	12.22
BS11	7	18.565	2.60	4.89	0.220	0.072	0.077	2.75	7.36	13.32
BS12	16	18.045	9.66	3.03	0.340	0.186	0.071	1.53	7.47	10.28
BS13	24	18.2	5.53	2.53	0.243	0.098	0.071	0.90	7.36	9.94
BS14	15	18.249	2.31	2.31	0.226	0.160	0.080	2.03	7.87	11.93
BS15	23	18.578	1.18	1.30	0.136	0.054	0.085	2.00	6.74	10.37
BS16	22	19.022	0.69	1.83	0.083	0.023	0.109	3.65	6.01	11.11
BS17	17	19.366	1.21	2.15	0.055	0.026	0.123	4.32	5.46	10.51
BS18	20	19.605	0.69	1.78	0.036	0.036	0.139	5.18	5.22	10.00
BS19	14	19.945	1.06	0.83	0.024	0.007	0.158	6.91	4.55	9.60
BS20	18	20.423	8.06	1.30	0.049	0.055	0.139	6.06	3.38	9.20
BS21	19	20.518	10.41	0.79	0.043	0.021	0.110	4.74	2.54	8.65
BS22	13	20.764	317.73	1.71	0.317	0.024	0.077	4.34	1.64	9.15
BS23	34	20.999	7048.37	12.97	5.559	0.003	0.009	3.20	0.69	11.33
BS24	36	21.121	7782.29	101.43	6.522	0.010	0.007	2.71	0.50	11.34
BS25	35	21.378	8791.42	212.40	6.528	0.000	0.003	1.40	0.54	11.16
BS26	32	21.421	8745.55	170.21	6.000	0.002	0.003	2.44	0.58	10.66
BS27	33	21.367	8592.65	183.60	5.303	0.000	0.002	1.54	0.57	10.41
BS28	30	21.56	8455.04	292.37	3.267	0.000	0.003	0.40	0.46	9.63
BS29	26	21.913	6604.96	47.32	0.691	0.005	0.004	0.19	0.36	9.81
BS30	28	22.069	6039.23	47.51	0.534	0.004	0.001	0.23	0.15	9.85

Code	TM bottle	Salinity (meas.)	MnD nM	FeD nM	CoD nM	PbD nM	CdD nM	ZnD nM	CuD nM	NiD nM
BS31	25	22.201	5397.05	26.60	0.372	0.005	0.002	0.73	0.03	10.07
BS32	29	22.269	5030.09	15.96	0.378	0.017	0.004	0.62	0.03	10.08
BS33	27	21.732	6115.68	107.12	0.906	0.002	0.007	0.69	0.61	9.85
BS34	46	17.079	11.79	4.08	0.309	0.068	0.049	2.20	7.89	13.16
BS35	38	17.391	16.90	7.87	0.288	0.030	0.063	1.39	9.31	13.19
BS36	45	17.56	14.27	7.47	0.183	0.023	0.102	5.02	8.80	12.86
BS37	43	18.055	6.87	3.81	0.164	0.019	0.107	4.41	8.58	12.91
BS38	44	18.196	9.69	5.39	0.177	0.024	0.114	5.34	8.67	12.63
BS39	47	14.921	9.33	10.05	0.340	0.061	0.033	3.30	12.61	12.89
BS40	37	14.912	11.68	9.02	0.314	0.033	0.041	2.06	11.86	14.82
BS41	48	16.105	11.64	19.02	0.230	0.045	0.066	5.29	9.15	13.41
BS42	40	16.875	86.01	23.51	0.343	0.014	0.095	4.14	10.18	13.12
BS43	39	15.328	43.35	28.22	0.437	0.030	0.039	3.22	11.28	13.36
BS44	65	15.432	153.43	56.30	0.492	0.057	0.043	2.43	11.78	13.16
BS45	42	16.305	1204.16	146.09	1.416	0.077	0.071	5.94	9.86	17.53
BS46	41	16.406	1347.89	174.79	1.597	0.032	0.067	3.16	9.44	17.24
BS47	60	17.387	21.93	6.14	0.319	0.043	0.056	1.01	7.88	11.69
BS48	66	17.309	44.25	16.21	0.287	0.024	0.107	2.60	8.03	11.15
BS49	55	17.455	28.81	10.39	0.245	0.048	0.093	4.86	9.02	11.75
BS50	53	17.928	18.93	8.93	0.277	0.090	0.093	6.11	8.53	12.58
BS51	56	18.252	54.49	31.04	0.255	0.014	0.125	5.33	7.66	14.54
BS52	57		22.69	42.28	0.429	0.069	0.067	1.82	15.98	12.98
BS53	54		672.67	72.06	1.551	0.033	0.144	7.14	8.83	13.24
BS54	49	8.894	103.88	180.81	0.689	0.614	0.139	5.57	28.81	13.04
BS55	52	14.465	15.20	14.14	0.362	0.115	0.075	2.74	14.74	11.38
BS56	59	15.23	17.19	25.54	0.353	0.211	0.066	1.79	13.84	12.15
BS57	50	12.005	46.70	20.22	0.478	0.121	0.096	2.34	21.43	12.27
BS58	71	16.563	103.88	42.89	1.198	0.069	0.092	2.79	10.94	12.57
BS59	51	17.571	1056.44	123.20	1.797	0.063	0.161	8.33	10.27	14.90
BS60	62	13.822	14.59	14.23	0.470	0.084	0.074	1.72	15.14	11.46
BS61	61	15.16	19.54	29.48	0.373	0.108	0.073	2.59	12.76	11.38

Code	TM bottle	Salinity (meas.)	MnD nM	FeD nM	CoD nM	PbD nM	CdD nM	ZnD nM	CuD nM	NiD nM
BS62	63	16.75	21.04	13.45	0.379	0.060	0.056	2.18	9.45	11.08
BS63	67	0.195	14.34	35.80	0.339	0.159	0.132	5.92	27.63	15.13
BS64										
BS65										
BS66	73		29.75	27.62	0.397	0.115	0.163	5.84	21.81	13.81
BS67										
BS68	69	15.282	14.04	12.06	0.379	0.060	0.066	1.48	13.02	11.16
BS69	70	17.218	14.10	8.81	0.361	0.052	0.059	1.52	9.24	11.15
BS70	68	17.65	24.43	6.92	0.341	0.052	0.071	2.59	8.29	11.08
BS71	74	18.18	171.16	15.94	0.474	0.034	0.134	6.49	8.69	12.11
BS72	84	14.864	13.36	9.78	0.390	0.045	0.067	1.27	13.10	11.34
BS73	89	17.323	10.92	6.08	0.194	0.033	0.058	1.58	8.29	12.35
BS74	87	17.809	23.36	5.72	0.223	0.028	0.087	3.38	8.16	13.05
BS75	85	18.248	27.03	4.15	0.173	0.034	0.100	6.34	7.57	12.09
BS76	86	18.188	54.13	7.02	0.180	0.018	0.118	4.40	7.50	12.28
BS77	88	16.428	14.02	10.59	0.249	0.048	0.102	2.87	10.61	11.42
BS78	82	17.385	11.31	6.02	0.199	0.040	0.075	2.21	8.31	11.64
BS79	83	17.718	15.47	8.83	0.232	0.030	0.107	4.13	9.40	13.61
BS80	79/90	18.26	3.75	1.31	0.117	0.028	0.109	2.53	7.77	12.29
BS81	75	18.297	13.59	7.48	0.133	0.044	0.093	5.93	9.28	12.15
BS82	92	16.689	7.77	4.42	0.219	0.047	0.048	1.10	9.78	12.54
BS83	93	17.654	9.24	31.80	0.268	0.068	0.055	2.51	8.76	13.55
BS84	91	18.133	6.91	2.80	0.229	0.065	0.060	1.42	7.90	12.21
BS85	81	18.223	7.74	4.32	0.220	0.070	0.056	1.73	7.97	11.62
BS86	95	18.171	8.87	1.32	0.171	0.044	0.085	1.58	7.68	11.56
BS87	99	16.793	6.16	6.33	0.205	0.024	0.060	2.39	9.25	10.98
BS88	102	17.497	10.08	6.72	0.239	0.031	0.067	1.86	8.91	12.59
BS89	101	17.504	29.36	6.68	0.314	0.019	0.108	4.90	10.14	14.13
BS90	96	18.229	351.67	5.99	0.577	0.018	0.109	3.79	8.51	13.94
BS91	94	18.23	567.26	9.76	0.846	0.015	0.105	4.66	9.11	15.07
BS92	106	16.138	8.47	4.74	0.238	0.032	0.045	2.08	10.88	12.80

Code	TM bottle	Salinity (meas.)	MnD nM	FeD nM	CoD nM	PbD nM	CdD nM	ZnD nM	CuD nM	NiD nM
BS93	109	16.737	8.67	3.70	0.268	0.027	0.047	8.24	9.83	12.07
BS94	108	17.211	7.34	4.18	0.230	0.039	0.063	2.12	9.72	13.47
BS95	100	17.418	9.05	3.69	0.232	0.031	0.089	45.40	9.65	13.41
BS96	98	17.685	18.07	8.95	0.248	0.027	0.122	6.45	9.36	10.85
BS97	97	18.201	154.43	14.02	0.304	0.016	0.124	6.06	9.41	14.56
BS98	111	15.006	11.88	16.61	0.268	0.026	0.069	3.17	12.69	9.58
BS99	112	15.754	16.12	20.55	0.355	0.034	0.077	4.19	11.99	12.61
BS100	113	17.001	109.83	18.86	0.532	0.022	0.115	4.47	10.20	11.59
BS101	107	17.982	148.05	15.28	0.343	0.015	0.136	7.80	9.65	12.58
BS102	110	18.088	172.52	14.53	0.368	0.020	0.152	6.23	9.81	11.44
BS103	123	18.256	8.62	1.77	0.293	0.110	0.059	1.32	7.38	8.90
BS104	125	18.244	8.49	1.85	0.269	0.115	0.053	2.18	7.72	8.85
BS105	105	18.145	8.21	2.12	0.285	0.086	0.053	2.40	8.16	9.47
BS106	114	18.179	4.98	1.59	0.278	0.084	0.061	2.09	8.02	8.73
BS107	103	18.456	1.53	0.42	0.151	0.069	0.073	1.77	7.43	10.38
BS108	104	18.676	1.85	1.38	0.137	0.034	0.089	2.65	7.20	9.40
BS109	115	18.629	1.24	1.14	0.132	0.029	0.080	2.27	7.07	9.07
BS110	119	18.797	3.33	1.44	0.093	0.021	0.091	3.12	6.73	9.22
BS111	117(pb)	18.937	2.87	1.37	0.080	0.013	0.097	5.45	6.41	10.68
BS112	118	18.93	1.64	1.02	0.069	0.016	0.092	5.29	6.49	10.45
BS113	120		1.30	0.86	0.047	0.007	0.114	4.59	5.79	10.62
BS114	124	20.463	9.54	0.80	0.037	0.020	0.095	4.47	2.97	9.59
BS115	122	20.516	32.00	0.57	0.062	0.003	0.080	4.19	2.91	9.27
BS116	138	18.154	10.24	2.83	0.297	0.091	0.056	1.13	7.71	9.98
BS117	135	18.118	12.31	2.81	0.312	0.093	0.058	1.84	8.59	9.53
BS118	137	18.145	5.28	1.77	0.242	0.071	0.058	3.58	8.25	9.07
BS119	116	18.27	1.83	0.60	0.176	0.053	0.066	4.28	7.50	8.56
BS120	136	18.449	14.74	3.70	0.144	0.038	0.090	3.22	8.45	9.62

Table AII3: General sampling parameters and particulate Mn and Fe (L=leachable fraction; R=residual fraction)

Code	Station	Depth m	Temperature °C	Salinity	SPM mg/l	MnL ng/l	MnL µg/g	MnR ng/l	MnR µg/g	FeL ng/l	FeL µg/g	FeR ng/l	FeR µg/g
BS6	1	5.4	23.06	17.63	0.708	184	260	17	23.5	185	261	1100	1554
BS7	1	9.9	23.03	17.63	0.41	204	498	12	29.3	230	560	1253	3057
BS9	1	39.5	20.03	17.83	0.45	47	105	6	14.2	146	324	581	1291
BS11	1	86.8	7.25	18.49	0.267	82	306	8	31.3	355	1331	966	3619
BS12	3	9.5	23.34	18.04	0.23	64	276	3	14.1	29	126	305	1327
BS14	3	31.2	9.35	18.24	0.22	114	519	6	29.5	15	67	116	528
BS15	3	60.5	7.06	18.49	0.053	86	1636	5	91.3	43	807	126	2381
BS17	3	91.3	7.26	19.37	0.13	329	2525	25	195.2	105	807	307	2364
BS19	3	110	8.15	20.6	0.226	1160	5124	93	410.0	123	544	225	995
BS20	3	130	7.81	20.15	0.17	1484	8740	111	654.8	89	522	164	966
BS21	3	140	8	20.4	0.136	911	6708	62	454.2	61	450	241	1771
BS22	3	150	8.26	20.75	0.109	748	6840	42	387.5	40	366	241	2213
BS24	3	170	8.49	21.12	0.407	126	309	8	20	283	696	570	1399
BS34	4	5.6	24.31	16.88	0.4	356	891	15	36	30	75	500	1250
BS34	4	5.6	24.31	16.88	0.453	570	1258	22	49	19	42	497	1097
BS37	4	27.4	9.54	18.06	0.38	2416	6357	122	322	211	556	604	1588
BS38	4	34.5	7.38	18.22	0.17	1921	11302	77	452	304	1789	461	2710
BS39	5	4.7	24.98	14.9	0.975	411	421			70	72		
BS39	5	4.7	24.98	14.9	0.8	353	441	29	36.4	65	81	426	533
BS40	5	12.2	24.38	15	0.711	416	585	22	31	147	206	484	680
BS41	5	17	23.49	15.98	2.3	6234	2710	242	105.3	3041	1322	1050	457
BS42	5	23	10.17	17.87	0.12	4517	37643	261	2177.8	1641	13672	763	6361
BS43	6	5	24.57	15.31	1.156	3120	2700	164	141.5	2668	2309	3599	3113
BS44	6	9.8	24.5	15.33	1.234	5851	4741	310	251.1	5965	4834	3737	3029
BS45	6	12.7	22.79	15.99	0.553	25433	45975	9242	16712.5	60631	109602	11199	20251
BS46	6	15.3	19.5	17.64	1.133	29278	25833	5599	4942	69683	61485	10572	9331
BS47	7	5.1	23.33	17.34	0.36	2748	7633	134	372	479	1329	755	2098
BS48	7	11.9	24.28	17.79	0.59	2184	3702	91	154.8	360	609	1278	2167
BS49	7	19.4	18.13	17.3	0.845	1647	1949	57	68	85	100	327	388
BS50	7	21.6	17.36	17.36	0.57	925	1623	45	79	86	150	428	750

Code	Station	Depth m	Temperature °C	Salinity	SPM mg/l	MnL ng/l	MnL µg/g	MnR ng/l	MnR µg/g	FeL ng/l	FeL µg/g	FeR ng/l	FeR µg/g
BS51	7	33.3	7.79	18.24	0.11	1493	13576	82	749.7	419	3809	914	8310
BS54	9	3.3	24.72	10.73	5.071	12732	2511	1357	267.5	33204	6547	114956	22669
BS55	9	6.9	24.69	12.91	1.54	3516	2283	210	136	3550	2305	16151	10488
BS55	9	6.9	24.69	12.91	1.522	4876	3204			4023	2644		
BS56	9	15.5	24.25	15.23	1.102	3413	3097	265	240.6	3236	2936	15694	14242
BS57	10	3.1	25.3	12.06	4	7849	1962	807	202	21667	5417	84978	21244
BS58	10	13.3	21.56	16.69	0.688	17515	25476	1479	2149	10606	15427	11634	16909
BS59	10	27.8	10.39	17.63	0.711	8124	11425	407	572	39006	54852	7024	9879
BS60	11	5.5	24.18	10.33	1.468	4705	3205	414	281.8	6100	4155	25106	17102
BS61	11	14.7	24.34	10.53	1.032	2582	2501	229	221.4	2826	2738	8431	8170
BS62	11	20.2	24.47	10.98	0.94	1820	1935	110	117.5	1104	1173	3135	3335
BS63	12	surface		0.1	35	47030	1344	10583	302.4	201323	5752	902754	25793
BS63	12	surface		0.1	21.167	32613	1541	5581	264	130990	6189	608930	28768
BS63	12	surface		0.1	38.033	49129	1292	9422	248	223988	5889	1023455	26910
BS66	15	surface		3.5	7.467	13165	1763	1893	253.5	54323	7275	173901	23289
BS66	15	surface		3.5	9.3	17545	1887	2384	256	69322	7454	291698	31365
BS68	17	4.8	24.57	11.79	1.289	3287	2551	255	198	3899	3026	14701	11405
BS69	17	21.7	23.81	13.36	0.52	1123	2160	52	100	447	860	1661	3193
BS70	17	28.3	23.48	13.44	0.638	1163	1824	65	102	456	715	901	1412
BS71	17	43.8	7.27	13.78	0.78	1942	2489	107	137	997	1278	4226	5418
BS72	18	3.7	24.34	13.03	1.433	2619	1828	179	125	2914	2033	10037	7004
BS73	18	10.4	23.84	15.02	1.09	1157	1061	49	45	646	593	2070	1899
BS74	18	19.7	21.82	15.47	0.92	1917	2084	83	90	561	610	1094	1189
BS75	18	31	8.64	15.79	0.087	1635	18865	77	885	405	4677	676	7769
BS78	19	10.2	23.71	14.11	0.95	1101	1159	48	50.1	134	141	601	632
BS79	19	20.4	18.16	14.45	0.764	1462	1914	71	92.6	169	221	462	605
BS80	19	36.4	8.68	14.71	0.347	334	964	20	57	74	213	244	704
BS81	19	46.3	7.63	14.76	0.669	345	516	12	19	64	96	255	381
BS82	20	1.7	24.2	{16.16}	0.922	294	319	19	20	55	60	589	639
BS83	20	10.4	24.05	{17.72}	0.69	202	293	10	14	39	57	229	333
BS84	20	19.6	22.52	{17.67}	0.787	72	92	5	6	9	11	122	155

Code	Station	Depth	Temperature	Salinity	SPM	MnL	MnL	MnR	MnR	FeL	FeL	FeR	FeR
		m	°C		mg/l	ng/l	µg/g	ng/l	µg/g	ng/l	µg/g	ng/l	µg/g
BS85	20	25.3	12.57	{17.88}	0.48	34	72	4	8	8	17	122	254
BS86	20	47.4	7.63	{18.12}	0.413	306	740	13	32	32	78	177	428
BS87	21	5.5	23.12	16.81	1.37	3303	2411	125	91	856	625	1787	1304
BS88	21	14.6	17.07	17.35	0.7	2297	3282	117	167	424	605	717	1024
BS89	21	23.6	9.14	17.53	1.05	5087	4844	253	241	620	590	957	912
BS90	21	40.2	7.12	18.15	0.52	2102	4043	100	192.0	539	1036	465	894
BS91	21	50.4	6.77	18.17	0.353	1452	4108	70	197	767	2170	555	1573
BS92	22	2	24.46	15.83	1.27	805	634	36	28	193	152	631	497
BS93	22	8.4	24.34	16.46	1.362	571	419	26	19	95	70	319	234
BS94	22	19.5	23.82	17.05	0.878	574	654	27	30	133	151	561	639
BS95	22	23	23.24	17.3	1.146	519	453	22	19	91	79	337	294
BS96	22	27.7	13.86	17.23	0.481	574	1192	26	53	104	217	286	594
BS97	22	50.9	6.51	18.14	0.6	665	1108	37	62	551	919	1008	1681
BS109	24	60.9	7.08	18.57		202			10	86			164
BS110	24	70.8	7.11	18.72		230			8	82			226
BS111	24	80.8	7.15	18.81		439			16	106			321
BS112	24	91.8	7.15	18.87		442			15	97			240
BS113	24	111.6	7.27	19.21		2169			113	156			304
BS114	24	141.8	8.04	20.39		13991			21957	37			998
BS115	24	151.8	8.11	20.5		13065			44720	22			1354
BS116	25	3.5	24.26	18.11	0.27	112	415			10	38		
BS120	25	70.3	7.32	18.42	0.31	292	941			59	190		

Table AII4: Leachable particulate trace metals

Code	CoL ng/l	CoL ug/g	PbL ng/l	PbL ug/g	CuL ng/l	CuL ug/g	NiL ng/l	NiL ug/g	ZnL ng/l	ZnL ug/g	CdL ng/l	CdL ug/g
BS6	0.82	1.16	3.26	4.61	7.99	11.27	3.13	4.41	32.92	46.47	0.34	0.48
BS7	0.28	0.67	2.66	6.48	8.1	19.76	6	14.63	4.53	11.04	0.22	0.54
BS9	0.27	0.59	2.02	4.49	4.9	10.89	1.9	4.22	47.15	104.78	0.23	0.5
BS11	0.53	1.99	2.98	11.19	2.81	10.54	0.79	2.95	18.5	69.38	0.3	1.13
BS12	0.36	1.57	2.72	11.8	11.35	49.35	17.85	77.61	36.5	158.7	<dl	<dl
BS14	0.47	2.15	2.17	9.86	4.73	21.48	1.5	6.82	7.04	31.99	0.31	1.42
BS15	0.46	8.71	0.61	11.46	2.15	40.71	1.66	31.43	2.08	39.46	0.32	6.14
BS17	0.76	5.8	2.05	15.71	3.02	23.21	3.56	27.32	0.78	5.98	0.47	3.63
BS19	1.41	6.24	2.32	10.27	2.81	12.42	4	17.67	8.76	38.71	0.41	1.8
BS20	1.55	9.1	1.55	9.11	3.28	19.33	3.6	21.22	9.24	54.39	0.36	2.1
BS21	1.17	8.61	0.93	6.82	2.4	17.64	2.51	18.47	8.08	59.44	0.27	1.97
BS22	1	9.17	0.95	8.66	17.09	156.21	1.87	17.07	8.98	82.07	0.16	1.48
BS24	0.74	1.82	7.63	18.75	50.85	124.9	3.17	7.79	79.94	196.35	1.63	4
BS34	0.8	1.99	3.52	8.8	8.25	20.63	4.47	11.18	18.6	46.5	0.85	2.12
BS34	<dl	<dl	2.52	5.56	11.68	25.77	5.12	11.29	23.52	51.88	0.64	1.41
BS37	4.15	10.91	5.08	13.38	11.2	29.46	4.96	13.05	31.28	82.32	0.36	0.96
BS38	2.76	16.26	3.43	20.15	5.48	32.22	1.56	9.18	18.72	110.12	0.32	1.87
BS39	1.24	1.27	3.74	3.83	17.88	18.33	16.5	16.92	79	81.03	2.66	2.73
BS39	2.53	3.16	2.24	2.8	18.3	22.88	18.6	23.25	49.15	61.44	1.82	2.28
BS40	1.51	2.13	3.39	4.77	16.44	23.12	13.11	18.44	26.56	37.34	1.58	2.22
BS41	9.91	4.31	5.45	2.37	31.3	13.61	19	8.26	74.45	32.37	1.48	0.64
BS42	4.65	38.78	3.67	30.56	27	225	2.6	21.67	31.1	259.17	0.75	6.22
BS43	4.99	4.32	7.72	6.68	19.11	16.54	28.44	24.62	47.83	41.39	1.6	1.38
BS44	3.31	2.68	9.38	7.6	16.31	13.22	9.45	7.66	40.98	33.21	1.58	1.28
BS45	4.33	7.83	8.05	14.56	20.96	37.88	17.98	32.5	82.66	149.42	0.88	1.6
BS46	9.53	8.41	8.3	7.32	27.21	24.01	10.67	9.41	406.33	358.53	0.38	0.34
BS47	3.81	10.59	6.96	19.32	14.29	39.69	6.5	18.06	19.95	55.42	0.77	2.14
BS48	3.58	6.07	11.72	19.86	12.82	21.73	6.85	11.61	31.55	53.47	1.2	2.03
BS49	4.56	5.39	6.92	8.18	11.31	13.38	7.44	8.8	29.82	35.28	1.83	2.16
BS50	1.03	1.81	4.08	7.15	5.8	10.18	4.95	8.68	17.5	30.7	0.99	1.74

Code	CoL ng/l	CoL ug/g	PbL ng/l	PbL ug/g	CuL ng/l	CuL ug/g	NiL ng/l	NiL ug/g	ZnL ng/l	ZnL ug/g	CdL ng/l	CdL ug/g
BS51	2.43	22.05	3.96	35.95	6.45	58.64	4	36.36	11.58	105.23	0.4	3.64
BS54	25.73	5.07	306.41	60.42	238.57	47.04	123.04	24.26	495.71	97.75	7.05	1.39
BS55	8.98	5.83	33.84	21.97	42.35	27.5	28.5	18.51	108.2	70.26	2.69	1.75
BS55	7.84	5.15	32.64	21.45	46.85	30.79	31.3	20.57	97.72	64.21	2.4	1.58
BS56	5.26	4.77	34.64	31.44	44.59	40.46	25.92	23.52	87.86	79.72	1.99	1.81
BS57	19.7	4.93	168.16	42.04	147.38	36.85	60.24	15.06	331.43	82.86	4.84	1.21
BS58	16.84	24.5	21.11	30.7	27.11	39.43	20.13	29.27	63.88	92.91	0.87	1.26
BS59	6.05	8.51	10.51	14.78	21.26	29.9	7.06	9.92	55.61	78.2	0.78	1.09
BS60	8.04	5.48	60.97	41.53	50	34.06	43.94	29.93	166.49	113.41	2.38	1.62
BS61	4.27	4.14	124.67	120.77	44.11	42.73	22.66	21.95	61.29	59.38	1.44	1.39
BS62	3.27	3.47	11.87	12.62	22.74	24.18	21.37	22.72	46.07	48.99	1.54	1.63
BS63	170.12	4.86	1033.65	29.53	1083.83	30.97	584.5	16.7	3129.33	89.41	20.23	0.58
BS63	122.28	5.78	732.32	34.6	709.83	33.54	282.67	13.35	1657.67	78.31	13.45	0.64
BS63	207.85	5.46	1095.47	28.8	1279	33.63	642	16.88	2539.33	66.77	21.87	0.57
BS66	45.12	6.04	332.58	44.54	287.83	38.55	138	18.48	643.17	86.14	6.47	0.87
BS66	56.52	6.08	403.4	43.38	343.17	36.9	174.17	18.73	828.92	89.13	8.48	0.91
BS68	5.9	4.58	27.21	21.12	37.42	29.04	24.09	18.7	98.46	76.41	1.98	1.54
BS69	2.84	5.45	7.88	15.15	<dl	<dl	7.05	13.56	19.05	36.63	0.84	1.62
BS70	1.55	2.43	2.47	3.88	4.81	7.55	2.88	4.51	7.34	11.52	0.34	0.53
BS71	3.29	4.22	13.24	16.97	18.62	23.88	10.3	13.21	37.1	47.56	1.08	1.38
BS72	3.5	2.44	24.12	16.83	35.28	24.61	22.39	15.62	64.67	45.12	1.58	1.1
BS73	3.3	3.03	9.05	8.3	15.8	14.5	8.55	7.84	28.5	26.15	1.22	1.12
BS74	2.43	2.64	6.67	7.24	11.29	12.28	5.75	6.25	21.8	23.7	0.74	0.8
BS75	2.86	33.02	5.45	62.92	11.19	129.16	2.93	33.85	19.2	221.54	0.54	6.27
BS78	1.55	1.64	4.55	4.79	10.95	11.53	5.64	5.94	37.68	39.66	0.91	0.95
BS79	3.47	4.55	6.11	8	10.92	14.3	7.12	9.33	21.76	28.49	1.11	1.45
BS80	1.05	3.02	3.97	11.46	5.49	15.85	0.93	2.69	10.5	30.29	0.27	0.78
BS81	1.57	2.34	3.14	4.7	3.17	4.74	1.79	2.68	8.9	13.3	0.64	0.96
BS82	1.83	1.99	5.01	5.43	13.23	14.34	8.83	9.58	22.61	24.52	1.48	1.6
BS83	0.85	1.24	6.32	9.17	19.91	28.87	6	8.7	23.07	33.45	0.98	1.43
BS84	0.37	0.47	2.18	2.78	6.42	8.16	5.47	6.95	18.6	23.64	1.05	1.33

Code	CoL ng/l	CoL ug/g	PbL ng/l	PbL ug/g	CuL ng/l	CuL ug/g	NiL ng/l	NiL ug/g	ZnL ng/l	ZnL ug/g	CdL ng/l	CdL ug/g
BS85	0.18	0.38	2.07	4.31	4.73	9.85	5.27	10.97	18.23	37.99	1.09	2.27
BS86	1.37	3.33	3.21	7.77	3.04	7.35	1.7	4.11	15.1	36.53	0.61	1.48
BS87	7.23	5.28	10.4	7.59	22.98	16.77	13.1	9.56	39.7	28.98	1.23	0.9
BS88	5.63	8.05	9.15	13.08	15.88	22.68	7.67	10.95	25.13	35.9	1.01	1.44
BS89	9.21	8.77	7.34	6.99	32.78	31.22	8.95	8.52	43.5	41.43	1.24	1.18
BS90	2.3	4.43	4.7	9.03	14.6	28.09	1.04	2	25.07	48.21	0.63	1.21
BS91	0.66	1.86	2.28	6.44	4.9	13.87	1.63	4.62	8.8	24.91	0.7	1.98
BS92	1.54	1.22	6.88	5.41	25.17	19.81	19.39	15.27	45.54	35.85	2	1.57
BS93	0.75	0.55	3.93	2.89	32.27	23.7	9.04	6.64	57.71	42.38	0.97	0.71
BS94	2.68	3.05	5.58	6.36	21.79	24.82	8.78	10	27.06	30.82	1.37	1.56
BS95	1.2	1.05	4.27	3.72	16.26	14.19	8.19	7.15	33.38	29.13	1.4	1.22
BS96	1.68	3.5	3.3	6.86	7.47	15.52	3.47	7.21	23.81	49.48	1.35	2.8
BS97	0.48	0.79	3.75	6.26	6.1	10.17	1.6	2.67	9.77	16.28	0.9	1.5
BS109	0.83		1.73		12.04		0.4		3.56		0.4	
BS110	0.44		1.91		3.44		0.25		2.88		0.77	
BS111	0.66		2.34		4.62		0.77		6.75		1.02	
BS112	0.7		1.96		2.63		0.14		14.04		0.75	
BS113	2.61		2.53		5.42		1.82		8.49		0.63	
BS114	2.78		0.08		8.33		6.08		49.04		0.4	
BS115	1.62		<dl		14.04		6.67		51.27		0.39	
BS116	0.17	0.64	2.88	10.67	21.17	78.42	2.7	10	24.78	91.78	0.59	2.18
BS120	0.29	0.93	2.73	8.81	15.36	49.56	0.48	1.53	12.43	40.08	0.66	2.12